Enhancing Tele-operation - Investigating the effect of sensory feedback on performance

By

JOSEPH OLUWATOBILOBA BOLARINWA

A thesis submitted in partial fulfilment of the requirements of the University of the West of England, Bristol for the degree of Doctor of Philosophy in Robotics

Faculty of Engineering and Technology, University of the West of England, Bristol

AUGUST 2022

Word count: Forty eight thousand, five hundred and fifty one

Abstract

The decline in the number of healthcare service providers in comparison to the growing numbers of service users prompts the development of technologies to improve the efficiency of healthcare services. One such technology which could offer support are assistive robots, remotely tele-operated to provide assistive care and support for older adults with assistive care needs and people living with disabilities. Tele-operation makes it possible to provide human-in-the-loop robotic assistance while also addressing safety concerns in the use of autonomous robots around humans. Unlike many other applications of robot tele-operation, safety is particularly significant as the tele-operated assistive robots will be used in close proximity to vulnerable human users. It is therefore important to provide as much information about the robot (and the robot workspace) as possible to the human operators to ensure safety, as well as efficiency. Since robot tele-operation is relatively unexplored in the context of assisted living, this thesis explores different feedback modalities that may be employed to communicate sensor information to operators.

The thesis presents research as it transitioned from identifying and evaluating additional feedback modalities that may be used to supplement video feedback, to exploring different strategies for communicating the different feedback modalities. Due to the fact that some of the sensors and feedback needed are not readily available, different design iterations were carried out to develop the necessary hardware and software for the studies. The first human study was carried out to investigate the effect of feedback on operator performance. Different combinations of video feedback, peripheral vision feedback, haptic feedback and verbal feedback were used to convey information about gripper orientation to participants who carried out a tele-operated assistive task. The different combinations of feedback were referred to as feedback scenarios. Performance was measured in terms of task completion time, ease of use of the system, number of robot joint movements, and success or failure of the task. The effect of verbal feedback between the operator and service users was also investigated. Feedback modalities have differing effects on performance metrics and as a result, the choice of optimal feedback may vary from task to task. Results show that participants preferred scenarios with verbal feedback relative to scenarios without verbal feedback, which also reflects in their performance. Gaze metrics from the study also showed that it may be possible to understand how operators interact with the system based on their areas of interest as they carry out tasks. This findings suggest that such studies can be used to improve the design of tele-operation systems.

The need for social interaction between the operator and service user suggests that visual and auditory feedback modalities will be engaged as tasks are carried out. This further reduces the number of available sensory modalities through which information can be communicated to operators. A wrist-worn Wi-Fi enabled haptic feedback device was therefore developed and a study was carried out to investigate haptic sensitivities across the wrist. Results suggest that different locations on the wrist have varying sensitivities to haptic stimulation with and without video distraction, duration of haptic stimulation, and varying amplitudes of stimulation. This

suggests that dynamic control of haptic feedback can be used to improve haptic perception across the wrist, and it may also be possible to display more than one type of sensor data to operators during a task.

The final study carried out was designed to investigate if participants could differentiate between different types of sensor data (gripper proximity and gripper orientation) conveyed simultaneously through different locations on the wrist via haptic feedback. The effect of increased number of attempts on performance was also investigated. Gripper proximity and orientation information was used to supplement video feedback. Total task completion time decreased with task repetition. Participants with prior gaming and robot experience had more significant reduction in total task completion time when compared to participants without prior gaming and robot experience. Reduction in task completion time was noticed for all stages of the task but participants with supplementary feedback had higher task completion time than participants without supplementary feedback. Reduction in task completion time varied for different stages of the task. Even though gripper trajectory reduced with task repetition, participants with supplementary feedback had longer gripper trajectories than participants without supplementary feedback, while participants with prior gaming experience had shorter gripper trajectories than participants without prior gaming experience. Perceived workload was also found to reduce with task repetition but perceived workload was higher for participants with feedback reported higher perceived workload than participants without feedback. However participants without supplementary feedback reported higher frustration than participants without supplementary feedback. Results show that the effect of supplementary feedback may not be significant where participants can get necessary information from video feedback. However, participants were fully dependent on feedback when video feedback could not provide requisite information needed.

The findings presented in this thesis have potential applications in healthcare, and other applications of robot tele-operation and feedback. Findings can be used to improve feedback designs for tele-operation systems to ensure safe and efficient tele-operation. The thesis also provides ways visual feedback can be combined with other feedback modalities. The haptic feedback designed in this research may also be used to provide situational awareness for the visually impaired.

Dedication and acknowledgements

I would like to thank God for the grace and strength to complete this research study (1 Samuel 2:9).

I would also like to express my gratitude to every one who advised and supported me in completing this research study.

My most sincere appreciation to my every member of my supervisory team: Professor Praminda Caleb-Solly (DoS), Professor Sanja Dogramadzi, and Dr Tom Mitchell. Thank you for your patience, supervision, expertise , and inspiration, which made it possible for me to fulfil the goals of this research. A special thanks to the technicians at the Bristol Robotics Laboratory (BRL), especially Jason Welsby and Ian Horsfield, for helping out with my hardware designs.

A special thanks to my Dad and Mum (Pastor and Pastor Josiah and Kemi Bolarinwa), and my Siblings (Timothy and Rebecca) for their prayers and support.

AUTHOR'S DECLARATION

I declare that the work in this dissertation was carried out in accordance with the requirements of the University's Regulations and Code of Practice for Research Degree Programmes and that it has not been submitted for any other academic award. Except where indicated by specific reference in the text, the work is the candidate's own work. Work done in collaboration with, or with the assistance of, others, is indicated as such. Any views expressed in the dissertation are those of the author.

Table of Contents

Page

List of Tables

List of Figures

List of Abbreviations

AC	Alternating current
ADC	Analog-to-digital converter
ADL	Activities of daily living
AF	Auditory feedback
AR	Augmented reality
DFF	Direct force feedback
DHS	Duration of haptic stimulation
ERM	Eccentric rotating mass
FOV	Field of view
GPIO	General-purpose input/output
HF	Haptic feedback
HG	Haptic guidance
HMD	head mounted display
HRI	Human robot interaction
ICF	International classification of functioning, disabilities, and health
ILHSP	Identification of location of haptic stimulation performance
LRA	Linear resonance actuators
MCU	Microcontroller unit
MDHI	Minimum detectable haptic intensity
MOSFET	Metal oxide semiconductor field effect transistor
PWM	Pulse width modulation
SARs	socially assistive robots

SDSI Simultaneous double-location stimulation identification

SFF Substituted force feedback

SSI Single-location stimulated identification

TRINA Tele-robotic intelligent nursing assistant

VAC Vergence-accomodation conflict

VE Virtual environment

VR Virtual reality

Chapter 1

Introduction

People are living longer and in some cases, with better health at older ages than in previous years. It is expected that the global population of people aged over 60 in 2017 would double by 2050 reaching nearly 2.1 billion [195]. However limited investments in health and social care, as well as lower numbers entering the social and healthcare workforce, is leading to shortages in the people available to provide a high quality of care to growing numbers of people who need more support. Age UK estimate that there are now nearly 1.2 million older people who do not receive the help they need with essential daily living activities, an increase of 48% since 2010 [5]. Nearly 1 in 8 older people in the UK now live with some level of unmet care need. According to [210], the United States of America, for example, will face an estimated shortage of 139,160 physicians by 2030, with the West having a physician to population ratio of 69:100,000 and the South 62:100,000.

The increasing cost of institutional long term care and preference of older persons (and younger persons with disability) to maintain independence continues to make a case for aging in place [197]. Aging in place encourages non-institutional care, which reduces the strain on institutional care providers, allowing families of older persons to support in the provision of necessary care and attention needed [6]. However, the increasing demand for medical care continuously undermines the supply efforts made to provide medical professionals. A promising approach however has been the introduction of computers and different technologies designed to help improve the efficiency of the healthcare system and the quality of care provided to patients.

While different technologies have be developed to enhance the quality of service/care provided by health care professionals, this research focuses on enhancing a relatively unexplored area: Robot tele-operation for providing assistance for older adults and people with disabilities. Robot tele-operation involves the control of a robot by a human operator located outside the vicinity or work environment of the robot. The justification for the consideration of robot tele-operation (in contrast to the use of autonomous robots) is that it ensures that human input is always present in the robotic solution provided. The application domain of this research is in helping older adults with assistive care needs and people living with disabilities with their activities of daily living (ADL).

Tele-operated robots allow for humans-in-the-loop remote operations of the assistive robots [23] which can also protect healthcare professionals when providing care for people with infectious disease [205]. This may help to solve some of the operational and safety challenges autonomous robots may experience as a result of the unpredictable nature of some work environments and service users for which care is provided [76]. For future implementations, it may be possible for a single carer to provide remote assistance for several people within a short period of time using tele-operated robots without the constraints of going to different locations (within healthcare institutions or private homes). Tele-operation can also allow family caregivers lead normal lives as they do not always have to be physically present to provide certain levels of care, hence allowing them pay sufficient attention to other areas of their lives.

1.1 Robot Tele-operation: Overview

The prefix ***tele*** has a Greek origin which means *at a distance* [70]. Robot tele-operation in general indicates the control of a robot at a distance. Hence, tele-operation extends human capability to manipulating robots in remote locations by providing the human operator with similar conditions as those in the remote location. This is achieved through a leader-follower system [24], which was formally referred to as the master-slave system. The leader robot, which could be a robot or a joystick, is situated at the human operator end while the follower robot (that performs the actual task) is situated at a location away from the operator. In a general setting, the human operator exerts a force on the leader robot which results in a displacement that is transmitted to the follower robot that mimics the movements of the leader robot.The follower robot's interaction with the remote environment may also be measured using force sensors and transmitted as external torque to the human operator via haptic senses along with visual senses, hence creating *bilateral* tele-operation.

From a control standpoint, stability and telepresence are two important goals of robot tele-operation. Whilst stability refers to the stability of the closed-loop system irrespective of how the operator or environment behaves, telepresence aims to provide the operator with feelings of being in the remote location. Instability is often introduced into the system via the communication medium (wired or wireless) between the leader and follower robots as it may contribute to the overall complexity of the system, as well as the introduction of distortion, and delays that impact stability and performance. This therefore motivates research on control theories on robot tele-operation.

1.1.1 Control methods/architectures for robot tele-operation

Early studies on the effect of delay in tele-operation involves that carried out by [45] who investigated the effects of delays in communication when reflecting force feedback to the leader robot. [46] also developed supervisory control to address the problems of delays, and inspired research in new tele-operation-oriented software languages [48], [166] and visual enhancements using predictive displays [20][69] to minimise communication exchange between the leader and follower robots. More advanced control methods include Lyapunov-based analysis [125], network theory through impedance representation [155], scattering theory and passivity-based control [12]. [96] presented research addressing transparency, dictating two-way transmission of force and velocity. The methods mentioned in this section are only a few of the existing methods as research in this field continues.

Whilst the various control methods address stability concerns in robot tele-operation, it is likewise important to examine the concept of telepresence as an important goal in robot tele-operation. Telepresence addresses the human operator's role in robot tele-operation as a whole.

1.1.2 Telepresence/Situational awareness in different applications

Telepresence in robot tele-operation refers to a human operator's feeling of being present at a remote location (follower robot's location) other than their true location. Situational awareness refers to the perception of events and elements in an environment with respect to time or space, their meanings and what their future status might be [42]. Researchers in the field of human-robot-interaction continue to explore several methods for combining remote robot sensing and data presentation to operators to improve telepresence and situational awareness [200]. This makes it possible to employ the use of robot tele-operation in several applications such as industrial robots [56], live-line maintenance [110], contact driven tasks [54], robot telesurgery [2][58], glovebox tele-operation for nuclear industry [190], excavator control [98], care assistance [120], education [94], and construction [153].

Most tele-operation setup provide visual information of the remote location to the human operator. However, depending on the application, limitations of the cameras often used to capture visual data, and limitations of human perception of distance via visual displays, supplementary information about the remote location and status of the follower robot may be conveyed to the operator. The supplementary information is gathered via sensors designed to capture relevant information needed. Some of the common sensors often employed in robot tele-operation include: stereo cameras, depth cameras, proximity sensors, LiDAR, Gyroscope, force sensors, slip sensors, motion sensors etc.

In a haptic-enabled tele-operation setup for a base-excited hydraulic manipulator intended for live power line maintenance, [17] examined how an operator's hand speed regulating scheme may enhance the lineman's performance as the system works under a wireless communication channel and the follower base is under excitation. This was carried out for two conditions: when the haptic device produces no force and when the regulating haptic force is added to the leader device. The force conveyed via the haptic device is built on the position error of the follower manipulator end-effector to regulate the operator's hand speed to achieve minimal follower position error. Evaluation of performance was carried out by measuring operator's success/failure in completing a task, the displacement of the end effector, follower manipulator controller effort, and the task completion time. Results show that the linemen function more effectively when haptic force is added to the system as the system is subject to base-excitement and communicates through a wireless network. Using the peg-in-hole task as the benchmark task, [99] evaluated the usefulness and inaccuracy of haptic guidance on the maintenance of nuclear power plant using tele-operation. The evaluation was done in virtual reality and participants were asked to position pegs in holes by manipulating the Geomagic Touch X haptic device. Performance evaluation was carried out by measuring task completion time and guidance force. They concluded that there is a reduction in task completion time, contact force and total force when there are no inaccuracies in haptic guidance.

Another application domain of robot tele-operation is in the area of Unmanned Ground Vehicles (UGV). An Unmanned Ground Vehicle is a vehicle designed to operate without a human presence on board while in contact with the ground [95]. Unmanned Ground Vehicles may be remotely controlled by a human operator to move from one location to the other, carrying out specific tasks. In evaluating the effect of haptic feedback on the tele-operation performance of an Unmanned Ground Vehicle (UGV), [81] conclude that the effect of haptic feedback is superior with regard to task performance and stability but not with regard to the control effort of the operator. The benchmark task used for evaluation is the UGV navigation task. A commercially available haptic device was used to control the UGV in a virtual environment displayed to the operator on a computer monitor. A Microsoft kinect2 camera was installed on the UGV and the operator controls the UGV using the depth and RGB information of the camera and a laser sensor during the experiment. The haptic feedback produced two repulsive forces: bounded force and obstacle avoidance force.

Minimising pain and increasing the speed of recovery are some of the major objectives of microsurgery. As a result, tele-operated robots continue to find application in robot-assisted surgery. In developing a framework for multilateral manipulation of surgical tasks, [134] tested these three collaboration models: fully autonomous exploration of tissue, shared control between human and robotic agents, supervised control where the operator dictates commands to the robot, traded control between human and robotic agents, and bilateral tele-operation. The leader and follower devices were two Phantom Premium 1.5A haptic devices. The human operator grasped the end effector of the leader robot while the follower device (with force-torque sensor) was positioned to palpate an artificial tissue. Results show tradeoffs in sensitivity, safety applications, maximum force applied and duration of experiment among the five models. [64] developed a new complete telesurgical robotic system called Al-Zahrawi, which comprises of a leader console and a follower console. Both the leader and follower consoles are connected through a communication link. The leader console was designed to have manipulators, visual information presentation apparatus, and foot pedals (to allow the surgeon to switch between endoscope control and forceps control modes). On the other hand, the follower console comprises of three manipulators labelled right, middle and left. Surgical instruments are attached to the left and right manipulators whereas the middle manipulator holds the endoscope. Al-Zahrawi is reported to have a smaller footprint than the Da Vinci surgical system, and also allows the flexibility of tool change during operation. [182] developed a prototype internet-based telesurgery system which was integrated on the existing "MicroHand S" and tested the system over a 150 km distance. Stereo image viewer on the leader robot side makes it possible to provide visual feedback to the operator who controls the follower robot manipulators. The system was used to carry out successful remote removal of gall bladder surgery on the sow of China. Results showed that the system possesses enough remote control performance and operability for telesurgery. Other research on the application of tele-operation for telesurgery also include work by [198], [186], [117], and [87].

Rehabilitation robotics is another growing research field for the purpose of helping people with disabilities to cope with their activities of daily living. Even in this field, the leader-follower slave structure continues to find popularity. [35] developed a novel mechatronics leader-follower setup for hand telerehabilitation. The setup consists of a sensorised glove designed to act as a remote leader and a powered hand exoskeleton. The leader interface is controlled by the therapist conducting the rehabilitation exercises while the patient can benefit from a robot-aided physical rehabilitation treatment without having to be physically present in the hospital. Likewise, [15] proposed the design of a bilateral telerobotic architecture for rehabilitation purposes. The proposed architecture was designed with a nonpassive, nonlinear, and autonomous dynamic behaviour that is needed for various types of complex therapies.

The introduction of robot tele-operation into assistive care environments has seen a steady rise. Unlike in some other applications, the tele-operated robot operates in close proximity to humans. [108] developed a telerobotic system which gives caregivers the capability of assisting older adults with dementia remotely using a dual-arm collaborative robot (YuMi). The system was based on inertia motion capture technology which translates the arm movement of the care giver to the arms of the robot. The design was verified by tele-operating the robot to pick up a medicine bottle and to remotely assist in picking up a cup. [108] concluded that the proposed system has potential use for improving the quality of life of older adults with dementia and care effects of caregivers. According to [90], patients trust the human operator more when they are able to see the operator. [90] investigated the use of tele-operated robots to allow health care workers to carry out their duties remotely from infected patients, especially when dealing with highly infectious diseases. A PR2 humanoid robot with two 7 degree-of-freedom arms was used. The Pr2 is equipped with two laser range-finding sensors, an Asus Xtion RGB-D camera, and stereo cameras to provide situational awareness to the robot-operator. Graphical user interface was provided for the operator to give access to a variety of information including live video feed from the remote location, and a model of the robot as it appears in the world. The tasks carried out in the study includes: the delivery of wrapped gauze to the medical tray, picking up a no-touch thermometer and holding it over participants' torso, moving IV pole closer to participants' cot, removing clothes hanging on a wall and placing in a bucket, and moving the bucket from the end of the cot to a different location.

Table 1.1: Applications of robot tele-operation

Publication Title	Sensors	Feedback Modalities
Haptic-enabled tele-operation of base-excited hydraulic manipulators applied to live-line maintenance [17]	Linear displacement sensors, Video camera	Haptic feedback
Preliminary user evaluation of inaccuracy in haptic guidance for teleoperated maintenance task of nuclear power plant [99]	Force sensor, Video camera	Visual feedback, Haptic feedback
Evaluation of Haptic Feedback in the Performance of a Teleoperated Unmanned Ground Vehicle in an Obstacle Avoidance Scenario [81]	Kinect camera, Laser sensor	Visual feedback, haptic feedback
A Framework for Multilateral Manipulation in Surgical Tasks [134]	Force-torque sensor, Position measurement sensor, Video cameras	Visual feedback
Al-Zahrawi: A Telesurgical Robotic System for Minimal Invasive Surgery [64]	Video camera, Instrument attach/detach sensing mechanism	Haptic feedback, Visual feedback
Development and experiment of the Internet-based telesurgery with MicroHand robot [182]	Video camera	Haptic feedback, Visual feedback
A Mechatronic System for Robot-Mediated Hand Telerehabilitation [35]	Pressure sensor, Accelerometer	Haptic feedback, Visual feedback
A Small-Gain Approach for Nonpassive Bilateral Telerobotic Rehabilitation: Stability Analysis and Controller Synthesis [15]	Video camera, Force sensor	Haptic feedback
Tele-operation of Collaborative Robot for Remote Dementia Care in Home Environments [108]	Video camera, IMU	Visual feedback
Seeing is comforting: Effects of teleoperator visibility in robot-mediated health care [90]	Laser range-finding sensor, Stereo camera, RGB-D camera	Visual feedback

Table 1.1 summarises some applications of robot tele-operation discussed and the sensors employed. It also shows the feedback modalities used to convey information to operators.

The application scenario of interest explored in this thesis involves using tele-operated robots for care provision for older adults with assistive care needs and people living with disabilities who are in need of assistance with their activities of daily living. With people living longer, and the decline in the number of health care professionals, this thesis addresses some of challenges faced when developing tools that may be used to improve the quality of care provided and also to reduce cognitive load on those providing care. When compared to other application scenarios, robot tele-operation is relatively unexplored in this context, hence the motivation for the research reported in this thesis.

1.2 Problem Scope

Safe human-robot interaction (HRI) is very important if robot tele-operation is to be employed for remote provision of care assistance. Unlike other applications of tele-operation, say in the use of industrial robots [175] [49] in manufacturing and hazardous environments, autonomous vehicles [133][141], mobile robots [164], the tele-operation of a robot manipulator to provide care assistance requires strict adherence to ensuring the safety of care receivers.

It is however not enough to pay attention to the safety of the human-robot interaction only, but also to the efficiency and effectiveness of the system. Attention should be paid to these parameters to ensure that all necessary components are available for the system to be useful as a tool in providing the necessary levels of assistance. The system should make the provision of care assistance easier for health care professionals. Robot tele-operation covers several concepts but in this thesis, the focus of research is identifying relevant sensor data and enhancing feedback modalities.

1.2.1 Human Sensory Perception

Human sensory perception involves the different ways information is gathered through our senses, namely: sight, smell, hearing, taste and touch [26]. The sensory modality for sight is light, and the sensory modality for hearing (or audition) is sound. Receptor cells located in taste buds on the tongue and pharynx encounter taste stimuli even though a combination of multiple sensory inputs create the taste perception [25]. The sense of touch is mediated by mechanoreceptors in the skin and is influenced by somatosensory modalities which include temperature, nociception (pain and itch), proprioception (body position and motion), visceral function, and discriminative touch. The sense of touch may then be used to detect properties such as motion (active or passive, velocity and direction), temperature, cognitive function (object recognition), surface texture, surface compliance and spatial dimensions [79].

It is vital to provide the operator with as much information (sensory feedback) as possible on the remote robot's conditions and the environment in which the robot is operating in. This can be done by identifying the relevant information needed for effective tele-operation and identifying the optimal sensory feedback modalities needed to present the sensor data to operators.

1.2.2 Feedback Modalities

After gathering information about the robot's conditions or its environment, effort should be made to correctly feed the information back to the operator for correct manipulation and control of the robot. In assistive care scenarios for example, where the operator may need to socially engage with the service user, sensor information may be passed across using other feedback modalities different from audio and visual feedback modalities. Some of the other feedback modalities often used include: force feedback, tactile (vibrotactile, etc.) [144], kinesthetic haptic feedback, contact feedback [188], auditory biofeedback [147].

The efficient transmission and interpretation of sensor data in tele-operation of robots for care assistance is thus very important. In this research, we aim to be able to identify ways to convey relevant sensor data to human operators with minimal cognitive load.

Little consideration has been given to verbal feedback in robot tele-operation because there has been little or no need for such in most of the other use cases of robot tele-operation. Another important component of providing care for the older adults with assistive care needs and people with disabilities is the understanding of the role social engagement plays in their well being. It is reported that often, older adults with assistive care needs feel lonely [135] and efforts have been made to meet such needs in addition to keeping them positive and engaging. By introducing social interaction into the tele-operation process could improve the tele-operation experience for both the operators (healthcare professionals and informal caregivers like family members) and service-users (older adults with assistive care needs and people with disabilities).

There remain a number of challenging and open research areas in the field of tele-robotics, particularly in the context of robotic tele-assistance. This PhD sets out to address a few of these challenges.

1.3 Aims and Research Questions

The aim of this research is to identify the optimal feedback modalities or combination of modalities for providing feedback to a telerobotics operator providing assistive care and ensure minimal cognitive load for the operator. As previously noted, this would be particularly important during collaborative assisted living task. It will involve mapping accurate real-time sensor data (of parameters like gripper orientation relative to the object orientation, gripper proximity to surrounding surfaces of interest, etc.) to different feedback modalities (Haptic feedback, Peripheral vision feedback) provided to the operator.

The objectives of the research are to identify necessary sensor information required for robot tele-operation, understand sensory substitution, how the sensor information can be conveyed through different feedback channels, and to investigate the effect of task repetition on operator performance.

The following research questions have been identified to address the aim and objectives.

1. What sensor data are required for effective tele-operation?
2. What are the hardware and software requirements for setting up efficient tele-operation systems for pick and place tasks in an assistive care scenario?
3. What feedback modality or combination of modalities (Peripheral vision, video feedback, haptic feedback, verbal feedback) are best suited for conveying sensor information to the operators? How does perceived workload change with different types of feedback?
4. What are the most appropriate feedback mechanisms?
   - To what extent can verbal feedback from the person being assisted at the remote location augment sensor data?
   - What knowledge of haptic sensitivities can be used to improve haptic perception?
   - Which sensory substitution strategies are best suited to convey sensor data ?
   - Can more than one type of sensor data be conveyed through a single feedback modality as operators carry out tasks?
5. What is the effect of task repetition on tele-operation performance?

1.4 Summary of Contributions

In investigating the above research questions, this thesis makes the following contributions.

1. The development of a wireless wrist-worn haptic feedback device for conveying multiple sensor data simultaneously to operators. This device was used for carrying the studies in chapter 5 and chapter 6 of the thesis.
2. Confirmation of the differences in haptic sensitivity of different locations across the wrist and its application for haptic feedback (Chapter 5). Factors that influence the changes are also highlighted.
3. Identification and justification of haptic display strategies for wrist-worn haptic feedback devices (Chapter 5).
4. Implementation and demonstration of the use of a wrist-worn haptic feedback device to convey 2 types of sensor data concurrently to an operator.

Within the context of the experimental tele-operation task, this thesis also makes the following contributions:

5. Identification of optimal feedback modalities to improve operator performance. Performance was measured in terms of task completion time, task completion, accuracy of gripper orientation, (Chapter 4).

6. Demonstration of the use of gaze metrics to understand how operators interact with a system (Chapter 4).

7. Demonstration of how verbal feedback can be used to improve operator performance. (Chapter 4).

8. Justification for the importance of understanding the role camera angles and field of view play tele-operation setup (Chapter 4).

9. Demonstration of the impact of task repetition on its own, and together with different feedback modalities, on operator performance (Chapter 6).

1.5 Publication

Journals

1. Bolarinwa, J.O., Eimontaite, I., Mitchell, T., Dogramadzi, S. and Caleb-Solly, P., Assessing the role of gaze tracking in optimizing humans-in-the-loop telerobotic operation using multimodal feedback. Frontiers in Robotics and AI, p.265.

2. Bolarinwa, J.O., Eimontaite, I., Mitchell, T., Dogramadzi, S. and Caleb-Solly, P., Wrist-worn Haptic Feedback: LocationSensitivities and Haptic Display Strategies forReal-Time Assistive Robot Tele-operation (In preparation).

Conference

1. J. Bolarinwa, I. Eimontaite, S. Dogramadzi, T. Mitchell and P. Caleb-Solly, "The use of different feedback modalities and verbal collaboration in tele-robotic assistance," 2019 IEEE International Symposium on Robotic and Sensors Environments (ROSE), 2019, pp. 1-8, doi: 10.1109/ROSE.2019.8790412.

2. Bolarinwa, J.O., I., Mitchell, T., Dogramadzi, S. and Caleb-Solly, P., Haptic Overload: Conveying Multiple Sensor Information using a Single Wrist-Worn Haptic Feedback Device for Assistive Tele-operation (In preparation).

1.6 Thesis Outline

The structure of the thesis is presented below, showing the different works that were carried out in the thesis.

- Chapter 2 describes the theoretical background to the research objectives. Reviews of concepts and studies that have be carried out is presented in this chapter.
- Chapter 3 describes the study methodology and the different iterations in the software and hardware design stages. The reasons for the choice of the designs are discussed. Illustration is also given for overall research progress and interactions between the software and hardware components.
- Chapter 4 discusses the first two studies carried out in the thesis. The first study is described as object characterization and sensor data identification. The second study involves a pilot study and the first study with human participants for the identification of optimal feedback modalities. Gaze metrics were also analysed to understand operators' interactions with the system.
- Haptic sensitivity across the different location on the wrist was investigated in chapter 5. Changes in the sensitivity based on haptic intensity, duration of haptic stimulation and distraction was also investigated. Haptic feedback display strategies were investigated in this chapter.
- Chapter 6 presents the demonstration of results of studies carried out in chapter 5 for real-life tele-operation task. Simultaneous display of 2 sensor data via a single wrist-worn haptic device was investigated in this chapter.
- Chapter 7 presents a summary of the entire thesis and possible future research that can be carried out to extend this thesis

Chapter 2

Literature Review

The literature review discusses existing work on the different components of robot tele-operation in relation to the use of robotic technologies in healthcare. It examines robot tele-operation approaches currently employed to support older adults with assistive care needs and people with disabilities with their activities of daily living. Section 2.1 provides an overview of service/assistive robots currently employed in healthcare institutions. Section 2.2 covers existing applications of tele-operation. In section 2.3, different stages of robot tele-operation are examined. Section 2.4 summarizes the examined literature.

2.1 Service/Assistive robots

Service robots are continually gaining acceptance and popularity in the health care sector as solutions to provide support for people in need of help in carrying out their activities of daily living [19]. The application of assistive robots in conjunction with smart home sensors can be useful to prompt and support people, enabling independent living in their homes [28]. Smart home technologies have played a huge role in providing older adults with assistive care needs living with dementia with services such as navigation support [127], schedule management [146], and responses to emergencies [61]. Due to the static nature of smart home technologies, limitations to the use of smart home technologies exist and hence limits their capacities to deliver assistance in some important scenarios and applications. In general, assistive robots are designed to improve the quality of life of older adults with assistive care needs or people with disabilities, and can have measurable psychological, social, and/or physiological effects on people [97].

In re-framing assistive robots to promote successful ageing, Lee et al. explored an alternative design approach to the study of ageing in human-robot interaction (HRI). With five ageing researchers and nine older adults taking part in the study, participants expressed their interpretation of ageing and suggested potential assistive robots. They found disability due to ageing as just one aspect of ageing but also recommended autonomy and resilience as themes that should be considered when designing assistive robots [100].

Telepresence robots like the Double [38] and Ohmni robot [138] continue to find applications as tools for providing care for older adults with assistive care needs and people with disabilities. With self drive and path planning capabilities, they are often used to ease communication between older adults with assistive care needs and caregivers (formal or informal). Telepresence robots have been documented to reduce loneliness often felt by older adults with assistive care needs [135].

Designed as a companion robot, the seal robot 'Paro' was developed to physically interact with people and is able to respond to touch, sound and temperature [199][72]. Paro was designed with a behaviour-generation system with two hierarchical layers of processing: proactive and reactive, generating three types of behaviour: proactive, reactive and physiological. Studies carried out showed that Paro improved the moods of older adults with assistive care needs, evident from good face scale scores gathered and high vigor scores. During the study, burnout scales were distributed to nursing staff (working with older adults with assistive care needs) that participated in the study. Results show that staff burnout gradually decreased as the study progressed, hence signally the positive effect assistive robots can have on staff. The decrease in burnout was attributed to a reduction in the dependency of older adults with dementia on their caregivers [199]. Pearl is another care robot designed with a differential drive system and two on-board Pcs [145]. It is equipped with wireless internet, laser range finders, sonar sensors, microphone for speech recognition, speakers for speech synthesis, touch-sensitive graphical displays, actuated head units and stereo camera systems. Using auto reminder technology, it reminds older adults with assistive care needs about events and schedules. Its intelligent mobility platform also provides support for indoor navigation.

Social robots have also been developed for engagements in rehabilitative therapies. Results gathered by Katie et al. provided evidence that socially assistive robots (SARS), like the pepper robot, can play a role in improving patients' engagement with self-directed exercise programs [204]. Obasayi et al., using the International Classification of Functioning, Disabilities and Health (ICF), measured the impact of robotics-aided care on the quality of life of older adults with assistive care needs. They found that the introduction of socially assistive robots into the care of older adults increased the frequency with which they socialised and made them more active and talkative [137]. Other studies also show that social robots appear to have positive impacts on the agitation, anxiety and quality of life of older adults after interaction [149][158]. Assistive humanoid robot 'Nao' was used in a study to detect fall [140]. It monitored service users as activities of daily living were carried out using OpenNI segments, tracking positions and posture. Upon detecting fall, Nao approached the service user and asked if support was needed. Pictures of the scene were sent to caregivers and family members who provided interventions. In different studies, Nao robot was used to provide emotional support for children with diseases such as diabetes mellitus type 1 and cancer [106][192][9]. Results showed that the interaction with Nao had positive effects on children's mood and openness.

As effective as the robots that have been discussed are, a noticeable limitation is that they do not have the capabilities to provide physical assistance. Chance et el. investigated strategies for planning and error handling in an assistive robot used to support independent dressing using the Baxter robot [73]. Participants were able to correct dressing errors using a fixed vocabulary of recognised speech commands [29]. With the use of low-cost sensors and simple HRI strategies, they demonstrated a successful robot assisted dressing task. Predictive tracking of the arm was further developed for robot assisted dressing [30]. For safe human-robot interaction, Ansari et al. exploited the compliance and dexterity of manipulators based on soft robotic technologies to develop a manipulator such as a shower arm to assist older adults with assistive care needs with assistive care needs in bathing [13]. However, the need to keep humans within the care process makes it difficult to adopt some of the technologies that help with physical assistance because of the missing element of social interaction. One of the technologies that combines the possibility of social interaction and physical assistance is robot tele-operation. This is in addition to the possibility of providing assistance to many service users without the need for care providers to travel between locations.

2.2 Robot Tele-operation

Essential to the care of older adults with assistive care needs with assistive care needs and people with disabilities is the need for human engagements in the care process. It is therefore recommended that the introduction of robots for healthcare service deliveries retains "human engagements", hence encouraging the adoption of tele-operation of robots within the healthcare system. Another consideration for tele-operation of robots are ethical concerns relating to the use of autonomous robots [55], one of which is safety. Tele-operated robots are in development in different forms and for varying applications; from a simple tele-operated arm using pneumatic artificial rubber muscles [82] to a fully-actuated and anthropomorphic hand [116]. In order to reduce the risk of healthcare workers to infections, Li et al, (2017) developed a Tele-robotic Intelligent Nursing Assistant (TRINA) mobile manipulator using an off-the-shelf dual-armed humanoid torso (Baxter robot by Rethink Robotics [73]). It was developed to serve as a human surrogate tele-operated to carry out light-to-medium-duty manipulation tasks like cleaning, food and medication delivery, and cart pushing [102]. Twenty six (26) common nursing tasks were carried out to examine the capabilities of TRINA, with result yielding success rates of 78% but longer task duration time (95x human completion time). Using a wearable sensory jacket, Ishac et al. developed a gesture based robotic arm control for mealtime care. The jacket, embedded with IMU and flex sensors to track the wearer's arm movements, controls the robot which mimics the motion of the human arm. To validate the effectiveness of the system, a water bottle transfer task was carried out. Results showed that the wearable jacket system demonstrated a lower average error distance than the conventional joystick. Task completion time was lower when the jacket was used than the time completion time when conventional joystick was used [75].

Research into the tele-operation of robots in assistive care scenarios continues to increase but whilst a lot of attention has been paid towards the development of relevant robotic technologies for application in healthcare, little attention has been paid to how operators interact with the system. Unlike other applications of tele-operation, the use of tele-operated robots to assist older adults with assistive care needs and people with disabilities requires that emphasis must be placed on the safety of care receivers, as well as the effectiveness and efficiency of the employed tele-operation system. To design an effective and efficient system capable of providing the level of safety required to achieve smooth tele-operation, it is important to provide operators with as much information as possible about the service user, the remote environment, and the tele-operated robot. Data gathering involves the use of relevant sensors chosen based on tasks to be carried out. The first study in this thesis involves identifying the necessary information about the remote location that can allow safe use of tele-operated robots in an assistive care context. Whilst it is important to gather relevant information, how the information is conveyed or communicated to the operators matters as well. This thesis also examines identifying optimal feedback modalities for conveying sensor data to human operators. In this research, we explore three important stages of tele-operation: Remote perception and data gathering, sensory substitution, and feedback modalities.

2.3 Stages of Tele-operation

To adequately employ robot tele-operation in the context of assistive care, we explored concepts relating to data gathering and feedback modalities.

2.3.1 Remote perception and data gathering

Human operator performance challenges are often classified into remote perception and manipulation [31]. Problems with remote perception often originate from sensory impoverishment due to lack of sufficient perception and situational awareness of the operators [132]. Human perception is often compromised in tele-operation as a result of the decoupling of natural perceptual processing from the physical environment. Since the operator is not physically present in the robot's remote environment, a good knowledge of the robot's physical and environmental conditions will inform decisions made during the tele-operation of the robot. Those conditions are gathered using relevant sensors which may be chosen based on the nature of the task to be carried out, capabilities of the tele-operated robot and the environment in which the robot operates.

Most tele-operated robots (e.g. [113], [122]) employ the use of monocular cameras (single camera sensor) [84] to capture visuals of the remote environment, providing operators with situational awareness of the remote environment and robot. A common problem with monovision cameras however is the constraint on the perception of depth caused by lack of parallax in monovision cameras [27]. As a result, depending on the application, other sensors are often employed to provide operators with information about the remote environment that cameras may not be able to provide.

Nutan et al achieved tele-operation using infra-red proximity sensors [32]. With an algorithm, the robot performed online adjustments in order to reach a pre-grasp pose for final grasp using three (3) infrared (IR) sensors mounted on the gripper. Their choice of infrared sensors was influenced by challenges of occlusion and possible time lag of image acquisition and processing. Pre-touch sensing with ranges between tactile sensors and vision were previously employed for short range perception [174]. For different applications, two (2) strategies were employed using seashell effect pretouch [33]. The first strategy employed detects extremely compliant objects but with sensor mount on only one side of the PR2 gripper used, it was difficult to determine the position of the object between the gripper which may lead to unsuccessful grasp. The second strategy was to use object scanning but there were challenges with doing that in real time. The challenges highlighted influenced the design developed by Nutan et al., using infrared sensors positioned to achieve object localization.

One application of sound is in the identification of different materials (or of different thickness) because of the varying sound frequencies they produce when struck. [119] focused on identifying wood, metal, glass, and plastic in a remote location using a tele-operated robot based on the amplitudes (measured in decibels (dB)) and frequencies (measured in hertz (Hz)) of the sounds produced. The tele-operated robot struck the material in the remote environment, and the sound produced was captured using microphones and transmitted to the operator. To correctly identify the different materials, analysis was carried out using the sound spectrum graph, frequency graph and force graph. They concluded that the thickness of the materials did not limit their ability to correctly identify the material. The setup can further be developed to make remote material identification possible in real time.

The peculiar context of robot tele-operation for care provision that this thesis addresses requires extra emphasis on identifying the information required to safety carry out tele-operated tasks. In general, tele-operation often involves gathering information like joint or gripper force, pressure, distance, speed, etc from the remote environment. In this research, we investigate required sensor data for efficient and effective tele-operation.

2.3.2 Sensory substitution and feedback modalities

Correctly providing operators with information about the remote robot end as they carry out tasks is as important as gathering the information. Feedback modalities are classified according to the sensory modality they address, say auditory, tactile, visual, or olfactory. For different applications of tele-operation, feedback modalities may be used individually or as a combination of two or more feedback modalities (multimodal feedback). Between gathering information about the remote environment using sensors and providing the information to operators is a very important data processing and sensory substitution stage. The stage helps to present the sensor information in ways operators can understand through different feedback modalities.

2.3.2.1 Visual Feedback

Most tele-operation setup require real-time visual feedback of the remote environment to the operators. Visual information of the remote environment is often gathered using 2-D and 3-D camera(s) which may be positioned static in the remote environment (thereby providing exocentric view) or on mobile platforms (e.g. robot [143] [185]) to provide dynamic egocentric view of the remote environment. Egocentric views are also known as first person view while exocentric views are third person views[123]. The visual information gathered is often displayed to operators through display glasses or on traditional screens (e.g., mobile devices [162], tablets, or computer screens). For better coverage of the remote environment, some studies employ the use of multiple cameras at the remote environment and display the video streams of the remote environment on multiple traditional screens to operators. This however, causes the divided attention paradigm as operators make constant context switches between monitoring the video streams and controlling the robot [67]. To reduce the distractions of switching between video screens and robot controller, [67] designed new interaction techniques by integrating virtual reality (VR).

In order to compensate for the delay induced by networks, [128] also introduced virtual reality into their system. Using virtual reality, remote environments and several senses (such as vision, hearing and touch) can be computer simulated [18]. Operators may then be immersed into such virtual environments and are able to interact with three-dimensional environments [131] with extended field of view (FOV). In most VR applications, visuals are displayed using the head-mounted display (HMD) [172] [80]. While virtual reality (VR) creates artificial environments, augmented reality (AR) simulates real environments with artificial objects [7]. However, both virtual reality (VR) and augmented reality (AR) can provide crystal clear views of the remote environment and teleoperated robot [209]. In order to provide multisensory exploration of the remote environment, [37] combined the domains of virtual and augmented realities by providing stereoscopic display and 3D interaction during an underwater robot tele-operation. [105] addressed the challenge of cognitive overload on robot operators by proposing the use of multi-sensor informed mixed reality visual aids to present sensor data to users. It should be noted that the mention of virtual reality and augmented reality in this section is in reference to visual displays and does not critically examine other functionalities that virtual reality and augmented reality provide. The use of AR and VR however comes with some challenges which may vary based on different applications. Some technical challenges include limited resolution, screen door effect, vergence-accommodation conflict (VAC) [209], complexity of integrating them with existing systems and long training time required [53]. Other associated challenges are usability and cognitive overload based on the task [34]. Hardware and software limitations [181], cost, concentration performance issues and visual fatigue [130] are also often encountered in the use of augmented reality (AR) [114].

To avoid some of the challenges posed by AR and VR in our studies, we elected to use static exocentric 2-D cameras to capture visual information of the remote environment and robot. Unlike the dynamic movements of cameras used in VR and AR settings, we employed several (at least 4) static cameras to capture different views of the remote environment. This also ensures that the operator can have different views of the remote environment without much movements. The multiple camera views/angles are displayed to operators on a computer display screen.

In order to compliment video feedback, some studies [167][23] employ peripheral feedback to convey information to operators through their peripheral field of view. This modality ensures that participants can focus on video feedback from the remote end and at the same time receive supplementary information about the remote end via their peripherals.

[52] explored the use of senses that are not used for controlling the tele-operation process in supporting the operator to enhance or if possible, substitute force feedback. Their work involved the application of sensory substitution in tele-operation, taking advantage of the plasticity of the human brain to establish alternative cognitive channels. Their goal was "to provide an interpretation of sensory information that can be easily and effectively perceived by the operator" [52], confirming the assumption that it is possible for the human peripheral vision to receive visual information independently from the central vision. Because of the need of conventional analogous and digital systems requiring direct focus on values being read and the difficulties that come with the operator reading values from complex systems, [52] then proposed new visualization methods with peripheral vision. They based their theoretical background on a mathematical model of the human photonic contrast sensitivity (the reciprocal of the minimum required contrast for a set detection probability). For tele-operation, they proposed that the feedback force is implemented separately from the position/force input using the principle of sensory substitution as opposed to the conventional bilateral control implementation having the position/force input and force/position display on the same device. Where getting accurate force-feedback is not realistic, substitutions may be made with cognitive info-communication. Experiments were carried out to check the possibilities of operators understanding the state of complex systems using only the peripheral vision.

Information on fuel level, oil pressure, temperature, altitude, engine rpm and speed displayed on analogue instruments were presented to participants to estimate the state of a virtual plane using the contrast sensitivity model. For the contrast sensitivity tests, three experiments were conducted with the participants. In experiment I, the participants could read an average of 2.9 instruments of the available 6 and only 2.5 were correctly perceived. In experiment II, on average 2.8 instruments were correctly perceived and 1.8 incorrectly perceived giving a higher perception ratio than experiment I. With the participants using peripheral vision in experiment III, on average 5.7 of the 6 instruments were perceived while dropping the ratio of ambiguity to zero. Even within a shorter time interval, peripheral vision still produced the best results but in real world application more sophisticated visualization techniques must be applied. Together with using peripheral vision to monitor complex systems, [52] also explored the possibility of passing gripping-force feedback to the operator using peripheral vision. This made it possible to compare the alternative feedback with the conventional force feedback. The operator was fed with both a normal vision feedback and an artificial vision-based force feedback located in the peripheral around the image or video of the scene showing the virtual slave gripper and the grasped object. A frequency modulated sinusoidal grate also showed the value of the difference between the instantaneous grasp force and the predefined reference grasp-force. When the difference was zero, a white surface was displayed. For positive error, upper half of the display starts to fade into a periodic signal while the same happens in the lower half of the display for negative error. Tests carried out showed that vision-based force-feedback gives less precise feeling of the remote side than the realistic force-feedback, but the subject could hold a predefined grasping force after a learning period.

2.3.2.2 Haptic Feedback

Often used together with visual feedback is the haptic feedback. Haptic feedback generally uses touch to communicate [194]. In robot tele-operation (involving a leader device and a follower), haptic feedback may be provided through the leader device (e.g a joystick or a robot) or through external (wearable and non-wearable) haptic devices. In general, haptic perception covers the cutaneous perception subsystem (referring to the sense of touch) and the kinesthetic perception subsystem (referring to body position and movement) [40]. Thermoreceptors (two types - responding to warmth and cold) and mechanoreceptors (four types: Meissner corpuscles, Merkel cell complexes, Ruffini endings, and Pacini corpuscles) embedded in the skin provide cutaneous perception information. Whilst thermoreceptors are sensitive to temperature, mechanoreceptors are sensitive to deformations caused by applied force. Kinesthetic information is provided by three main types of mechanoreceptors (muscle spindles, Golgi tendon organs and joint receptors) within the muscles and joints. It is therefore possible to convey sensor data gathered from the remote end and remote robot to operators through either of the haptic perception subsystems to improve dexterous manipulation [40]. Depending on the application or hardware and software required, it may be possible to convey the measured parameter directly to operators via similar modalities or in some cases substitute the sensory modality with a different feedback modality via sensory substitution. For example, it may be intuitive to present the forces felt by a robot's hands and fingers as forces on the operator's hands and fingers. Alternatively, feedback on the forces felt by the robot's hands and fingers may be provided through other feedback modalities like haptic or visual cues. This creates telepresence known as transparency [39]. Transparency is a telepresence concept where operators feel direct interaction with remote environments [152][68]. According to [39], cutaneous feedback is more stable and less transparent while force feedback is more transparent and less stable, hence the need for multimodal haptic feedback in order to identify the best trade-off between both haptic modalities.

[93] examined the effect of and need for haptic feedback in a tele-operated task. They designed an experiment to test performance on tele-operated box and blocks tasks (a portable manual dexterity and hand function test). The experiment was carried out with no feedback, direct force feedback (DFF), substituted force feedback (SFF) and a combination of direct force feedback and substituted force feedback (DFF and SFF). The tele-operated robot consists of four-digit; 13 degrees of freedom humanoid robotic hand equipped with 3D force sensors on its fingertips. The robot was controlled with a haptic glove, enabled with finger tracking capabilities, and designed to also provide passive force feedback on each of the fingers. Vibrotactile feedback was provided using 16 strategically placed pancake motors in a custom vibrotactile glove worn underneath the haptic control glove. Two types of haptic feedback were employed: direct force feedback (DFF) at the fingertips and vibrations at the fingertips (which is the substituted force feedback SFF). When providing direct force feedback (DFF) to the fingertips, each fingertip was blocked when the Euclidean norm of the force (vector) measured at the corresponding robot finger exceeded 0.1 N. The substituted force feedback (SFF) was provided in the form of vibratory feedback at each fingertip using the vibrotactile glove. The SFF was calibrated such that a force with a norm greater than 0.05 N is linearly scaled to a maximum vibration at 2 N. The tele-operated task was an adapted box and block task where participants were asked to move as many blocks as possible from the higher side of a box to a lower side within two minutes. Results showed that participants' preference was towards the different feedback types over no feedback. However, none of the forms of haptic feedback on the fingers (DFF, SFF and DFF + SFF) significantly improved performance (objective and subjective measures) on the number of blocks moved within the given time frame [93].

Haptic feedback (HF) has also been studied extensively for use in robotic surgery involving robot tele-operation. Prior to the introduction of haptic feedback in robotic surgery, surgeons had to estimate forces exerted on organs based on visual deformation of organs. The systematic review carried out by [10] on the application of haptic feedback in robotic surgery suggests that majority of research consider kinesthetic feedback while a smaller number cover cutaneous feedback. In a study designed to use a tele-operated image-guided robot (neuroArm [183]) in the neurosurgical treatment of glioma, [184] implemented a haptic notification system designed to warn surgeons when forces of tool-tissue interaction exceed certain limits. It was implemented as an alternative to the safety measure of limiting the robot in physical space (no-go zone virtual fixture) to avoid causing damage to healthy tissues. Two titanium Nano17 force sensors were installed in each arm of the neuroArm to measure force in real time. The haptic device used (for control and feedback) was an Omega 7 haptic device with 7 degrees of freedom (DOFs) positional sensing and 4 degrees of freedom (DOFs) force feedback. The haptic device allowed the natural range of motion of the human wrist pivoting around the wrist and can produce force as high as 12 N as well as a grasping force feedback up to 8 N. The haptic capability of the hand-controllers made it possible for the surgeon to remotely experience and monitor the tool-tissue interaction. Surgical tasks in a robot-assisted glioma surgical operation performed by the neuroArm were a combination of manipulation, coagulation, and pick and place motions of cotton strips. The robot-assisted surgery took about 33 minutes and the end-effector was shown to travel 9.8, 11.1, and 11.8 mm along the x, y, and z axes. Maximum force components measured were 1.37, 1.84, and 2.01 M along the x, y, and z axes respectively, from which the maximum total force was calculated. This case study setup makes it possible to quantify position and force ranges of the robotic arm for use as reference training in robot-assisted glioma surgery [184].

[142] reported the clinical series of unicompartmental knee arthroplasties (UKAs) using a semiactive robotic system. For precise planning and execution of an inlay unicondylar knee arthroplasty, haptic guidance in combination with a navigation module were employed. During surgical operation, the robot was moved by the surgeon who guides the force-controlled tip within the defined boundaries. The setup was such that the surgeon could sense when cutting is done and feedback was also introduced to prevent inaccurate motion to the designated areas. As predefined boundaries of the implant position was approached, the robot provided audio feedback and haptic feedback via active stiffness of the robotic arm. The setup was successfully trialled on 10 patients and the technique may be able to improve positioning based on patients' individual anatomy and also with regard to planned leg alignment (Pearle, O'Loughlin and Kendoff, 2010). In a study on tele-operated robot-assisted endovascular catheterization, [176] demonstrated that haptic feedback decreases the contact force between the catheter and blood vessel phantom.

Studies have also suggested that haptic feedback and haptic guidance can be combined when carrying out tele-operated tasks. However [173] and [196] suggest that the effect of haptic guidance and haptic feedback can overlap when combined on the same haptic interface, hence making it difficult for the operator to distinguish between the two. In order to augment haptic information, [167] explored a combination of haptic feedback (force) and haptic guidance (according to a surgical plan) for tele-operated robotic surgery using a Phantom OMNI [1] and real-time control software QUARC [151]. They carried out two studies: a simulated pedicle screw placement and milling tasks similar to those performed during knee replacement surgeries. The first study involved the evaluation of the superposition of haptic feedback and haptic assistance during depth control of a simulated drilling task. The task was carried out for different combinations of visual, tactile, tactile (vibration) + peripheral, kinesthetic wall (stiffness) + peripheral and haptic feedback. Visual feedback was used for a representation of the current drilling depth indicated by a grey sphere. The tactile feedback represented the current depth by an increasing vibration rate until the target depth is reached after which the vibration becomes constant. The peripheral feedback is represented by a coloured semi-transparent frame at the edges of the screen at the target depth. The kinesthetic wall represents stiffness on the haptic device. Combining haptic feedback and kinesthetic wall represents a mode where haptic feedback and haptic assistance are superimposed in the same degree of freedom. Performance was measured based on the final distance to the target depth (effectiveness) and user satisfaction. Results on effectiveness indicate a significant improvement in target depth deviation by the augmentation of haptic feedback and there were no discrepancies between assistance and force feedback information. Drilling accuracy was significantly improved by modes that incorporate kinesthetic wall and a combination of haptic feedback and peripheral feedback. The combination of haptic, visual, and peripheral feedback constituted a good compromise between increasing the effectiveness and the detection of discrepancies between haptic guidance/assistance and force feedback. The second study was divided into two phases (P1 and P2). P1 targets milling tasks for which assistance can be provided. P2 targeted interventions (e.g., craniectomies) where assistances could not be offered in all degrees of freedom (DOF). Haptic and visual assistance constituted of speed restriction, haptic boundary constraint, haptic trajectory guidance (stiffness) based on deviation from optimal milling path, velocity (haptic) guidance to maintain constant velocity, and scaling (depth direction). For the assisted milling tasks in P1, there was statistically significant improvements with respect to effectiveness if motion is constrained by boundaries haptically. In P2 when assistance could not be provided in all degrees of freedom, improvements were not noticed with respect to the scenario where no feedback was applied [167].

[129] worked on the use of vibrotactile feedback for the restoration of texture recognition especially for upper limb amputees. The use of haptic feedback (placed on any sensitive part of the skin) by amputees can restore the sense of touch and can invariably complete the communication loop between an external stimulus and the amputee's brain. This was made possible by converting the external stimulus (like object's texture and motion) that could not be perceived by the user into a different type of stimulus the user could recognise (substitution). The choice of vibrotactile feedback can be linked to the advantages of vibrations in such applications. Vibration (applied to an intact sensory area of the skin) does not interfere with the peripheral nerves [154] and can be recognised easily and quickly [171][206]. It is also possible to create a sense of motion on the skin using multiple vibrator motors [187]. The multimodal functionality of vibrotactile feedback makes it applicable under static (e.g. awareness of how an object is grasped) and dynamic conditions (e.g. ability to recognise texture). [129] proposed a haptic feedback designed to allow the user to recognise different textures during active touch sensing and checked the effect of further training (of users) on the effectiveness of such sensory substitution. 10 multi-modal capacitive tactile sensors were mounted on a three-finger adaptive robot gripper from Robotiq, [160]. The gripper was mounted on a UR5 universal robot [161]. The sensors were designed to capture pressure and speed of movement based on data generated under static and dynamic conditions. As the sensor's surface moved over different textures, unique vibrations were generated based on the differing depths and patterns of each texture. A vibrating motor attached to the user's skin applied a

corresponding type of vibration as detected by the sensor. Using linear and circular textures, [129] examined the impact of linear and rotary motion as dynamic feedback was transmitted from the haptuator to the skin. The frequency of the vibrations produced by the haptuator corresponded to the texture's unique amplitude as measured by the tactile sensor. Subjects familiarized themselves with the texture and were told to identify different textures blindfolded as well as being given noise-cancelling headphones. Subjects who had previous knowledge of haptic systems identified the different textures with better accuracy then those new to haptics. In confirming the efficiency of the haptuator, it was discovered that the system could successfully reproduce vibrations corresponding to the textures when there were distinct dissimilarities between the textures but the efficiency began to drop as the textures began to get similar. As much as the research was successful in sensory substitution, more work still must be carried out on being able to differentiate textures with very minute differences with real world applications. With their research focusing on dynamic conditions, research also will be done in integrating sensing in both static and dynamic conditions. The third issue that should be worked also is the inherent delays during sensing and processing.

2.3.2.3 Auditory Feedback (AF)

Relative to video feedback and haptic feedback, auditory feedback is either unexplored or less preferred [89] in robot tele-operation. This may be because of the difficulties in correctly mapping sensor data to auditory cues or the difficulties in interpreting auditory cues. However, with developments in technology and sensory substitution techniques, audio feedback continues to find increasing applications. In general, audio feedback may be generated from other sensory modalities (by sensory substitution) [208] or by reproducing scenes of the remote environment [14][104].

In order to compensate for insufficient leader-follower force feedback in a tele-operated construction task, [208] introduced auditory feedback into their setup. Using sonification, they mapped force gain (obtained by using hydraulic pressure sensors) to sound produced with differing tempo. They are able to conclude that auditory feedback has the potential to improve force perception and in return operator's performance [208]. It is however possible that auditory feedback may not have significant effect on improving performance (e.g. task completion time) when compared to scenarios that do not employ feedback at all but may significantly reduce perceived difficulty of tasks as [115] discovered.

Auditory feedback has also found application in the tele-operation of tubular continuum robots. Lack of haptic feedback and camera occlusion however decreases accuracy and path-following efficiency, hence increasing cognitive load. As a solution, [22] developed a novel auditory display to convey navigational cues to operators. They evaluated the effects of auditory display on parameters such as task completion time, accuracy, usability, subjective workload, and efficiency in a test environment designed to simulate transnasal intervention with simulated continuum robot. Relative to visual-only display, participants demonstrated significant increase in accuracy, efficiency and task completion time using auditory display with visual display [22]. Similarly, auditory display was found to improved accuracy for resection guidance in navigated liver surgery according to [62]. Auditory feedback also significantly reduced time spent looking at the screen in a test carried out by [62] by about 86%.

2.3.2.4 Multimodal Feedback

Visual feedback, haptic feedback and auditory feedback modalities are the most used feedback modalities in robot tele-operation and each of these modalities also have different varieties. For example, auditory feedback may be realised as auditory icons, earcons, verbal messages [178] or the reproduction of sound captured from the remote location. Studies have been carried out to compare the effects of the different modalities or their varieties of which some might be more effective than others depending on applications [16]. In some other studies, two or more feedback modalities have been combined to covey the same information to operators. This concept is known as multimodal feedback. The simplest form of multimodal feedback is observed when any (or some) of the different varieties of other feedback modalities are combined with visual feedback of the remote environments (video(s) of the remote end displayed on computer screen(s)). However, because of the importance of visual feedback, most studies consider visual feedback as a compulsory component of tele-operation. Hence, the mention of multimodal feedback often focuses on the combinations of other feedback modalities, their varieties, and in some cases other varieties of visual feedback. Some studies however have found multimodal feedback to be not as effective as single feedback [109] when compared in terms of task performance [86] and perception [213][78]. This indicates that further investigation is needed to examine the impact of multimodal feedback.

In order to evaluate the impact of multimodal feedback for tele-operated assembly task in a virtual environment, [207] focused on the utility of vibrotactile feedback in addition to auditory feedback in displaying vibrations experienced while operating an actual impact wrench. They also investigated the effectiveness of vibrotactile feedback (versus force feedback) and auditory feedback in enhancing operator's awareness of the state of the tool, as well as forces experienced during collision and coupling. Visual feedback (of the virtual impact wrench and virtual working objects: bolts and nuts) was provided via a VR head-mounted display (HMD) as the impact wrench in the virtual environment was controlled by a 3d-printed haptic manipulator mechanically coupled to the stylus of a SenAble PHANtoM Omni Haptic device. The SensAble PHANToM renders force feedback to the to the manipulator while vibrotactile feedback is provided by four vibrating mini motor discs [3] distributed on the 3D-printed manipulator. Each vibrating motor (driven with pulse width modulation (PWM)) was distributed to be in contact with the operator's hand for effective and distinguishable haptic feedback.

The accelerations of different levels of vibration feedback, as well as the accelerations of the real impact wrench were measured using ADXL 3-axis accelerometer. 0.01 g, 0.07 g, 0.20 g, and 0.24 g, at corresponding frequencies of 39.60 Hz, 84.16 Hz, 99.01 Hz, and 118.81 Hz were the accelerations recorded for each intensity level generated by the vibrating motors. The accelerations of two typical working states of the real impact wrench were measured as 0.30 g and 0.32 g at frequencies of 69.31 Hz and 49.02 Hz respectively. The maximum vibrating level of the haptic feedback was chosen after [207] conducted some pilot studies. Repetitive pulses generated with the motor discs was used to convey the hammering state of the impact wrench at 50% duty cycle (cycle period = 300 ms). Auditory feedback was provided using a pair of speakers by playing back recorded sounds of a real impact wrench. The study task required participants to move the impact wrench to a randomly selected nut and bolt, couple the wrench socket to the nut and tighten the nut on the bolt under three feedback conditions. The first condition consisted of graphical and auditory feedback only. For the second condition, vibrotactile feedback was used to represent the working states of the of the impact wrench and indicate collisions and coupling of the impact wrench with the nut. Vibrotactile feedback was also used to represent the working states of the impact wrench and indicate coupling of the impact wrench with the nut for the third condition. However, force feedback was used to indicate collisions of the impact wrench with nut. [207] observed that the introduction of force feedback did not significantly improve task completion time, contrary to their initial hypothesis even though participants reported greater perceived realism of the interaction when force feedback was introduced. This also implied that mechanically simpler ungrounded haptic systems (e.g. vibrotactile feedback) may support similar level of performance in VR assembly tasks as their grounded (e.g. force feedback) counterparts. Arm fatigue was also observed when conditions 2 and 3 were applied because of the inclusion of haptic feedback [207].

Different feedback modalities (or varieties of the same feedback modality) may also be used to convey different task related information to operator carrying out tasks at the same time. Such combinations may vary depending the feedback modality or task being carried out. The use of the human natural limb during dexterous manipulations integrate multiple haptic signals which become absent during tele-manipulation. [109] designed and presented an experimental framework to explore continuous dual-modality haptic feedback to enable dexterous tele-operated manipulation. Participants were required to carry out a virtual grasp-and-hold task under several conditions using a 1-DOF custom 3D printed gripper or myoelectric control. During the task, participants were instructed to grasp and hold a virtual object while the object was pulled downwards with a logarithmically increasing load force. Participants received grip force feedback through the haptic display to prevent slip when too little grasp force is applied and breakage of the object if too much grasp force is applied. The aperture of the gripper was mapped to positions of the virtual environment (VE) grippers. The conditions include no feedback, vibrotactile feedback (via a C-2 tactor [43]) of object slip, squeeze feedback of grip force (designed with an MG90S servo that tightens the Velcro strap around participants' wrists in proportion to grip force produced in the virtual environment), and a combination of vibrotactile and squeeze feedback. Results suggested that vibration may have dominated the squeeze cues. However, there were indications that carrying out the task with feedback may be better than receiving no feedback at all [109].

This PhD thesis reports tele-operation studies carried out with different feedback. The reasons for the choice of each feedback modality are also outlined, as well as how operators performed using each feedback modality. We explored the use of video feedback, peripheral vision, auditory feedback, and haptic feedback for an assisted living task.

2.3.3 Robot Control

Increase in applications of robot tele-operation has also seen the development of different modes of operation for tele-operated robots. Some of the most popular modes of operating tele-operated robots include direct manipulation [111], supervised manipulation [66], and shared control [107]. Using direct manipulation, remote robots (follower robots) either replicate the movements of the leader robot as controlled by the operator or respond to control instructions from operators using other technologies. Other technologies employed for direct manipulation include traditional input devices like joystick, game controllers and 2D mouse [77], gaze, gesture control, voice control [31], and haptic control interface using haptic gloves [93][101]. In supervised manipulation, humans supervise execution processes of robots carrying out tasks according to predetermined programs [107]. Shared control combines the characteristics of direct manipulation and supervised manipulation. In shared control, humans interact with semi-autonomous robots, allowing humans to make critical decisions during tele-operated tasks.

Control algorithms have also been developed to enhance tele-operation system performance. Since tele-operation performance is often affected by time delay and transmission distance, control methods are being employed to achieve good natural control performance. Neural networks (NN) control methods have been developed to deal with the uncertainties of kinematics and dynamics [103]. To solve problems of time delay and backlash-like hysteresis, [103] developed a synchronization control method. Another alternative to compensate for time delay in robot tele-operation is the fuzzy theory [103]. To compensate for system's dynamics uncertainties and influences of time delays, [71] developed an integrated control method that combined radial basis function NNs with wave variable-based passivity theory. Impedance control schemes have also been employed for non-linear tele-operation system in practical applications [165][156].

Due to the aims and objectives of this thesis, emphasis was placed on understanding the role feedback modalities play in tele-operation. In the different studies carried out, we either used a joystick (remote) or an X-box controller (direct manipulation mode of operation) to control a 6-degree of freedom robot ($Jaco^2$) in an assisted living environment. The $Jaco^2$ is a 6 degree of freedom robot arm capable of reaching 900mm at full stretch [88]. The gripper has three under-actuated fingers capable of being controlled individually, and whose combinations enable the arm to perform pick and place tasks. Kinova's 3-axis, 7-button joystick allows users to operate in three (3) different modes: translate, rotate and grip. When the X-box controller was used, buttons on the X-box controller were also mapped to allow users operate in three (3) different modes: translate, rotate and grip.

2.4 Summary

Literature on different components of a tele-operation system was reviewed in this chapter, providing insight into some of the concepts of robot tele-operation. Previous studies on the use of feedback in robot tele-operation have also been examined. This provides a foundation for the studies reported in this thesis as we explore feedback modalities in the context of assisted living.

Table 2.1 summarises the review of some of the research on the use of service robots to improve the quality of care provided by health care professionals, as well as their impact on service users and care professionals. A review of some of these robots provides insight into some of the requirements that should be considered when employing robots in health care service delivery.

However, As previously highlighted, one of the limitations of most service robots is their inabilities/limitations in providing physical assistance. This therefore encourages the need for tele-operation of robots that may be used to provide physical assistance.

This chapter also provides insights into the concepts of robot tele-operation in the context of assistive care provision. Emphasis has been placed on safe and effective robot tele-operation since the tele-operated robots are designed to operate in the vicinity of human care receivers. The concepts examined contribute to ensuring that safe and effective robot tele-operation is achieved. These concepts include: remote perception and data gathering, sensory substitution and feedback modalities, and robot control. Some of the feedback modalities explored include: visual feedback, haptic feedback, auditory feedback, and multi-modal feedback.

Table 2.2 and Table 2.3 provide a summary of studies that cover the different concepts examined. Whilst Different studies have explored some of the different modalities mentioned in different applications, very few studies have been carried out in the context of assistive care provision. This therefore influenced the different studies reported in this thesis.

Table 2.1: Review of Service robots

Research/Publication Title	Insight	Impact on research

Continued on next page

Table 2.1 – continued from previous page

Research/Publication Title	Insight	Impact on research
Reframing Assistive Robots to Promote Successful Aging. [100]	Study of ageing in human robot interaction	The article recommended autonomy and resilience as themes that should be considered when designing assistive robots
Telepresence robots [38], Ohmni robot [138]	Examples of telepresence robots that are in use to enhance communication between healthcare professionals and service users	Encouraging use of telepresence robots establish the need to introduce telepresence in remote care giving
Robot assisted activity for elderly people and nurses at a day service center [199]	The study was designed to interact with older adults with dementia by generating three types of behaviour: Proactive, reactive, and physiological	Results show that staff burnout reduces as the dependency of service users on staff reduces.
Towards robotic assistants in nursing homes: Challenges and results [145]	The study was designed to provide reminders about events and schedules to older adults	This study provides an example of how robots can be employed to help older adults with assistive care needs be less dependent on care givers.
Social Robots for Engagement in Rehabilitative Therapies: Design Implications from a Study with Therapists [204]	Social robots can be used to provide self directed exercises for physiotherapy	This study provides an example of how robots can be employed in rehabilitation exercises.
Robust fall detection with an assistive humanoid robot [140]	In this study, a robot was used to monitor users as they carried out activities to detect fall.	Results confirm that the use of robots can be used to monitor activities of care receivers and improve moods, creating openness.
Elbows Out"—Predictive Tracking of Partially Occluded Pose for Robot-Assisted Dressing [30]	In this study, strategies were developed for planning and error handling in an assistive robot to support independent dressing	The study shows that robots are capable of providing physical assistance but also highlights the limitation for real time applications

Table 2.2: Concepts in Robot tele-operation (Remote perception and data gathering)

Study/Concepts	Sensor	Insight
Use of monocular cameras [113], [122]	Single cameras	There is often a constraint of perception of depth. This prompts the use of other sensors.
Assistive grasping in teleoperation using infra-red proximity sensors [32]	Infra-red proximity sensors	This study was designed to address the challenge of occlusion and possible time lag of image acquisition and processing. They achieved object localization with infrared sensors.
Utilising tele-operation and mobile application in identifying materials of varied thickness and sizes [119]	Microphones	The goal was to identify different materials in a remote location based on amplitude and frequency of the captured sound when struck.

Table 2.3: Concepts in Robot tele-operation (Sensory Substitution/Feedback modalities)

Study/Concepts	**Feedback Modality**	**Insight**
Improving Collocated Robot Teleoperation with Augmented Reality [67]	Visual feedback (Augmented reality)	Augmented Reality was introduced to reduce the distraction of switching between computer monitors to receive visual information of the remote location.
Human-Robot-Interfaces based on Mixed Reality for Underwater Robot Teleoperation [37]	Visual feedback (VR and AR)	Combined the domains of virtual and augmented realities by proving stereoscopic display and 3D interaction during underwater teleoperation.
Intuitive Robot Teleoperation Through Multi-Sensor Informed Mixed Reality Visual Aids [105]	Visual Feedback (Multi sensor informed mixed reality visual aids)	The aim was to address the challenge of cognitive overload.
Peripheral vision [167][23]	Visual feedback (Peripheral vision)	This feedback modality provides supplementary data as participants focus on video streams.

Continued on next page

Table 2.3 – continued from previous page

Study/Concepts	Feedback Modality	Insight
Visual feedback techniques for telemanipulation and system status sensualization [52]	Visual feedback (Peripheral vision)	Employed sensory substitution to convey the state of a system (fuel level, oil pressure, temperature, speed, and engine rpm) to an operator via peripheral vision.
Haptic Feedback in a Teleoperated Box & Blocks Task BT - Haptics: Science, Technology, Applications [93]	Haptic feedback	Examined the need for direct force feedback and substituted force feedback on a tele-operated box and blocks task. Participants preferred the use of feedback over no feedback scenario.
Robotics in the neurosurgical treatment of glioma [184]	Haptic Feedback	Implemented a haptic notification system designed to warn surgeons when forces of tool tissue interaction exceed certain limits.
Robot-Assisted Unicompartmental Knee Arthroplasty [142]	Haptic guidance	Employed haptic guidance in combination with a navigation module for precise planning and execution of an inlay unicondylar knee arthroplasty.
Augmentation of haptic feedback for teleoperated robotic surgery [167]	Haptic feedback + haptic guidance	Explored the combination of haptic feedback and haptic guidance for teleoperated robotic surgery
The Use of Vibrotactile Feedback to Restore Texture Recognition Capabilities, and the Effect of Subject Training [129]	Vibrotactile feedback	Explored the use of vibrotactile feedback for the restoration of texture recognition especially for upper limb amputees.
Operational Evaluation of a Construction Robot Teleoperation with Force Feedback [208]	Auditory feedback	Using auditory feedback (sonification) to compensate for insufficient leader-follower feedback. Force perception improved with auditory feedback.
Auditory Display for Telerobotic Transnasal Surgery Using a Continuum Robot [22]	Auditory feedback	Using auditory feedback to display navigation cues to human operators

Continued on next page

Table 2.3 – continued from previous page

Study/Concepts	Feedback Modality	Insight
[207]	(multimodal feedback) Vibrotactile + auditory feedback	Investigated whether the combination of feedback enhances operator's awareness of the state of the tools.
Evaluating Multimodal Feedback for Assembly Tasks in a Virtual Environment [207]	(multimodal feedback) Vibrotactile + auditory feedback	Investigated whether the combination of feedback enhances operator's awareness of the state of the tools.
Towards an Understanding of the Utility of Dual-Modality Haptic Feedback in Teleoperated Medical Devices [109]	Multimodal (vibrotactile, squeeze feedback.)	Results highlight the knowledge gap in the use of continuous multimodal feedback in different tele-operation scenarios

Chapter 3

Methodology and Software/Hardware Design

The methods adopted to address the research questions in this thesis combine the review of relevant literature, different iterations of software and hardware developments, and experimental studies. The literature review provides a theoretical background for the studies carried out and outlines knowledge gaps in the implementation of feedback modalities for assistive care tele-robotics. This chapter describes the different software and hardware design iterations made as different experimental studies were carried out. Deductive and inductive approaches were combined in the design of the feedback modalities examined in the studies. Whilst the inductive approach to design involves testing the performance of devices with user studies to understand the device parameters that ensure satisfactory human parameters, the deductive approach investigates parameters that are important for the design of devices [40]. Qualitative and/or quantitative research methods were employed during the user studies. The quantitative method of data collection typically uses numeric measurements, is deductive, requires hypothesis and may focus on cause and effect. The qualitative method of data collection, on the other hand, uses words, is inductive, does not require hypothesis and focuses on the understanding of phenomena in their social, institutional, political and economic context [4].

This thesis starts with a qualitative inductive research study which involves the review of already existing technologies, and research studies that have been carried out on tele-operation of robotic systems. The review explores previous works carried out on applications of various combinations of feedback modalities, especially with applications in robotics. The knowledge gained from reviewing previous research on the challenges of health care institutions and technologies that are employed as solutions shed more light on the challenges of tele-operated robots. Limited work has been done on the use of tele-operated robots in assistive care, prompting the need for this PhD research. Therefore this thesis addresses issues relating to remote perception, sensory substitution, and the effect of different feedback modalities on tele-operated assistive tasks, both on the care givers (operators) and service users.

3.1 Scope of Study

In this thesis, we investigated different sensor data required in assistive tele-operation, sensory substitution, and the role of feedback modalities on operator performance while also examining how task repetition affects performance. The cognitive load brought about as a result of the use of each feedback modality was also investigated to reduce the over-exploitation of certain sensorial information, majorly vision and proprioception.

An ethical concern in the application of robots in healthcare is “dehumanisation and cold care” [179]. There is a general concern that robots may replace health care providers, therefore removing the warm human care from the care process. To ensure that natural human communication remains in the care process, collaboration between operators and service users was introduced in the study [168]. The collaboration does not just allow for human feel but should also help the operator in delivering quality service [211] and enhance adaptation to the information about the remote environment conveyed to operators [204].

Relative to the environments where industrial robots and other types of robots operate, robots that are used in health care service applications (service robots) operate in environments and under conditions designed for humans which are less mature, unstable, uncontrolled and unpredictable (i.e. heterogeneous environments) [99]. To provide tele-operated assistive support, it is important to be aware of the operational conditions which helps to put in place mechanisms that ensure the safety of both the service users and service robots while also delivering quality service in real time .

The design of tele-operated systems for assisted living involves careful consideration of the human users. The users include the service users and service providers (as operators). The service providers could be professional carers and operators as well as informal operators which may be friends or relatives. The major difference between these two categories of service providers is the level of training they receive in order to carry out tele-operative tasks.

Having the user groups in mind influences the research decisions that will be taken as well as the experimental designs to achieve the aims and objectives of this PhD research. Since the human operators do not necessarily involve only professional operators who spend an appreciable amount of time learning the process, it is important to develop a system that is not only easy to use but easy to learn. Some of the general challenges operators (formal and informal) may face include:

(i) Robot mobility and manoeuvrability

(ii) System control and usability for carers

(iii) Object grasping and manipulation

(iv) Recognition and interpretation of human behaviour (social interaction between the service user and operator)

(v) Safety of service users and of the robots

(vi) Reliable detection of objects

(vii) Positional awareness of the robots for the safety of the service user and the robot itself

(viii) Service time: where automation is possible, shared control can be introduced

(ix) Operator concentration and increasing cognitive load.

The list above is inexhaustible but this thesis focuses on the use of feedback modalities to tackle a few of the challenges operators may face when carrying out assistive tasks.

Key themes include:

- Data gathering for object grasping and manipulation.
- Sensory substitution
- Operator concentration and minimising cognitive load.
- Usability and ease of learning.
- Effect of task repetition.

3.2 Research Progress

This section describes the hardware and software developments carried out to provide answers to the research questions. It also describes the different studies carried out throughout the PhD research.

Figure 3.1 shows the block diagram summarising tasks carried out in different phases of the research. It shows the flow of hardware and software developmental work done before and after different studies were carried out. There was a need to develop software and hardware for sensors and feedback modalities because of the unavailability of off-the-shelf devices that meet the specific requirements of the studies carried out. A few of the available ones were found to be very expensive, hence the need to develop hardware and the supporting software to integrate all the necessary components of the system. The sensors and hardware were calibrated according to technical reference manuals of the components used in the designs (section 4.1.3, section 4.2.2.2, section 4.2.2.3, and section 3.3.1). The processes of manual calibration have also been documented. 5 studies were carried out and have been reported in this thesis.

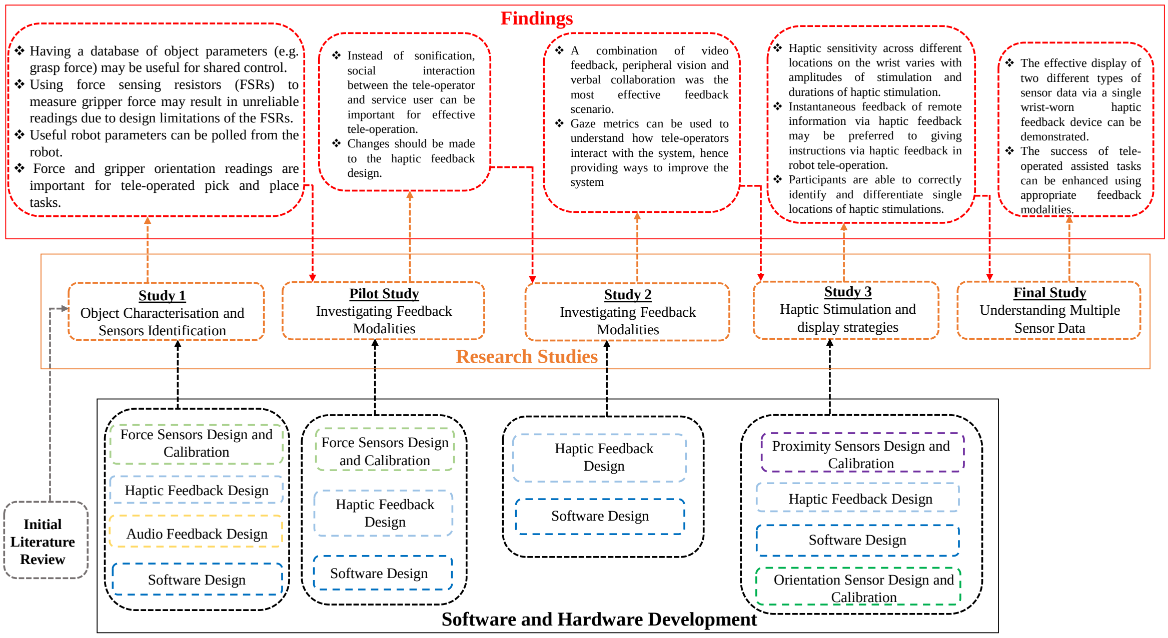

Figure 3.1: Overall Research Stages: Hardware and Software development including studies carried out.

3.3 Software and Hardware Design

The setup for the different studies carried out in the PhD required accompanying software and hardware. For the studies carried out in the thesis, the accompanying hardware developed may be grouped into feedback modalities and sensors.

3.3.1 Feedback Modalities

Feedback modalities define the different forms through which information is presented to a human user. Each individual form is classified by the sensory modality it addresses (e.g. auditory, visual, or tactile). Haptic feedback, auditory feedback, and visual feedback (video and peripheral vision) were explored in this study.

3.3.1.1 Haptic Feedback

Haptic feedback involves the use of touch to communicate [193]. Of the five human senses (touch, sight, hearing, smell, and taste [26]), sight and hearing have been the channel of communication between humans and electronic devices. This is quickly changing with the introduction of haptic devices that simulate the sense of touch. There are two types of haptic feedback: tactile feedback and kinesthetic feedback [63]. Tactile feedback initiates feel on/in the skin, allowing the brain to get the feeling sensations of vibration, pressure, touch, texture etc. Kinesthetic feedback on the other hand initiates feeling sensations in the muscles, joints, tendons etc [51]. For example, when you hold a cup in your hand, you get the approximate size of the cup, its weight, and the position of the cup relative to your body through kinesthetic feedback. References to haptic feedback in this research will involve the use of vibrotactile haptic feedback.

There are five main types of haptic feedback technologies: force feedback, vibrotactile, electrotactile, ultrasound and thermal feedback. Haptic devices whose effects are felt on the top layers of the skin are referred to as cutaneous devices. Force feedback on the other hand has effects on the ligaments and muscles through the skin into the musculoskeletal system [121]. By their more complex designs, force feedback devices have impacts on large areas of the body like arms and legs. Force feedback devices are of two kinds namely: biomimetic and non-biomimetic. Biomimetic force feedback devices are designed to look and move as human limbs making their designs difficult. Non-biomimetic force feedback devices may be designed different from the human body. In general, force feedback devices may be classified as active and resistive devices. Resistive devices limit users' movement using brakes while active devices restrict movements in space using motors [191]. A wider range of interactions can be achieved through active devices, but they need to be more powerful and are more difficult to control.

Electrotactile feedback involves the stimulation of receptors and nerve endings with electrical impulses. With this type of feedback, most sensations (e.g. texture, breeze etc) can be simulated using electrical impulses. The sensations may be based on how it is simulated using current, voltage, material, form of wave, electrode size, hydration, contact force and skin type. Very important advantages of this type of feedback are the absence of moving/mechanical parts and the wide range of stimulations that can be achieved. Feedback through electrical stimulations is also seen by many as simple and inexpensive [139].

The ultrasound tactile feedback uses sound wave of high frequency. Several emitters are combined to create invisible tangible interfaces in the air that can be felt through the skin. As an advantage, ultrasound tactile feedback does not require users to wear any accessories.

Thermal feedback is relatively easier to design, and the actuators are required to be in direct contact with the skin. This though requires a lot of energy and for realistic feel, the process must be done quickly.

Vibrotactile feedback is the last and most common of the haptic feedback technologies. This is done by applying pressure to definite human skin receptors (Pacinian Corpuscle) capable of picking up vibrations up to 1000 hertz [163]. The fundamental frequency range of a female voice is 350Hz – 3KHz, while that of a male is 100Hz – 8KHz [177]. This means that the skin can feel many of the sound we hear, and this includes speech. Vibrotactile feedback devices are simple, relatively cheap and consume little power. This type of feedback also has its disadvantages. One of such is ghosting effect that may appear with prolonged/strong impact. Miniaturising the vibrating motors is also hard and deep penetration is also another side effect after prolonged usage [121].

In this research, the haptic feedback designed and used is the vibrotactile haptic feedback.

It is designed to produce effects on the skin and therefore has no effect on joints. The effects of prolonged vibration were not investigated as participants for the studies only used haptic feedback when needed.

Haptic Feedback Hardware

In order to develop the haptic feedback device, specifications were set for the functionality and ease of use requirements of the device. The requirements are listed below:

1. The haptic device should be portable and small.
2. The haptic device should be wireless. For usability and safety, the haptic device should communicate with the control system via Bluetooth or over a network (Wi-Fi).
3. The haptic device should be easy to integrate with the available setup.
4. The haptic device should be worn on the wrist or arm
5. The haptic device should be safe to use and without any exposed electronics.

Market research was carried out to purchase a suitable haptic feedback device that meets the above listed requirements, but none was found. Therefore, a suitable haptic feedback was developed for use in the studies carried out. However, several design iterations had to be made to achieve the set requirements. The actuators used are the coin eccentric rotating mass (ERM) motors shown in figure 3.2 below. The coin type is used to reduce the overall size of the haptic device. Linear resonant actuators (LRAs) are another type of actuator that may be used but they are driven by AC signals. Since the device is intended to run on batteries, LRAs are not suitable.

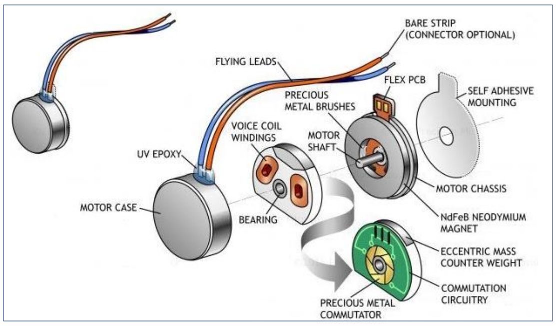

(a) Eccentric rotating mass (ERM) motor

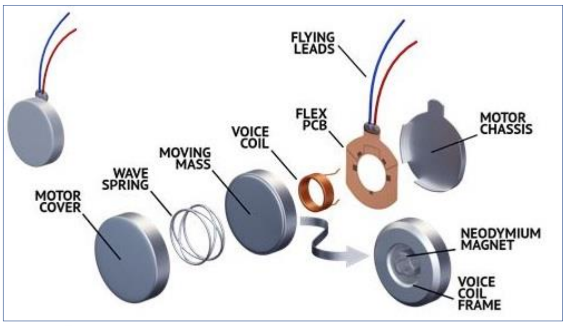

(b) Linear resonant actuators (LRA) motor

Figure 3.2: Haptic Motors

The phase-1 haptic device design is shown in figure 3.3. The design is made up of a grove module integrated with DRV2605L (a haptic driver for ERM/LRA) [169]. It has an easy-to-use library which makes it capable of simulating 123 kinds of vibrating modes. However, the haptic stimulations produced were not strong enough to be distinguishable when embedded into a wrist strap. Likewise, due to the size of the control board (Seeduino: a derivative of the Arduino uno), it was difficult to miniaturise the phase-1 haptic feedback device.

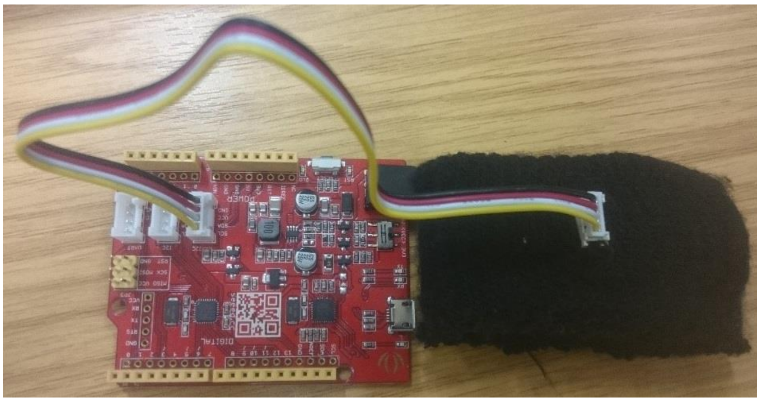

Figure 3.3: Haptic device in a wrist band with the Seeduino board

The phase-2 design is shown in figure 3.4. The required power was provided using a 9V battery and the processing board used is the ESP8266 NodeMCU [136]. In Phase 2, wired connections between the haptic device and the central processing PC were eliminated. The board was powered with a 9 V battery and data transfer between the central processing PC and haptic feedback device was done over a Wi-Fi network.

(a) (b)

Figure 3.4: Phase-2 haptic feedback device, (a) complete design (b) haptic motor and control board

A problem encountered with the use of the phase-2 design is partial wire disconnection when the wrist band was worn by participants with relatively large fists. Because of the varying fist sizes of participants, participants with smaller hands found it easier to put on the phase-2 haptic feedback device than participants with relatively larger hands. As the wrist band is stretched beyond certain limits, the wires connecting the control board to the haptic motors broke, thus causing the haptic feedback to fail. To solve the disconnection problem noticed in the phase-2 design, a 3D-printed case was designed to house the haptic feedback electronics and the haptic motors. Figure 3.5 shows the 3D model of the phase-3 design. Two haptic motors were used to provide haptic stimulation when the case is strapped to the wrist. The problem encountered in phase-2 design was solved but the casing was heavy and bulky. The motors also had more work to do for vibrations to be noticeable and distinguishable due to the position of the motors and the casing.

(a) (b)

Figure 3.5: Phase-3 Haptic feedback device, (a) complete design (b) CAD design for the casing

The off-the-shelf ESP8266 NodeMCU used contributed to the bulky nature of the designs up to this phase. To reduce the overall size of the haptic control circuit for a phase-4 design, a customised board was designed using the ESP8266MOD module. Another problem that was encountered with the phase-2 and phase-3 designs was that the haptic motors had slow responses to the input value changes. The maximum current that can be drawn from each individual GPIO pin of the ESP8266 NodeMCU is 12 mA, which is too low to generate quick response from the motors. In the phase 4 and phase 5 designs, switching transistors (MOSFET) were introduced to the design and the motors were driven using software pulse width modulation (PWM).

Phase-4 design was smaller (48 mm x 35 mm) than the previous designs but was still considered bigger than preferred.

Figure 3.6: Phase-4 Haptic feedback device

The circuit redesign in phase 5 (28 mm x 27 mm) was done using the ESP32 module. The ESP32 module has an extra CPU core and has more GPIOs when compared to the ESP8266MOD module. The increased number of GPIOs was especially important to include additional functionalities to the final design. Figure 3.7 shows the schematic for the final haptic feedback device.

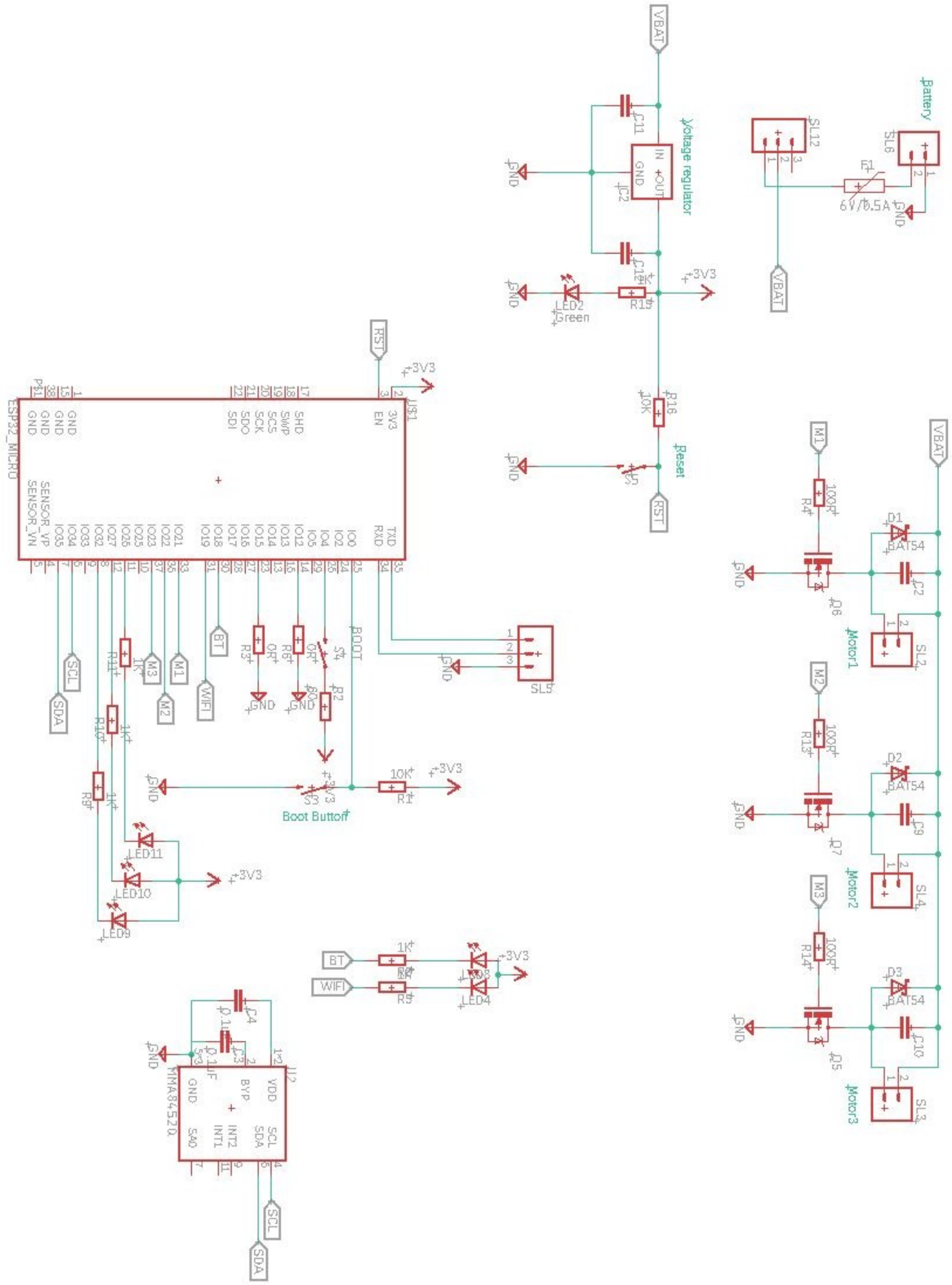

Figure 3.7: Phase-5 Haptic feedback schematic diagram

A maximum of 4 haptic motors may be controlled with the phase-5 haptic motor control board and users also have the option of choosing the number of motors to be used depending on the application. Different LEDs were also added to show different states of use. Some of the states include power on, network connectivity, and the number of motors in use. 3D-printed casing was also designed to house the circuitry (fig. 3.8).

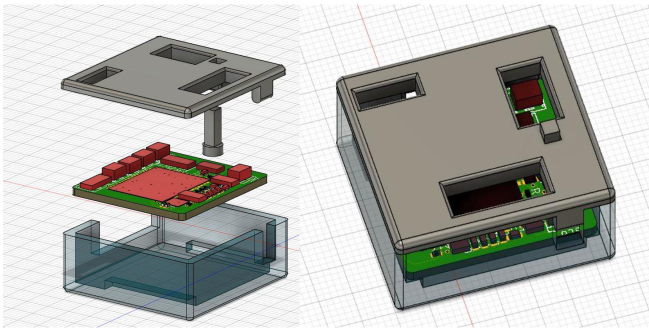

Figure 3.8: 3D model of the phase-5 haptic feedback circuitry

Figure 3.9 shows the finished wrist-worn haptic feedback device containing the circuitry and embedded haptic motors.

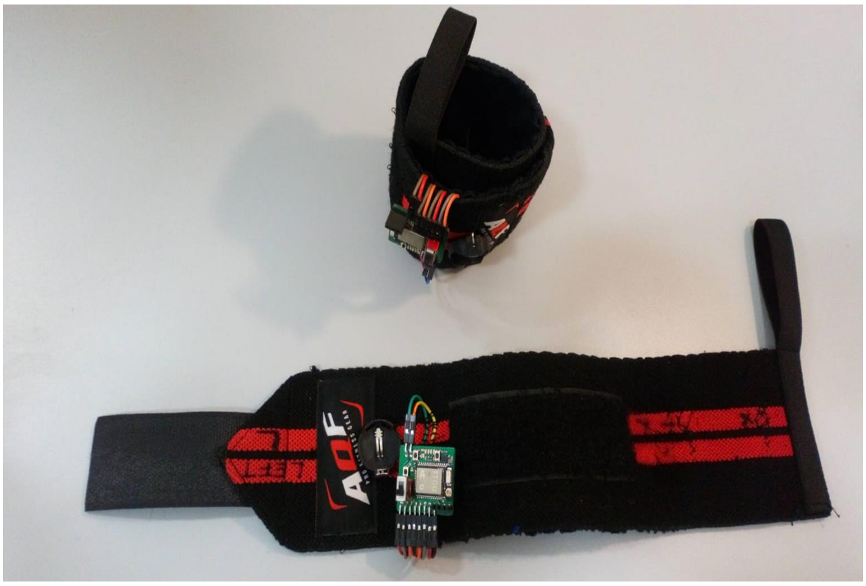

Figure 3.9: Phase 5 haptic feedback device

Iterations to the haptic feedback design are summarized in figure 3.10

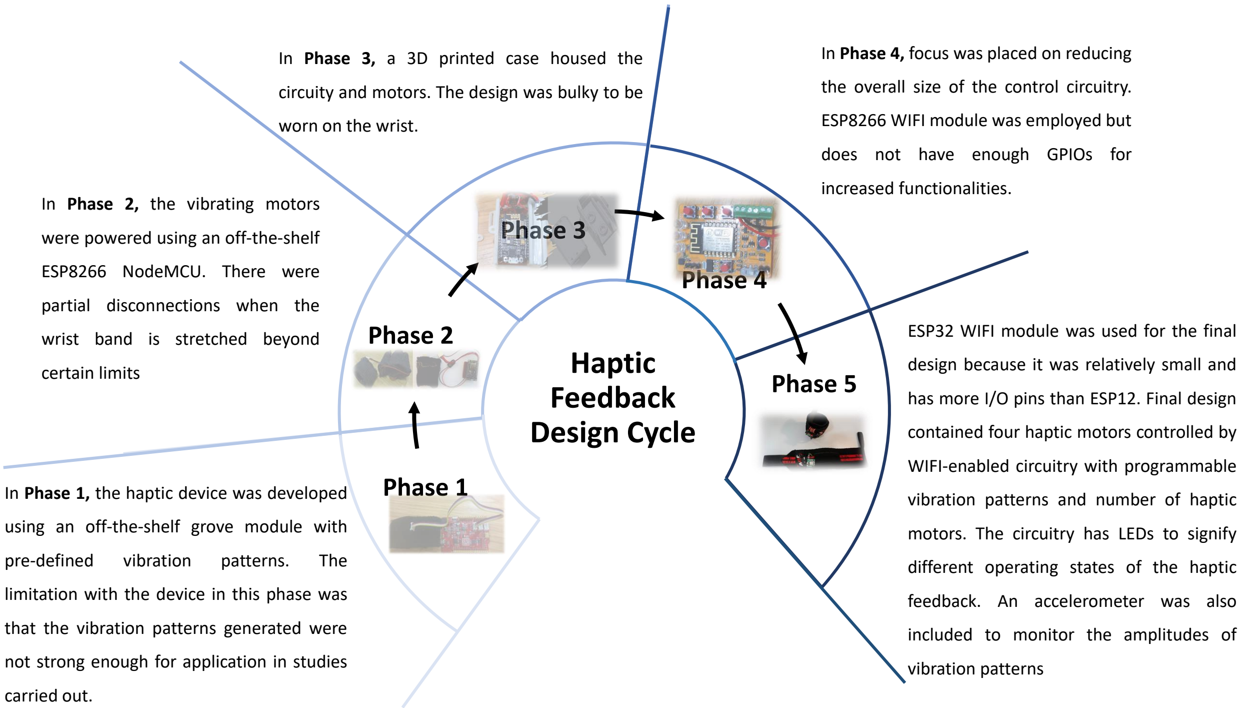

Figure 3.10: Haptic feedback design iterations

Haptic Feedback Software

Pulse with modulation (PWM) is a technique used to supply electrical power to loads with relatively slow response [157]. It is also regarded as a way of using digital output (0s and 1s) to control analog devices [65]. Pulse width modulation simulates analog-like outputs by applying power in pulse or short bursts of regulated voltage. A square wave can be created using digital signal switched between on and off, simulating voltages between full on (5V) and off (0 volts). This is done by changing the amount of time the signal spends on relative to the time the signal spends off. Pulse width is the duration of "on time". In a DC motor, the motor windings store energy that smooths the energy bursts delivered by the input pulses. This makes it possible to control the electrical power input by adjusting the width of the pulses. The brightness or dimness of light emitting diodes can also be controlled by adjusting the width of energy pulses supplied. Pulse width modulation is often described using frequency and duty cycle.

For a voltage signal with pulses of duration τ_o, repeated every τ_c unit of time as shown in figure 3.11, the output voltage of a PWM channel is either V_s or zero. Supplying the signal to a device with response time much larger than τ_c, the signal will be experienced as an approximate DC input with an effective voltage of

$$V_{eff} = V_s \frac{\tau_o}{\tau_c} \tag{3.1}$$

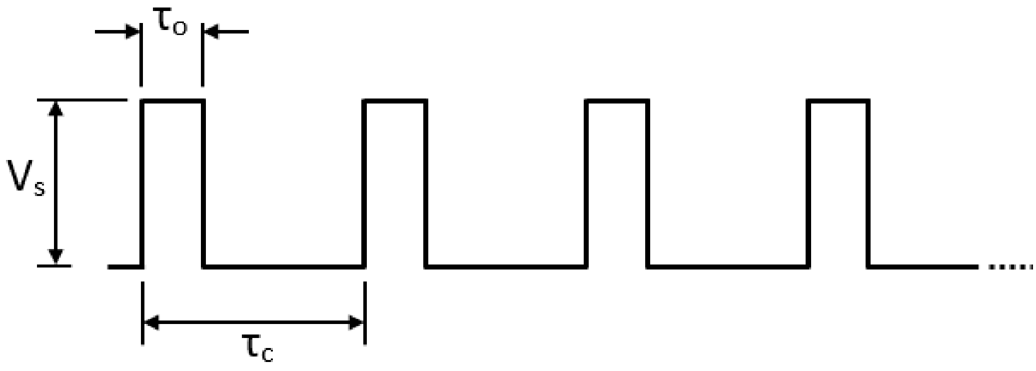

Figure 3.11: Duty cycle of pulse width modulation

$\frac{\tau_o}{\tau_c}$ from equation 3.1 is the duty cycle of the square wave pulses. Adjusting the duty cycle controls the effective DC voltage.

Different haptic effects can be implemented by altering the vibration intensity and pattern of vibration. The amplitude of vibration (magnitude of wave) and frequency are related in eccentric rotating masses (ERMs). As the magnitude increases, the frequency increases (meaning the period shortens) [148]. The frequency should also be set for vibrations detectable by mechanoreceptors in the skin. The Pacinian Corpuscle best detects vibration in the 40 – 800 Hz range and have peak perception between 200 and 300Hz. Frequency also affects displacement as the motor vibrates. Comparing the displacement of two motors with the same vibration amplitude but different frequencies, the motor with the lower frequency will have the highest displacement of the two and this can affect vibration perception.

The relationship between the centripetal force of a rotating mass (F), its mass (m), eccentricity (r) and rotational speed (ω in radians per second) can be expressed as

$$F = m \times r \times \omega^2 \tag{3.2}$$

The relationship between motor speed and amplitude of vibration is not linear but exponential, and therefore increasing the speed will result in a larger increase in amplitude. In ERMs, motor speed (revolutions per minute) and the vibration frequency (Hertz) imply the same thing. This means that by simply increasing the motor speed, the frequency and amplitude are increased. This is further shown in figure 3.12.

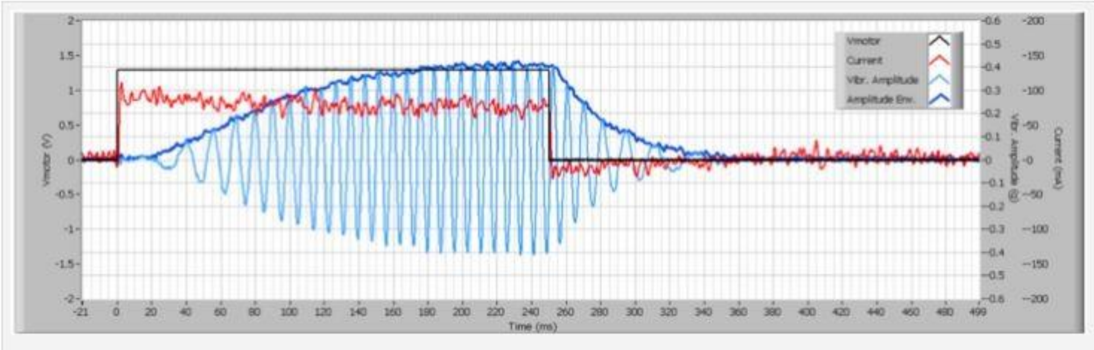

Figure 3.12: Motor voltage, amplitude, and frequency [148]

To control the motor speed, the driving voltage (V_{eff}) is adjusted. To control haptic motors, four important voltages should be taken note of. They are, typical start voltage, certified start voltage, rated voltage, and maximum operating voltage.

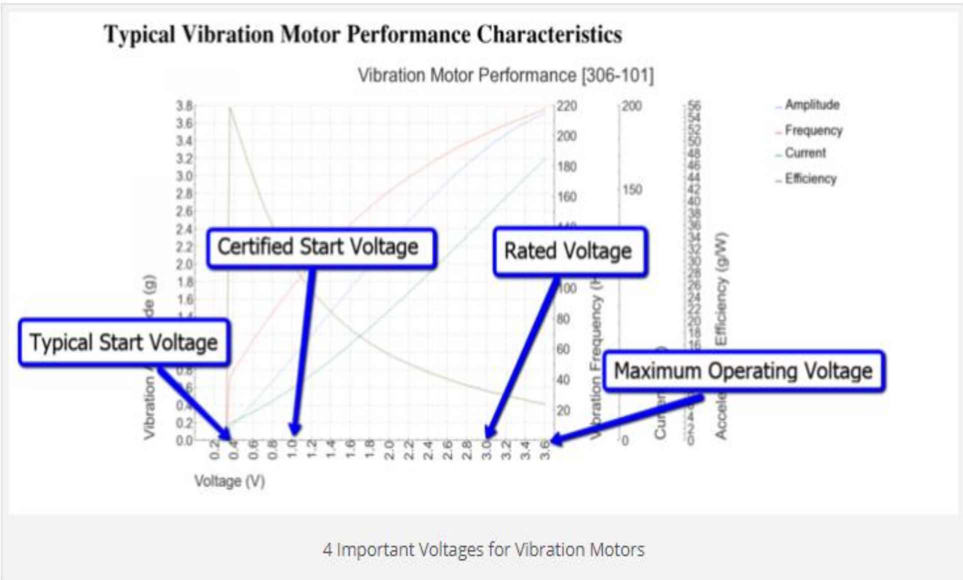

Figure 3.13: Vibrating motor voltages [148]

The typical start voltage is the minimum voltage required to start the motor, however the maximum operating voltage for the motor should not be exceeded to avoid damages to them. The control circuit designed to power the haptic motors was programmed using the Arduino IDE. Pulse width modulation (PWM) can be implemented using analogWrite and DigitalWrite [170].

Using the analogWrite function, varied square wave can be generated by changing the duty cycle. A 100% duty cycle occurs if the value is set to 255 and 0 for 0% duty cycle. The frequency of the PWM is determined by the GPIO pin used.

The analogWrite value is set by multiplying the duty cycle by 255.

$$duty\,cycle \times 255 = analogWrite\,value \tag{3.3}$$

Creating a square wave using the digitalWrite function is done with delay functions since the digitalWrite function can only provide a High (5 V) or a Low (0 V).

The duty cycle can be calculated using the equation below

$$\frac{delay\,time\,HIGH}{delay\,time\,HIGH + delay\,time\,LOW} = Desired\,duty\,cycle \tag{3.4}$$

An advantage of using the digitalWrite function is that the frequency of the pulse can be changed. Changing the total time for each cycle will also change the frequency since frequency is inversely proportional to time.

In the phase-2 design, the analogWrite function was used to generate the PWM in the ESP8266 wifi board. The ESP32 however does not allow the use of the analogWrite function, being different from Arduino. ESP32 uses 8 (value range between 0 and 254),10,12,15-bit resolution to generate PWM value. The ledWrite(pinChannel, dutyCycle) function is called in order to use PWM on the ESP32 module.

3.3.1.2 Peripheral Vision Feedback

The development of this feedback modality was done in software. It is presented as colour changes on a screen placed in the peripheral of users to display specific information. This feedback can be adapted to different applications and studies. Table 3.1 below shows a use of the peripheral feedback in providing feedback about the orientation of a robot gripper.

Orientation classification	Gripper orientation ranges (degrees)	Colour representation
Aligned with the vertical axis of the cup	125 – 134, 482 – 492, -221 – -231	Green
A little tilted to the the left	135 – 140	Light blue
Farther to the left from the aligned position	141 – 482	Deep blue
A little tilted to the right	120 – 125	Light red
Farther to the right from the vertical alignment	-221 – 120	Deep red

Table 3.1: Gripper Orientation ranges mapped to different colours

3.3.2 Sensors

Video feedback of the remote end was projected to all participants that took part in the different studies as operators. To assist with carrying out different tasks, more sensor data had to be gathered. This sensor data includes gripper force, robot gripper orientation and gripper proximity (to tables or cooking surface). Sensor data like the robot gripper orientation originally were polled from the robot but customised circuits had to be designed and populated to enable us gather information about the gripper force, orientation and proximity.

3.3.2.1 Force Sensors

Force Sensors Hardware

To measure gripper force, force sensing resistors (FSRs) were initially calibrated and used as described in the study phase 1. However, readings from the FSRs were found to be unreliable with use, especially if they are bent. Therefore, more reliable force sensors were designed. This involved the use of barometric sensors. Figure 3.14 shows the 3D model of the force sensor and force sensor controller designed and implemented. A total of nine (9) sensors were used on the three fingers of the gripper. A force sensor controller was also developed to poll sensor data from all the sensors, and wirelessly transfer the force sensor data to the central processing computer. Each force sensor has an MPL115A absolute pressure sensor and an i^2c translator to give it a unique address. The lower part of the casing is made of 3D printed plastic while the upper part of the casing is made of 3D printed rubber filled with silicone gel.

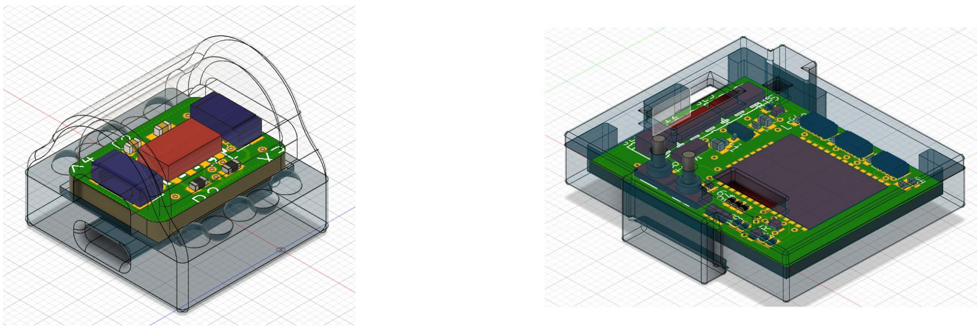

(a) (b)

Figure 3.14: 3D model of the barometric force sensor, (a) force sensor (b) force sensor controller

Figure 3.15 below shows the force sensors mounted on one of the Jaco^2 fingers.

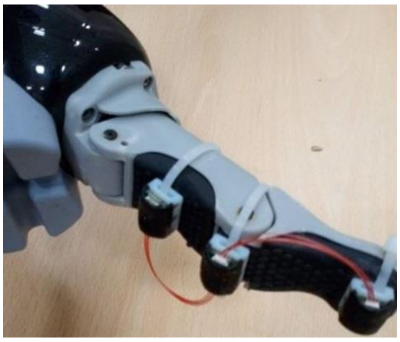

Figure 3.15: Force sensor mounted on the Jaco^2 robot gripper

Force Sensors Software

Each force sensor was given a unique i^2c address. On set up the force sensor controller polls sensor data from each force sensor using their unique i^2c addresses and transmits the sensor readings to the processing computer for processing. The force sensor controller is programmed in C programming language using the Arduino IDE.

3.3.2.2 Proximity Sensors

To prevent operators from driving the robot into the cooking surface and table (of the setup used), proximity sensors were also implemented. This information will make operators aware of the proximity of the gripper to surfaces. This design is made up of the proximity sensor (fig. 3.16a) and the Wi-Fi enabled proximity controller (fig. 3.16b).

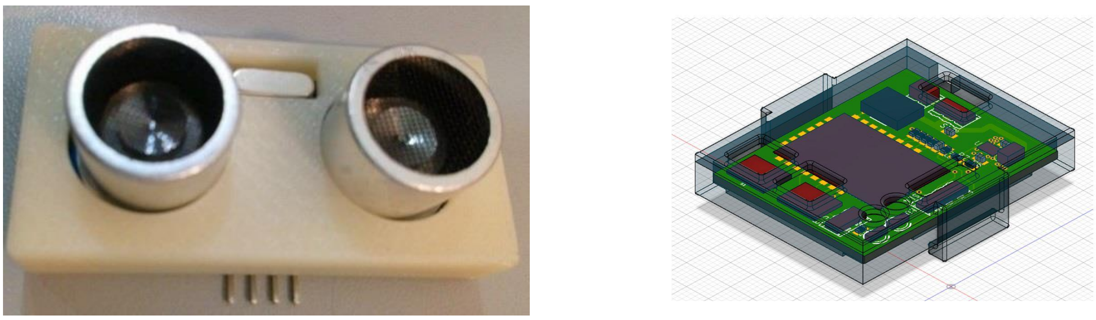

(a) (b)

Figure 3.16: Gripper proximity sensor, (a) sensor (b) 3D model of the proximity sensor controller

3.3.2.3 Orientation Sensors

In order to make the gripper orientation sensor independent of the robot, a modular orientation sensor was developed using an 3-axis accelerometer and a Wi-Fi module.

3.3.3 Software Interactions

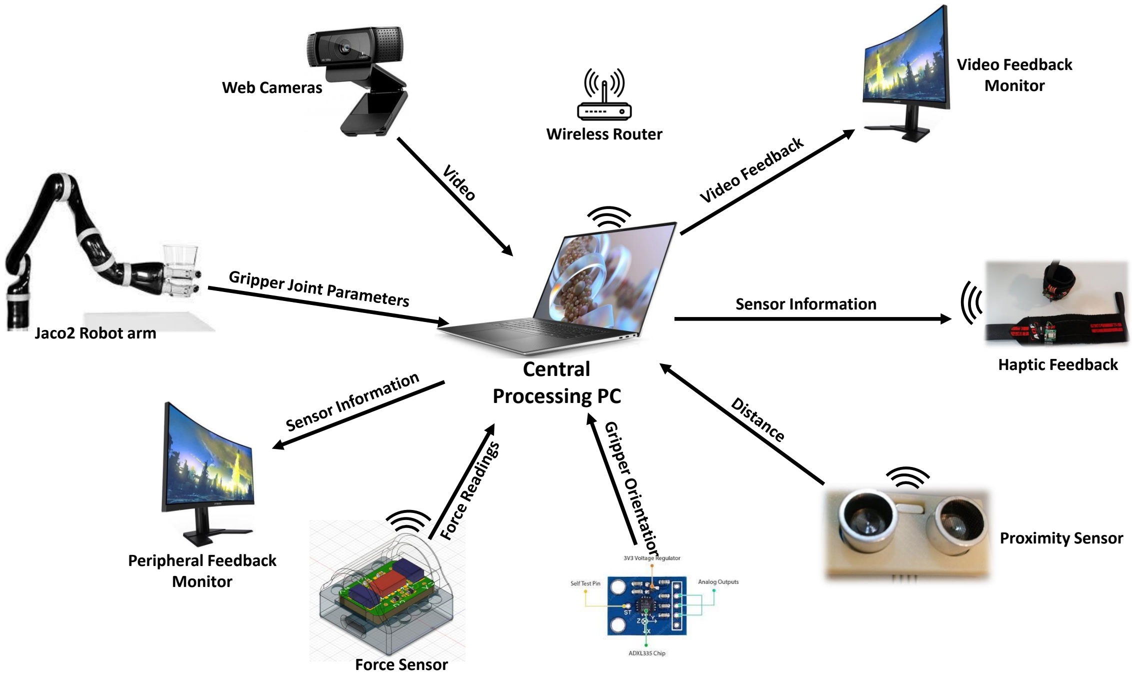

Figure 3.17: Software interactions

The Central processing software was written with C++ programming language, but the software of the force sensor, proximity sensor, orientation sensor and haptic feedback were written in C.

3.3.4 Ethical Applications and Approval

Ethics approval for all the studies carried out was sought and granted by the research ethics committee of the university of the west of England, Bristol (UWE).

Ethics Application : UWE REC REF No: FET.17.12.015

An amendment was made to the original application for the study in chapter 5 and chapter 6 which was approved.

CHAPTER 4

RESEARCH STUDIES

To achieve the aim and objectives of the thesis, studies were carried to provide answers to the research questions. This chapter reports the first 3 studies that were carried out in this thesis. The first study investigated required sensor data. The second was a pilot study which validated the setup before the third study was carried out with participants. For each study, combinations of the hardware and software developed in chapter three (3) were used.

4.1 Study Phase1: Object Characterization and Identification of Relevant Sensor Data for Pick and Empty Tasks

4.1.1 Introduction

Due to the complexity of robot control and the high level of safety needed in close proximate human-robot interaction, the operator needs to be mindful of the remote environment, robot conditions and conditions under which the interactions take place. Even for simple pick and place tasks, for example, that might be used when supporting a person with eating and drinking, or other assistive tasks such as support with dressing, it may be important to provide the operator with information about objects to be picked. One of such information often mentioned in the literature is grasp force. This knowledge is similar to the information human beings retain in their memory of different objects having previously interacted with them. Such knowledge is also important where the operator wants to hand over control of certain tasks to the robot for quicker execution of tasks. In such cases, having a database of household objects together with their characteristic properties (e.g. weights, width, height, etc.) may also be important. The results can also be used to make contributions to cloud-based robot grasping databases using object recognition [83][112]. This ensures that object characteristics are reusable by other robots in as many locations as possible.

This study was designed to investigate relevant sensor data required for effective and efficient tele-operation. The identified sensors may be used to measure different characteristics of objects to be manipulated. For many of our everyday activities, humans relate with the environment and actions are taken as a result of prior knowledge of the environment in which they operate. Such prior knowledge thus help us to measure how we relate with different things in the environment.

4.1.2 Methods

The aim of this study is to identify parameters (types of sensor data) that may be useful to achieve grasp. We start with exploring the need for grasp force and extend to other parameters. The hardware and software requirements are outlined below.

4.1.2.1 Hardware Requirements

The hardware requirements are listed below:

1. Kinova 6-DOF Jaco^2 robot arm with 3-fingered gripper.
2. Force sensing resistors (FSRs).
3. Arduino Nano.
4. 3 KΩ, 10 KΩ, 30 KΩ, 43 KΩ, and 100 KΩ Resistors
5. Unity gain amplifier (LM324)
6. Vero Board
7. Jumper wires
8. Cup

4.1.2.2 Software Requirements

The software used to carry out the study are listed below:

1. Microsoft Visual Studio Professional

   This is the development environment for programming the robot using the robot's application programming interface. It is also important for gathering and processing sensor data.

2. Kinova Development Center (The GUI for interacting with the robot)

   This is the graphical user interface developed by Kinova [88] for controlling the robot and visualising sensor information.

3. Microsoft Excel

   This is used for analysing results and presenting the data in graphical forms.

4.1.3 Force sensing resistor calibration

In order to measure gripper grasp force, force sensing resistors (FSRs) were attached to the fingers of the robot gripper. Interlink Electronics FSR402SHORT 0.5" diameter short tail force sensing resistors [74] with actuation force range of 0.2 N - 20 N were used. Weights of varying sizes of 50 g - 700 g range with 50 g weight intervals were used to calibrate the force sensing resistors. The dependent variable measured is the voltage reading while the independent variables include force values of the weights and resistors.

Each force sensing resistor was connected to an Arduino (nano), programmed to convert analog sensor (force) readings to digital signals (read as voltages). To read the values using a microcontroller, resistors of known values were connected in series with the FSR which will help to approximate the resistance of the FSR as a function of voltage drop across the known resistor. The voltage divider circuit is shown in figure 4.1 below.

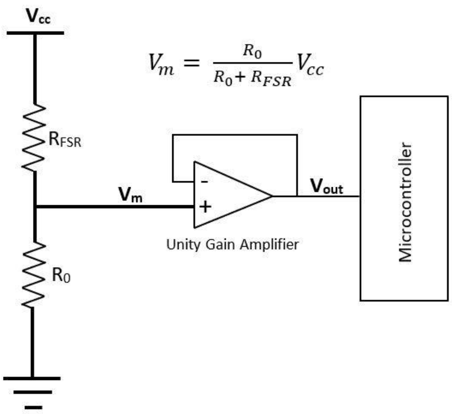

Figure 4.1: Schematic diagram of the FSR circuit

Where,

R_{FSR} = Resistance of the FSR

R_0 = known resistance

V_{cc} = supply voltage

V_m = voltage measured by the unity gain amplifier, fed to the Arduino's (nano) analog to digital (ADC) converter.

As different weights were applied to the FSR, the output readings of the unity gain amplifier were converted to digital signals (millivolts) by the microcontroller's analog to digital (ADC) converter and saved into a text file for a duration of 60 seconds. Placing the weights on the

FSR and recording the corresponding voltage readings was repeated for different known resistor values as shown in table 4.1. Averages of the recorded voltages were taken and plotted against their corresponding weights. Figure 4.2 shows the circuit hardware connecting the force sensing resistors in a voltage divider to the microcontroller.

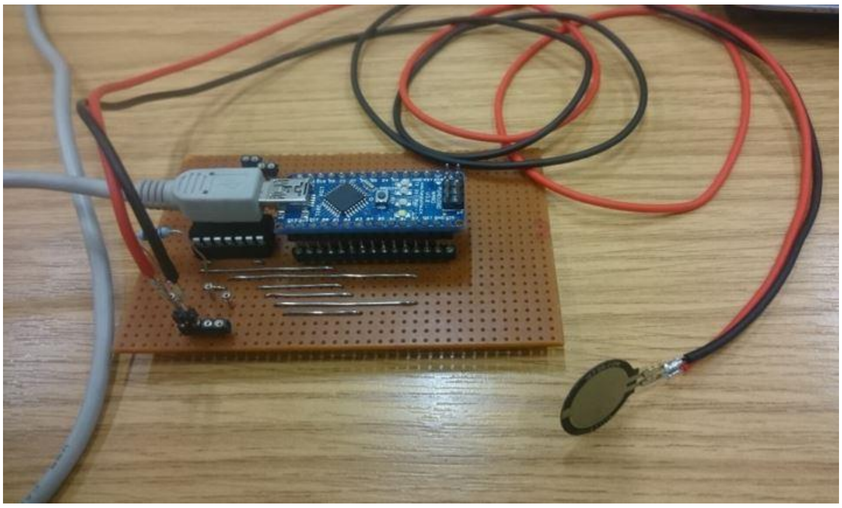

Figure 4.2: FSR and microcontroller circuit

Figure 4.3: Weights placed on the FSR

Figure 4.3 shows the weights placed on the FSR during calibration. Table 4.1 shows the table of force values and their corresponding voltages (in millivolts) for different resistor values. The values are averages of continuous readings taken over a 60-second period.

Table 4.1: Force values and the corresponding output voltages(mV) for different known resistor values.

Force (g)	3 KΩ	10 KΩ	30 KΩ	43 KΩ	100 KΩ
50	904.7298	1264.813	2064.399	1964.19	2659.959
100	1526.848	2500.194	3786.423	3340.446	3810.976
150	1988.287	2984.977	4244.67	3988.47	4487.445
200	2391.704	3332.698	4435.663	4310.835	4698..26
250	2659.178	3588.216	4514.493	4498.235	4808.627
300	2876.575	3816.598	4546.34	4608.198	4845.813
350	3013.482	3931.492	4614.883	4688.685	4872.668
400	3087.201	3986.993	4664.6	4736.703	4893.678
450	3191.963	4061.514	4692.964	4766.977	4910.081
500	3335.099	4066.785	4718.374	4790.941	4914.27
550	3437.914	4140.819	4744.11	4797.221	4919.276
600	3402.424	4149.332	4752.585	4815.342	4921.941
650	3484.824	4202.781	4762.994	4818.265	4927.629
700	3520.611	4238.575	4775.178	4830.456	4934.56

The values in table 4.1 were plotted for different known resistor values as shown in figure 4.4.

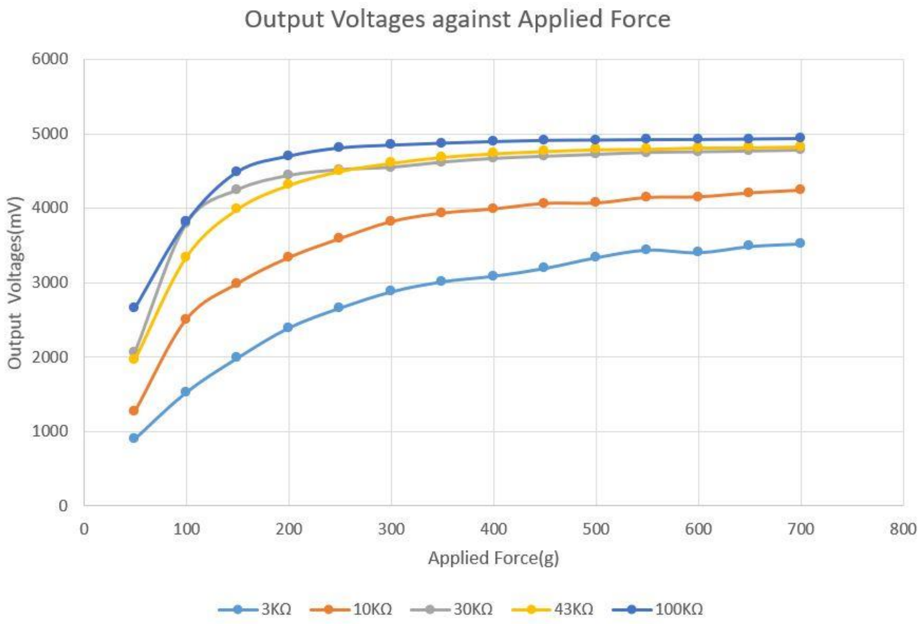

Figure 4.4: Plot of output voltages against applied force for the different known resistor values

In order to derive an equation showing the relationship between applied force and the voltage read by the microcontroller, force reading was plotted against voltage for the 3K resistor. The choice of the force and corresponding voltage values of the 3K resistor amongst other known resistor values was random.

Figure 4.5 shows the plot of the force values against their corresponding output voltage values for a 3K resistor.

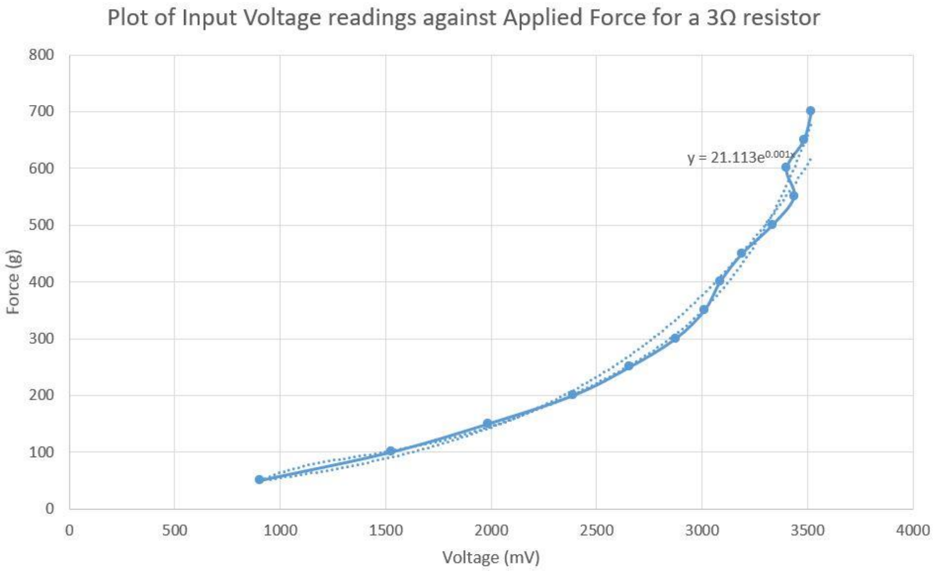

Figure 4.5: Plot of applied for against output voltages for a 3K resistor

The graph in figure 4.5 above can be represented by the equation below.

$$y = 21.113e^{0.001x} \tag{4.1}$$

Equation 4.1 was therefore used to program the force sensing resistors.

4.1.4 Study 1: Gripper Force Detection and Gripper Orientation Requirements

This study was designed to develop methods of characterizing objects for pick and place tasks. This involves identifying optimal force required grasp an object and investigating the need for gripper orientation during such tasks.

In this study, grasp of a cup was attempted mid air with the gripper of a Jaco^2 robot (with four force sensing resistors attached to the fingers). The grasp force was gradually increased as the gripper was close until the force applied was high enough to prevent slip and sufficiently grasp the cup for movement and manoeuvring. The Gripper setup with the force sensing resistors (FSRs) is shown in figure 4.6. For simplicity, only two of the three gripper fingers were used. Pairs of force sensing resistors were used on each finger and the force readings summed for each finger. During the study, FSRs provided gripper grasp force readings while the joint motor currents readings at each finger were polled from the robot.

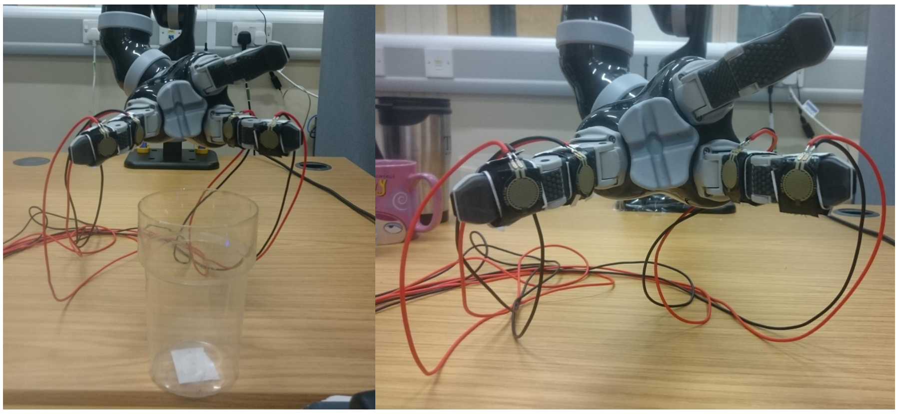

Figure 4.6: FSRs setup on the robot gripper

The gripper-finger joint motor currents (A) in the two fingers used were added together and plotted against time together along with the force readings (N) from the FSRs attached to the fingers.

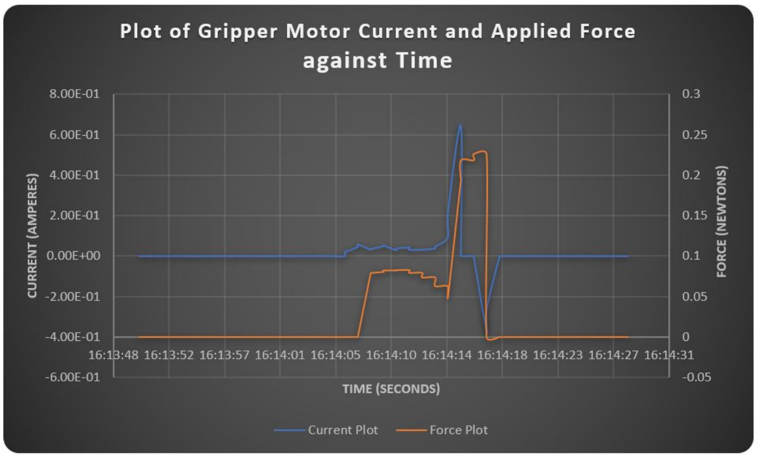

Figure 4.7: Determining optimal grasp force by plotting gripper grasp force and motor currents against time

In this study, optimal grasp force is defined as the force with which the gripper grasps an object without the possibility of slip. From figure 4.7 above, the optimal grasping force for a randomly chosen cup (fig. 4.6) is measured as the force reading corresponding to the peak motor current. The motor current rises as the gripper force is increased and falls immediately the grasp is released. Plotting the motor current and force against time makes it possible to identify the measured gripper corresponding to the highest gripper joint motor current. As shown in figure 4.7, the optimal gripper force corresponds to 0.21854 N. The gripper joint motor current readings were polled from the robot continuously via the serial ports for about three seconds with a 200 ms delay in each loop. The task was repeated three times and averages taken.

This provides a methodology for use in applications where predetermined grasp forces are needed to guide operators carrying out tele-manipulation tasks using different feedback modalities. It may also be important to provide guidance for robots carrying out tasks autonomously. Building a database of grasp forces for different objects can potentially make tele-operated tasks easier.

This study also involves the investigation of the effect of gripper orientation on grasp force. This was done by measuring the grasp force when grasp was achieved under two different scenarios. In scenario 1, the gripper was aligned vertically with the object to be grasped while in scenario 2, the gripper was intentionally misaligned with the object to be grasped. Vertical alignment is achieved if grasping takes place with the gripper parallel to the vertical axis of the object to be picked. Figure 4.8 and figure 4.9 show the optimal grasp forces for another randomly chosen plastic cup with and without correct gripper alignment respectively. The optimal grasp force measured when the cup was vertically aligned with the gripper from figure 4.8 is 0.22452 N while that measured without vertical alignment is 0.169638 N (fig. 4.9).

The reduced force values for the unaligned configuration may be because of the non-alignment of the force sensing resistors mounted on the fingers of the gripper to the object to be grasped. If the gripper is not aligned with the cup, the force sensitive resistors do not all make contact with the object and as a result, lower contact force is recorded. Another effect of the non-alignment of the gripper and object is that objects are picked up tilted and for objects with liquids in them, spillage may occur. This may also make it difficult to place objects on surfaces. Attempting to achieve grasp with the tip of the gripper resulted in greater amount of force being applied and did not present the robot with large enough contact surface for sufficient grasp. Also, the chances of having slip while attempting grasp were higher. The success of such attempts may vary based on the size and weight of the object to be picked.

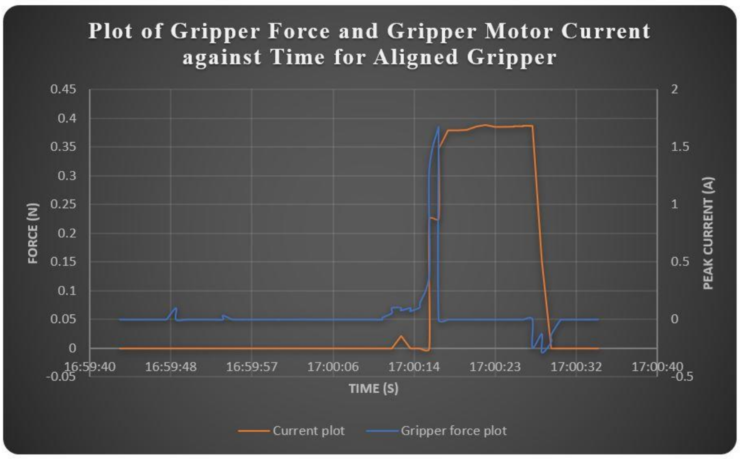

Figure 4.8: Determining optimal grasp force for a correctly aligned gripper

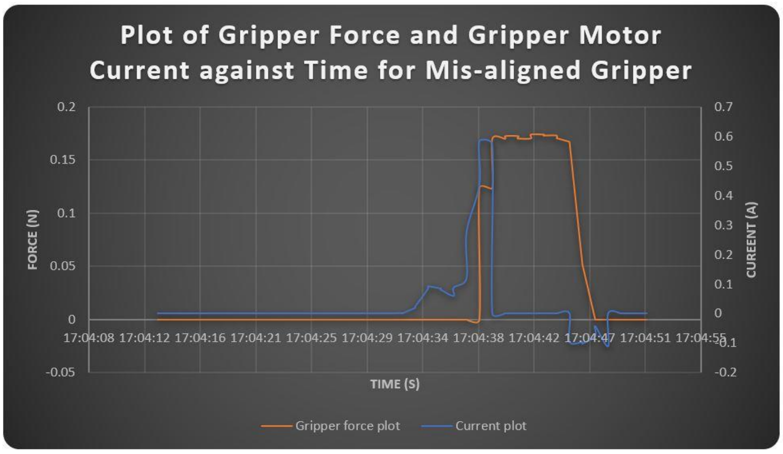

Figure 4.9: Determining optimal grasp force for a wrongly wrongly-aligned gripper

4.1.5 Discussion

In the study reported on subsection 4.1, we investigated the need to measure grasp force in a tele-operated pick-and-place task, and how changes in gripper orientation affect grasp force. The investigation was carried out using force sensing resistors (FSRs) calibrated and mounted on the robot gripper. Object grasp was carried out mid-air in order to make visual inspection of the grasp easier as well as to ensure that the weight of the cup used was fully supported by the robot gripper. This is particularly important as grasp force is difficult to determine using video cameras and the human operator will carry out a manipulation task solely with information conveyed via other feedback modalities. For other applications of robot tele-operation,grasp force may not be as important if the manipulated objects have fixed rigidity and shapes. However, in the context of assisted living, different objects of different characteristics and sizes will be manipulated which makes the measurement of grasp force very important. Results show that different grasp forces were recorded as gripper orientation changed, suggesting that it is also important to measure the orientation of the gripper. Likewise, changes in gripper orientation also influenced the ease with which the grasped cup could be successfully placed back on a table, further supporting the need to convey information about the gripper orientation to operators. An alternative to measuring gripper grasp force may be to use active soft end effectors as suggested by [8]. However, developing miniaturised grippers with such capabilities may required more work.

The findings of this study (which support need to convey gripper orientation to human operators) informed the design of the next study where we investigated optimal feedback modalities for conveying gripper orientation to the operator.

4.2 Study Phase 2: Investigating Optimal Sensory Feedback Modalities

4.2.1 Introduction

A very important factor to consider when providing remote support to people, especially when helping with activities of daily living is 'the feeling of being present' with the service users. This concept is often referred to as 'tele-presence'. To achieve that, a human operator should be provided with as much information (through feedback) about the remote environment as possible. Providing feedback to an operator however comes with a lot of challenges, some of which include:

1. Identification of the most effective feedback modality or combination of feedback modalities for each sensor data required for successful tele-operation.

2. Identifying suitable transformations needed to map sensor data into useful information through feedback.

3. Minimising cognitive load on the operator without compromising the information content of the feedback.

4. Provision of diagnostic information to the operator to ensure safe task completion.

To provide answers to the questions asked above, this study is designed to explore the use of different feedback modalities to convey sensor data (gripper orientation) to participants. Before the actual study, a pilot study was carried out to validate the study setup with human participants. Results of the pilot study influenced a re-evaluation of the methodology for the main study.

4.2.2 Feedback Mechanisms

After an extensive literature review on feedback modalities, some feedback modalities were chosen for exploration based on the application domain of this thesis, as well as availability and cost.

4.2.2.1 Video feedback

For all feedback scenarios examined in the studies carried out, video feedback of the tele-operated robot and work environment was provided. Real time video feedback was provided to participants on a computer monitor. Each camera view was displayed on separate quadrants on the video feedback screen as shown in figure 4.10. For the piot study, three camera angles (fig. 4.10a) were provided but was increased to four (fig. 4.10b) in the actual study.

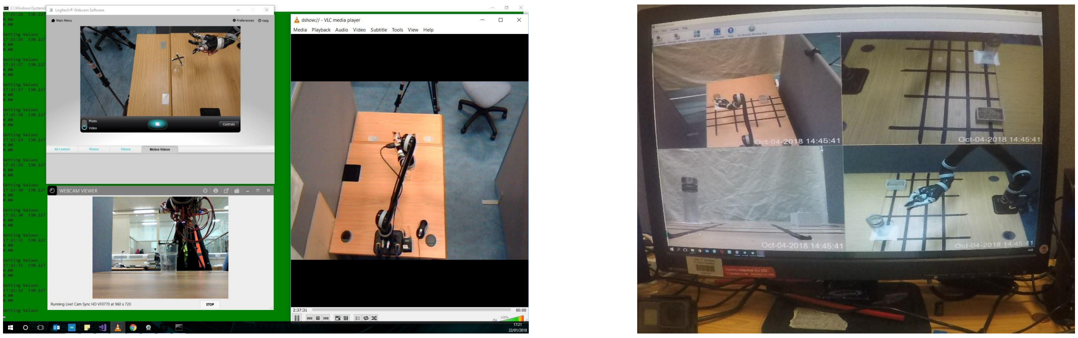

(a) (b)

Figure 4.10: Video feedback, (a) pilot study (b) actual study

4.2.2.2 Haptic feedback

The methodology chapter of this thesis extensively describes the different iterations to the haptic feedback device.

For the pilot study carried out by the principal researcher, haptic feedback was provided through a grove haptic motor [169] embedded in a wristband and driven by a haptic controller board, Seeeduino V4.2 (Seeed, 2021). The actuators are the same used by Andualem et al, in their publication titled “Wearable Vibrotactile Haptic Device for Stiffness Discrimination during Virtual Interactions” [112].

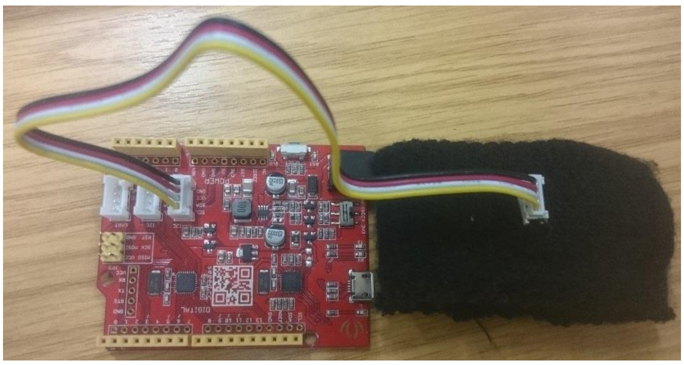

Figure 4.11: Wrist-worn haptic feedback device powered with the Seeduino board

The control board was designed with a library of 123 vibration patterns, of which three (3) distinguishable patterns were chosen for use in the pilot study.

In order to improve the usability of the wrist-worn haptic feedback device, Wi-Fi enabled haptic wristbands (fig. 4.12) were designed to provide haptic feedback to participants in the next study with human participants. A wrist-worn haptic feedback device is worn on each arm to signify the direction of orientation of the robot gripper.

(a) (b)

Figure 4.12: Phase-2 haptic feedback device, (a) complete design (b) haptic motor and control board

The orientation of the robot gripper was mapped to the amplitude of vibrations of the haptic feedback device using the mathematical map() function in the Arduino IDE. Two different ranges of values can be mapped using 'fromLow to toLow' and 'fromHigh to toHigh'. In-between values are taken care of in the function. The syntax is given below:

$$Y = map(value, fromLow, fromHigh, toLow, toHigh) \tag{4.2}$$

Parameters
Value: the number to map
fromLow: the lower bound of the value's current range
fromHigh: the upper bound of the value's current range
toLow: the lower bound of the value's target range
toHigh: the upper bound of the value's target range

The orientation of the robot gripper was grouped as a range of values into three (3) states, namely:

1. Vertically aligned: From empirical tests carried out, the ranges of values of the orientation of the gripper (in degrees) which correspond to the vertically aligned state of the gripper were identified (table 4.2). In this state, there are no vibrations from either of the two wrist-worn haptic devices.

2. Tilted left: The 'tilted left' state is achieved if the gripper's orientation is to the left of the vertical axis of the object to be grasped. In this state, the haptic device worn on the left hand vibrates. The farther away the gripper's orientation is from the object's vertical axis, the higher the amplitude of vibration of the haptic feedback device.

3. Tilted right: Gripper orientations to the right of the vertical axis of the object is referred to as the gripper being tilted right. Its range of values was found to be $-221^0 – 124^0$.

Table 4.2: Gripper orientation ranges for the haptic feedback

Orientation classification	**Wrist haptic feedback**	**Gripper orientation ranges (degrees)**
Vertically aligned	No vibration	125^o – 134^o, 482^o – 492^o, and -231^o – -234^o
Gripper tilted left	Left	134^o – 482^o
Gripper tilted right	Right	-221^o – 124^o

The gripper orientation values in table 4.2 above are specific to the Kinova Jaco^2 robot [88].

4.2.2.3 Peripheral Vision Feedback

This involves conveying gripper orientation information via colour changes in the peripheral of participants' field of view.

Table 4.3 shows how peripheral vision was used to display the orientation of the gripper to participants.

Table 4.3: Colour code interpretation for peripheral vision feedback

Orientation classification	**Gripper orientation ranges (degrees)**	**Colour Representation**
Aligned with the vertical axis of the cup	125 – 134, 482 – 492, -221 – -231	Green
A little tilted to the the left	135 – 140	Light blue
Farther to the left from the aligned position	141 – 482	Deep blue
A little tilted to the right	120 – 125	Light red
Farther to the right from the vertical alignment	-221 – 120	Deep red

This study involves the use of 3 colours - Blue, Green and Red as well as a shade of red and blue. The colours chosen were chosen with reference to the three types of photopigments contained in the three types of cones contained in the retina. The cones are referred to as short (S), medium (M), and long (L) wavelength cones. The naming convention implies that each type of cone provides colour information for the wavelength of light that excites them best [150].

4.2.2.4 Verbal Feedback

Considering the need for social interaction, the researcher provided verbal cues prompting participants to adjust the position of the robot end effector whilst avoiding providing information about the orientation of the robot end effector. Some of the key words used were: move up, move downwards, to the left, to the right, OK, let's go deliver the content, open the gripper, close the gripper, etc. Answers were also provided based on the questions asked by participants. Verbal interactions also comprised comments relating to how they were feeling and the occurrence of video lags.

4.2.3 Pilot study

To test the functionality of the system and in preparation for experiments with human participants, the principal researcher carried out a pilot study on the task using three feedback scenarios. The task was repeated three times with each feedback modality scenario to check for the possibility of learning. The feedback modality scenarios are listed below:

1. With only video feed of the robot environment

2. With peripheral vision and video feed of the robot environment.

3. With peripheral vision, haptics feedback and video feed of the robot environment.

The video feedback showed video feed of the robot environment and environment captured by three cameras (fig. 4.10a). Gripper orientation was mapped to peripheral vision feedback and haptic feedback. Feedback on the grasp force was not presented but the grasp force was recorded as the task was repeated.

4.2.3.1 Procedure for pilot study

The study protocol is listed below

1. Using the robot controller to control the robot arm, grasp the cup at the right position

2. Move the object to the desired position

3. Release the object

4. Move the robot arm back to its home position

4.2.3.2 Results for pilot study

Table 4.4: Time taken to carry out a tele-operated task using different feedback scenarios

Feedback Scenarios	**Attempt 1 task completion time**	**Attempt 2 task completion time**	**Attempt 3 task completion time**	**Average task completion time**
1: With only video feedback of the robot end	305.915 secs	262.123 secs	247.71 secs	271.916 secs
2: With peripheral vision and video feed of the robot end	230.78 secs	265.691 secs	275.745 secs	257.405 secs
3: With periph- eral vision, haptics feedback and video feed of the robot end	248.267 secs	199.198 secs	183.102 secs	210 secs

Table 4.4 shows the time taken to carry out the task for different feedback scenarios. The highest task completion time was recorded for the feedback scenario with only video feedback from the three cameras. Lower task completion times were recorded when additional feedback was introduced. It is yet to be statistically confirmed if trial order has any significant effect on the task completion time for the different feedback scenarios. The lowest task completion time was recorded for the feedback scenario with a combination of peripheral vision feedback, haptic feedback, and video feedback. Figure 4.13 shows the plot of task completion time of different attempts for different feedback scenarios. Task completion time reduced for scenarios 1 and 3 as the task was repeated.

Table 4.5 shows the final position of the grasped cup after the task was completed. 'NU' in the table implies 'Not Upright' while 'U' implies 'Upright'. The regions shaded green implies that the gripper was successfully aligned with the vertical axis of the cup before it was picked up while sections shaded blue imply that the gripper orientation was slightly to the left of the aligned orientation. As shown in the table, 75% of cases where the gripper orientation was not aligned before grasp, the cups fell over at the end of the task.

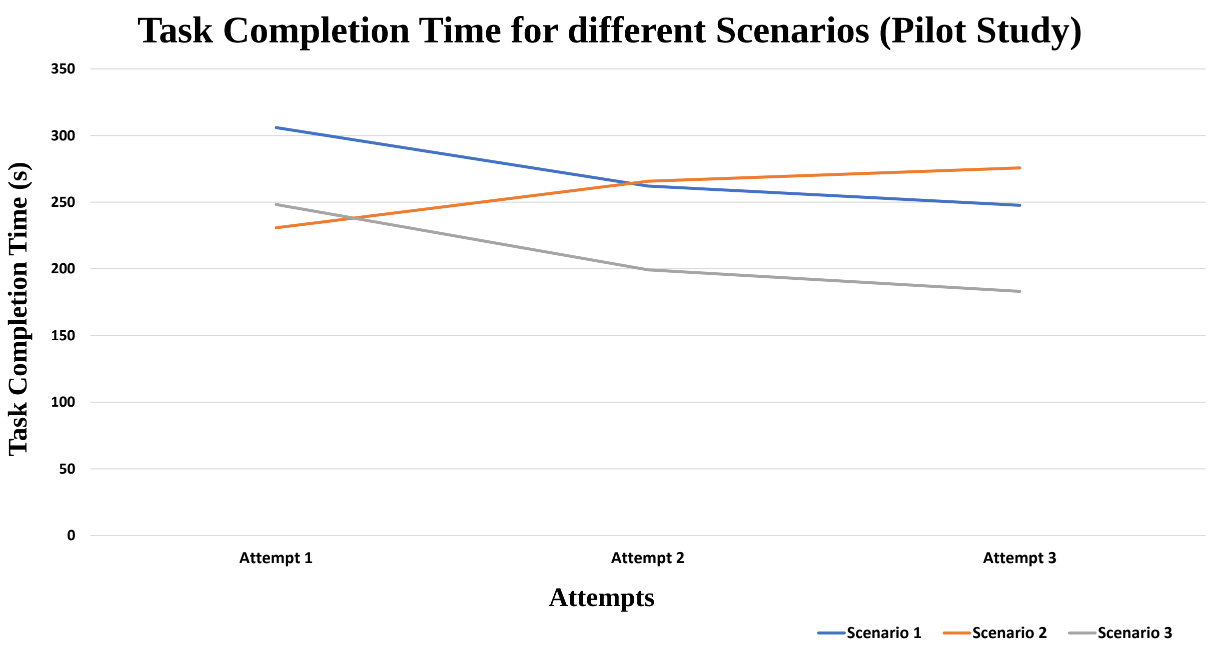

Figure 4.13: Task completion time for different feedback scenarios (pilot study)

Table 4.5: Effect of gripper orientation on final position of an object

	Feedback Scenario 1	**Feedback Scenario 2**	**Feedback Scenario 3**
Attempt 1	NU	NU	U
Attempt 2	U	U	NU
Attempt 3	U	NU	U

Table 4.6 below shows the gripper grasp force readings applied during each attempt. It also shows the average grasp forces for the different scenarios.

Table 4.6: Gripper grasp force readings

	Feedback Scenario 1	**Feedback Scenario 2**	**Feedback Scenario 3**
Attempt 1	0.276262 N	0.10731 N	0.139454 N
Attempt 2	0.494704 N	0.093492 N	0.954716 N
Attempt 3	0.172872 N	0.674534 N	0.213542 N
Average grasp force	0.314613 N	0.291778 N	0.435904 N

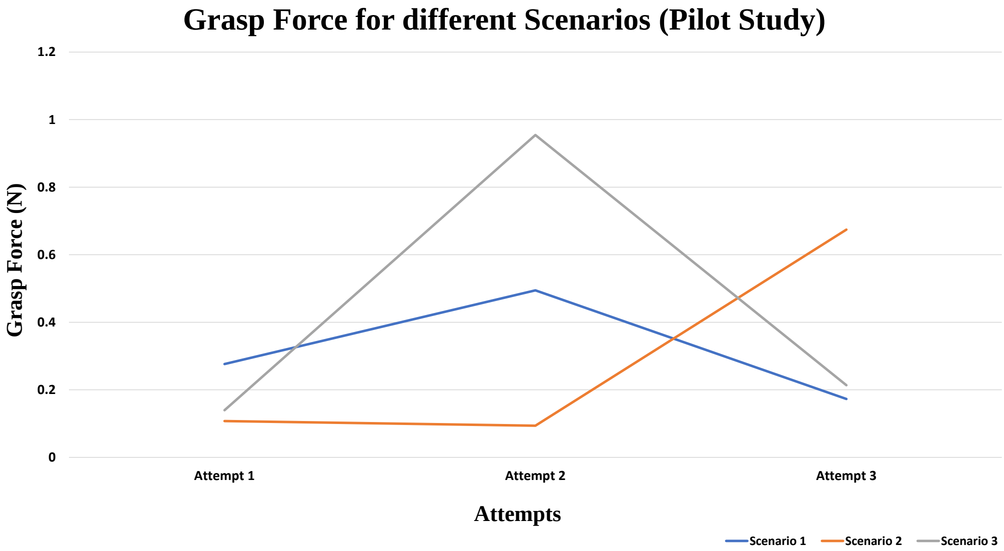

Figure 4.14: Plot of gripper grasp force for different scenarios (pilot study)

Plot of gripper grasp force for different scenarios is shown in figure 4.14. Whilst the grasp force reduces with repetition for scenarios 1 and 3, it increased for scenario 2.

4.2.3.3 Discussion and Conclusion

Average recorded task completion time was highest for scenario 1. The high task completion time may be because the principal researcher had to extract all information needed from video feedback alone. Table 4.4 shows that the average task completion time reduced with supplementary feedback, but it is also important carry out further studies to understand the significance of each additional feedback introduced. Having force feedback may not be enough to successfully carry out tasks but a combination of the force applied and an understanding of how the grasp takes place using robot gripper orientation. However, feedback on gripper orientation, if not used carefully may distract an operator and cause an increase in task completion time.

Using a pick and place task (of a cup) to understand the role correct gripper orientation plays in grasp, table 4.5 shows results for different feedback scenarios. In 83.3% of attempts where the gripper was correctly aligned with the vertical axis of the object before grasp, the cup was successfully placed without tipping off. This further confirms the need for feedback about the gripper orientation.

Grasp force shown in table 4.7 was recorded as the task was carried out. The goal was to examine how gripper orientation affects grasp. The results were non-conclusive, and more studies will be carried out. The use of 3 cameras did not capture all views of the robot environment. 4 cameras will be used in the next study.

4.2.4 Identifying Optimal Feedback Modalities for Conveying Gripper Orientation

Results from the pilot study prompted adjustments to the study setup. The number of camera views of the remote service user environment was increased to four from three (fig. 4.10b). Iterations were also made to the hardware and software of the haptic feedback device.

The pilot study confirmed the need for feedback on the gripper orientation and grasp force. It also confirms the usefulness of haptic feedback and peripheral vision. A third modality introduced in the next study is verbal feedback. The verbal feedback introduced was in the form of social interaction between the principal researcher (acting as the service user) and participants (acting as operators).

Participants were required to move a jar filled with sunflower seeds from one location to another and then empty the content into another jar. The task was carried out under different feedback scenarios with varying combinations of feedback and verbal collaboration. The different feedback scenarios were designed to communicate the gripper orientation to participants.

4.2.4.1 Experimental set-up

Figure 4.15: Study setup

The study setup in figure 4.15 was designed to represent the operator interface (left) and the remote service-user environment (right).

Figure 4.16 shows the operator interface of the setup.

Figure 4.16: Operator Interface of the study setup

The different hardware requirements for the operator interface setup is examined.

Operator-interface hardware

1. Laptop Computer

   The laptop was used as the central processing hub of the study. Input from the Jaco^2 robot, web cameras, and button input from the principal researcher are processed in software with the laptop computer. The laptop also communicates via Wi-Fi with the haptic devices. Two additional computer monitors were used to extend the computer screen. This makes it possible to have the web-cam views on one screen and display the peripheral information on another screen.

2. Web Camera display monitor and Peripheral Vision display monitor

   Videos of the remote service user environment captured by web cameras were displayed to the participants on a monitor as shown in figure 4.17. The peripheral vision display monitor displays gripper orientations in participants' peripheral vision as series of colours.

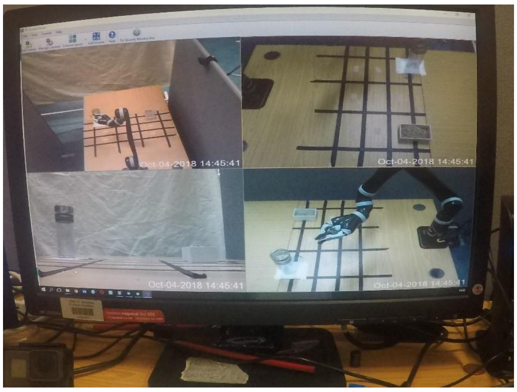

Figure 4.17: Video feedback of the remote service user environment displayed to participants (operators)

3. Tobii eye tracker

   The Tobii eye tracker was used to capture participants' gaze metrics as they carried out the task during the study.

Figure 4.18: Tobii eye tracker [189]

4. Wearable haptic wristbands (fig. 3.4)

   The wrist band was designed to provide participants with information about the orientation of the gripper using haptic feedback. This is the phase-2 haptic design with four (4) vibrating motors. Data was sent from the control PC to the haptic devices over a wireless network using Client-Server communication (WinSock). Each wristband has an IP address through which the client identifies the individual wristband over a network and connects to them. The calibration and feedback use are described in section 4.2.2.2.

Operator interface software

Different software was written or used by/for different hardware used for the study.

1. Visual Studio Professional (IDE)

   The processing software on the control pc was written in C++ using the visual studio integrated development environment (IDE). The software allows data to be polled from the Jaco^2 robot using the kinova API, mapped, and displayed through different feedback modalities.

2. Arduino IDE

   Software for the haptic control boards and the principal researcher's stage success/completion buttons were written in c programming language using the Arduino IDE.

3. IP Camera viewer

   The IP camera viewer was used to display live video from four (4) web cameras to participants on a single computer screen.

Service-user environment hardware

Figure 4.19: Remote service user environment of the study setup

Figure 4.19 shows the service-user end of the study setup. It comprises a Jaco^2 robot, web cameras, a jar and a container in which sunflower seeds was emptied.

1. Kinova Jaco^2 robot

Figure 4.20: Kinova Jaco^2 robot

2. Web Cameras

   Four (4) web cameras were used to capture video of the remote service user environment. The four (4) cameras capture four different views and are displayed to the participants on a computer display.

3. Researcher feedback button

   With the principal researcher performing the role of service user, an array of buttons was created to signal task stage completion and success or failure. This makes it possible to log the completion time for each stage of the task, as well as whether the stage was successfully completed or not.

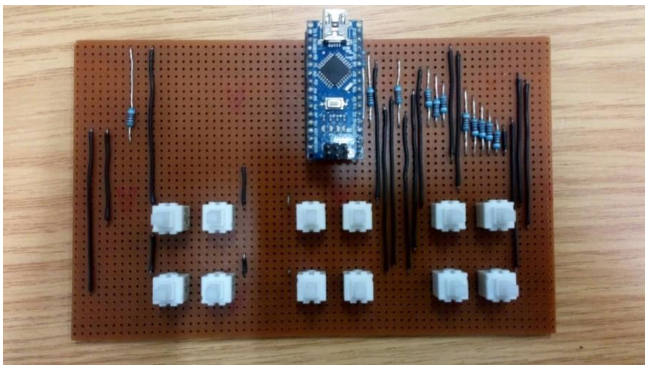

Figure 4.21: Researcher feedback button

Figure 4.22 shows the block diagram for the study hardware and software interaction. It also shows the data interaction between the different components.

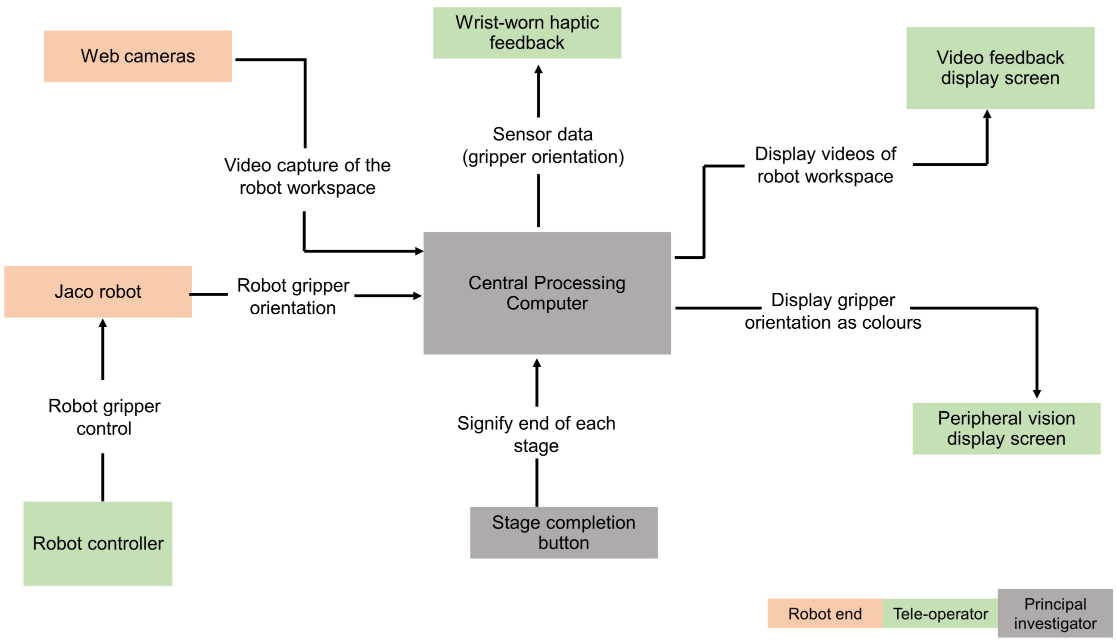

Figure 4.22: Block diagram for the study hardware and software interaction setup

4.2.4.2 Feedback Scenarios

Feedback scenarios refer to different combinations of feedback modalities provided to participants as they carried out the task. Feedback scenarios were used to display information about gripper orientation to participants. Table 4.7 shows the different feedback scenarios employed.

Table 4.7: Feedback scenarios showing the different combinations of feedback modalities

	Video Feedback	**Peripheral Video Feedback**	**Verbal collaboration**	**Haptic feedback**
Scenario 1 (Video Feedback only)	✓			
Scenario 2 (Verbal collaboration)	✓		✓	
Scenario 3 (Peripheral vision)	✓		✓	
Scenario 4 (Peripheral vision and Verbal collaboration)	✓	✓	✓	
Scenario 5 (Haptic feedback)	✓			✓
Scenario 6 (Haptic feedback and Verbal collaboration)	✓		✓	✓
Scenario 7 (Haptic feedback, Peripheral vision, and Verbal collaboration)	✓	✓	✓	✓

To ensure that the experiment is fair, counterbalance measures were put in place to ensure that participants did not carry out the tasks in the same order with feedback modalities.

Counter Balancing order for feedback scenarios

1. Carry out the task with video feedback only.
2. Carry out the task with video feedback and in collaboration with the researcher.
3. Carry out the task with video feedback and peripheral vision only.
4. Carry out the task with video feedback and peripheral vision with collaboration with researcher.
5. Carry out the task with video and haptic feedback only.
6. Carry out the task with video and haptic feedback in collaboration with the researcher.
7. Carry out the task with video feedback, peripheral vision, and haptic feedback in collaboration with the researcher.

The randomised task orders assigned to participants is shown in table 4.8 below

Table 4.8: Randomised order of feedback scenarios for participants

Participants	**Order of scenario**
4,11	1,2,3,4,5,6,7
3,5	2,3,4,5,6,7,1
6,7	3,4,5,6,7,1,2
2	4,5,6,7,1,2,3
8,9,10	5,6,7,1,2,3,4
1	6,7,1,2,3,4,5

4.2.4.3 Hypotheses

To carry out the task, participants were required to pick up a jar containing sunflower seeds and empty the content of the jar into an empty container. Participants were also required to return the emptied jar to its initial location. The task was repeated seven (7) times using different feedback scenarios. Each task repetition is referred to as an attempt. For detailed analysis, the task was divided into four (4) stages described below:

1. Free-space translation and rotation of the gripper from its start position to a position close enough for grasp.

2. Grasping the jar and making free-space translation to a position where it's content can be emptied.

3. Free-space rotation and translation of the jar to empty its content.

4. Free-space translation and rotation of the emptied jar to its pickup position.

As participants carried out the task, certain parameters were measured for analysis. The measured parameters include:

1. Task stage completion, success, and completion time

   To understand how the different feedback scenarios impacted the success of the task, the task stage completion and the overall task completion time were recorded. As participants carried out the task, the principal researcher, acting as a service user, signalled the end of each stage of the task and the success or failure of each stage with an array of buttons. At each signal the completion times and success of each stage of the task was recorded. .

2. Participants' gaze metrics

   The Tobii eye tracker [189] was used to record gaze data (gaze duration and fixation count) needed to understand how participants interacted with the setup and the feedback modalities.

3. Robot joint steps

   We recorded the sum of robot joint movements in the x-y-z coordinates as participants controlled the robot. It is values are polled from the robot using the Kinova API. It was important to understand how the sum of robot joint steps vary under different feedback scenarios.

Having identified the variables to be measured the hypotheses listed below were made.

1. **H1:** Task repetition improves the task completion time, as well the overall robot joint steps.
2. **H2:** The use of feedback improves the accuracy with which the jar is grasped.
3. **H3:** Verbal collaboration between the operator and a service user improves operator's ease of use of the system and success in completing the task.
4. **H4:** Prior gaming and robotics experience improves operators' performance (task completion time and accuracy of grasp).
5. **H5:** The introduction of feedback reduces the task completion time.
6. **H6:** Feedback modalities affect the operator's gaze time on different camera views.
7. **H7:** There is a learning effect in the operator's control of the robot as the task is repeated.

4.2.4.4 Study

Ethics approval was granted by the research and ethics committee of the university of the west of England. Appendix A shows the consent form participants read and signed before taking part in the study. Appendix B shows the demographic questionnaire used to gather participant data. With Appendix C information about the study was conveyed to participants. At the end of each study attempt, participants were required to fill a system usability questionnaire shown in Appendix D. Appendix D also contains ease of use questionnaire participants completed. The study protocol is shown in Appendix E.

4.2.4.5 Results

The study was carried out with 13 participants (data gathered from two (2) participants was eventually excluded from the analysis due to incomplete data) with varying demographics and previous experiences with games and robots. Each participant repeated the task seven (7) times according to table 4.8.

1. **Ease of Use**

Analysis was caried out to compare participants' subjective rating of the ease of use of the different feedback modalities. Non-parametric Friedman's ANOVA [44] showed a significant main effect of scenario $\chi^2(6) = 37.56, p < .001$, suggesting that participants perceived some scenarios to be easier to use than others. Having a priori hypothesis that adding any type of feedback to visual information will improve perceived ease(H3), all scenarios (S2, S3, S4, S5, S6 and S7) were compared to the scenario with only visual feedback(S1). The comparison with Wilcoxon Signed Rank tests showed that all conditions with verbal feedback significantly improved participants' ease of use ratings on the task. Comparing S1 with S3 showed a trend after adjusting for multiple comparison with Bonferroni test (p = .009) (table 4.9).

Table 4.9: Means and standard deviation for ease of use scores across conditions and Wilcoxon signed rank test result for pairwise comparison.

Feedback Scenarios	**Mean**	**SD**	**S2**	**S3**	**S4**	**S5**	**S6**	**S6**
S1	5.5	2.84	Z = 2.83, p = .005, r = .60	Z = 2.32, p = .02, r = .50	Z = 2.82, p = .005, r = .60	Z = 0.76, p = .439, r = .17	Z = 2.68, p = .007, r = .57	Z = 2.81, p = .005, r = .60
S2	8.00	1.55		Z =1.87, p = .062, r = .40	Z = 2.12, p = .034, r = .45	Z = 1.96, p = .05, r = .42	Z = 0.96, p = .336, r = .21	Z = 2.41, p = .016, r = .51
S3	6.82	2.27			Z = 2.38, p = .017, r = .51	Z = 1.22, p = .22, r = .26	Z = 2.12, p = .034, r = .45	Z = 2.44, p = .015, r = .52
S4	8.55	1.04				Z = 2.44, p = .015, r = .52	Z = 0.56, p = .58,r = .12	Z = 1.67, p = .096, r = .36
S5	5.91	3.11					Z = 2.68, p = .007, r = .57	Z = 2.62, p = .009r = .56
S6	8.36	1.29						Z = 1.82, p = .068, r = .39
S7	9.00	0.89						

Multiple Wilcoxon Signed Rank tests with Bonferroni multiple comparison adjustment were performed (table 4.9) to confirm H3. The results confirm that scenarios with verbal feedback relates to participants' increased ease of use rating with S7 being reported as easiest to use. The Wilcoxon Signed Rank test indicated trend differences with S2, S3 and S5, but no significant difference with S4 and S5. This result further confirms that participants' perception of task difficulty was reduced with verbal feedbak (task completion was perceived as easier compared to conditions with no verbal feedback). As a second step, analysis on the System Usability Scale (SUS) [57] was conducted to investigate if the system was more usable with particular modalities (a SUS score above a 68 is considered average, table 4.10). Results, although not significant (Friedman's ANOVA $p \geq .312$; table 4.10), confirms the same pattern of perceived usability scores – S1 condition was scored with the lowest scores, while conditions with verbal feedback (S2, S4, S6, S7) received higher results.

2. **Task Performance**

   Friedman ANOVA's was conducted on the sum of robot joint steps and time needed to complete stage 1, and accuracy of gripper orientation before grasp (table 4.10). Higher scores imply higher gripper accuracy. Figure 4.23, figure 4.24, figure 4.25, and figure 4.26 show the plots of parameter mentioned on table 4.10. The mentioned parameters were analysed for stage 1 because of the effect the success or failure of stage 1 has on the overall success of the task. Also, stages 2 and 3 can be carried out without supplementary feedback to the video feedback and so consideration was given to not including data measured across these stages. Wilcoxon Singed rank test was used to explore further differences for a prior hypothesis that the introduction of additional feedback modalities will yield improved performance (H2 and H5) compared to the scenario where only video feedback was used.

Table 4.10: Mean and standard deviations for robot joint movements and stage one completion time, stage 1 orientation accuracy and SUS Scores or each scenario

Feedback Scenarios	**Sum of discrete number of robot joint movements**		**Completion time (seconds)**		**Orientation accuracy scores**		**SUS**	
	Mean	**SD**	**Mean**	**SD**	**Mean**	**SD**	**Mean**	**SD**
S1	266.50	113.84	84.92	28.36	2.27	1.95	63.18	22.08
S2	155.50	12.02	87.02	33.35	1.64	1.91	73.64	15.43
S3	150.50	27.58	125.16	71.64	3.55	2.11	66.36	16.06
S4	135.50	6.36	110.61	44.56	5.00	0.00	73.64	13.48
S5	327.50	236.88	138.74	69.20	1.55	2.30	64.32	18.27
S6	391.50	133.64	115.54	50.91	1.91	2.17	70.45	17.85
S7	122.50	62.93	121.27	27.24	4.45	1.21	71.82	16.21

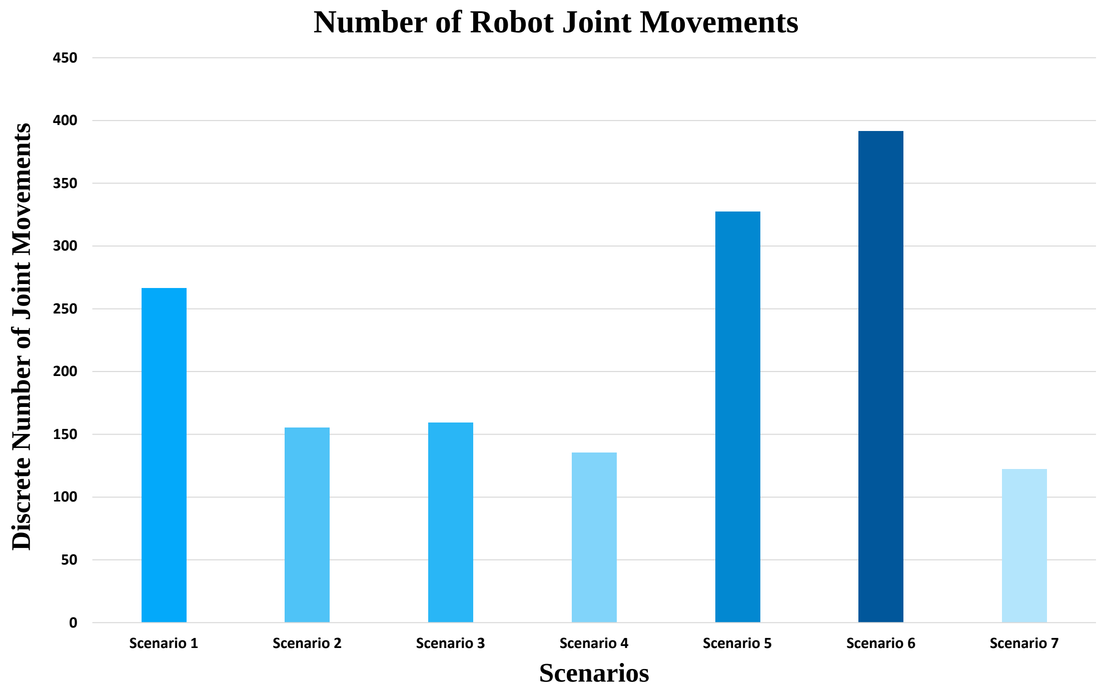

Figure 4.23: Sum of robot joint steps for all scenarios

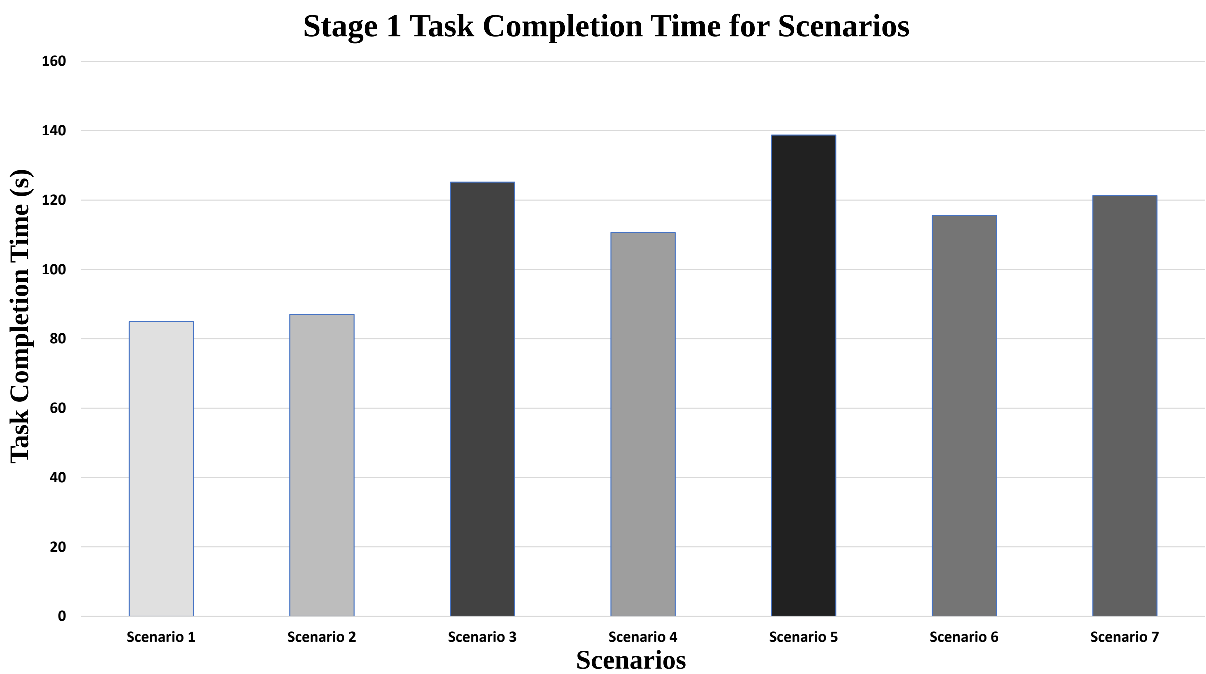

Figure 4.24: Stage 1 task completion time for all scenarios

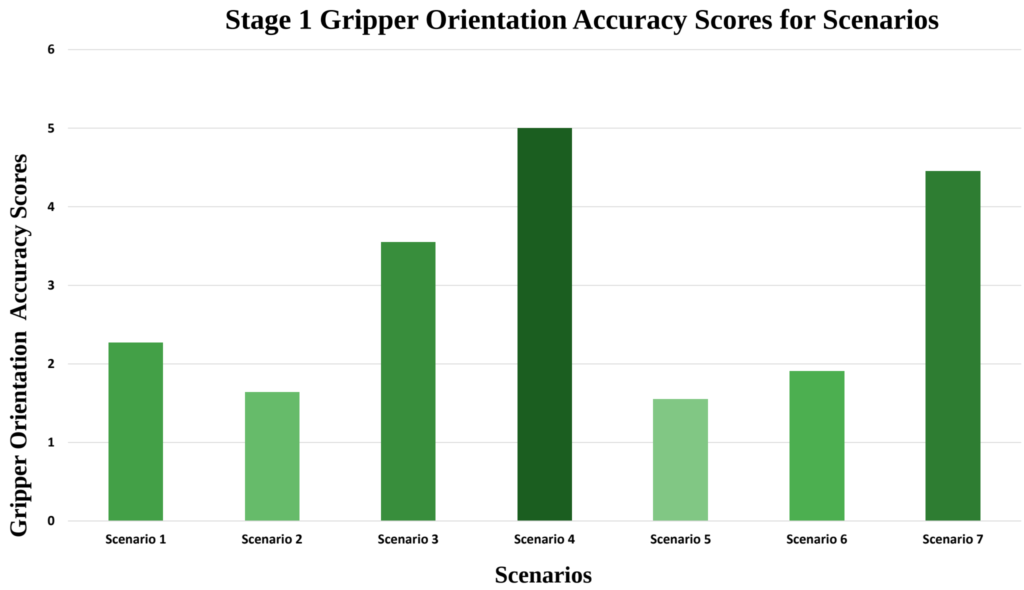

Figure 4.25: Stage 1 gripper accuracy scores for all scenarios

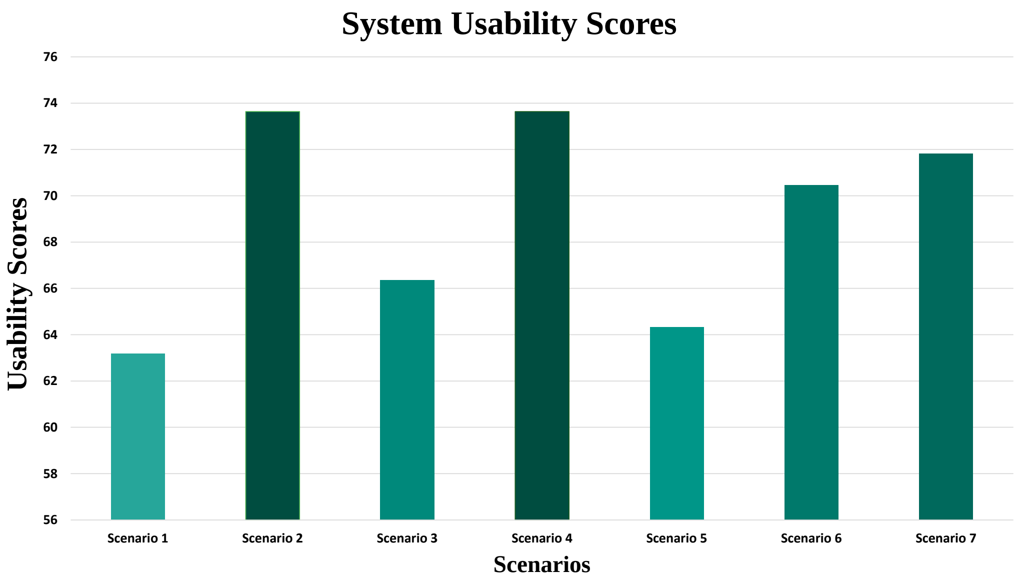

Figure 4.26: System usability scores

a) **Sum of robot joint steps (joint movements):** Friedman's ANOVA was not significant (p = .259), indicating that the joint movements taken were similar across all conditions. However, Scenarios S5 and S6, compared with S1 required the most convoluted joint movements (highest values for the sum of joint movements), while S7 had the simplest trajectory needed to complete the task.

b) **Stage Completion Time:** Friedman's ANOVA on time needed to complete stage 1 suggests that there was a main effect of modality ($\chi^2(6) = 13.01, p = .043$). Paired Wilcoxon Signed Rank test comparisons between all scenarios with S1 indicated differences with S3, S4, S5, S6 and S7 ($p = .026, p = .033, p = .010, p = .041 and p = .021$, respectively; table 4.11). However, these differences were not significant after multiple comparison correction. The only approaching significance difference was between S1 and S5 – Video and Haptic Feedback ($Z = 2.58, p = .010$).

c) **Gripper Orientation:** Friedman's ANOVA on robot orientation while completing stage 1 suggests that there was main effect of feedback modality ($\chi^2(6) = 26.79, p < .001$; table 4.11). Paired Wilcoxon Signed Rank test comparisons between all conditions with S1 (video feedback only) indicated a significant improvement in orientation in S4 ($Z = 2.60, p = .009$) and a trend significance between S1 and S7 after multiple comparison adjustment ($Z = 2.41, p = .016$).This result is consistent with the subjective ease of use and SUS results, indicating that verbal feedback is important for successful task completion.

d) **Impact of Gaming and Robot Usage Experience:** It was hypothesised that participants' gaming and robot usage experience improves participants' tele-operation performance (H4). Spearman's rho correlation coefficient indicates that there was a significant negative correlation between participants gaming experience and stage 1 completion time in S7 ($Spearman'srho = -.707, p = .022$). This suggests that participants with greater gaming experience completed stage 1 in S7 more quickly. Furthermore, robot experience was negatively correlated to the time needed to complete stage 1 in S1 ($Spearman'srho = -.66, p = .027$) and the sum of the number of discrete robot arm joint movements (overall robot arm trajectory) needed to complete stage 1 in S5 ($Spearman'srho = -.7815, p = .025$). The more robotics experience participants had, the less time they needed to complete stage 1 in S1. Similarly, with greater robotics experience, the sum of the number of discrete robot arm joint movements needed to complete stage 1 in S5 decreased. As S1 and S5 were conditions without verbal feedback, this suggests that verbal feedback helps people without gaming or robotics experience to perform as highly as people familiar with such tasks (gamers and robot users/researchers).

e) **Order effects:** To control for possible order effects, Friedman's ANOVA was performed to investigate if participants' ability to correctly orient the gripper, perceived ease of use, completion time and sum of the number of discrete robot arm joint movements needed to compete stage 1 reduced with every attempt at completing task. Investigation on the completion time for stage 1 of the task with non-parametric Friedman ANOVA showed that participants were significantly quicker to complete the task depending on the attempt, $\chi^2(6) = 22.35, p = .001$. The Wilcoxon Signed Rank test indicated that compared to attempt 1, time needed to complete attempt 4, attempt 6 and attempt 7 significantly decreased ($Z = 2.70$, $p = .007$, $r = .58$, $Z = 2.67$, $p = .008$, $r = .57 and Z = 2.67$, $p = .008$, $r = .57$, respectively), while this decrease was at a trend compared to attempt 3 and attempt 5 ($Z = 2.30$, $p = .022$, $r = .49 and Z = 2.50$, $p = .013$, $r = .53$). Using the Friedman's ANOVA test, neither ease of use, completion time nor sum of the number of discrete robot arm joint movements needed to compete stage 1, were affected by having more practice at completing the task ($\chi^2(6) \leq 19.14$, $p \geq .166$; table 4.11).

Table 4.11: Mean values for time needed to complete stage 1, orientation accuracy, and sum of the number of discrete robot arm joint movements for stage 1 as well as ease of use rating as a function of condition presentation order

Order	**Time to complete stage 1**		**Orientation accuracy for stage 1**		**Robot joint steps for stage 1**		**Ease of use**	
	Mean	**SD**	**Mean**	**SD**	**Mean**	**SD**	**Mean**	**SD**
1	358.50	96.54	2.18	2.36	653.00	192.67	7.64	2.11
2	315.52	81.93	2.18	2.36	563.20	270.68	7.64	2.54
3	288.15	89.58	3.73	1.85	467.75	233.67	7.09	2.47
4	270.97	97.69	3.09	2.30	482.29	160.28	7.09	2.55
5	243.60	83.22	2.55	2.11	489.13	262.11	7.64	1.80
6	206.63	51.60	3.27	2.10	325.25	166.49	7.73	2.53
7	199.83	58.92	3.36	2.34	284.25	142.67	7.64	2.50

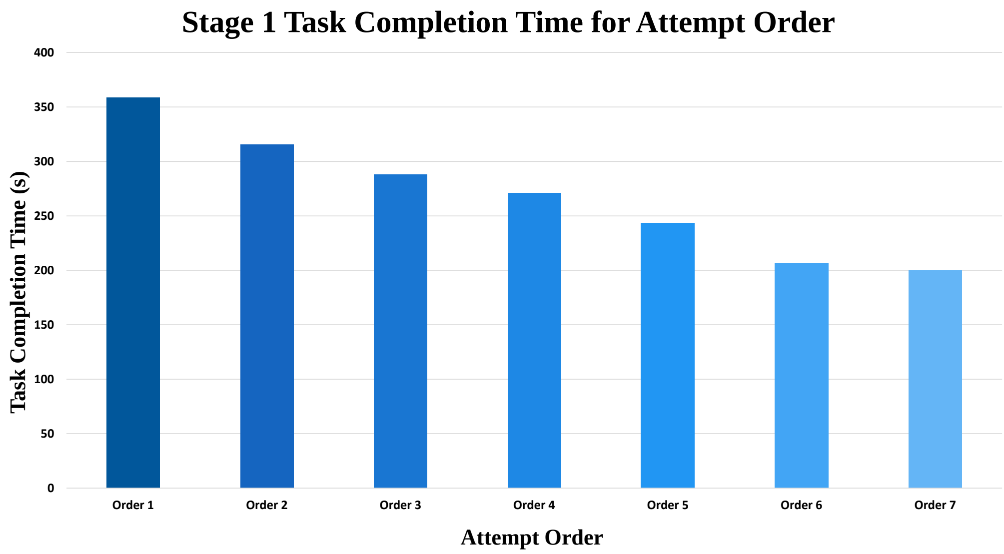

Figure 4.27: Stage 1 task completion time showing attempt order effects

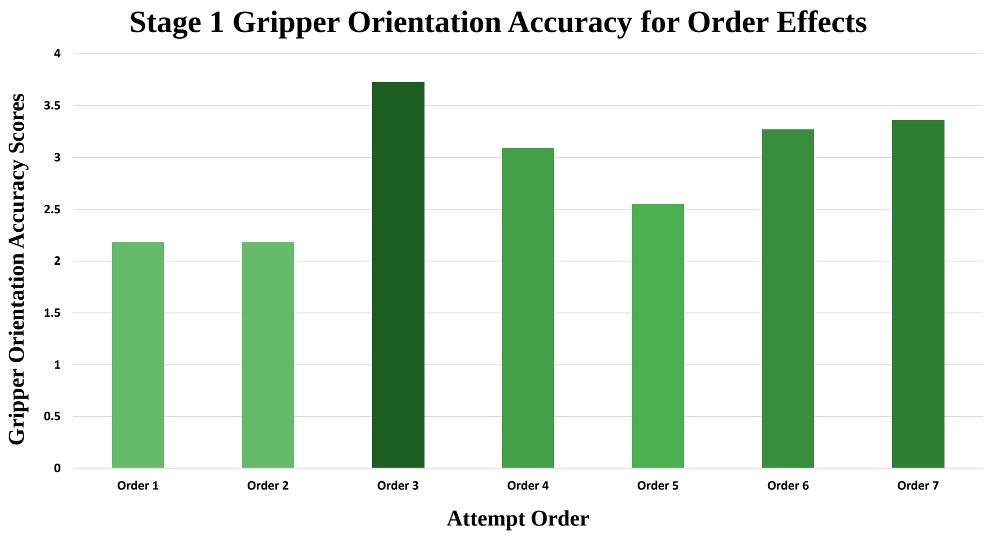

Figure 4.28: Stage 1 gripper orientation accuracy showing order effects

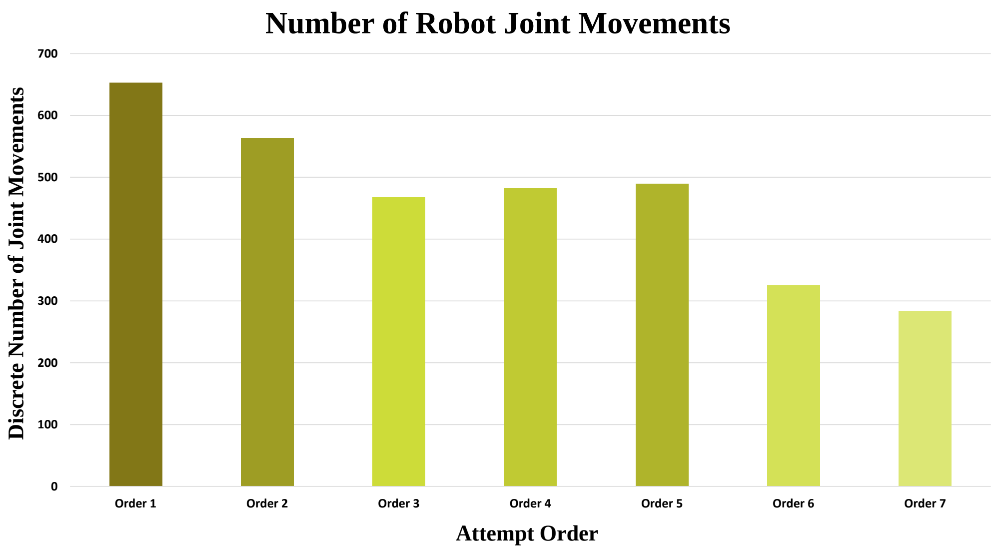

Figure 4.29: Sum of robot joint movements for all scenarios

3. **Scenario Ranking**

   Having examined the effect of each feedback scenario on the parameters measured, scores and rank were given to the scenarios based on how positive their effects were on the parameters measured. Scores were attributed based on the rankings for each parameter and overall mean. Rankings from 1-7 are attributed as score of 10, 8, 6, 4, 2, 1, 0 respectively. table 4.12 shows the rankings and attributed scores of each feedback scenario for parameters measured. Each feedback scenario is a combination of two or more feedback modalities, as shown in table 4.7. These parameters include ease of use scores, number of robot steps taken, task completion time, orientation accuracy and system usability scale.

Table 4.12: Mean values for time needed to complete stage 1, orientation accuracy, and sum of the number of discrete robot arm joint movements for stage 1 as well as ease of use rating as a function of condition presentation order

Scenarios	Ease of use		Robot joint steps		Completion time		Orientation accuracy		System usability scores		Total	Average
	R	S	R	S	R	S	R	S	R	S		
1	7	0	5	2	1	10	4	4	7	0	16	3.2
2	4	4	4	4	2	8	6	1	1	10	27	5.4
3	5	2	3	6	6	1	3	6	5	2	17	3.4
4	2	8	2	8	3	6	1	10	1	10	42	8.4
5	6	1	6	1	7	0	7	0	6	1	3	0.6
6	3	6	7	0	4	4	5	2	4	4	16	3.2
7	1	10	1	10	5	2	2	8	3	6	36	7.2

From the total scores and averages attributed in table 4.12 above, Scenario 4 (video, peripheral vision, and verbal collaboration) has the highest score of all the scenarios explored. Figure 4.30 shows the plots of overall scenario performances.

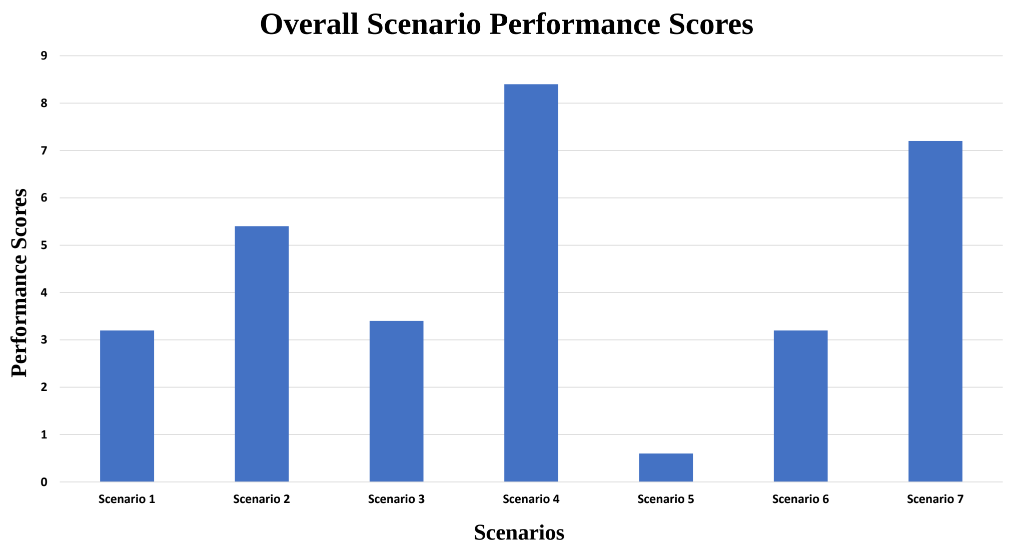

Figure 4.30: Scenario performance scores

4.2.4.6 Eye Tracking Data Analysis

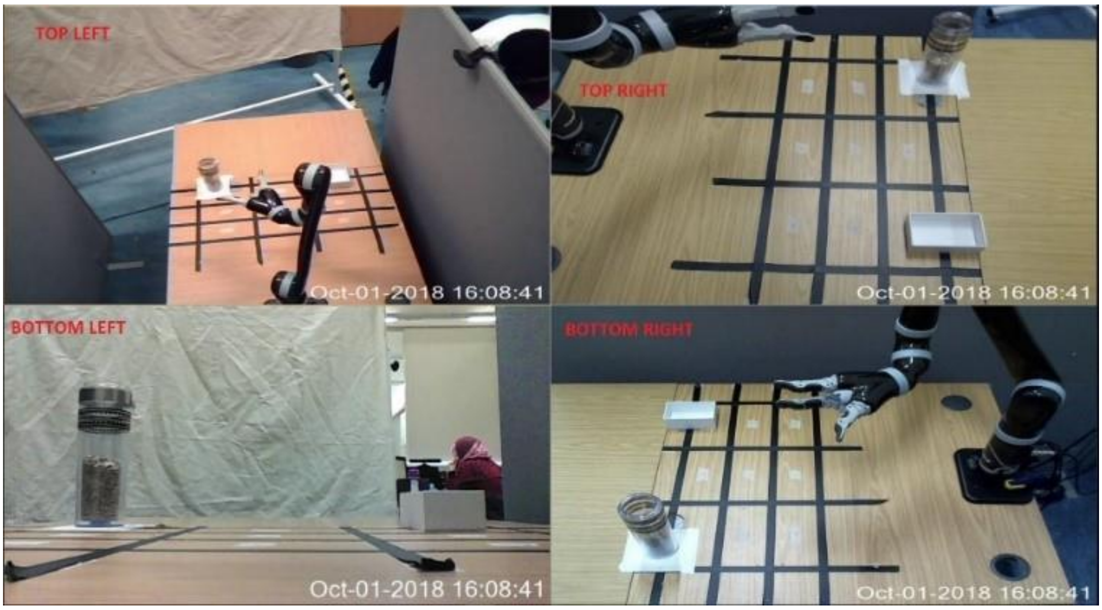

Figure 4.31: Video feedback quadrants

1. Learning effect in use of robot controller

   Video feedback was the constant source of feedback throughout all the conditions. The next stage of the analysis investigated the participants' eye gaze duration towards the instruction sheet for all scenarios (i.e. as a measure of the familiarity with instructions), as well as investigating which camera view was consulted the most throughout the study. As eye gaze was continuous data with normal distribution, the parametric tests for inferential statistics were used.

   The top-left quadrant of the screen showed the aerial view of the robot's workspace, while the quadrant labelled 'top-right' provides participants with a view of the right-hand side of the workspace. The quadrant labelled 'bottom-left' focused on table-level view of the workspace to help participants see the distance between the gripper and the table, as well as the placement of the jar on the table. The bottom-right quadrant showed the left-hand side of the robot workspace.

   To investigate whether with time participants looked at the instruction sheet changed with increasing familiarity, an ANOVA with a repeated measure of trial (trial one to trial seven) was conducted on the eye gaze duration towards the instruction sheet.

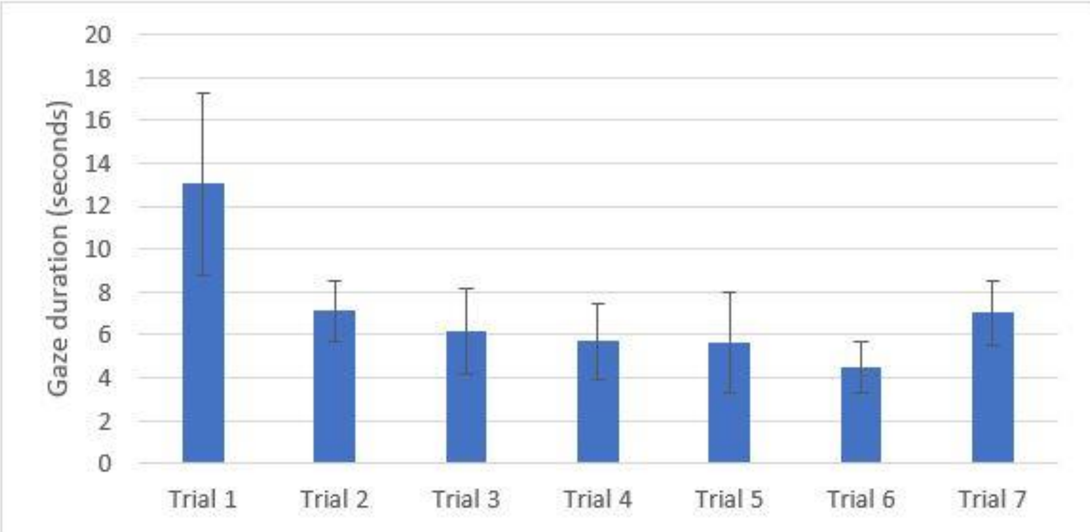

Figure 4.32: Gaze duration towards robot joystick instructions

There was a trend main effect of Trial Order ($F(2.08, 16.61) = 2.54$, $p = .107$, $\eta^2 = .241$; fig. 4.32). The descriptive statistics indicate that indeed participants consulted the instructions less with each attempt they make, compared to the first trial. As participants' completion time was related to their gaming experience, in the follow-up analysis we included participants' Gaming Experience as a covariate. The result showed a significant main effect of Trial Order ($F(6,30) = 3.63, p = .008, \eta^2 = .420$), yet, the interaction Trial order gaming experience were not significant ($F(6, 30) = 1.29$, $p = .290$, $\eta^2 = .260$).

The equivalent analysis on scenarios (S1 to S7), did not show a significant main effect of feedback scenario without covariate and with covariate of gaming experience ($F(6, 42) \leq 0.90, p \geq .506, \eta^2 = .114$). The results indicate, that although gaze duration towards the instructions did not depend on feedback modalities, yet, participants got more familiar and spent less time looking at instructions (therefore negating H7) with time.

2. Camera angle

Next, the quadrants that participants consulted the most was investigated for the scenario with only video feedback (S1, control scenario). The repeated measures ANOVA was significant ($F(1,10) = 21.91, p = .001, \eta^2 = .687$). Participants consulted the Bottom-Right quadrant significantly more than to other quadrants. Furthermore, gaze duration on other quadrants did not significantly differ (table 4.14).

Table 4.13: Gaze duration mean (s), standard deviation (SD), and post hoc comparison between significance levels of four (4) quadrants in S1

	Mean	**SD**	**N**	**Top-Left**	**Top-Right**	**Bottom-Left**
Top-Left	9.32	8.79	11			
Top-Right	2.54	5.38	11	.249		
Bottom-Left	9.72	6.87	11	≥ .999	.212	
Bottom-Right	35.93	16.19	11	.007	.001	.002

To investigate which video quadrant was most used depending on feedback modality, a 4 (camera view: Top Left; Top Right; Bottom Left; Bottom Right) x 7 (Scenarios: S1- S7) ANOVA with a covariate of gaming experience was conducted on the eye tracker gaze duration for each scenario. The results showed a significant main effect of Quadrant ($F(3,21) = 19.48, p \leq .001, \eta^2 = .736$), and main effect of Scenario ($F(6,42) = 2.41, p = .043, \eta^2 = .256$). The interaction, Scenario x Quadrant and interactions with the covariate of gaming experience did not yield significant result ($F(6,42) \leq 1.85$, $p \geq .113, \eta^2 = .209$)

Further investigation of main effect of camera view showed that participants overall had a significantly longer gaze duration towards bottom right quadrant compared to other views (table 4.13). This suggests that participants' preference towards this quadrant was not significantly influenced by feedback modality (opposed to H6).

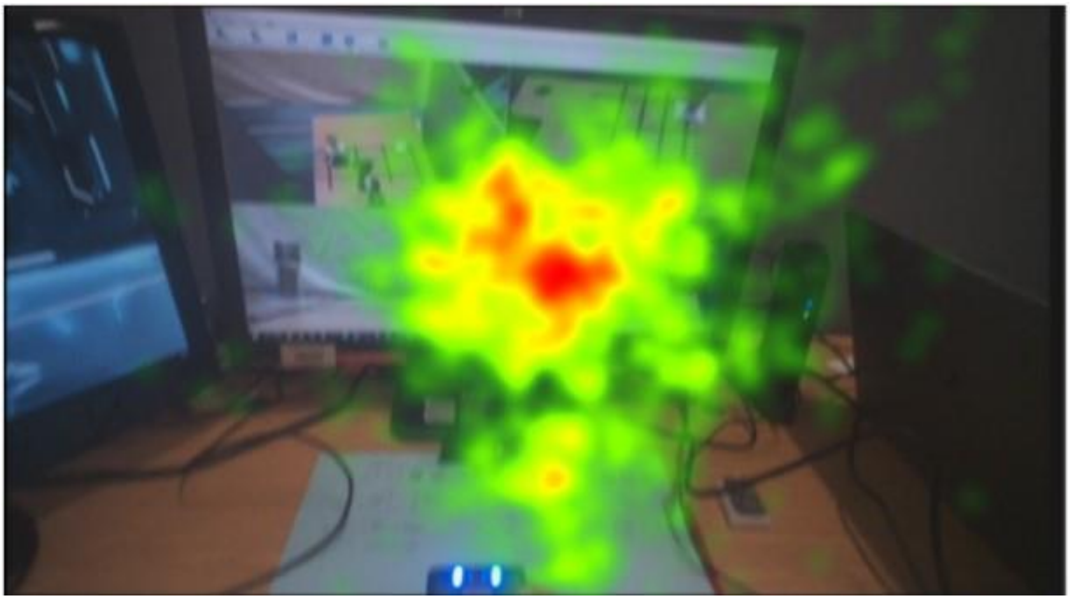

Figure 4.33: Heat map of average gaze duration

Table 4.14: Gaze duration mean, standard deviation (SD) and post hoc comparison between 4 camera views significance level across all Scenarios

	Mean	**SD**	**N**	**Top-Left**	**Top-Right**	**Bottom-Left**
Top-Left	10.87	8.53	9			
Top-Right	3.33	2.92	9	.185		
Bottom-Left	11.87	9.49	9	≥ .999	.173	
Bottom-Right	41.61	18.95	9	.028	.004	.010

Although the analysis yields the main effect of scenario to be significant, post hoc comparisons did not reveal participants having longer gaze duration in any condition ($p \geq .419$).

As the analysis shows that only bottom-right camera view was the most viewed (table 4.14), it was further explored to see if different modalities affect the viewing of this camera perspective compared to the video only scenario. We compared the bottom-right quadrant of video only scenario with other scenarios. The paired t-test between the S1 and S4 was significant ($t(10) = 2.74$, $p = .021$), indicates that participants in the S4 had significantly longer gaze duration. Other comparisons were not significant ($t(10) \leq 1.62$, $p \geq .136$). Furthermore, in checking the relationship between longer gaze duration and participants' performance on the task, Pearson correlation coefficient was used to establish relationship between gaze duration in S1 and steps needed to complete the task. There was a significant positive correlation between gaze duration and steps ($r = .715, p = .013$).

Table 4.15: Gaze duration means and and standard deviation (SD) across four (4) quadrants as a function of scenario

Scenarios	Top-Left		Top-Right		Bottom-Left		Bottom-Right	
	Mean	SD	Mean	SD	Mean	SD	Mean	SD
S1	9.32	8.79	2.54	5.38	9.72	6.87	35.93	16.19
S2	9.64	12.62	1.95	4.50	7.41	5.71	26.78	9.16
S3	12.93	11.31	7.96	11.18	12.34	10.97	42.16	39.90
S4	6.85	7.04	2.14	3.80	11.69	10.75	49.39	26.63
S5	14.03	10.49	5.71	7.85	12.87	16.42	40.42	23.32
S6	12.61	12.36	4.80	4.35	12.33	15.51	39.62	30.54
S7	13.41	15.96	2.41	1.85	11.48	11.70	48.51	28.37

Considering the results of the number of robot joint steps needed to complete stage 1 across all scenarios, and the ease of use (table 4.11), S4 was reported to be among the easiest conditions for participants. Furthermore, the gaze duration at bottom-right quadrant in scenario 4 was longest when compared to other scenarios (table 4.15). Descriptively, for this scenario participants hardly consulted other quadrants. This suggests that focusing longest on the bottom right quadrant while ignoring other camera views and having verbal collaboration and peripheral vision as additional feedback allows the participants to complete the task quickly and increase their perceived ease of use.

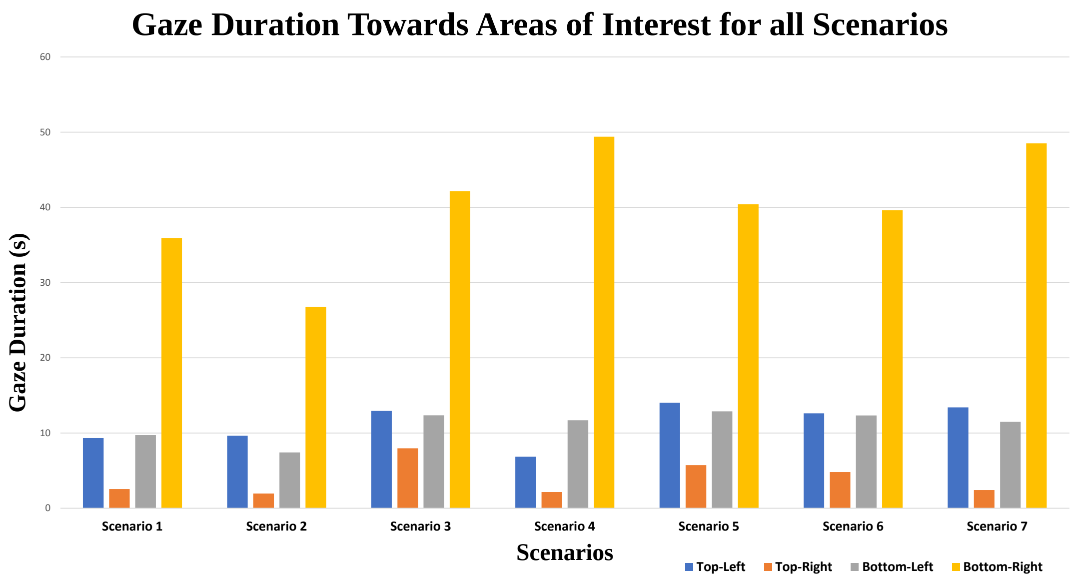

Figure 4.34: Gaze duration for areas of interest across scenarios

3. Gaze distractions by feedback modalities

   Because of the importance of video feedback in tele-operation, it was also important to see the effect of each feedback scenario on participants' gaze during the tele-operation task. Distraction would occur if operators look away from areas of interest because of any of the feedback scenarios. The areas of interest are defined as the screen for video feedback, the robot controller, and robot control instructions. The distraction time was calculated by subtracting the sum of gaze time on areas of interest from the total time of interest duration. The total time of interest duration is the time spent on the task. A repeated measures ANOVA with independent measure of seven scenarios and dependent measure of gaze duration outside areas of interest with covariant of gaming experience, showed the main effect of scenario to be significant ($F(6,48) = 2.46$, $p = 0.37, \eta^2 = .235$). The interaction Scenario x Gaming experience was not significant ($F(6,48) = 1.95$, $p = .092$, $\eta^2 = .196$.)

   Post hoc investigation with the Bonferroni adjustment for multiple comparison did not indicate any significant differences between scenarios ($p \geq .999$). The equivalent analysis on the attempt order showed that the main effect of attempt was significant ($F(6,48) = 2.86$, $p = .018$, $\eta^2 = 263$), as well as the interaction between attempt and Gaming Experience ($F(6,48) = 3.11$, $p = .012, \eta^2 = .280$). Further investigation of the main effect of Attempt with

Bonferroni adjustment for multiple comparison did not indicate any significant difference between Attempts ($p \geq .222$). Result suggests that participants gaze outside the areas of interest was both dependent on condition and dependent on which attempt it was. However, post hoc results did not indicate significant difference between attempts and scenario and as such further investigation is needed with increased number of participants.

4.2.4.7 Discussion

The challenge of tele-operating an assistive task remotely presents many problems which could reduce the efficiency with which the tasks are carried out. In the study presented in this chapter, participants completed a pick-and-empty task, picking up a jar containing sunflower seeds and emptying the contents into another container using different feedback and collaboration scenarios.

Results from the ease of use questionnaires completed after each task showed that the use of feedback improved how easily participants were able to carry out the task which comprised varying levels of difficulties (the four stages comprising the whole task). How easily participants were able to carry out the tasks varied with the different types of feedback provided. Results also show that verbal feedback improved participants' perceived ease of use of the system for all feedback scenarios, with Scenario 7 (Video feedback, Haptic feedback, Peripheral vision, and Verbal feedback) proving to be the easiest. This confirms hypothesis 3, H3 and the findings of Kraut et al. in their study on the effect of collaboration in performance of physical tasks [91]. Verbal collaboration between the operator and a service user improves operator's ease of use of the system and success in completing the task. For scenarios without feedback (S1, S3, and S5), Scenario 3 (Video feedback and Peripheral vision) had the highest ease of use score while Scenario 1 (Video Feedback only), the baseline scenario, had the lowest ease of use score. This pattern also reflects in Scenario 1 having the lowest score on the system usability scale, while scenarios with verbal collaboration have higher scores on the system usability scale. It can be suggested that the more information about the system and process that the operators have, the more confident and comfortable they were. There are suggestions of improved performance from research involving multimodal feedback when additional modalities are employed to support or enhance user activities [41][144].

Task repetition reduced the task completion time as hypothesized in H1 and confirmed by [126] but did not have any effect on the accuracy with which the task was carried out. The results did not agree with the second part of H1, stating that task repetition reduces the overall trajectory as the task is carried out. The introduction of feedback did increase the task completion time for all scenarios, in contrast to what was initially hypothesized in H5. The increased task completion time is also in contrast to expected general effect of the use of feedback. [60] and [81], for example found that the use of feedback reduced the task completion time in their tele-operated vehicle for obstacle avoidance. The type of haptic feedback according to [203] also has an effect on results.

Several factors could have contributed to the increase in task completion time. One of such could be the amount of information operators have to process whilst carrying out the task. Whilst the time increased, it was not significant enough to cause a major discouragement in its use. Another possible reason could be the task type and difficulty level. Even though the introduction of feedback did increase the time taken to complete the task, there was significant improvement in the gripper orientation performance before grasp, confirming H2. Although not significant, the sum of the number of discrete robot arm joint movements in x, y and z planes taken to complete stage 1 also decreased with the introduction of feedback, confirming the second part of H2. With each attempt, participants became quicker to complete a task. However, this did not influence their perceived ease of use (no significant order effect). Considering the influence that feedback had on the trajectory taken to complete the task, even though there was no statistically significant effect, scenario 7 had the least values for the sum of the number of discrete robot arm joint movements in x, y and z planes. Scenario 2 (Video feedback and Verbal collaboration) produced the highest mean value for the sum of the number of discrete robot arm joint movements in x, y and z planes for task completion.

For gripper orientation accuracy, scenario 4 (Video feedback, Peripheral vision, and verbal collaboration) resulted in the operator being able to achieve the most accurate gripper orientation, followed by Scenario 7 and Scenario 3 (Video feedback and Peripheral vision). The gripper orientation accuracy is very important for successful grasp and can therefore affect the overall result of the task. Even though the scenarios that yielded the best gripper orientations had a longer task completion time, this might be acceptable for high-risk tasks.

As hypothesized in H4, prior gaming experience was indeed an advantage to successfully completing Stage 1 of the task, but as shown, verbal collaboration increased the chance of success for participants without prior gaming and/or robot experience. For tele-operation applications that emphasise safety and precision, like assisted care provision or tele-surgery [10], these results are positive as task completion time can be traded for greater accuracy, task success and better user satisfaction and socialisation. Based on our experiments described in this paper, when verbal collaboration does not take place, a combination of video and peripheral feedback, was found to be the optimal way for providing feedback (Scenario 3). This is based on the ease of use rating given by operators. However, when verbal feedback is introduced then using a combination of video, peripheral and haptic feedback results in the highest rating of ease of use (Scenario 7). This combination also results in the highest gripper orientation accuracy and lowest joint movements.

While the results of the gaze data do not indicate whether feedback modalities affect the operators' gaze time on different camera angles (H6), recording gaze may be a useful method to determine an operator's preference of camera views in relation to the task difficulty. This information could be very useful in taking an adaptive approach to the information provided, by enhancing the specific information, such as the magnification of the camera view, as the operator proceeds with the task.

The studies reported in this chapter were designed such that two wrist-worn haptic feedback devices were worn by participants. Each device was worn on each arm to represent directions of gripper orientation. To simplify the setup, we explored the use of a single wrist-worn haptic feedback device to convey sensor data to participants. In order to achieve this, the next chapter examines the sensitivity of different locations across the wrist. In chapter 5, we also examine participant's abilities to pinpoint locations of haptic stimulation across the wrist and different haptic display strategies.

CHAPTER 5

Investigating Haptic Stimulation Sensitivity Across the Wrist and Haptic Display Strategies

5.1 Introduction

With haptic feedback modality finding increasing use in many tele-operation applications, it is important to understand how to effectively use this modality to convey information to operators. The nature of the underlying information may also determine the choice of haptic sensation employed (tactile or kinesthetic) and how users interpret haptic data. Different haptic sensations can be caused by different stimuli (e.g. mechanical force) generated by specific haptic interfaces [201]. In robot tele-operation, haptic feedback modality is typically used to convey force data to an operator through robotic manipulators often referred to as the slave [118] [212] [56]. However, some tele-operation interfaces have employed wearable haptic feedback to convey force data [21]. In the study presented in this chapter, three phases of experiments were carried out to investigate the haptic sensitivity of various locations across the wrist and to investigate participants' abilities to pinpoint locations of haptic stimulation across the wrist.

Sensitivity to haptic stimulation varies from person-to-person and, consequently, it is important to explore the need to calibrate a haptic feedback device for individual users. Phase 1 of the study had three aims. The first aim was to examine the minimum detectable haptic intensity (MDHI) at different locations across the wrist. MDHI was measured in terms of the duty cycle of pulse width modulation powering the haptic motors. As well as indicating the sensitivity of different locations across the wrist to varying intensities of haptic stimulation, it may also be possible to explore the potential for simultaneous stimulation at these locations to convey more than one data stream to the operator. The second aim was to determine whether there are differences in MDHI between the different locations across the wrist for various durations of haptic stimulation (DHS). The third aim was to determine whether MDHI varies when video distraction is introduced, examining whether social interaction may affect haptic perception in assistive tele-operation.

In Phase 2 of the study, information gathered from phase 1 was used to provide personalised calibration of the haptic device as participants were asked to pinpoint locations of haptic stimulation across the wrist. Phase two had five aims. The first aim was to establish whether calibrating the haptic device with results from the phase one study would produce similar performances in pinpointing locations of haptic stimulation and sensitivities to haptic stimulation across different locations on the wrist for all participants. The second aim was to compare the overall identification of locations of haptic stimulation performances (ILHSP) for single-location stimulation identification (SSI) and simultaneous double-location stimulation identification (SDSI). This is important because it helps to understand the ease with which haptic stimulation can be identified by increasing the number of possible stimulation strategies. The third aim was to identify how ILHSP and sensitivity varies between different locations across the wrist. The fourth aim was to identify how ILHSP varies with stimulation frequency and intensity. The fifth aim was to examine the chances of correctly identifying two simultaneously stimulated locations across the wrist. This is particularly useful in applications where instructions are to be given to operators by concurrently stimulating two different locations on the wrist.

The information conveyed to operators may be provided using different sensory substitution strategies: to provide situational awareness of the remote environment or to instruct the operator on what to do. The third phase focuses on identifying the most appropriate strategy for conveying different sensor data to operators. The aim was to determine whether operators find it more useful to be provided with situational awareness or to be instructed on what to do.

5.2 Design/Setup

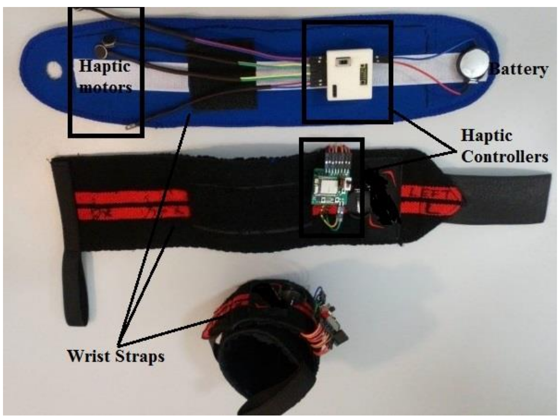

Figure 5.1: WI-FI enabled haptic feedback device

The study setup was made up of a Wi-Fi enabled wrist-worn haptic feedback device (Phase-5 haptic feedback device) shown in figure 5.1. The haptic motors in the wrist-worn haptic feedback device were positioned across the wrist such that they appear across the wrist as shown in figure 5.2. The positioning was influenced by Weinstein's two-point discrimination. Experimentally, the minimum distance between two distinguishable locations of tactile stimulations was found to be 38 mm [202]. Figure 5.2 allows for such considerations.

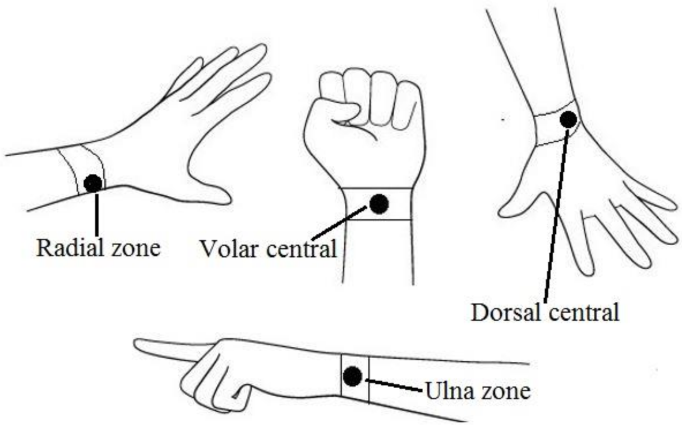

Figure 5.2: Haptic motor placements across the wrist

Several parameters may be varied to provide haptic stimulation to convey information. The choice of parameter depends on the application. Below are some of the parameters that may be varied.

1. Method of haptic motor activation: This describes how the motors are powered. Each motor could be powered through a DC voltage (with minimum voltage equal to the start voltage of each motor) or pulse width modulation (PWM) signal. The haptic motors were powered using PWM in the prototype haptic feedback device used in the study reported in this chapter.

2. Vibration intensity: This parameter controls the vibration strength of the haptic motors. This can be changed by varying the duty cycle of the pulse width modulated signal or the supplied DC voltage.

3. Frequency: Haptic feedback can be perceived when the stimulation frequency is within the range that is detectable by the mechanoreceptors in the skin. The frequency is inversely proportional to the time interval between each tactile stimulation.

4. Vibration duration: This parameter controls the duration of each stimulation.

For the phases of the study, control information about the haptic stimulation was sent from a software (written with C++) on the control PC to the haptic feedback device.

5.3 Wrist Sizes

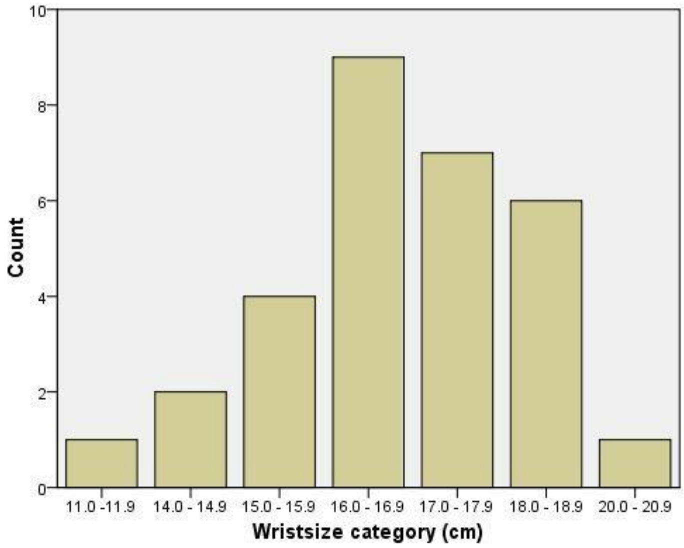

Figure 5.3: Bar chart for different wrist size categories of participants

A total of 30 people participated in the study. Appendix A and Appendix B were used to gather participants' information. Figure 5.3 shows the wrist size category distribution for all participants (N = 30). The wrist size is a measure of the circumference of the wrist of each participant. The ratio of male to female representation was 16:14 amongst participants.

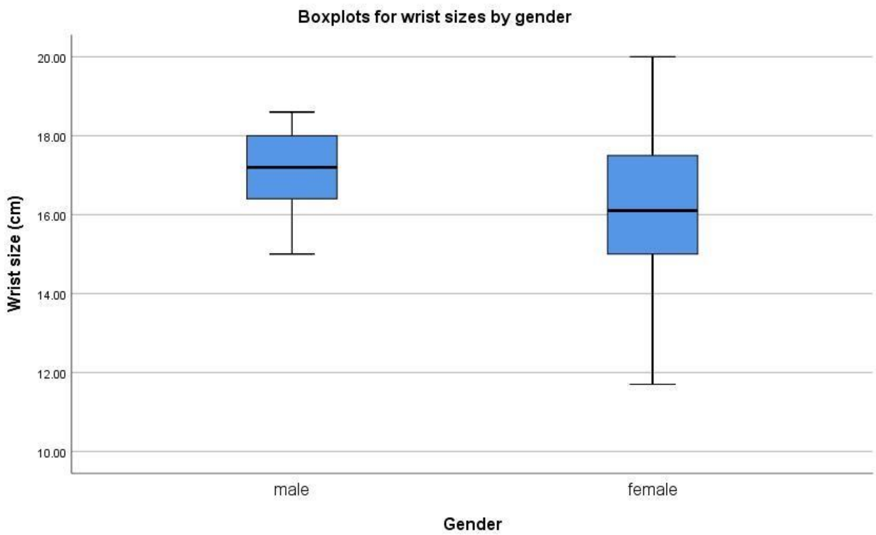

Figure 5.4: Box plot for participants' wrist sizes

Figure 5.4 below shows the boxplots for male and female wrist sizes represented in the study. The mean wrist size for male participants was 17.11 cm while the mean wrist size for female participants was 16.04 cm. The plots show that the wrist sizes for female participants were more widely dispersed than the male participants.

Shapiro-Wilk test of normality for wrist sizes give levels of significance of 0.725 and 0.917 for male and female respectively. Wrist size measurements for participants (male and female) had a normal distribution. [85][180].

5.4 Phase 1 Study: Minimum Detectable Haptic Intensity (MDHI)

Phase 1 of the study investigates the MDHI of different locations across the wrist under varying conditions of video distractions. The wrist was chosen because wrist-worn devices are commonplace, do not affect everyday tasks and are aesthetically acceptable [47].

While previous studies have employed the use of wrist-worn haptic devices, [47][159][36], there are limited studies employing such haptic devices for robot tele-operation. It is important to understand how minimum detectable haptic intensity (MDHI) varies between locations across the wrist and between different participants.

The study was carried out by constantly stimulating different locations across the wrist until each participant could correctly identify the location of haptic stimulation. The locations as highlighted in figure 5.2 are referred to as Ulna zone, Dorsal central, Radial zone, and Volar central. In order to stimulate each location on the wrist, data packets were sent from the control PC to the wrist-worn haptic device to generate haptic stimulation. Each packet contained values for PWM duty cycle. The principal researcher sent the packets by clicking on each position of haptic stimulation shown in figure 5.5. Each button was repeatedly clicked until each participant correctly identified the location of haptic stimulation. Also, for each repeated click, the duty cycle of the PWM was increased by a factor of 10. The starting PWM duty cycle was 10% and at 100%, the PWM duty stayed the same. The principal researcher clicked on the 'YES' button when each participant correctly identified the location of stimulation. The minimum detectable haptic intensity is saved in a text file for each location on the wrist. The phase is repeated eight times for different combinations of duration of haptic stimulation (DHS) and video distraction.

This phase of the study involves three independent variables and one dependent variable. The independent variables are the duration of haptic stimulation (250 ms, 500 ms, 750 ms, and 1000 ms), distraction (with and without video distraction), and locations of haptic stimulation across the wrist (Ulna zone, Dorsal central, Radial zone, and Volar central). The dependent variable is the minimum duty cycles (as a percentage) of haptic stimulation that can be correctly perceived across different locations on the wrist.

The video played during the study is an interview called 'David Attenborough on His Decades-Long Career' (GURUS, 2018).

Figure 5.5: (a) Graphical user interface for triggering haptic stimulation at the Dorsal central. (b) Graphical user interface for triggering haptic stimulation at the Radial zone. (c) Graphical user interface for triggering haptic stimulation at the Volar central zone. (d) Graphical user interface for triggering haptic stimulation at the Ulna zone.

5.4.1 Results

Normality was assumed for the recorded minimum detectable haptic intensity (measured as PWM duty cycles) based on graphical inspection of the data and the central limit theory. The central limit theorem was used to assume normality for the recorded values since the number of participants was up to 30 [50][92].

A 2-way repeated measures ANOVA (analysis of variance) was carried out to evaluate the null hypothesis that there is no significant difference between the corresponding PWM duty cycles of the minimum detectable haptic intensity (MDHI) across different locations on the wrists of participants (with and without the introduction of video distraction) for varying durations of haptic stimulation (DHS). The two-way ANOVA was carried out on the corresponding PWM duty cycles for minimum detectable haptic intensity (MDHI) recorded for the different durations of haptic stimulation.

5.4.1.1 Minimum Detectable Haptic Intensity for Duration of Haptic Stimulation = 250 ms

Table 5.1 shows the descriptive statistics (mean and standard deviations) for the duty cycles corresponding to the minimum detectable haptic intensity (MDHI) at different locations across the wrist for duration of haptic stimulation (DHS) of 250 ms.

Table 5.1: Descriptive statistics for recorded minimum duty cycles for haptic stimulation felt (DHS = 250 ms)

Location on the wrist	With Video Distraction		Without Video Distraction		Number of Participants
	Mean duty cycle (%)	Standard Deviation	Mean duty cycle (%)	Standard Deviation	
Dorsal central	58.6667	12.79368	53.6667	10.66200	30
Volar central	50.3333	8.89918	50.3333	8.50287	30
Ulna zone	63.0000	12.35956	61.6667	14.16244	30
Radial zone	66.0000	10.69966	58.3333	11.47211	30

Figure 5.6 shows the boxplots of the duty cycles for different locations across the wrist. It also allows for comparisons for the effect of video distractions.

The assumption of sphericity was met for stimulation locations and the interaction between stimulation locations and distraction. The significance levels for StimulationLocation ($p = 0.939$) and interaction StimulationLocation*Distraction ($p = 0.641$) were greater than 0.05. 95% confidence interval was used for all calculations.

Results of the two-way repeated measures ANOVA revealed that there was a significant main effect of location of stimulation on MDHI (N = 30). $Wilk'sLambda = 0.420, (F(3,87) = 14.525, p < 0.001, \eta_p^2 = 0.334)$. Thus, there is significant evidence to reject the null hypothesis that there is no significant difference between the corresponding PWM duty cycles of the minimum detectable haptic intensity (MDHI) across different locations on the wrists of participants. Results also display large effect size ($\eta_p^2 = 0.334$) of locations of stimulation.

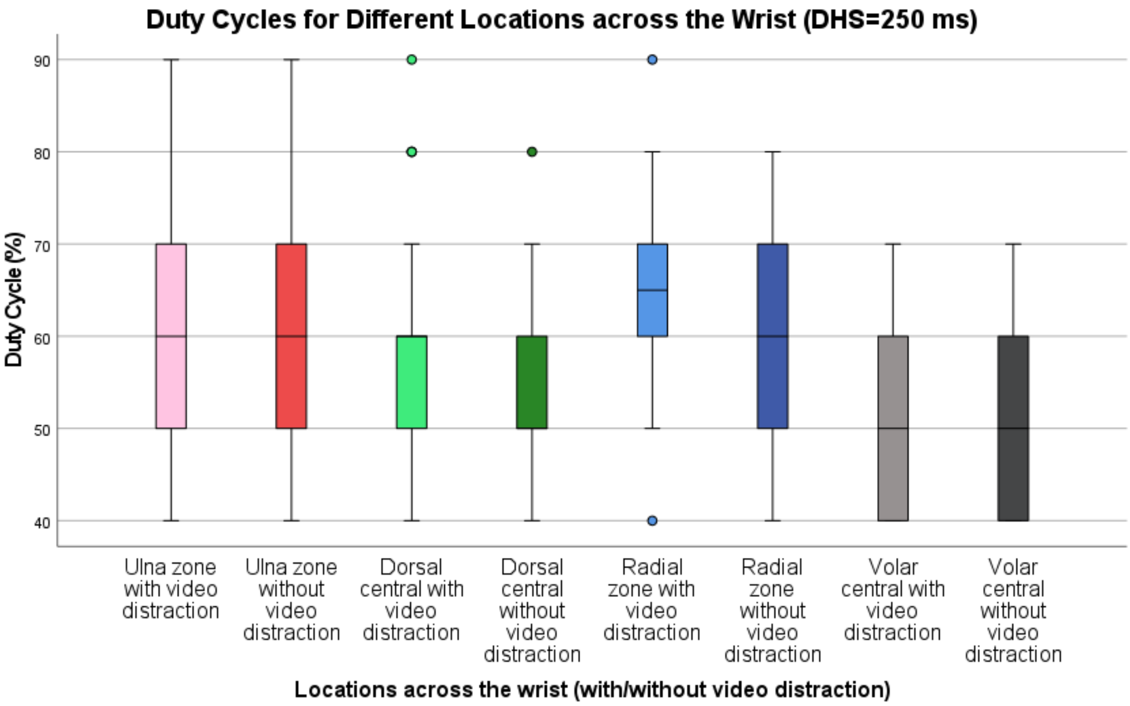

Figure 5.6: Boxplots for PWM duty cycles of MDHI with and without video distraction (stimulation duration = 250 ms)

The mean minimum PWM duty cycles recorded for the different locations on the wrist regardless of the distraction varied as shown in table 5.2.

Table 5.2: Mean duty cycles regardless of distraction (DHS = 250 ms)

Stimulation locations	**Mean duty cycle (%)**	**Standard error**
Dorsal central	56.167	1.805
Volar central	50.333	1.221
Ulna zone	62.333	2.045
Radial zone	62.167	1.432

Follow up comparisons indicated that pairwise difference of the mean minimum PWM duty cycles corresponding to the MDHI between the Dorsal central and Volar central was significant ($p = 0.011$). The Dorsal central also significantly differed in MDHI from the Ulna zone ($p = 0.004$) and Radial zone ($p = 0.006$). Pairwise difference of MDHI between the Volar central and Ulna zone ($p < 0.001$), as well as Radial zone ($p < 0.001$) was also significant. MDHI for the Ulna zone and Radial zone was similar ($p = 0.938$).

There was a significant main effect of distraction on MDHI. $Wilk's Lambda = 0.815$, ($F(1,29) = 6.579$, $p = 0.016$, $\eta_p^2 = 0.185$). Thus, there is significant evidence to reject the null hypothesis. Results also display large effect size ($\eta_p^2 = 0.185$) of distraction on MDHI. The mean duty cycle of the haptic stimulation felt when video distraction was introduced (59.5%) was higher than the mean duty cycle of haptic stimulation felt without video distraction (56.0%). Pairwise comparison for the two levels of distraction (with video, without video) was significant ($p = 0.016$).

The interaction between locations of haptic stimulation and distraction did not yield any significant main effect, $Wilk's Lambda = 0.850$, ($F(3,87) = 2.127$, $p = 0.103$, $\eta_p^2 = 0.068$).

Figure 5.7 below shows the profile plot for the estimated marginal means of the minimum duty cycles for the different stimulation locations across the wrist. Levels 1 and 2 of the distraction level represent duty cycle measurements with and without video respectively. Figure 5.7 shows similar patterns for the duty cycles with and without the introduction of video distraction. With and without video distraction, the volar central can be seen to have the lowest MDHI.

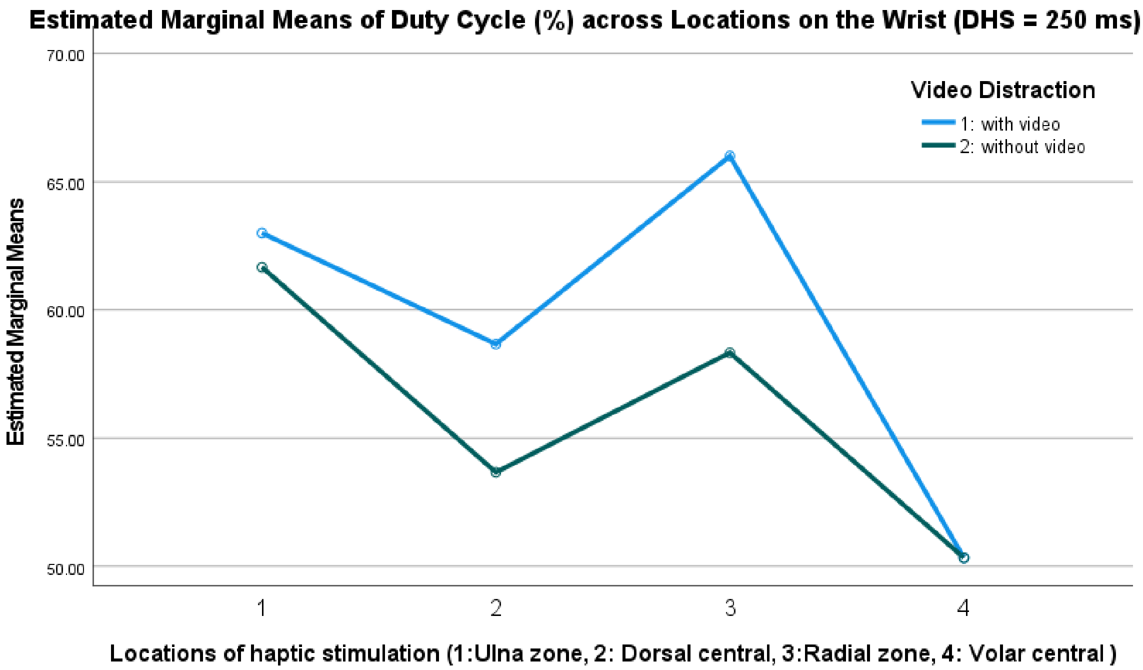

Figure 5.7: Profile plots for duty cycles (DHS = 250 ms)

5.4.1.2 Minimum Detectable Haptic Intensity for Duration of Haptic Stimulation = 500 ms

Table 5.3 shows the descriptive statistics (mean and standard deviations) for the duty cycles corresponding to the minimum detectable haptic intensity (MDHI) across different locations on the wrist for duration of haptic stimulation (DHS) of 500 ms.

Table 5.3: Descriptive statistics for recorded minimum duty cycles for haptic stimulations felt (stimulation duration = 500 ms)

Location on the wrist	With Video Distraction		Without Video Distraction		Number of Participants
	Mean duty cycle (%)	Standard Deviation	Mean duty cycle (%)	Standard Deviation	
Dorsal central	50.6667	11.12107	46.6667	8.441882	30
Volar central	44.6667	8.60366	40.0000	8.30455	30
Ulna zone	55.6667	13.04722	53.0000	12.90549	30
Radial zone	56.0000	12.48447	56.0000	14.76249	30

Figure 5.8 shows the boxplots of the duty cycles for different locations on the wrist. It also allows for comparisons for the effect of video distractions.

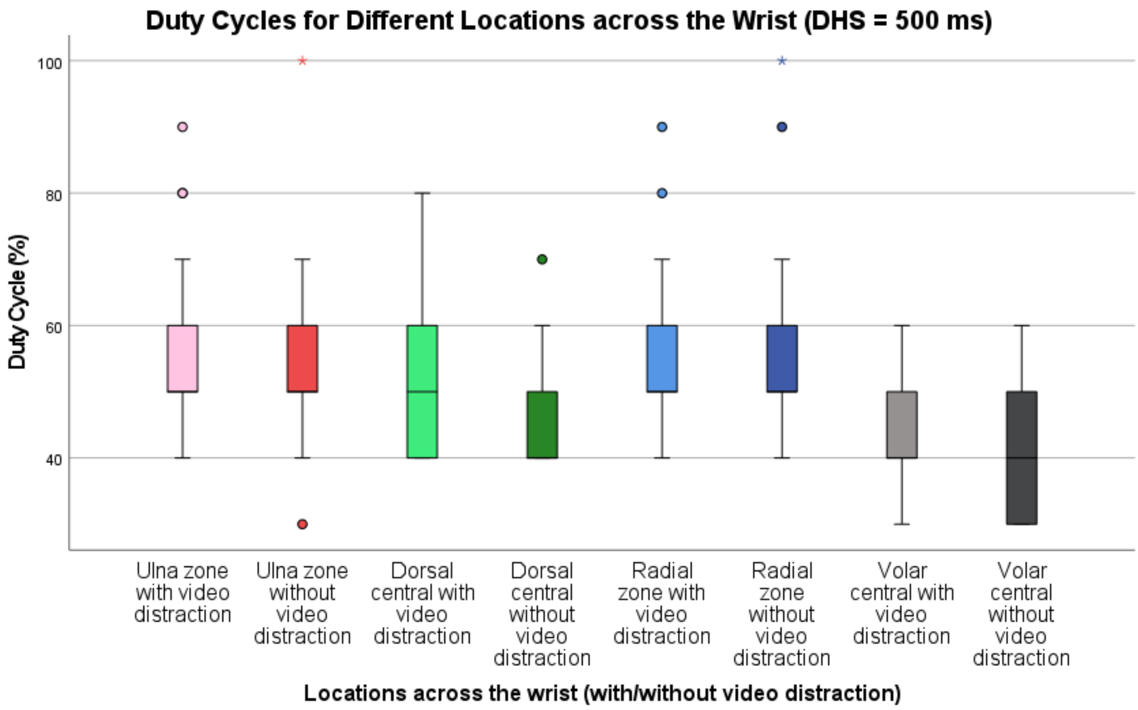

Figure 5.8: Boxplots for PWM duty cycles of MDHI with and without video distractions (DHS = 500 ms)

The assumption of sphericity was met for stimulation locations and the interaction between stimulation locations and distractions. The significance levels for StimulationLocations (p =

0.191) and interaction StimulationLocations*Distraction ($p = 0.054$) were greater than 0.05. 95% confidence interval was used for all calculations.

Results of the two-way repeated measures ANOVA revealed that there was a significant main effect of locations of stimulation on MDHI (N = 30). $Wilk'sLambda = 0.394, (F(3,87) = 15.137, p < 0.001, \eta_p^2 = 0.343)$. Thus, there is significant evidence to reject the null hypothesis that there is no significant difference between the corresponding PWM duty cycles of the minimum detectable haptic intensity (MDHI) across different locations on the wrists of participants. Results also display large effect size ($\eta_p^2 = 0.343$) of locations of stimulation.

The mean minimum PWM duty cycles recorded for the different locations on the wrist regardless of the distraction varied as shown in table 5.4.

Table 5.4: Mean duty cycles regardless of distraction (duration of haptic stimulation = 500 ms)

Stimulation locations	**Mean duty cycle (%)**	**Standard error**
Dorsal central	48.667	1.477
Volar central	42.333	1.192
Ulna zone	54.333	1.929
Radial zone	56.000	1.953

Follow up comparisons indicated that pairwise difference of the mean minimum PWM duty cycles corresponding to the MDHI between the Dorsal central and Volar central was significant ($p < 0.001$). The Dorsal central also significantly differed in MDHI to the Ulna zone ($p = 0.019$) and Radial zone ($p = 0.005$). Pairwise difference of MDHI between the Volar central and Ulna zone ($p < 0.001$), as well as Radial zone ($p < 0.001$) was also significant. MDHI for the Ulna zone and Radial zone was however similar ($p = 0.506$).

There was a significant main effect of distraction on MDHI. $Wilk'sLambda = 0.815, (F(1,29) = 6.594, p = 0.016, \eta_p^2 = 0.185)$. Thus, there is significant evidence to reject the null hypothesis. Results also display large effect size ($\eta_p^2 = 0.185$) of distraction on MDHI. The mean duty cycle of the haptic stimulation felt when video distraction was introduced (51.750%) was higher than the mean duty cycle of haptic stimulation felt without video distraction (48.917%). Pairwise comparison for the two levels of distraction (with video, without video) was significant ($p = 0.016$).

The interaction between locations of haptic stimulation and distraction did not yield any significant main effect, $Wilk'sLambda = 0.926, (F(3,87) = 0.624, p = 0.601, \eta_p^2 = 0.021)$.

Figure 5.9 below shows the profile plot for the estimated marginal means of the minimum duty cycles for the different stimulation locations on the wrist. Levels 1 and 2 of the distraction level represent duty cycle measurements with and without video respectively. Figure 5.9 shows similar patterns for the duty cycles with and without the introduction of video distraction. With and without video distraction, the Volar central can be seen to have the lowest MDHI.

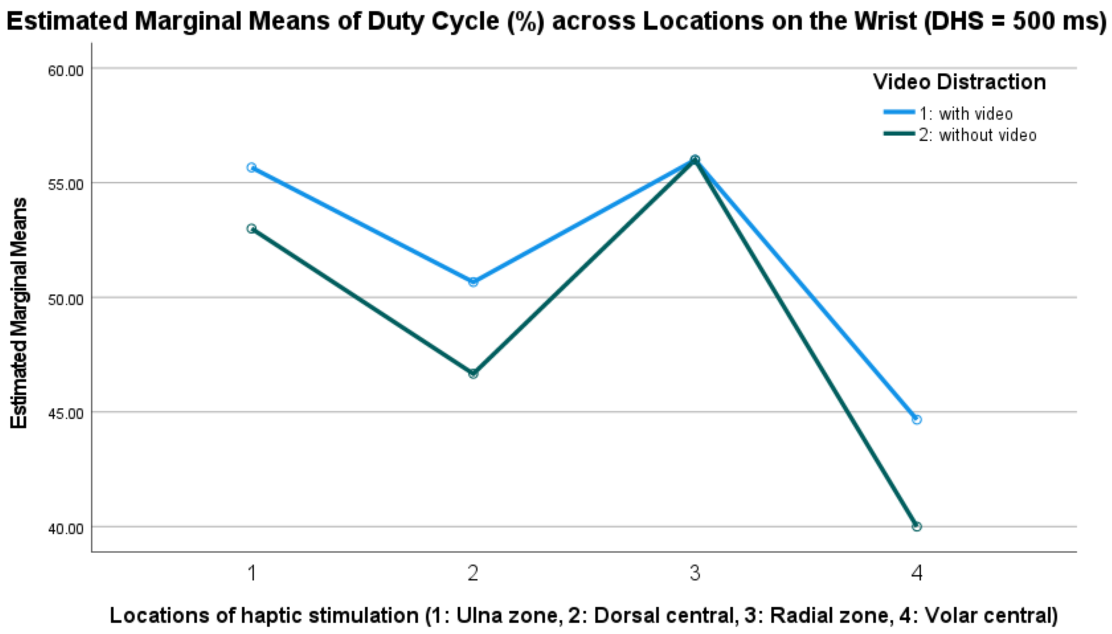

Figure 5.9: Profile plots for duty cycles (DHS = 500 ms)

5.4.1.3 Minimum Detectable Haptic Intensity for Duration of Haptic Stimulation = 750 ms

Table 5.5 shows the descriptive statistics (mean and standard deviations) for the duty cycles corresponding to the minimum detectable haptic intensity (MDHI) at different locations on the wrist for duration of haptic stimulation (DHS) of 750 ms.

Table 5.5: Descriptive statistics for recorded minimum duty cycles for haptic stimulations felt (DHS = 750 ms)

Location on the wrist	With Video Distraction		Without Video Distraction		Number of Participants
	Mean duty cycle (%)	Standard Deviation	Mean duty cycle (%)	Standard Deviation	
Dorsal central	49.3333	12.84747	47.6667	13.04722	30
Volar central	41.6667	8.74281	39.6667	9.27857	30
Ulna zone	50.0000	13.39068	53.6667	11.88547	30
Radial zone	53.3333	11.54701	49.6667	12.99425	30

Figure 5.10 shows the boxplots of the duty cycles for different locations on the wrist. It also

allows for comparisons for the effect of video distractions.

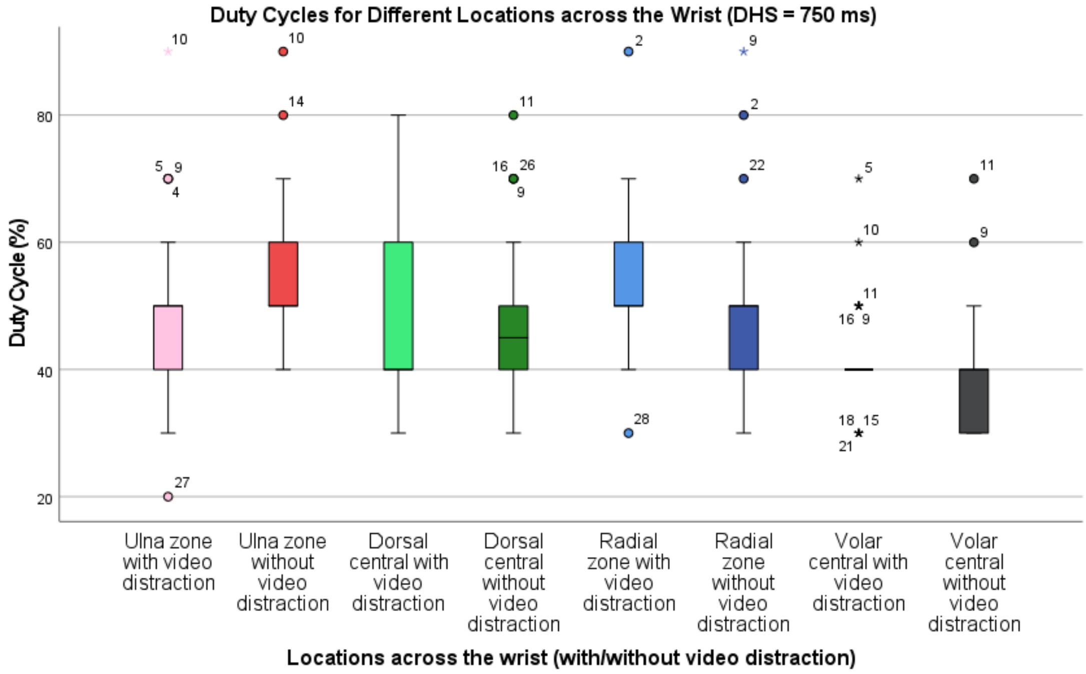

Figure 5.10: Boxplots for PWM duty cycles of MDHI with and without video distractions (DHS = 750 ms)

The assumption of sphericity was met for stimulation locations and the interaction between stimulation locations and distractions. The significance levels for StimulationLocation (p = 0.963) and interaction StimulationLocation*Distraction ($p = 0.276$) were greater than 0.05. 95% confidence interval was used for all calculations.

Results of the two-way repeated measures ANOVA revealed that there was a significant main effect of locations of stimulation on MDHI (N = 30). $Wilk's Lambda = 0.417, (F(3,87) =$ 11.676, $p < 0.001$, $\eta_p^2 = 0.287$). Thus, there is significant evidence to reject the null hypothesis that there is no significant difference between the corresponding PWM duty cycles of the minimum detectable haptic intensity (MDHI) across different locations on the wrists of participants. Results also display large effect size ($\eta_p^2 = 0.287$) of locations of stimulation.

The mean minimum PWM duty cycles recorded for the different locations on the wrist regardless of the distraction varied as shown in table 5.6.

Follow up comparisons indicated that pairwise difference of the mean minimum PWM duty cycles corresponding to the MDHI between the Dorsal central and Volar central was significant ($p < 0.001$). MDHI between the Dorsal central and both the Ulna ($p = 0.154$) and Radial ($p < 0.174$) zones was not significant. Pairwise difference of MDHI between the Volar central and Ulna zone ($p < 0.001$), as well as Radial zone ($p < 0.001$) was also significant. MDHI for the Ulna zone and

Radial zone was however similar ($p = 0.886$).

Table 5.6: Mean duty cycles regardless of distraction (duration of haptic stimulation = 750 ms)

Stimulation locations	**Mean duty cycle (%)**	**Standard error**
Dorsal central	48.500	1.935
Volar central	40.667	1,350
Ulna zone	51.833	1.895
Radial zone	51.500	1.796

There was a significant main effect of distraction on MDHI. $Wilk's Lambda = 0.984$, ($F(1,29) = 0.474$, $p = 0.016$, $\eta_p^2 = 0.474$). Thus, there is significant evidence to reject the null hypothesis. Results also display large effect size ($\eta_p^2 = 0.474$) of distraction on MDHI. The mean duty cycle of the haptic stimulation felt when video distraction was introduced (48.583%) was higher than the mean duty cycle of haptic stimulation felt without video distraction (47.667%). Pairwise comparison for the two levels of distraction (with video, without video) was not significant ($p = 0.497$).

The interaction between locations of haptic stimulation and distraction did not yield any significant main effect, $Wilk's Lambda = 0.864$, ($F(3,87) = 1.674$, $p = 0.178$, $\eta_p^2 = 0.055$).

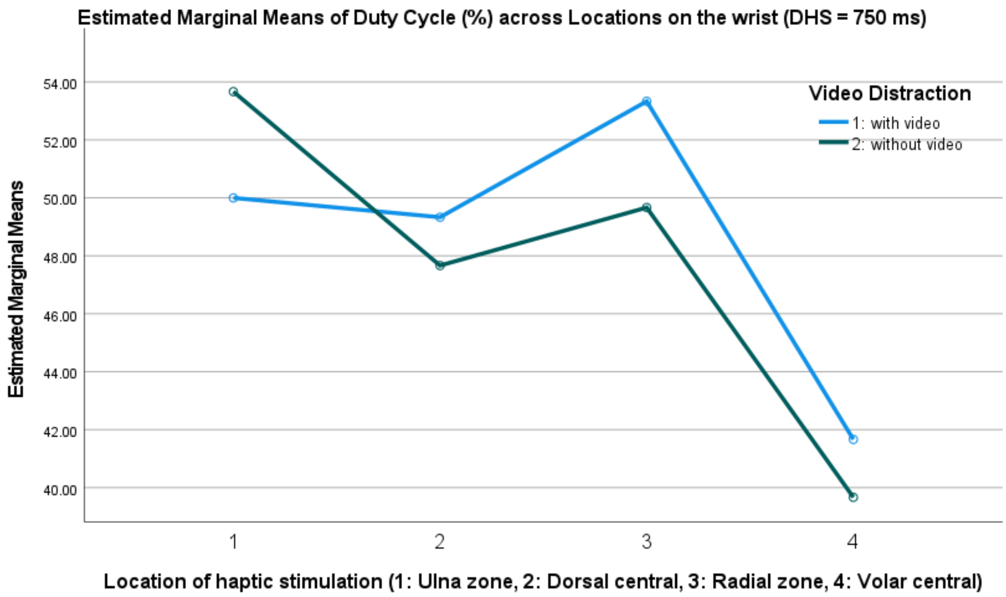

Figure 5.11: Profile plots for duty cycles (DHS = 500 ms)

Figure 5.11 shows the profile plot for the estimated marginal means of the minimum duty cycles for the different stimulation locations on the wrist. Levels 1 and 2 of the distraction levels represent duty cycle measurements with and without video respectively. Figure 5.11 shows similar patterns for the duty cycles with and without the introduction of video distraction. With and without video distraction, the volar central can be seen to have the lowest MDHI.

5.4.1.4 Minimum Detectable Haptic Intensity for Duration of Haptic Stimulation = 1000 ms

Table 5.7 shows the descriptive statistics (mean and standard deviations) for the duty cycles corresponding to the minimum detectable haptic intensity (MDHI) at different locations on the wrist for duration of haptic stimulation (DHS) of 1000 ms.

Table 5.7: Descriptive statistics for recorded minimum duty cycles for haptic stimulation felt (stimulation duration = 1000 ms)

Location on the wrist	Video Distractions		Without Video Distractions		Number of Participants
	Mean duty cycle (%)	Standard Deviation	Mean duty cycle (%)	Standard Deviation	
Dorsal central	41.0000	7.58856	46.6667	11.54701	30
Volar central	38.6667	7.76079	42.0000	14.47947	30
Ulna zone	49.0000	10.93870	51.3333	13.32183	30
Radial zone	47.6667	8.97634	48.6667	11.95778	30

Figure 5.12 shows the boxplots of the duty cycles for different locations on the wrist. It also allows for comparisons for the effect of video distractions.

The assumption of sphericity was met for stimulation locations and the interaction between stimulation locations and distractions. The significance levels for StimulationLocations (p = 1.000) and interaction StimulationLocations*Distraction (p = 0.211) were greater than 0.05. 95% confidence interval was used for all calculations.

Results of the two-way repeated measures ANOVA revealed that there was a significant main effect of locations of stimulation on MDHI (N = 30). $Wilk'sLambda = 0.536, (F(3,87) = 8.568, p < 0.001, \eta_p^2 = 0.228)$. Thus, there is significant evidence to reject the null hypothesis that there is no significant difference between the corresponding PWM duty cycles of the minimum detectable haptic intensity (MDHI) across different locations on the wrists of participants. Results also display large effect size ($\eta_p^2 = 0.228$) of locations of stimulation.

The mean minimum PWM duty cycles recorded for the different locations on the wrist regardless of the distraction varied as shown in table 5.8.

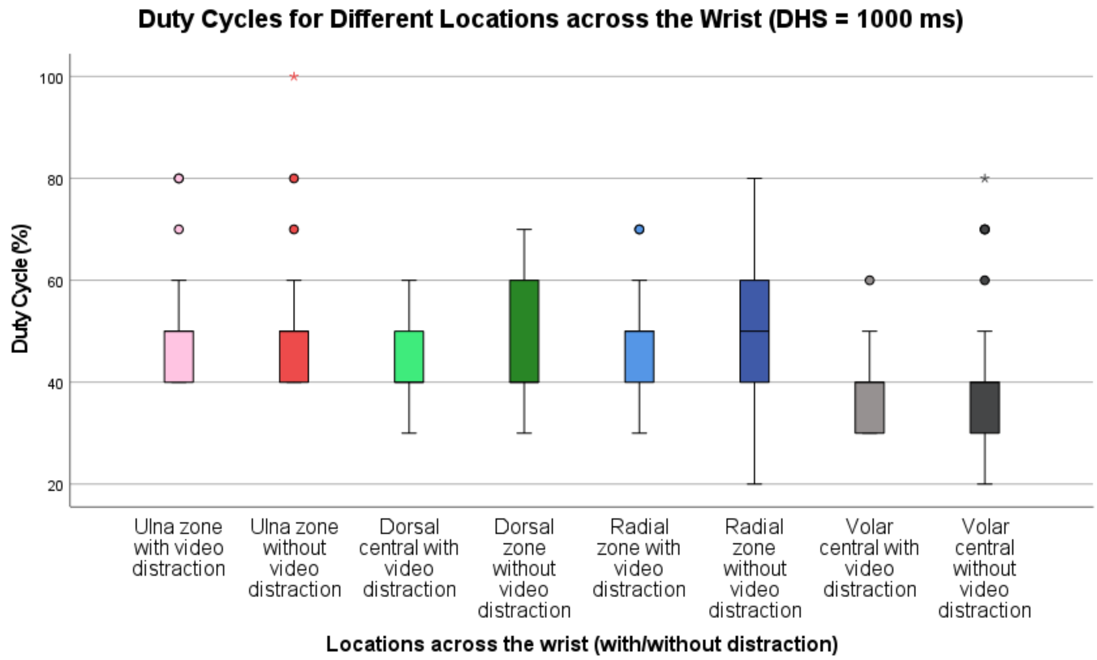

Figure 5.12: Boxplots for PWM duty cycles of MDHI with and without video distractions (DHS = 1000 ms)

Follow up comparisons indicated that pairwise difference of the mean minimum PWM duty cycles corresponding to the MDHI between the Dorsal central and Volar central was not significant ($p = 0.105$). MDHI between the Dorsal central and the Ulna ($p = 0.005$) was however significant. Pairwise difference of MDHI between the Volar central and Ulna zone ($p < 0.001$), as well as Radial zone ($p < 0.001$) was significant. MDHI for the Ulna zone and Radial zone was however similar ($p = 0.363$).

Table 5.8: Mean duty cycles regardless of distraction (duration of haptic stimulation = 1000 ms)

Stimulation locations	**Mean duty cycle (%)**	**Standard error**
Dorsal central	43.833	1.472
Volar central	40.333	1,642
Ulna zone	50.167	1.753
Radial zone	48.167	1.617

There was a significant main effect of distraction on MDHI. $Wilk's Lambda = 0.848$, ($F(1,29) = 5.182$, $p = 0.030$, $\eta_p^2 = 0.152$). Thus, there is significant evidence to reject the null hypothesis. The mean duty cycle of the haptic stimulation felt when video distraction was introduced (44.083%) was lower than the mean duty cycle of haptic stimulation felt without video distraction (47.167%). Pairwise comparison for the two levels of distraction (with video, without video) was significant ($p = 0.030$).

The interaction between locations of haptic stimulation and distraction did not yield any significant main effect, $Wilk's Lambda = 0.882$, ($F(3,87) = 0.732$, $p = 0.535$, $\eta_p^2 = 0.025$).

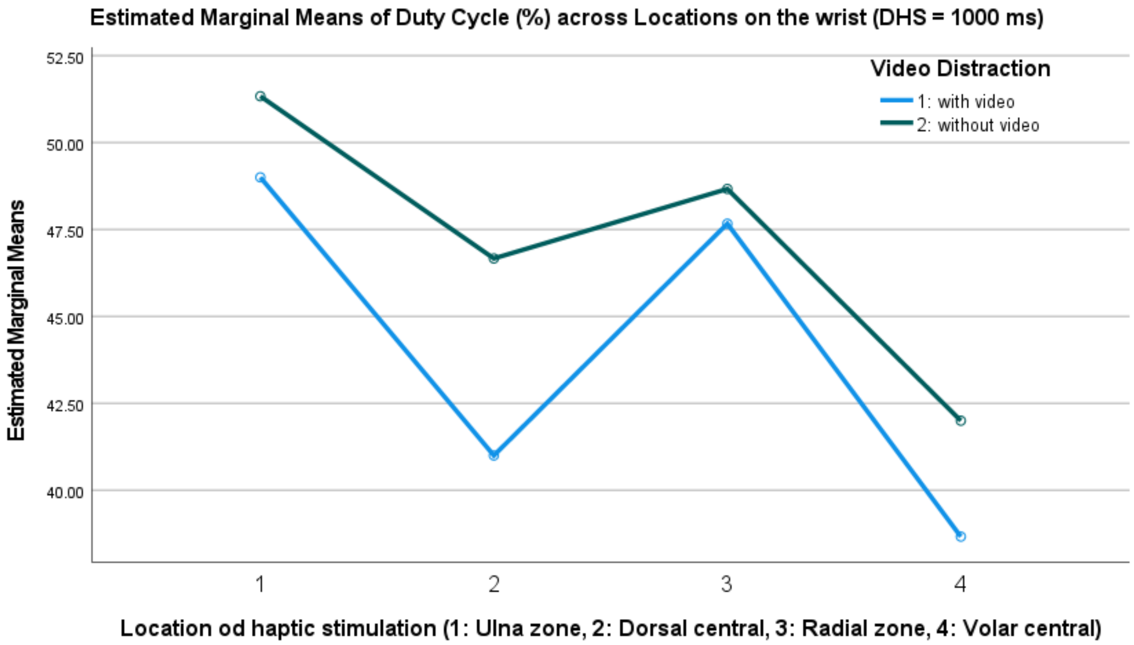

Figure 5.13: Profile plots for duty cycles (DHS = 1000 ms)

Figure 5.13 shows the profile plot for the estimated marginal means of the minimum duty cycles for the different stimulation locations on the wrist. Levels 1 and 2 of the distraction levels represent duty cycle measurements with and without video respectively. Figure 5.13 shows similar patterns for the duty cycles with and without the introduction of video distraction. With and without video distraction, the Volar central can be seen to have the lowest MDHI.

5.4.1.5 Examining the Significance of Durations of Haptic Stimulation

Subsections 5.4.1.1, 5.4.1.2, 5.4.1.3, and 5.4.1.4 describe how the minimum detectable haptic intensity (MDHI) varies across different locations on the wrist for different durations of haptic stimulation. Here, the MDHI for each point of haptic stimulation on the wrist is compared across the different durations of haptic stimulation (DHS).

In this section, the aim is to determine if there is statistical difference between duty cycles of MDHI at different locations on the wrist for different durations of haptic stimulations. Table 5.9 shows the mean minimum detectable duty cycles for varying durations of haptic stimulation. Across the locations on the wrist for different DHS, paired samples t-test was carried out on the duty cycles recorded when video distraction was used.

Table 5.9: Variability of the MDHI (duty cycles) with durations of haptic stimulation

Duration of Haptic Stimulation	Mean Duty Cycle (With Video Distraction)				Mean Duty Cycle (Without Video Distraction)			
	Ulna zone	Dorsal central	Radial central	Volar central	Ulna zone	Dorsal central	Radial zone	Volar central
250	63.0000	58.6667	66.0000	50.3333	61.6667	53.6667	58.3333	50.3333
500	55.6667	50.6667	56.0000	44.6667	53.0000	46.6667	55.6667	40.0000
750	50.0000	49.3333	53.3333	41.6667	53.6667	47.6667	49.6667	39.6667
1000	49.0000	41.0000	47.6667	38.6667	51.3333	46.6667	48.6667	42.0000

Table 5.10 shows the pairs (DHS comparison) for which the test was significant. Table 5.10 contains results with video distraction. The null hypothesis (that the difference of the means of the pairs equals zero) will be rejected if the calculated t value is greater than the critical t value or if sig. (2-tailed) is less than 0.05 [124](df = 29, confidence level = 95%).

Table 5.10: Paired samples t Test for duty cycles based on duration of stimulation (All with video distraction)

		Duration of Hapic Stimulation (DHS)					
		250 - 500	250 - 750	250 - 1000	500 - 750	500 - 1000	750 - 1000
Ulna zone	Calculated t	2.665	5.407	6.433	1.951	2.339	~~0.423~~
	Critical t	2.045	2.045	2.045	2.045	2.045	2.045
	Sig. (2-tailed)	0.006	< .001	< .001	0.030	0.013	~~0.338~~
Dorsal central	Calculated t	3.077	3.006	6.652	~~0.548~~	4.690	3.470
	Critical t	2.045	2.045	2.045	2.045	2.045	2.045
	Sig. (2-tailed)	0.005	0.005	<.001	~~0.588~~	<.001	0.002
Radial zone	Calculated t	3.942	6.071	7.792	~~1.034~~	3.878	2.538
	Critical t	2.045	2.045	2.045	2.045	2.045	2.045
	Sig. (2-tailed)	<.001	<.001	<.001	~~0.155~~	<.001	0.008
Volar central	Calculated t	2.984	4.292	6.727	~~1.608~~	3.071	~~1.874~~
	Critical t	2.045	2.045	2.045	2.045	2.045	2.045
	Sig. (2-tailed)	0.003	<.001	<.001	~~0.059~~	0.002	~~0.036~~

Figure 5.14 shows clustered bar chart for different locations across the wrist. For each location across the wrist, mean duty cycles for different durations of haptic duration are compared. It shows that MDHI decreases as DHS increases for all the locations examined.

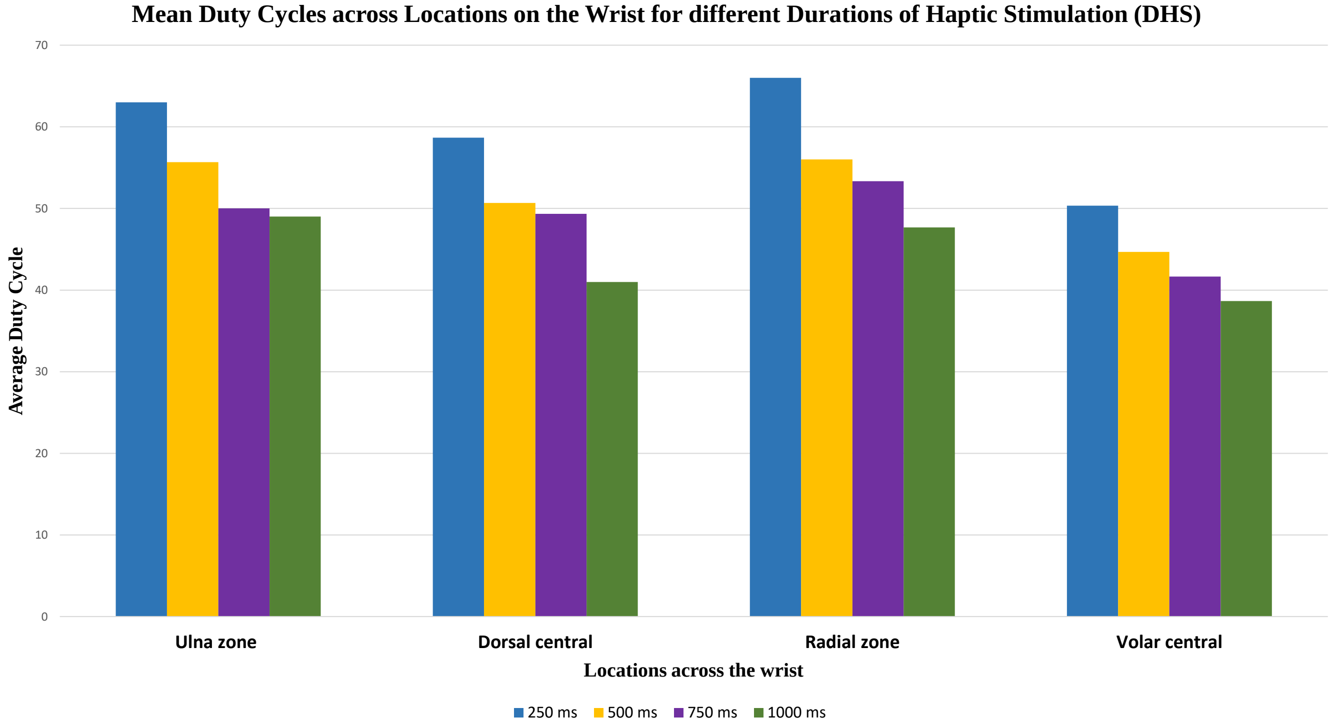

Figure 5.14: Mean duty cycles for different DHS across locations on the wrist(with video distraction)

It is also important to examine the effect of video distraction on MDHI for locations across the wrist as DHS changes. Table 5.11 shows the paired samples t-test results when duty cycles are paired with and without distractions for the different locations on the wrist. Table 5.11 shows only the significant results.

Table 5.11: Paired samples t-test for duty cycles based on distraction

DHS	**Point on the Wrist**	**Calculated t-value**	**Critical t-value**	**Sig. (2-tailed)**
250	Top	2.140	1.96	0.041
250	Right	2.677	1.96	0.012
500	Bottom	2.379	1.96	0.024
1000	Top	2.811	1.96	0.009

Table 5.10 shows the paired t-test for different locations on the wrist based on duration of stimulation. There were significant differences between most of the duration of stimulation as shown for the different locations on the wrist. We can conclude that the duration of stimulation has significant effect on the MDHI of haptic stimulation across different locations of the wrist examined. From Table 5.11, the introduction of distraction only had significant effect in a few cases at different locations and duration of stimulation.

5.5 Study Phase 2: Identification of Location of Haptic Stimulation Performance (ILHS)

Phase 2 of the study examined the participants' abilities to correctly identify the locations of haptic stimulation on the wrist. The study was repeated for five (5) scenarios (with and without video distractions), taking a total time of approximately 30 minutes. For each participant, the highest MDHI (measured as duty cycle of PWM) for across locations on the wrist in phase 1 was used. Table 5.12 below shows the DHS and average duty cycles for the different scenarios.

Table 5.12: Scenarios of the haptic-stimulated point identification task

Scenarios	Duty Cycles (%)	Duration of haptic Stimulation (ms)	Average Duty Cycle (%)	
			With Video	Without video
S1	Highest duty cycle for each participant, derived in phase 1	250	70	66.82
S2	Highest duty cycle for each participant, derived in phase 1	500	64.09	62.27
S3	Highest duty cycle for each participant, derived in phase 1	750	56.36	62.72
S4	Highest duty cycle for each participant, derived in phase 1	1000	50.91	58.18
S5	90	750	90	90

Scenario 5 is the control scenario. The parameters (duty cycle and duration of haptic stimulations) in scenario 5 are kept constant for all participants. For scenarios 1-4, corresponding maximum duty cycles recorded for each participant from the phase 1 study were used. In the phase 1 study, the minimum detectable haptic intensity (MDHI) at each location on the wrist is recorded with and without video distraction for each stimulation duration. Since the recorded minimum DHI of haptic stimulations at the different locations on the wrist are not the same, the highest duty cycles (with and without video distraction) recorded for the different locations are used in this phase. The task which involved identifying the locations of haptic stimulation was carried out in two stages. In the first stage, participants were required to identify single locations of haptic stimulation. The locations in this phase were tagged as directions as shown in figure 5.15 . Each location tag corresponds to the naming convention in figure 5.2 respectively.

1. Right: Radial zone
2. Down: Volar central
3. Left: Ulna zone
4. Up: Dorsal central

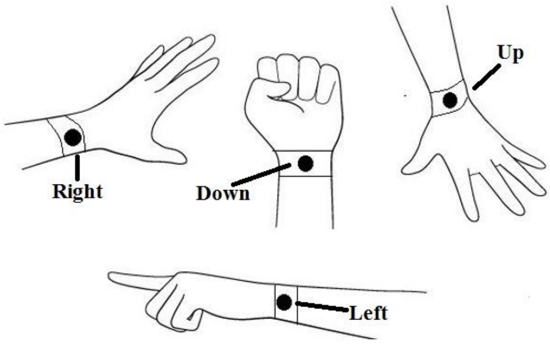

Figure 5.15: Phase 2 study graphical user interface

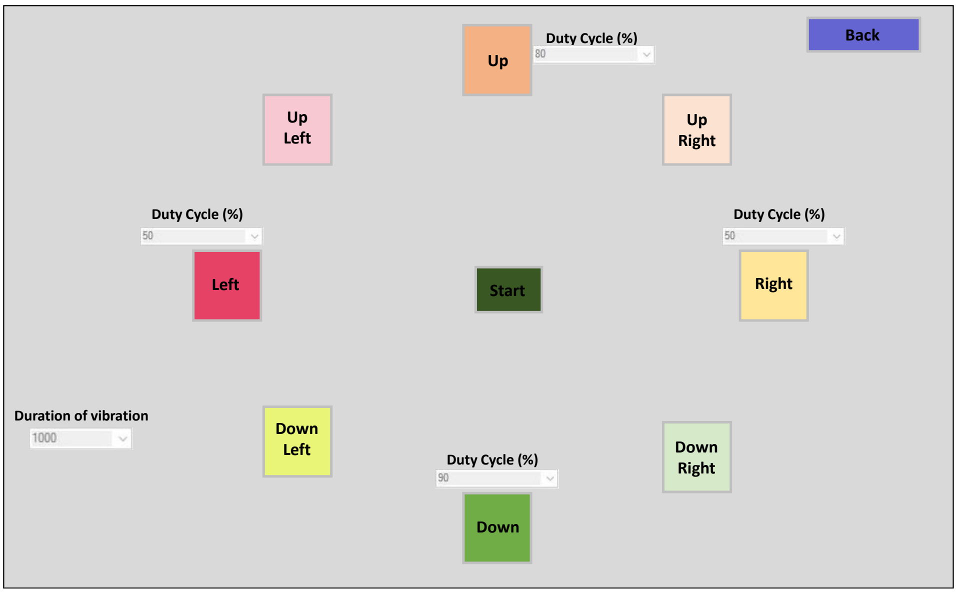

Figure 5.16: Phase 2 study graphical user interface

In the second stage, participants were required to identify two simultaneously stimulated locations of haptic stimulation. The combinations of double-locations stimulation are Dorsal central - Radial zone, Dorsal central - Ulna zone, Volar central - Ulna zone, and Volar central - Radial zone. Each single location (and combination of locations) was stimulated three times. Each scenario for which the task was carried out was used with and without video distraction. Figure 5.16 shows the graphical user interface of the control program used to control haptic stimulation. The duty cycles of the PWM for each haptic motor can be set.

Twenty eight of all participants were right-handed with only two participants being left-handed. The haptic feedback device was worn on the non dominant hand and so the results of the two left-handed participants were adjusted to ensure that references to the different locations across the wrist are the same for all participants.

5.5.1 Results

Participants' abilities to correctly identify locations of haptic stimulation on the wrist in this thesis is referred to as identification of location of haptic stimulation performance (ILHSP). Table 5.12 shows the haptic stimulation durations and average duty cycles for the different scenarios.

The task, which involved the identification of locations of haptic stimulation was carried out in two stages. In the first stage, participants were required to identify single locations of haptic stimulation. The single locations are at the Dorsal central, Radial zone, Volar central and Ulna zone of the wrist. In the second stage, participants were required to identify two simultaneously stimulated locations of haptic stimulation. The combinations of double locations for stimulation are Dorsal central - Radial zone, Dorsal central - Ulna zone, Volar central - Radial zone, and Volar central - Ulna zone. Each location (or combination of locations) was haptic stimulated three times. Each scenario for which the task was carried out was used with and without video distraction.

A score of 1 is given for every correctly identified location (or combination of locations) of haptic stimulation. Each stage attempt requires that all the locations (or combinations of locations) are stimulated three times. This implies that participants can score a maximum score of 3 (average=1) for each point (or combination of locations) of haptic stimulation in each attempt.

		Haptic stimulation (Signal)	
		Present	Absent
Response	Present	Hit	False Alarm
	Absent	Miss	Correct Rejection

Figure 5.17: Decision table

Although the performance scores for the different locations tells us how participants performed in correctly identifying the stimulated locations, it is difficult to interpret high performance scores as the sensitivity of the locations on the wrist. There is therefore the need to eradicate false responses. Signal detection theory was employed to determine the sensitivity of the different locations on the wrist to haptic stimulation. It is often used to evaluate sensitivity in decision-making [11]. Signal detection theory is built on the premise that signal (e.g. haptic stimulation) and noise are represented probabilistically within the decision maker.

Figure 5.17 shows the response matrix for all signal-response combinations. Response decisions are made relative to set criterion (β). Haptic stimulation is reported present when the signal is stronger than β and absent when the signal is weaker than β. For each haptic stimulation, a hit represents the probability that participants report the presence of haptic stimulation at a point on the wrist when it is (fig. 5.18A green), and a false alarm represents the probability that participants report the presence of haptic stimulation at a point on the wrist when it is absent (fig. 5.18B red). Alternatively, a miss represents the probability that participants report the absence of haptic stimulation when it is present (fig. 5.18A red), and a correct rejection represents the probability that participants report the absence of haptic stimulation when it is absent (fig. 5.18B green).

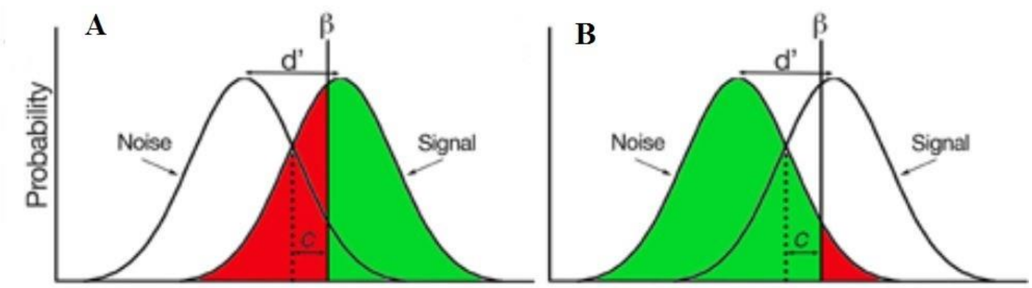

Figure 5.18: Normal plots for signal and noise representations

Sensitivity can be estimated as:

$$d^{'} = Z(P_{hit}) - Z(P_{FA}) \tag{5.1}$$

Given: Z(P_{hit}) is the z-value (standard deviation) associated with the probability of a hit. Z(P_{FA}) is the z-value (standard deviation) associated with the probability of a false alarm.

Sensitivity d' reflects the probability of a hit and the probability of a false alarm. It is also independent of participants' bias (c).

$$c = -\frac{Z(P_{hit}) + Z(P_{FA})}{2} \tag{5.2}$$

A negative value of c implies that participants are more likely to report that haptic stimulation is present (liberal criterion). A positive value of c means that participants are less likely to report that haptic stimulation is present (conservative criterion). The strength of participants' bias is provided by the absolute value of c [11].

5.5.1.1 Overall Identification of Location of Haptic Stimulation Performance (Overall ILHSP)

Table 5.13 shows the descriptive statistics for the overall performance scores when participants were tasked with identifying locations of haptic stimulation on the wrist. It shows the performance statistics for the two stages of haptic stimulation (single - location stimulation identification (SSI) and simultaneous double-locations stimulation identification (SDSI)). For each attempt, a maximum score of twelve can be achieved when the scores are added for the four single locations of haptic stimulation (as well as for the four double locations of haptic stimulation). Taking an average of the performance scores by the overall number of stimulation-attempts for each task attempt resolves the score to a maximum of 1.

Table 5.13: Overall Identification of Location of Haptic Stimulation Performance (ILHSP) Scores

Scenarios	Overall Identification of Location of Haptic Stimulation Performance (Overall ILHSP) Scores for Single-Location Stimulation Identification (SSI). (Up, Right, Down and Left)				Overall Identification of Location of Haptic Stimulation Performance (Overall ILHSP) Scores for Simultaneous Double-Location Stimulation Identification (SDSI). (Up-Right, Up-Left, Down-Right and Down-Left)			
	With Video Distraction		Without Video Distraction		With Video Distraction		Without Video Distraction	
	Mean	Standard Deviation	Mean	Standard Deviation	Mean	Standard Deviation	Mean	Standard Deviation
1	0.7318	0.22417	0.6773	0.21121	0.0605	0.07859	0.0986	0.10503
2	0.7086	0.19389	0.7273	0.17734	0.1632	0.17573	0.1814	0.21656
3	0.6550	0.14982	0.7355	0.16442	0.1627	0.19855	0.2423	0.21150
4	0.6514	0.14942	0.6705	0.22154	0.1618	0.15759	0.2123	0.18249
5 (Control)	0.8218	0.14911	0.8527	0.14862	0.3264	0.23746	0.3291	0.27589

Figure 5.19 shows the boxplots for haptic stimulation identification performances of the participants shown in Table 5.13 for different haptic stimulation durations. The boxplots show the difference in performance scores for location identification when single-locations and double-locations are haptic stimulated. Figure 5.19 shows that it is easier to correctly identify single haptic stimulated locations than correctly identifying 2 simultaneously stimulated locations on the wrist. The effects of video distractions on the performance was also examined.

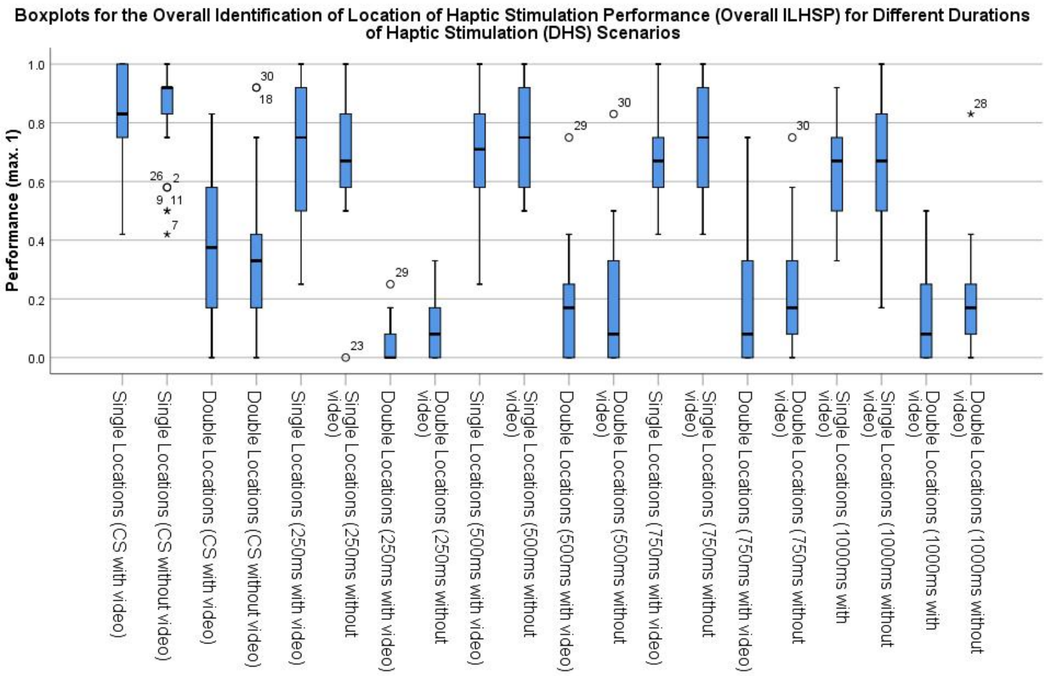

Figure 5.19: Boxplots for Overall Identification of Locations of Haptic Stimulation Performance (Overall ILHSP) for various scenarios of SSI and SDSI.

5.5.1.2 Overall Identification of Location of Haptic Stimulation Performance (Overall ILHSP) Scores for Single-Location Stimulation Identification (SSI)

Overall performance scores are derived by adding performance scores for each individual location of haptic stimulation. The assumption of sphericity was not met for the different scenarios ($p = 0.037$) but was met for the interaction scenarios*distractions ($p = 0.709$).

Results of the two-way repeated measures ANOVA revealed that there was a significant main effect of the scenario (different haptic stimulation durations) on participants' performance scores ($F(3.12, 65.55) = 7.087, p = 0.00, \eta_p^2 = 0.252).Wilk's Lambda = 0.00.$). Follow up comparisons indicated that the pairwise difference of performance scores between scenarios 1-4 was not significant ($p_{1-2} = 1.00, p_{1-3} = 1.00, p_{1-4} = 1.00, p_{2-3} = 1.00, p_{2-4} = 1.00, p_{3-4} = 1.00$). This implies that there is no significant difference in overall performance scores between scenarios 1- 4. The overall performance scores for the difference scenarios were similar. Using the results of the haptic calibration stage yields similar overall results irrespective of the duration of haptic stimulation. The Pairwise differences for performance scores between scenario 5 (control scenario) and scenario 1($p = 0.059$) as well as scenario 2($p = 0.053$ were not significant. However, the pairwise difference between scenario 5 and 3($p = 0.001$), as well as 4($p = 0.00$) were significant. The test of within-subjects contrasts between scenario 5 and all other scenarios was significant, $p < 0.05$. It can be noted from table 5.17 that scenarios 1 and 2 have higher mean duty cycles when compared to scenarios 3 and 4. Participants had high performance scores when the duty cycles were high (even though the durations of haptic stimulations were low). The performance in scenario 5 was significantly different from other scenarios. At sufficiently high duty cycles, irrespective of the duration of haptic stimulation, identifying points of haptic stimulation becomes easier.

Results also showed that there was no main effect of distractions on identifying points of haptic stimulations ($F(1,21) = 0.739$, $p = 0.400$, $\eta_p^2 = 0.034). Wilk'sLambda = 0.40$. Follow up comparisons indicated that the pairwise difference different levels of distraction was not significant ($p = 0.400$). The within-subjects contrasts was also not significant ($p = 0.400$). The interaction between the scenarios of the task and distraction was not significant ($p = 0.366$).

Figure 5.20: Profile plots for overall haptic stimulation identification performance (HSIP) scores for single-location stimulation identification (SSI)

Figure 5.20 shows the profile plots of performance for overall single-Location haptic stimulation identification. It also shows the effect of video distraction. Scenario 5 clearly had better performance scores than scenarios 1-4.

5.5.1.3 Overall Identification of Location of Haptic Stimulation Performance (Overall ILHSP) Scores for Simultaneous Double-Location Stimulation Identification (SDSI)

In this stage of the study, participants were required to identify two locations of simultaneous stimulation. Table 5.13 shows the descriptive statistics for the performance scores for the different scenarios. Scenario 5 has the highest overall ILHSP scores with and without videos. Results show relatively low performance scores for all the scenarios examined as participants struggled to correctly identify two simultaneously stimulated locations on the wrist. The assumption of sphericity was not met for the different scenarios ($p = 0.020$) and for the interaction scenarios *distractions ($p = 0.000$).

Two-way repeated measures ANOVA revealed that there was a significant main effect of scenarios on the overall performance scores of participants ($F(2.78, 58.3) = 10.52$, $p = 0.00$, $\eta_p^2 = 0.334$). $Wilk'sLambda = 0.001$. Performance scores were affected by scenarios. Follow up comparisons indicated that the pairwise difference of performance scores between scenario 5 and scenarios 1($p = 0.00$) and 2(0.011) were significant. Furthermore, it also shows that the pairwise difference of performance between scenario 5 and scenarios 3($p = 0.097$) and 4(0.099) were not significant. The within-subjects contrasts between scenario 5 and all other scenarios were significant ($p < 0.05$). This implies that there is significant difference in ILHSP scores for SDSI between scenario 5 and other scenarios.

There is also a significant main effect of distraction on performance of participants ($F(1,21) = 6.396$). $Wilk'sLambda = 0.020$. Follow up comparisons indicated that the pairwise difference between the different levels of distraction was significant ($p = 0.020$). Within-subjects contrasts was also significant ($p = 0.020$).

The interaction between the scenarios of the task and distraction was not significant ($p = 0.553$). Figure 5.21 shows the profile plots for different scenarios for the overall performance in identifying two concurrently stimulated locations. The scenarios without video distraction scored higher and scenario 5 had the highest overall scores (with and without video distraction)

The overall ILHSP scores reveal how participants fared in identifying single and double locations of haptic stimulation in general. However, they do not reveal in detail the sensitivity of the different locations on the wrist and the how easily haptic stimulation could be correctly identified (individual performance scores) at the different locations on the wrist.

Next, we explored in detail the sensitivity of the different locations on the wrist to haptic stimulation for various scenarios and the ease with which stimulation was correctly identified at the different points on the wrist.

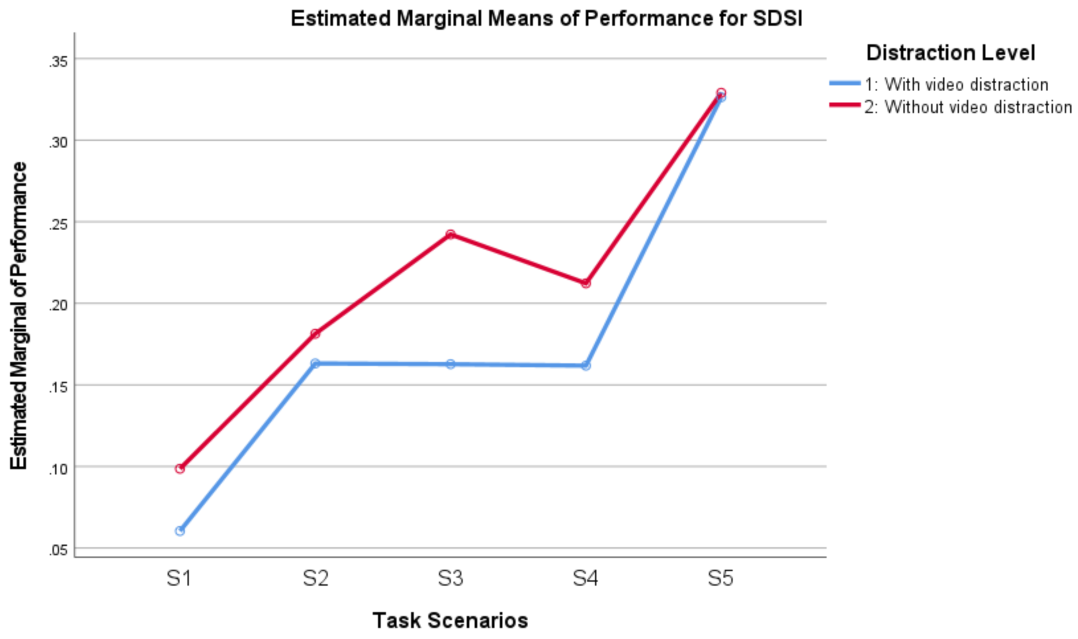

Figure 5.21: Profile plots for overall haptic stimulation identification performance (HSIP) scores for simultaneous double-location stimulation identification (SDSI)

5.5.1.4 Individual Identification of Location of Haptic Stimulation Performance (Individual ILHSP) for Single-Location Stimulation Identification (SSI) and Sensitivity Measurements

In this section, the accuracy with which participants correctly identified single locations of haptic stimulation on the wrist for the various scenarios in table 5.12 was examined. The probabilities of identification by chance was also examined by estimating the sensitivity of the different locations on the wrist.

1. **Control scenario (Duration of Haptic Stimulation (DHS) = 750 ms, Duty cycle = 90%)**

   The overall ILHSP scores for correctly identifying the locations of haptic stimulation was highest for this scenario (table 5.13). Results were further analysed to see how participants correctly identified haptic stimulation at each of the specified location on the wrist.

   The descriptive statistics for the ILHSP scores for each location is shown in table 5.14. The down location had the highest ILHSP score, and the location on the left of the wrist had the least performance score. With and without video distraction, the least performance score is greater than 70%.

   A 2-way repeated measures ANOVA (analysis of variance) was carried out to evaluate the null hypothesis that all haptic stimulated locations on the wrist can be equally identified.

The assumption of sphericity was not met for location of stimulation ($p = 0.013$) and interaction location*distraction ($p = 0.011$).

Table 5.14: Individual Identification of Location of Haptic Stimulation Performance scores for control scenario

Location on the wrist	With Video Distractions		Without Video Distractions		Number of Participants
	Mean Performance Score (max. = 1)	Standard Deviation	Mean Performance Score (max. = 1)	Standard Deviation	
Dorsal central	0.8673	0.24092	0.8560	0.25792	30
Volar central	0.9337	0.16108	0.9337	0.16108	30
Ulna zone	0.7440	0.36883	0.7783	0.30759	30
Radial zone	0.7447	0.32435	0.7673	0.30529	30

There was significant main effect of location of haptic stimulation on correctly identifying points that were haptic stimulated ($F(2.414, 70.004) = 4.730$, $p = 0.008$, $\eta_p^2 = 0.140$). Wilk's Lambda = 0.526. We can therefore reject the null hypothesis that all haptic stimulated locations on the wrist can be equally correctly identified. Pairwise difference for the performance scores between the Volar central and the Dorsal central was not significant ($p = 0.512$). However, the pairwise difference for the performance scores between the Volar central and Ulna zone ($p = 0.011$) as well as the Radial zone ($p = 0.005$) were significant. This implies that there are similarities in performance scores when identifying haptic stimulation at the Dorsal central and Volar central. Results show that it was more difficult to identify haptic stimulation at locations at the Ulna and Radial zones relative to the Dorsal central and Volar central.

There was no significant effect of distraction on correctly identifying locations of haptic stimulation on the wrist ($F(1,29) = 0.120$, $p = 0.732$, $\eta_p^2 = 0.004$). We can also reject the null hypothesis that distraction affects the ability to correctly identify locations of haptic stimulation on the wrist. Likewise, there was no significant main effect of the interaction location*distraction ($F(2.154, 62.471) = 0.165$, $p = 0.920$, $\eta_p^2 = 0.006$).

The profile plot in figure 5.22 shows that it was easier to identify haptic stimulation at the Volar central but there is no significant difference in the ease at which haptic stimulation could be pinpointed between the Ulna and Radial zones for the control scenario.

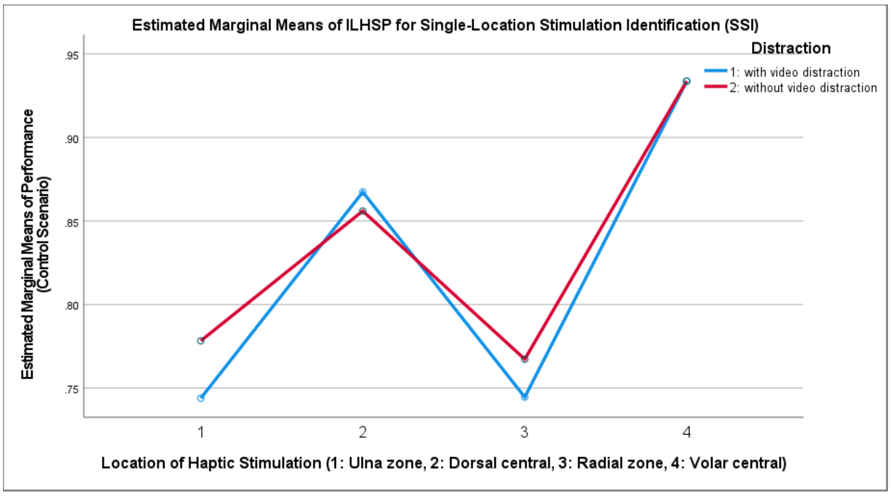

Figure 5.22: Profile plots of ILHSP for single-location stimulation identification (Control scenario)

Table 5.15: Sensitivity and bias values for different locations on the wrist (Control scenario)

(a) With video distraction

Scenarios	With Video Distraction					
	Hit		False Alarm		Sensitivity, d'	Bias, c
	p	z scores	p	z scores		
Ulna zone	0.743	0.6526	0.011	-2.290	2.943	0.819
Dorsal central	0.867	1.114	0.018	-2.089	3.203	0.488
Radial zone	0.745	0.658	0.015	-2.179	2.837	0.761
Volar central	0.934	1.504	0.022	-2.014	3.683	0.255

(b) Without Video Distraction

Scenarios	Without Video					
	Hit		False Alarm		Sensitivity, d'	Bias, c
	p	z scores	p	z scores		
Ulna zone	0.756	0.693	0.041	-1.743	2.436	0.525
Dorsal central	0.854	1.052	0.022	-2.014	3.066	0.481
Radial zone	0.767	0.730	0.011	-2.290	3.325	0.78
Volar central	0.933	1.504	0.04	-1.747	3.251	0.122

Using Equation 5.1 and Equation 5.2, the participants' sensitivity and bias values were calculated for the different locations on the wrist. Table 5.15 shows the calculated values for the control scenario.

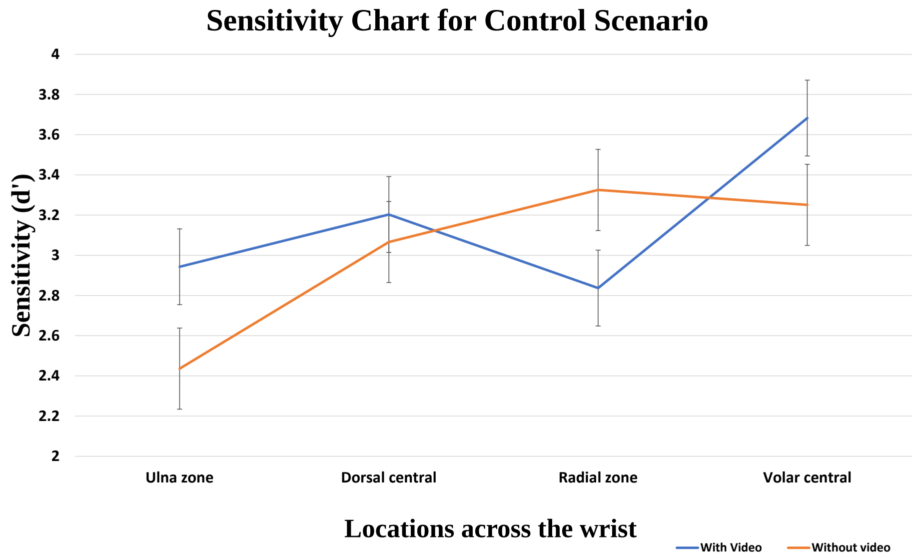

Figure 5.23: Sensitivity chart for locations on the wrist (Control scenario)

Figure 5.23 shows that participants were more sensitive to haptic stimulation at the Volar central when video distraction was introduced. This is in line with the identification performance score rankings for the different locations on the wrist. It also shows that the identification performance scores for the different locations on the wrist did not happen by chance.

Without distraction, participants were more sensitive to haptic stimulation at the Radial zone as shown in figure 5.23. Positive values for bias shows that participants demonstrated a more conservative bias which means that participants were less likely to report that the stimulation is present.

2. **Scenario 1 (Duration of Haptic Stimulation (DHS) = 250 ms)**

   In this scenario, the duration of haptic stimulation used was 250 ms. For each participant, the highest recorded duty cycle for phase 1 of all locations on the wrist was used as the duty cycle in this phase.

   Table 5.16 shows the descriptive statistics of individual ILHSP scores for stimulation duration of 250 ms. With and without video distraction, the minimum performance score (ILHSP score) is 66.73% and 53.05% respectively. The lowest ILHSP score was recorded for the left side of the wrist.

Table 5.16: Individual identification of location of haptic stimulation performance scores for scenario 1

Location on the wrist	With Video Distraction		Without Video Distraction		Number of Participants
	Mean Performance Score (max. = 1)	Standard Deviation	Mean Performance Score (max. = 1)	Standard Deviation	
Dorsal central	0.7882	0.33426	0.7732	0.29827	22
Volar central	0.8032	0.30316	0.7427	0.37015	22
Ulna zone	0.6673	0.38518	0.6673	0.32596	22
Radial zone	0.6673	0.38518	0.5305	0.3522	22

A 2-way repeated measures ANOVA (analysis of variance) was carried out to evaluate the null hypothesis that all haptic stimulated locations on the wrist can be equally identified. The assumption of sphericity was met for locations of stimulation ($p = 0.636$) and interaction location*distraction ($p = 0.406$).

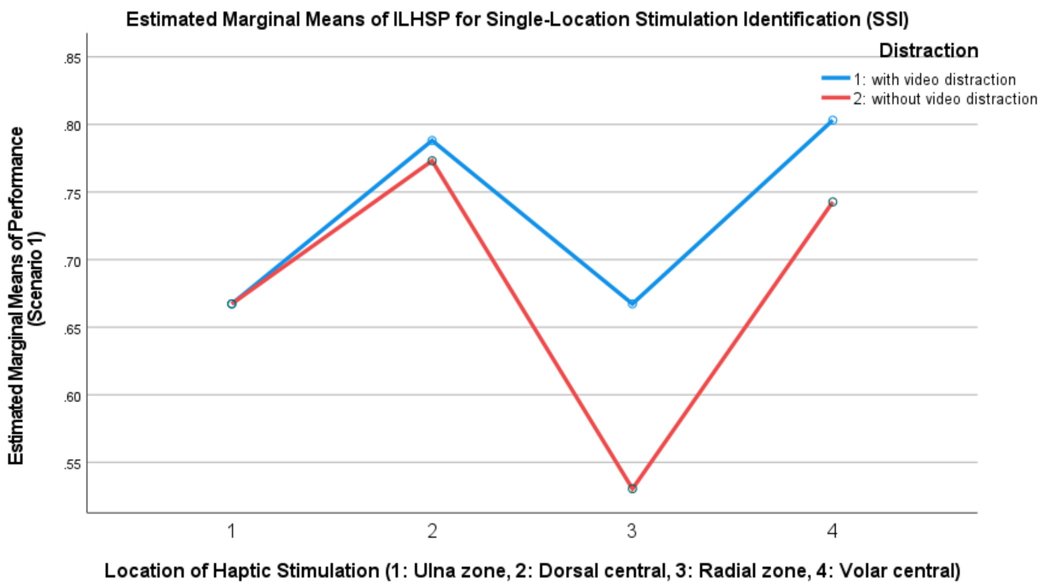

Figure 5.24: Profile plots of ILHSP for single-location stimulation identification (Scenario 1)

There was no significant effect of location of haptic stimulation on participant's abilities to correctly identify the points of haptic stimulation ($F(3,63) = 2.732$, $p = 0.051$, $\eta_p^2 = 0.115$).

The null hypothesis is confirmed. There was also no significant effect of distraction on the ability of participants to correctly identify locations of haptic stimulation ($F(1,21) = 1.383$, $p = 0.253$, $\eta_p^2 = 0.062$). The interaction location*distraction was also found to have no significant effect on ILHSP of participants ($F(3,63) = 0.603$, $p = 0.615$, $\eta_p^2 = 0.028$).

Figure 5.24 shows the profile plots for the marginal means of performance scores for different locations across the wrist. Though not statistically different from other locations on the wrist, haptic stimulation at the Dorsal central and Volar central were easier to pinpoint.

Table 5.17 shows participants' sensitivity and bias values for scenario 1.

Table 5.17: Sensitivity and bias values for different locations on the wrist (Scenario 1)

(a) With video distraction

Scenarios	With Video Distraction					
	Hit		False Alarm		Sensitivity, d'	Bias, b
	p	z scores	p	z scores		
Ulna zone	0.667	0.4324	0.04	-1.7507	2.1831	0.659
Dorsal central	0.788	0.8001	0.055	-1.5982	2.3983	0.399
Radial zone	0.667	0.4324	0.055	-1.5982	2.0306	0.5829
Volar central	0.803	0.8530	0.085	-1.3693	2.2223	0.258

(b) Without Video Distraction

Scenarios	Without Video					
	Hit		False Alarm		Sensitivity, d'	Bias, b
	p	z scores	p	z scores		
Ulna zone	0.667	0.4324	0.03	-1.8808	2.3132	0.724
Dorsal central	0.773	0.7494	0.055	-1.5982	2.3476	0.424
Radial zone	0.530	0.0764	0.070	-1.4724	1.5488	0.698
Volar central	0.788	0.8001	0.11	-1.2536	2.0537	0.227

Table 5.17 shows that for scenarios with video distraction, participants were more sensitive to haptic stimulation at the Dorsal central. However, it also shows close sensitivity values

for the different locations on the wrist (fig. 5.25). The close sensitivity values are consistent with the results showing no significant effect of location of haptic stimulation on the participants' abilities to correctly identify locations of haptic stimulation.

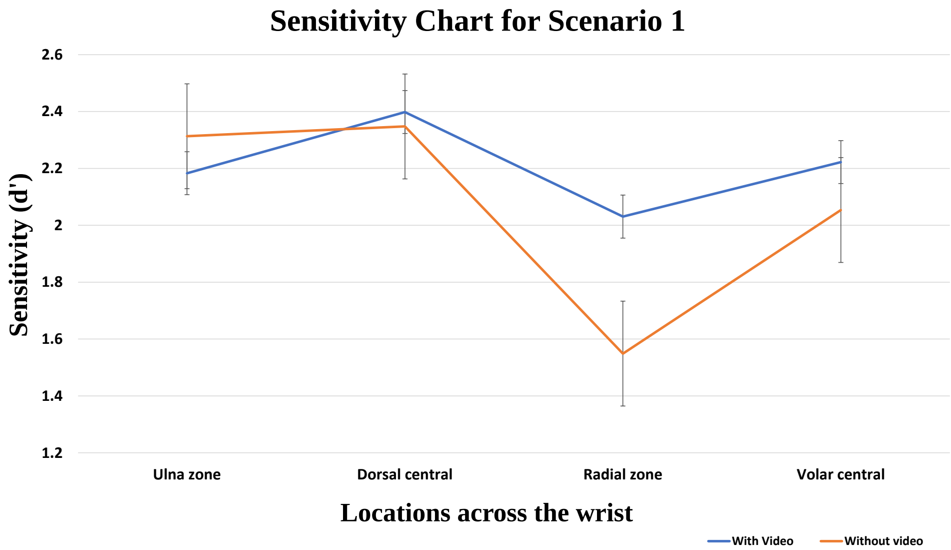

Figure 5.25: Sensitivity chart for locations across the wrist (Scenario 1)

3. **Scenario 2 (Duration of Haptic Stimulation (DHS) = 500 ms)**

The duration of haptic stimulation used was 500 ms. Duty cycle used was the maximum recorded of the locations on the wrist from phase 1.

Table 5.18: Individual Identification of Location of Haptic Stimulation Performance scores for scenario 2

Location on the wrist	With Video Distraction		Without Video Distraction		Number of Participants
	Mean Performance Score (max. = 1)	Standard Deviation	Mean Performance Score (max. = 1)	Standard Deviation	
Dorsal central	0.8191	0.26647	0.7432	0.32434	22
Volar central	0.8341	0.26697	0.8341	0.30386	22
Ulna zone	0.5150	0.38191	0.6982	0.27085	22
Radial zone	0.6664	0.35725	0.6368	0.38411	22

The descriptive statistics of ILHSP scores for each point on the wrist for scenario 2 is shown in table 5.18. With and without video distraction, the minimum ILHSP scores are 51.5%

and 63.7% respectively. The ILHSP score was highest at the Volar central.

A 2-way repeated measures ANOVA (analysis of variance) was carried out to evaluate the null hypothesis that all haptic stimulated locations across the wrist can be equally identified. The assumption of sphericity was met for locations of stimulation ($p = 0.912$) and interaction location*distraction ($p = 0.087$).

There was a significant main effect of location of haptic stimulation on ILHSP, $Wilk'sLambda = 0.637$, $F(3,63) = 4.307$, $p = 0.008$, $\eta_p^2 = 0.170$. Null hypothesis is not confirmed. Pairwise difference for ILHSP between the Ulna zone and Volar central was significant ($p = 0.040$). All other pairwise differences between the different locations across the wrist were not significant.

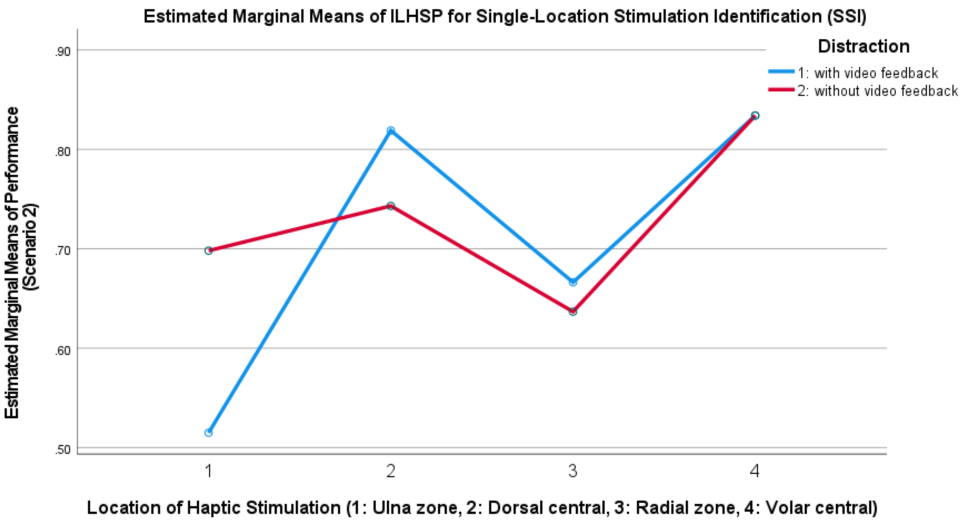

Figure 5.26: Profile plots of ILHSP for single-location stimulation identification (Scenario 2)

Results also showed a non-significant effect of distraction on participants' abilities to correctly identify locations of haptic stimulation, $Wilk'sLambda = 0.994. F(1,21) = 0.135$, $p = 0.717$, $\eta_p^2 = 0.006$. There was no effect of the interaction location*distraction, $F(3,63) = 2.040$, $p = 0.117$, $\eta_p^2 = 0.089$. The profile plots in figure 5.26 show how participants identified the locations of haptic stimulation.

Table 5.19 shows that for scenarios with video distraction, participants were more sensitive to haptic stimulation at the Volar central. This is shown in figure 5.27.

Positive values for bias shows that participants demonstrated a more conservative bias which means that participants were less likely to report that the stimulation is present.

Table 5.19: Sensitivity and bias values for different locations on the wrist (Scenario 2)

(a) With video distraction

Scenarios	With Video Distraction					
	Hit		False Alarm		Sensitivity, d’	Bias, b
	p	z scores	p	z scores		
Ulna zone	0.515	0.0376	0.045	-1.6954	1.733	0.8289
Dorsal central	0.819	0.9119	0.085	-1.3693	2.2812	0.229
Radial zone	0.666	0.4299	0.025	-1.9600	2.3899	0.927
Volar central	0.834	0.9705	0.045	-1.6954	2.6659	0.362

(b) Without video distraction

Scenarios	Without Video Distraction					
	Hit		False Alarm		Sensitivity, d’	Bias, b
	p	z scores	p	z scores		
Ulna zone	0.698	0.5192	0.03	-1.8808	2.4	0.6808
Dorsal central	0.743	0.6532	0.07	-1.4758	2.129	0.411
Radial zone	0.667	0.4324	0.075	-1.4395	1.8719	0.5036
Volar central	0.834	0.9705	0.055	-1.5982	2.5687	0.3139

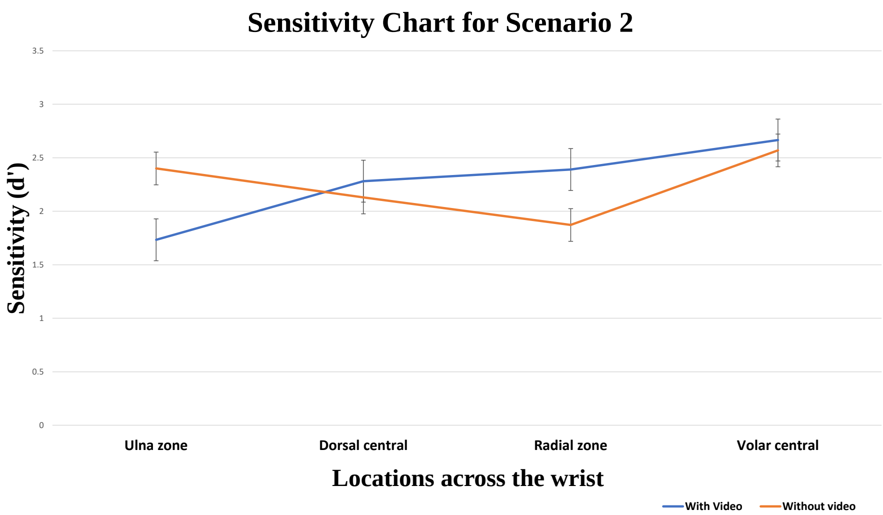

Figure 5.27: Sensitivity chart for locations on the wrist (Scenario 2)

4. **Scenario 3 (Duration of Haptic Stimulation (DHS) = 750 ms)**

   Here, the duration of haptic stimulation used was 750 ms, and the duty cycle used was the maximum recorded of locations from phase 1.

Table 5.20: Individual Identification of Location of Haptic Stimulation Performance scores for scenario 3

Location on the wrist	With Video Distraction		Without Video Distraction		Number of Participants
	Mean Performance Score (max. = 1)	Standard Deviation	Mean Performance Score (max. = 1)	Standard Deviation	
Dorsal central	0.6368	0.38411	0.8195	0.19778	22
Volar central	0.8186	0.28608	0.7882	0.36440	22
Ulna zone	0.5768	0.34475	0.6214	0.41566	22
Radial zone	0.6068	0.30335	0.7277	0.33588	22

The descriptive statistic of ILHSP for scenario 3 is shown in table 5.20. With and without video distractions, the minimum performance scores are 57.7% and 62.1% respectively. The lowest performance scores were for the Ulna zone. With video distraction, the Volar central had the highest performance score.

A 2-way repeated measures ANOVA (analysis of variance) was carried out to evaluate the null hypothesis that all haptic stimulated points on the wrist can be equally identified. The assumption of sphericity was met for locations of stimulation ($p = 0.778$) and interaction location*distraction ($p = 0.745$).

There was no significant effect of location of haptic stimulation on participants' abilities to correctly identify each stimulated location on the wrist, $Wilk's Lambda = 0.788, F(3,63) = 2.178, p = 0.099, \eta_p^2 = 0.094$. There was no significant effect of distraction on participants' abilities to correctly identify locations of haptic stimulations, $Wilk's Lambda = 0.861, F(1,21) = 3.392, p = 0.080, \eta_p^2 = 0.139$. The interaction location*distraction also yielded no significant effect on the participants' abilities to correctly identify locations of haptic stimulation, $Wilk's Lambda = 0.858, F(3,63) = 1.157, p = 0.333, \eta_p^2 = 0.052$.

The profile plots shown in figure 5.28 shows the performance scores for the different locations across the wrist. The Ulna zone was the least correctly identified location of haptic stimulation.

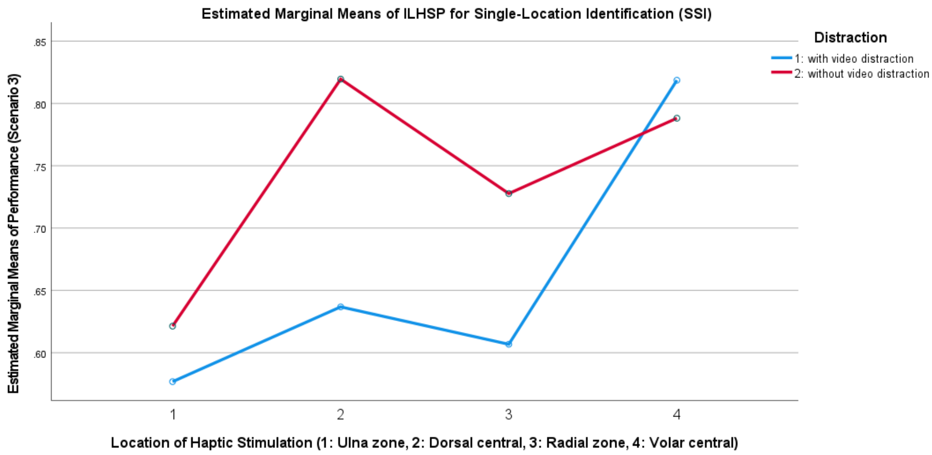

Figure 5.28: Profile plots of ILHSP for single-location stimulation identification (Scenario 3)

Table 5.21: Sensitivity and bias values for different locations on the wrist (Scenario 3)

(a) With video distraction

Scenarios	With Video Distraction					
	Hit		False Alarm		Sensitivity, d’	Bias, b
	p	z scores	p	z scores		
Ulna zone	0.577	0.1938	0.065	-1.5141	1.7079	0.660
Dorsal central	0.637	0.3500	0.085	-1.3722	1.7222	0.511
Radial zone	0.591	0.2311	0.025	-1.9600	2.1911	0.864
Volar central	0.819	0.9101	0.080	-1.4020	2.3121	0.246

(b) Without video distraction

Scenarios	Without Video Distraction					
	Hit		False Alarm		Sensitivity, d’	Bias, b
	p	z scores	p	z scores		
Ulna zone	0.606	0.2687	0.035	-1.8119	2.0806	0.772
Dorsal central	0.820	0.9136	0.05	-1.6449	2.5585	0.366
Radial zone	0.728	0.6060	0.03	-1.8808	2.4868	0.637
Volar central	0.788	0.8001	0.06	-1.5548	2.3549	0.377

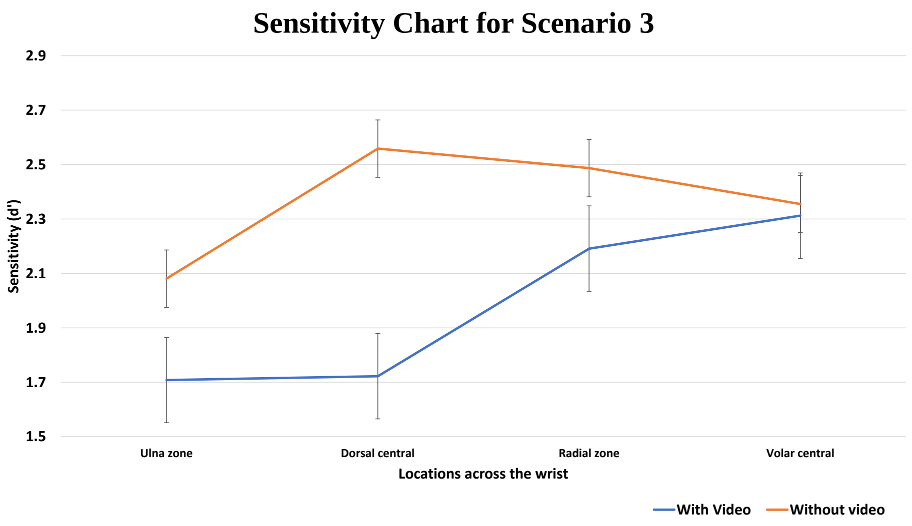

Figure 5.29: Sensitivity chart for locations on the wrist (Scenario 3)

As shown in Table 5.21, for scenarios with video distraction, participants were more sensitive to haptic stimulation at the Volar central (fig. 5.29).

5. **Scenario 4 (Duration of Haptic Stimulation (DHS) = 1000 ms)**

   The duration of haptic stimulation (DHS) employed was 1000 ms, and the duty cycle used was as recorded from phase 1 of the different locations on the wrist.

Table 5.22: Individual Identification of Location of Haptic Stimulation Performance scores for scenario 4

Location on the wrist	With Video Distraction		Without Video Distraction		Number of Participants
	Mean Performance Score (max. = 1)	Standard Deviation	Mean Performance Score (max. = 1)	Standard Deviation	
Dorsal central	0.5918	0.29089	0.7727	0.34758	22
Volar central	0.7873	0.30203	0.7732	0.33179	22
Ulna zone	0.7286	0.22184	0.5150	0.38191	22
Radial zone	0.5164	0.39540	0.6209	0.37590	22

The descriptive statistics of ILHSP scores for scenario 4 is shown in table 5.22. With and without video distractions, the minimum performance scores are 51.6% and 51.5%

respectively. Performance scores were highest at the volar central.

A 2-way repeated measures ANOVA (analysis of variance) was carried out to evaluate the null hypothesis that all haptic stimulated points on the wrist can be equally identified. The assumption of sphericity was met for location of stimulation ($p = 0.392$) but not for interaction location*distraction ($p = 0.025$).

There was no significant effect of location of haptic stimulation on correctly identifying points that were haptic stimulated, $Wilk's Lambda = 0.746, F(3,63) = 2.551$, $p = 0.064$, $\eta_p^2 = 0.108$. This implies that for this scenario, the participants' abilities to identify the different locations of haptic stimulation were similar for each location. Pairwise differences for performance between the different points of haptic stimulations were not significant, ($p > 0.05$).

Results also showed no significant effect of distraction on participants' abilities to correctly identify haptic stimulation on different locations on the wrist, $Wilk's Lambda = 0.997, F(1,21) = 0.065$, $p = 0.801$, $\eta_p^2 = 0.003$. However, there was a significant effect of the interaction location*distraction on the identification of location performance of participants ($Wilk's Lambda = 0.500, F(3,63) = 5.282$, $p = 0.003$, $\eta_p^2 = 0.201$).

Figure 5.30 shows the performance scores for the different locations across the wrist.

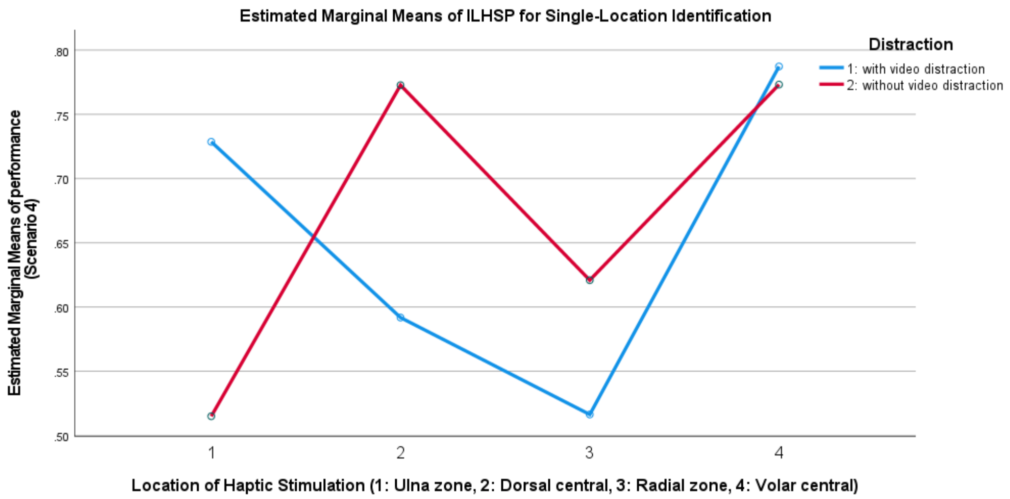

Figure 5.30: Profile plots of ILHSP for single-location stimulation identification (Scenario 4)

Participants' sensitivity and bias values for scenario 4 are shown in table 5.23

Table 5.23: Sensitivity and bias values for different locations on the wrist (Scenario 4)

(a) With video distraction

Scenarios	With Video Distraction					
	Hit		False Alarm		Sensitivity, d'	Bias, b
	p	z scores	p	z scores		
Ulna zone	0.713	0.5627	0.095	-1.3106	1.8733	0.374
Dorsal central	0.592	0.2322	0.03	-1.8808	2.113	0.824
Radial zone	0.516	0.0410	0.01	-2.3264	2.3674	1.143
Volar central	0.787	0.7970	0.06	-1.5547	2.3517	0.379

(b) Without video distraction

Scenarios	Without Video Distraction					
	Hit		False Alarm		Sensitivity, d'	Bias, b
	p	z scores	p	z scores		
Ulna zone	0.5	0	0.03	-1.8808	1.8808	0.940
Dorsal central	0.773	0.7479	0.025	-1.9600	2.7079	0.606
Radial zone	0.621	0.3079	0.025	-1.9600	2.2679	0.826
Volar central	0.773	0.7494	0.111	-1.2217	1.9711	0.236

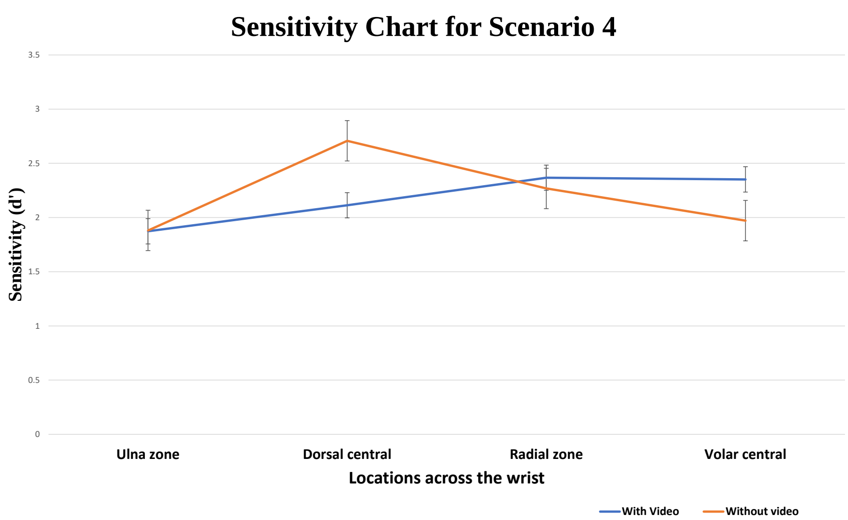

Figure 5.31: Sensitivity chart for locations on the wrist (Scenario 4)

Table 5.23 shows that with video distraction, there was no significant difference between Radial zone and Volar central. Figure 5.31 shows the sensitivity chat for scenario 4.

Positive values for bias shows that participants demonstrated a more conservative bias which means that participants were less likely to report that the stimulation is present.

6. **Comparing ILHSP for Single-Location Stimulation Identification (SSI) across Scenarios**

Table 5.24 shows the descriptive comparisons for ILHSP scores of different locations on the wrist across the scenarios. Visual comparisons are done horizontally. Table 5.25 shows the colour representations for the performance rankings. The darker the cell, the higher the performance score.

Table 5.24: : Performance comparisons of the different locations on the wrist across scenarios

Scenarios	With Video Distraction Mean Performance Scores (max. = 1)					Without Video Distraction Mean Performance Scores (max. = 1)				
	Scenarios					Scenarios				
	1 (N=22)	2 (N=22)	3 (N=22)	4 (N=22)	5 (N=22)	1 (N=22)	2 (N=22)	3 (N=22)	4 (N=22)	5 (N=22)
Dorsal central	0.7882	0.8191	0.6368	0.5918	0.8795	0.7732	0.7432	0.8195	0.7727	0.8941
Volar central	0.8032	0.8341	0.8186	0.7873	0.9395	0.7427	0.8341	0.7882	0.7732	0.9700
Ulna zone	0.6673	0.5150	0.5768	0.7286	0.7268	0.6673	0.6982	0.6214	0.5150	0.7582
Radial zone	0.6673	0.6664	0.6368	0.5164	0.7427	0.5305	0.6368	0.7277	0.6368	0.7886

Table 5.25: Colour codes for table 5.24

Performance Ranking	**1**	**2**	**3**	**4**	**5**
Colour Representation					

Plots of normalised mean performance scores at each location across all examined scenarios are shown in figure 5.32. Figure 5.32a shows the performance plots when participants had video distraction, while figure 5.32b shows the plots for performance plots without video distraction.

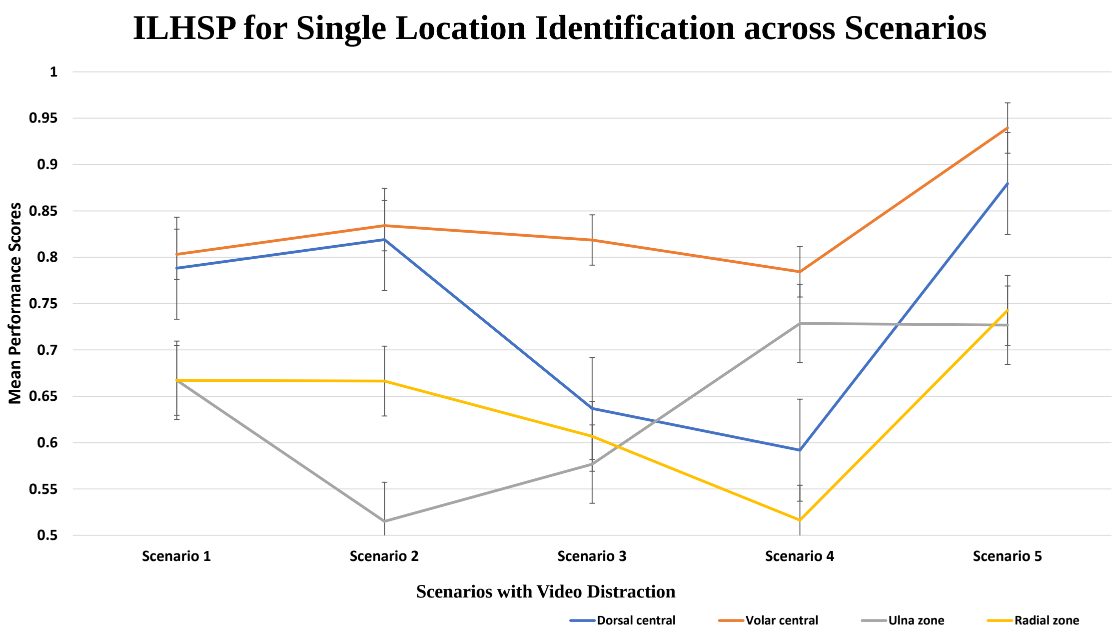

(a)

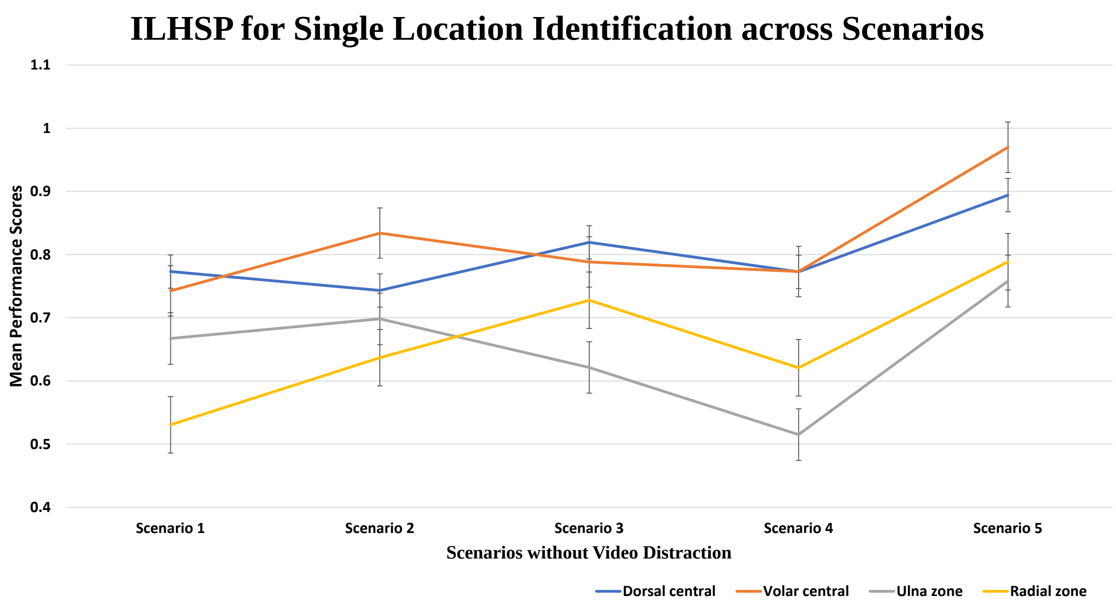

(b)

Figure 5.32: ILHSP for SSI across scenarios, (a) with video distraction (b) without video distraction

Figure 5.33 shows 3D bar charts of normalised ILHSP scores for SSI across scenarios. Across all scenarios, participants were able to pinpoint haptic stimulation easiest at the Volar central.

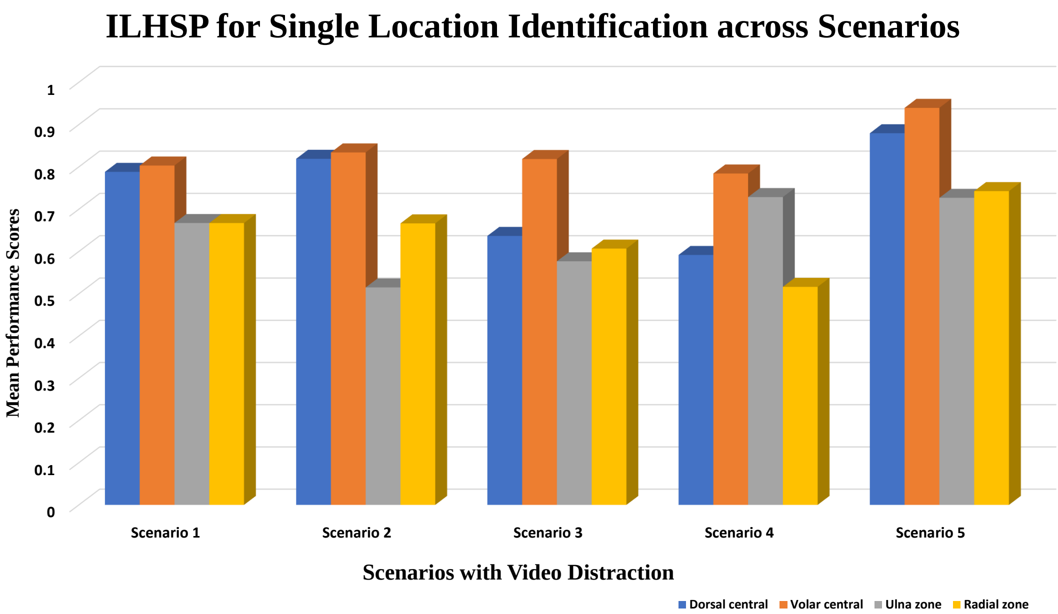

(a)

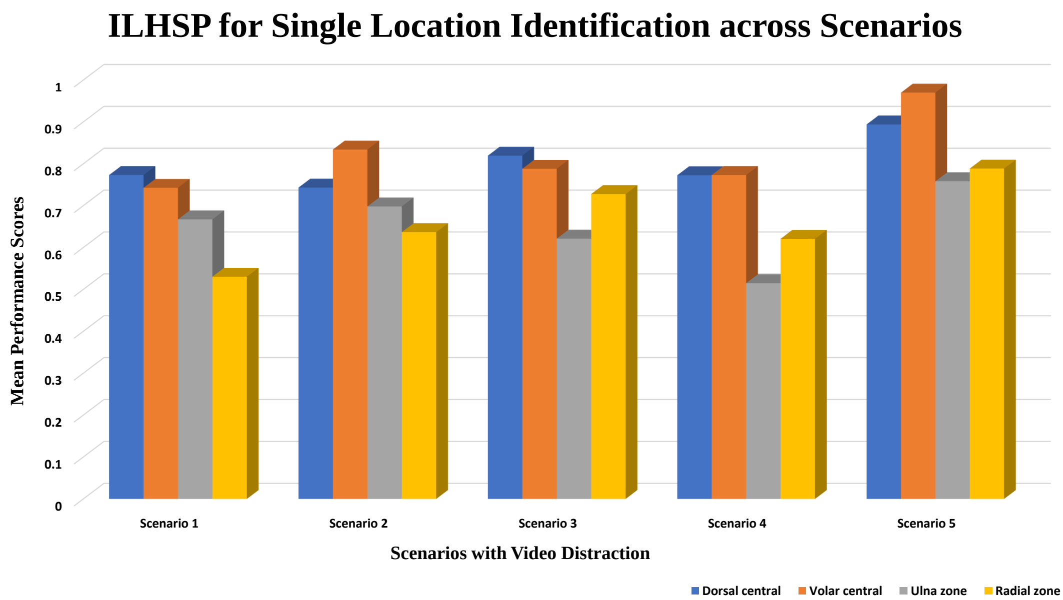

(b)

Figure 5.33: ILHSP for SSI across scenarios, (a) with video distraction (b) without video distraction

Paired samples t-test was carried out on the SSI ILHSP scores for each location on the wrist across the various scenarios examined. Table 5.26 shows the comparison results for significant outcomes of the t-test. We reject the null hypothesis (that the difference between the means of the scenario pairs of each location is equal to zero) if the calculated t value is greater than the critical t value (df = 21, confidence level = 95%).

Table 5.26: Paired samples t test for duty cycles based on duration of stimulation (All with video distraction)

		Ulna zone		Dorsal central		Radial zone		Volar central	
		With Video	Without Video	With Video	Without Video	With Video	Without Video	With Video	Without Video
c - 250 (video)	Calculated t	0.612	0.973	1.069	1.354	0.860	3.041	1.819	2.732
	Critical t	2.080	2.080	2.080	2.080	2.080	2.080	2.080	2.080
	Sig. (2-tailed)	0.547	0.342	0.297	0.190	0.399	0.006	0.083	0.012
c - 500 (video)	Calculated t	1.946	0.650	0.809	1.925	0.843	1.638	1.492	1.903
	Critical t	2.080	2.080	2.080	2.080	2.080	2.080	2.080	2.080
	Sig. (2-tailed)	0.065	0.523	0.428	0.068	0.409	0.116	0.150	0.071
c - 750 (video)	Calculated t	1.500	1.485	2.842	1.395	1.890	1.004	1.782	2.162
	Critical t	2.080	2.080	2.080	2.080	2.080	2.080	2.080	2.080
	Sig. (2-tailed)	0.149	0.152	0.010	0.178	0.073	0.327	0.089	0.042
c - 1000 (video)	Calculated t	- 0.021	2.211	3.461	1.319	2.540	1.924	2.215	2.525
	Critical t	2.080	2.080	2.080	2.080	2.080	2.080	2.080	2.080
	Sig. (2-tailed)	0.984	0.038	0.002	0.202	0.019	0.068	0.038	0.020
250-500 (video)	Calculated t	2.022	- 0.534	-0.58	0.414	0.009	- 1.319	-0.50	-1.25
	Critical t	2.080	2.080	2.080	2.080	2.080	2.080	2.080	2.080
	Sig. (2-tailed)	0.056	0.599	0.570	0.683	0.993	0.201	0.621	0.226
250-750	Calculated t	1.022	0.623	1.930	-0.58	0.657	-2.14	-0.26	-0.59

Continued on next page

Table 5.26 – continued from previous page

		Ulna zone		Dorsal central		Radial zone		Volar central	
		With Video	Without Video	With Video	Without Video	With Video	Without Video	With Video	Without Video
(video)	Critical t	2.080	2.080	2.080	2.080	2.080	2.080	2.080	2.080
	Sig. (2-tailed)	0.318	0.540	0.067	0.569	0.518	0.045	0.800	0.560
250-1000 (video)	Calculated t	-.615	1.694	2.328	0.006	1.632	-1.29	0.224	-0.37
	Critical t	2.080	2.080	2.080	2.080	2.080	2.080	2.080	2.080
	Sig. (2-tailed)	0.545	0.105	0.030	0.995	0.117	0.213	0.825	0.713
500-750 (video)	Calculated t	-.904	0.936	2.240	-1.11	0.708	-.84	0.199	0.554
	Critical t	2.080	2.080	2.080	2.080	2.080	2.080	2.080	2.080
	Sig. (2-tailed)	0.360	0.160	0.036	0.281	0.487	0.410	0.844	0.586
500-1000 (video)	Calculated t	-2.05	1.878	2.827	-0.41	1.669	0.160	0.850	1.002
	Critical t	2.080	2.080	2.080	2.080	2.080	2.080	2.080	2.080
	Sig. (2-tailed)	0.053	0.074	0.010	0.688	0.110	0.875	0.405	0.328
750-1000 (video)	Calculated t	-1.80	1.164	0.522	0.564	1.231	1.105	0.397	0.186
	Critical t	2.080	2.080	2.080	2.080	2.080	2.080	2.080	2.080
	Sig. (2-tailed)	0.086	0.662	0.607	0.579	0.232	0.053	0.696	0.854

Cells shaded green in table 5.26 show the pairs with significant mean difference and the areas shaded red show pairs with non-significant mean difference. Table 5.26 confirms results shown in table 5.24 and displayed in figure 5.32 and figure 5.33. For most of the paired scenarios, there was no significant mean difference in performance for individual locations of haptic stimulation. This confirms that individual duty cycle calibration of each location based on duration of stimulation may be important to achieve similar performance scores across scenarios. Table 5.27 shows the comparisons of the performance within each scenario from subsection 5.5.1.4. It shows that locations at the Volar central and Dorsal central are easiest locations at which haptic stimulation can be pinpointed. Visual comparisons are done vertically. Figure 5.32 shows the result.

Table 5.27: : Comparisons of the performance scores across different locations on the wrist within each scenario

Scenarios	With Video Distraction Mean Performance Scores (max. = 1)					Without Video Distraction Mean Performance Scores (max. = 1)				
	Scenarios					Scenarios				
	1 (N=22)	2 (N=22)	3 (N=22)	4 (N=22)	5 (N=30)	1 (N=22)	2 (N=22)	3 (N=22)	4 (N=22)	5 (N=30)
Dorsal central	0.7882	0.8191	0.6368	0.5918	0.8673	0.7732	0.7432	0.8195	0.7727	0.8560
Volar central	0.8032	0.8341	0.8186	0.7873	0.9337	0.7427	0.8341	0.7882	0.7732	0.9337
Ulna zone	0.6673	0.5150	0.5768	0.7286	0.7440	0.6673	0.6982	0.6214	0.5150	0.7783
Radial zone	0.6673	0.6664	0.6068	0.5164	0.7447	0.5305	0.7277	0.7732	0.6209	0.7673

Table 5.28: Colour codes for table 5.27

Performance Ranking	**1**	**2**	**3**	**4**
Colour Representation				

Table 5.29 shows ILHSP scores and the estimated sensitivity values at the different locations on the wrist. Table 5.29 shows that high sensitivity does not necessarily imply high performance scores. Sensitivity values consider the probabilities of stimulation identification by chance and such factors should be considered when carrying out tasks involving haptic stimulation.

Table 5.29: Performance scores and sensitivity comparisons

		Control Scenario		Scenario 1		Scenario 2		Scenario 3		Scenario 4	
		Score	d'	Score	d'	Score	d'	Score	d'	Score	d'
Video	Dorsal central	0.867	3.199	0.788	2.398	0.819	2.281	0.637	1.722	0.592	2.113
	Volar central	0.934	3.518	0.803	2.222	0.834	2.666	0.819	2.312	0.787	2.352
	Ulna zone	0.744	2.943	0.657	2.183	0.515	1.733	0.577	1.708	0.729	1.873
	Radial zone	0.744	2.837	0.667	2.031	0.666	2.390	0.607	2.191	0.516	2.367
No Video	Dorsal central	0.856	3.066	0.773	2.348	0.743	2.129	0.820	2.559	0.773	2.708
	Volar central	0.934	3.250	0.743	2.054	0.834	2.569	0.788	2.355	0.773	1.971
	Ulna zone	0.778	2.436	0.667	2.313	0.698	2.4	0.621	2.081	0.515	1.881
	Radial zone	0.767	3.325	0.667	1.549	0.637	1.872	0.728	2.487	0.621	2.268

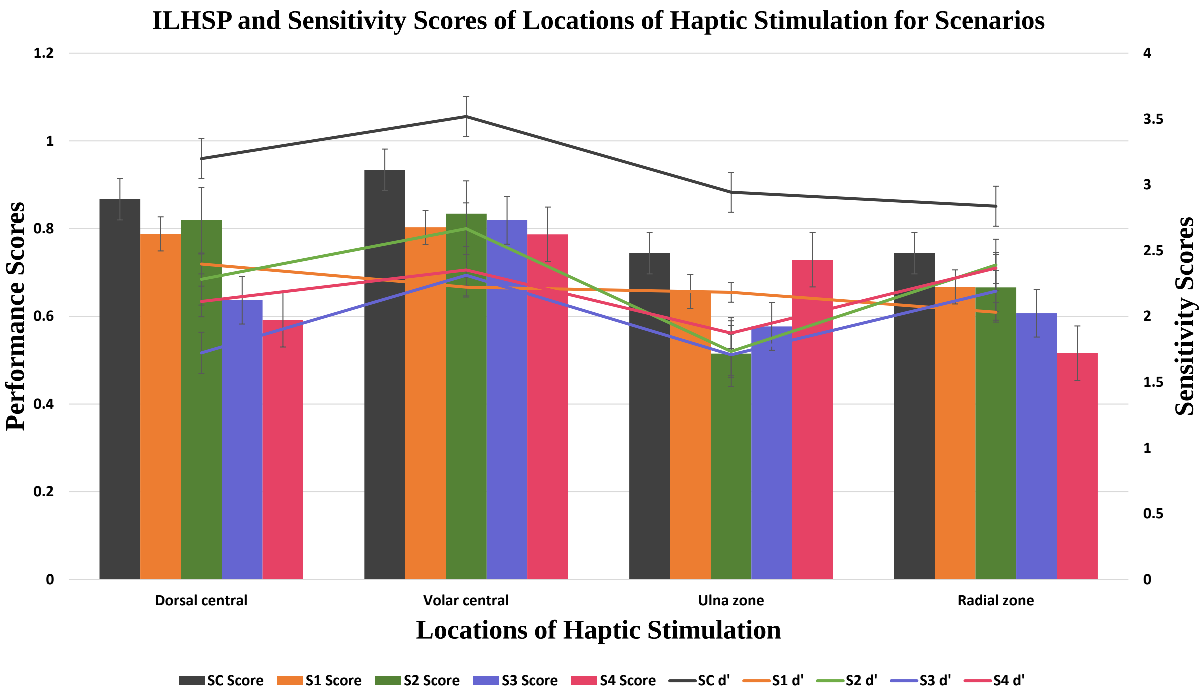

Figure 5.34: ILHSP and Sensitivity plots for locations across the wrist

5.5.1.5 Individual Identification of Location of Haptic Stimulation Performance (Individual ILHSP) for Simultaneous Double-Location Stimulation Identification (SDSI) and Sensitivity Measurements

The overall accuracy with which participants were able to correctly identify two simultaneously stimulated locations on the wrist for various scenarios highlighted in table 5.13.

1. **Control scenario (Duration of Haptic Stimulation = 750 ms, Duty cycle = 90%)**

   The overall ILHSP score was highest in this scenario for SDSI (table 5.13). Further analysis was then carried out to identify the accuracy of correctly identifying each double-locations of concurrent haptic stimulation.

   The descriptive statistics of the ILHSP scores for the control scenario is shown in table 5.30. ILHSP scores at the "Dorsal central - Radial zone" had the highest score compared to other double locations with video distraction.

Table 5.30: ILHSP scores for SDSI (Control scenario)

Location on the wrist	With Video Distraction		Without Video Distraction		Number of Participants
	Mean Performance Score (max. = 1)	Standard Deviation	Mean Performance Score (max. = 1)	Standard Deviation	
Dorsal central - Radial zone	0.4110	0.3249	0.3433	0.3556	30
Dorsal central – Ulna zone	0.4330	0.4125	0.3227	0.3669	30
Volar central – Ulna zone	0.2783	0.3520	0.3667	0.3953	30
Volar central - Radial zone	0.3440	0.3560	0.3223	0.3967	30

A 2-way repeated measures ANOVA (analysis of variance) was carried out to evaluate the null hypothesis that the ILHSP scores for identifying two simultaneously stimulated locations is the same across the wrist. Assumption of sphericity was met for location of stimulation ($p = 0.361$) and interaction location*distraction ($p = 0.877$).

There was no significant effect of location of haptic stimulation on participants' abilities to correctly identify two simultaneously stimulated locations on the wrist ($F(3,87) = 0.362$, $p = 0.781$, $\eta_p^2 = 0.012$). There was also no significant effect of distraction on participants' abilities to correctly identify two simultaneously haptic-stimulated locations on the wrist ($F(1,29) = 0.585$, $p = 0.450$, $\eta_p^2 = 0.020$). The interaction location*distraction also yielded no significant effect on participants' abilities to correctly identify two concurrently stimulated locations on the wrist ($F(3,87) = 1.502$, $p = 0.220$, $\eta_p^2 = 0.049$).

2. **Scenario 1 (Duration of stimulation = 250 ms)**

Here, the duration of haptic stimulation (DHS) used was 250 ms, and the duty cycle used was the maximum recorded of all location from phase 1.

Table 5.31 shows the average ILHSP scores for duration of stimulation of 250 ms. A 2-way repeated measures ANOVA (analysis of variance) was carried out to evaluate the null hypothesis that the ILHSP scores for identifying two simultaneously stimulated locations is the same for all double simultaneous stimulations on the wrist. Assumption of sphericity was not met for location of stimulation ($p = 0.048$) and interaction location*distraction ($p = 0.043$).

Table 5.31: Individual ILHSP scores for SDSI (Scenario 1)

Location on the wrist	With Video Distraction		Without Video Distraction		Number of Participants
	Mean Performance Score (max. = 1)	Standard Deviation	Mean Performance Score (max. = 1)	Standard Deviation	
Dorsal central - Radial zone	0.0300	0.0971	0.1359	0.2221	22
Dorsal central – Ulna zone	0.0905	0.2337	0.1214	0.2831	22
Volar central – Ulna zone	0.0455	0.1562	0.1059	0.2600	22
Volar central - Radial zone	0.0755	0.1760	0.1205	0.2616	22

There was no significant effect of location of haptic stimulation on participants' abilities to correctly identify two simultaneously stimulated locations on the wrist ($F(2.187, 45.922) = 0.225$, $p = 0.879$, $\eta_p^2 = 0.011$). There was also no significant effect of distraction on participants' abilities to correctly identify two simultaneously stimulated locations on the wrist ($F(1,21) = 3.291$, $p = 0.084$, $\eta_p^2 = 0.135$). The interaction location*distraction also yielded no significant effect on participants' ILHSP scores ($F(3, 47.324) = 0.265$, $p = 0.850$, $\eta_p^2 = 0.012$).

3. **Scenario 2 (Duration of stimulation = 500 ms)**

Here, the duration of haptic stimulation (DHS) used was 500 ms, and the duty cycle used was the maximum recorded of all locations from phase 1.

Table 5.32 shows the average ILHSP scores for SDHI given duration of stimulation of 500 ms.

A 2-way repeated measures ANOVA (analysis of variance) was carried out to evaluate the null hypothesis that the ILHSP scores for identifying two simultaneously stimulated locations is the same for all double simultaneous stimulations on the wrist. Assumption of sphericity was met for location of stimulation (p = 0.644) and interaction location*distraction (p = 0.054).

There was no significant effect of location of haptic stimulation on participants' abilities to correctly identify two simultaneously haptic-stimulated locations on the wrist ($F(3,63) =$ 1.701, $p = 0.176$, $\eta_p^2 = 0.075$). There was also no significant effect of distraction ($F(1,21) =$ 0.221, $p = 0.643$, $\eta_p^2 = 0.010$). The interaction location*distraction also yielded no significant effect ($F(3,63) = 0.637$, $p = 0.594$, $\eta_p^2 = 0.029$).

Table 5.32: ILHSP scores for SDSI (Scenario 2)

Location on the wrist	With Video Distraction		Without Video Distraction		Number of Participants
	Mean Performance Score (max. = 1)	Standard Deviation	Mean Performance Score (max. = 1)	Standard Deviation	
Dorsal central - Radial zone	0.1968	0.3032	0.2873	0.3305	22
Dorsal central – Ulna zone	0.1814	0.2861	0.1664	0.3212	22
Volar central – Ulna zone	0.1359	0.2653	0.1209	0.3005	22
Volar central - Radial central	0.1355	0.1961	0.1509	0.2236	22

4. **Scenario 3 (Duration of stimulation = 750 ms)**

Here, the duration of haptic stimulation used was 750 ms, and the duty cycle used was the maximum recorded of all locations from phase 1. Table 5.33 shows the average ILHSP scores for SDSI given duration of stimulation of 750 ms.

A 2-way repeated measures ANOVA (analysis of variance) was carried out to evaluate the null hypothesis that the ILHSP scores for identifying two concurrently stimulated locations is the same for all double simultaneous stimulations on the wrist. Assumption of sphericity was met for location of stimulation (p = 0.165) and interaction location*distraction (p = 0.355).

There was no significant effect of location of haptic stimulation on participants' abilities to correctly identify two simultaneously haptic-stimulated locations on the wrist ($F(3,63) = 0.316$, $p = 0.814$, $\eta_p^2 = 0.015$). However, there was a significant effect of distraction on participants' abilities to correctly identify two simultaneously haptic-stimulated locations on the wrist ($F(1,21) = 5.040$, $p = 0.036$, $\eta_p^2 = 0.194$). The interaction location*distraction also yielded no significant effect ($F(3,63) = 0.014$, $p = 0.998$, $\eta_p^2 = 0.001$).

Table 5.33: ILHSP scores for SDSI (Scenario 3)

Location on the wrist	With Video Distraction		Without Video Distraction		Number of Participants
	Mean Performance Score (max. = 1)	Standard Deviation	Mean Performance Score (max. = 1)	Standard Deviation	
Dorsal central - Radial zone	0.1973	0.3205	0.2718	0.3195	22
Dorsal central – Ulna zone	0.1364	0.2851	0.2273	0.3158	22
Volar central – Ulna zone	0.1664	0.2471	0.2423	0.3444	22
Volar central - Radial zone	0.1509	0.2666	0.2264	0.2796	22

5. **Scenario 4 (Duration of stimulation = 1000 ms)**

   Here, the duration of haptic stimulation used was 1000 ms, and the duty cycle used was the maximum recorded of all locations from phase 1.

   Table 5.34 shows the average ILHSP scores for SDSI given duration of stimulation of 1000 ms. The 2-way repeated measures ANOVA (analysis of variance) was carried out to evaluate the null hypothesis that the ILHSP scores for identifying two simultaneously stimulated locations is the same for all double simultaneous stimulations on the wrist. Assumption of sphericity was met for location of stimulation ($p = 0.311$) and interaction location*distraction ($p = 0.387$).

   There was no significant main effect of location of haptic stimulation on participants' abilities to correctly identify two simultaneously haptic-stimulated locations on the wrist

($F(3,63) = 1.367$, $p = 0.261$, $\eta_p^2 = 0.061$). There was also no significant main effect of distraction on participants' abilities to correctly identify two simultaneously haptic-stimulated locations on the wrist ($F(1,21) = 2.479$, $p = 0.130$, $\eta_p^2 = 0.106$). The interaction location*distraction also yielded no significant main effect on participants' abilities to correctly identify two simultaneously haptic-stimulated locations on the wrist ($F(3,63) = 1.461$, $p = 0.234$, $\eta_p^2 = 0.065$).

Table 5.34: ILHSP scores for SDSI (Scenario 4)

Location on the wrist	With Video Distraction		Without Video Distraction		Number of Participants
	Mean Performance Score (max. = 1)	Standard Deviation	Mean Performance Score (max. = 1)	Standard Deviation	
Dorsal central - Radial zone	0.1668	0.3049	0.3027	0.3700	22
Dorsal central – Ulna zone	0.1818	0.3044	0.3027	0.3404	22
Volar central – Ulna zone	0.1509	0.2666	0.1214	0.2430	22
Volar central - Radial zone	0.1664	0.2866	0.2423	0.3124	22

6. **Scenario Comparisons**

Table 5.35: Comparisons of the SDSI performance scores across different locations on the wrist within each scenario

Scenarios	With Video Distraction Mean Performance Scores (max. = 1)					Without Video Distraction Mean Performance Scores (max. = 1)				
	Scenarios					Scenarios				
	1 (N=22)	2 (N=22)	3 (N=22)	4 (N=22)	5 (N=22)	1 (N=22)	2 (N=22)	3 (N=22)	4 (N=22)	5 (N=22)
Dorsal central - Radial zone	0.0300	0.1968	0.1973	0.1668	0.4557	0.1359	0.2873	0.2718	0.3027	0.3657
Dorsal central – Ulna zone	0.0905	0.1814	0.1364	0.1818	0.3883	0.1214	0.1664	0.2273	0.3027	0.3003
Volar central – Ulna zone	0.0455	0.1359	0.1664	0.1509	0.3007	0.1059	0.1209	0.2423	0.1059	0.3887
Volar central - Radial zone	0.0755	0.1355	0.1509	0.1664	0.3217	0.1205	0.1509	0.2264	0.2577	0.3000

Table 5.36: Colour codes for table 5.35

Performing Ranking	**1**	**2**	**3**	**4**	**5**
Colour Representation					

In general, participants struggled to correctly identify the two simultaneously stimulated locations on the wrist. With and without video distraction, scenario 5 had the highest performance scores when compared to other scenarios.

5.5.1.6 Chances of Correctly Identifying Two Simultaneously Stimulated Locations

Section 5.5.1.6 describes how participants performed when tasked with correctly identifying two simultaneously stimulated locations on the wrist. In this section, we explored the probability of correctly identifying the stimulated points. Two locations on the wrist were simultaneously stimulated three times and the locations participants reported they felt the stimulations were recorded. Table 5.37 shows the colour code for the ranking of probability of each locations or combination of locations being reported as locations stimulated during simultaneous double-location stimulation identification (SDSI).

Table 5.37: Colour codes for section 5.5.1.6

Performing Ranking	**1**	**2**	**3**
Colour Representation			

1. **Dorsal central – Radial zone**

Table 5.38: Probability of haptic stimulation identification of different locations for simultaneous haptic stimulation of Dorsal central - Radial zone

	Scenario 1		Scenario 2		Scenario 3		Scenario 4		Scenario 5	
	With Video	Without Video	With Video	Without Video	With Video	Without Video	With Video	Without Video	With Video	Without Video
Volar central	0.00	0.00	1.50	3.00	3.05	3.05	7.50	3.00	0.00	1.10
Radial zone	22.73	21.14	22.64	24.23	21.14	19.68	15.14	22.73	14.4	17.77
Ulna zone	7.59	7.55	0.00	3.00	0.00	4.50	10.59	1.50	1.10	1.10

Continued on next page

Table 5.38 – continued from previous page

	Scenario 1		Scenario 2		Scenario 3		Scenario 4		Scenario 5	
	With Video	Without Video	With Video	Without Video	With Video	Without Video	With Video	Without Video	With Video	Without Video
Dorsal central	57.59	54.59	46.95	30.32	51.55	27.32	25.73	30.23	32.17	34.4
Ulna zone - Volar central	3.00	1.50	1.50	3.00	0.00	1.50	6.00	1.50	0.00	0.00
Radial zone - Volar central	0.00	1.50	1.50	3.00	1.50	4.50	4.50	4.50	0.022	0.044
Dorsal central - Ulna zone	3.05	0.00	3.05	4.50	6.05	12.05	9.05	9.05	3.30	5.53
Dorsal central - Radial zone	3.00	12.05	19.68	27.23	19.73	28.73	16.68	24.18	41.1	34.3
No Idea	3.00	1.50	3.00	3.00	1.50	3.00	4.50	3.00	5.50	1.10

Table 5.38 shows the probability with which participants felt haptic stimulation when locations at the Dorsal central and Radial zone were simultaneously stimulated.

2. **Dorsal central – Ulna zone**

Table 5.39 shows the probability with which participants felt the haptic stimulation when locations at the Dorsal central and Ulna zone were simultaneously stimulated.

Table 5.39: Probability of haptic stimulation identification of different locations for simultaneous haptic stimulation of Dorsal central - Ulna zone

	Scenario 1		Scenario 2		Scenario 3		Scenario 4		Scenario 5	
	With Video	Without Video	With Video	Without Video	With Video	Without Video	With Video	Without Video	With Video	Without Video
Volar central	3.00	4.55	4.50	1.50	3.00	1.50	1.5	3.05	0.00	0.00
Radial zone	0.00	0.00	1.50	6.05	0.00	4.55	1.5	0.00	0.00	1.10
Ulna zone	25.77	25.68	19.64	22.73	16.64	15.14	24.23	21.14	12.20	17.73
Dorsal central	56.09	46.95	53.09	36.32	53.09	45.41	45.32	33.27	35.53	38.90
Ulna zone - Volar central	3.00	4.55	1.50	1.50	9.14	7.55	6.0	3.00	2.23	6.63
Radial zone - Volar central	0.00	0.00	0.00	0.00	1.50	0.00	0.00	1.50	1.10	0.00
Dorsal central - Ulna zone	9.05	16.55	18.14	19.68	13.64	22.73	16.65	25.73	43.3	31.13
Dorsal central - Radial zone	1.50	1.50	0.00	6.05	1.50	1.50	1.50	9.05	3.30	2.20
No Idea	1.50	0.00	1.50	4.50	1.50	4.55	3.00	3.00	2.1	2.20

3. **Volar central – Radial zone**

Table 5.40: Probability of haptic stimulation identification of different locations for simultaneous haptic stimulation of Volar central - Radial on the wrist

	Scenario 1		Scenario 2		Scenario 3		Scenario 4		Scenario 5	
	With Video	Without Video	With Video	Without Video	With Video	Without Video	With Video	Without Video	With Video	Without Video
Volar central	65.14	56.05	50.09	48.46	53.00	39.41	43.86	33.32	35.57	36.63
Radial zone	24.27	15.14	22.73	22.73	16.64	18.18	15.14	25.73	12.1	13.3
Ulna zone	0.00	1.50	0	1.50	0.00	0.00	0.00	0.00	1.1	1.1
Dorsal central	1.5	7.50	1.50	0.00	0.00	1.50	6.05	1.50	0.00	0.00
Ulna zone - Volar central	0.00	1.50	6.00	1.50	4.50	1.50	6.05	4.50	3.3	0.00
Radial zone - Volar central	6.00	7.50	12.05	15.09	15.09	27.18	15.14	21.18	34.4	32.23
Dorsal central - Ulna zone	0.00	1.50	1.50	0.00	3.05	1.50	3.00	0.00	0.00	0.00
Dorsal central - Radial zone	1.50	1.50	3.05	7.555	3.00	6.05	3.05	9.09	5.5	12.2
No Idea	1.50	7.55	3.00	3.01	4.50	4.55	4.55	0.00	4.43	1.1

Table 5.40 shows the probability with which participants felt the haptic stimulation when locations at the Volar central and Radial zone of the wrist were simultaneously stimulated. As shown in table 5.40, when the Volar central and Radial zone were stimulated at the same time, there was a greater chance of pinpointing the Volar central as the location of stimulation.

4. **Volar central – Ulna zone**

Table 5.41 shows the probability with which participants felt the haptic stimulation when locations at the Volar central and Ulna zone were simultaneously stimulated.

Table 5.41: Probability of haptic stimulation identification of different locations for simultaneous haptic stimulation of the Volar central and Radial zone

	Scenario 1		Scenario 2		Scenario 3		Scenario 4		Scenario 5	
	With Video	Without Video	With Video	Without Video	With Video	Without Video	With Video	Without Video	With Video	Without Video
Volar central	75.77	60.64	62.14	56.05	63.64	45.41	37.86	60.64	54.4	46.7
Radial zone	1.50	3.00	3.05	7.55	0.00	7.55	1.50	6.09	2.2	1.1
Ulna zone	15.14	24.14	10.64	9.09	10.55	9.09	19.68	9.09	5.53	11.1
Dorsal central	1.50	1.50	0.00	1.50	3.05	0.00	6.05	0.00	2.23	0.00
Ulna zone - Volar central	6.05	3.05	13.59	12.09	16.64	19.68	15.09	12.09	27.83	36.63
Radial zone - Volar central	0.00	1.50	3.00	1.50	0.00	7.59	7.55	3.00	2.23	3.33
Dorsal central - Ulna zone	0.00	1.50	4.50	6.05	0.00	6.05	7.59	1.50	2.23	1.1
Dorsal central - Radial zone	0.00	0.00	3.00	4.55	6.05	0.00	1.50	3.00	1.1	0.00
No Idea	0.00	3.05	0.00	1.50	0.00	4.55	3.00	4.55	2.2	0.00

5. **Discussion**

Subsection 5.5.1.5 suggests the probabilities of correctly identifying 2 simultaneously stimulated locations on the wrist. For each attempt, there were 9 different possible responses participants could give as shown in table 5.38, table 5.39, table 5.40, and table 5.41. Each stimulation was repeated three times. Each response is assigned a score of 1/3 and for the three attempts, a maximum of 1. The average scores for all responses were calculated and tabulated.

Table 5.38 shows that when the Dorsal central and Radial zone were simultaneously stimulated, participants reported that they felt the stimulation at the Dorsal central more times than other locations on the wrist for scenarios 1-4. However, for the control scenario, participants felt the stimulation correctly more times that other locations. When the Dorsal central and Ulna zone were simultaneously stimulated, table 5.39 shows that participants felt the stimulation at the Dorsal central more times than other locations on the wrist for most of the scenarios examined. For control scenario with video distractions however, most of the stimulation were correctly identified. Table 5.40 shows that participants reported stimulation more at the Volar central when the Volar central and Radial zone were simultaneously stimulated. Also, when Volar central and Ulna zone were simultaneously stimulated, participants reported the stimulation significantly more at the Volar central than other locations for all the scenarios examined. In other cases, participants reported 'No idea' where it was difficult to accurately identify simultaneous locations of haptic stimulation.

Results in section 5.5.1 show that for the various durations of haptic stimulation, the Volar central and Dorsal central had the lowest duty cycles for minimum detectable haptic intensity (MDHI). The difference in MDHI may be used to explain why participants reported more haptic stimulations at the Dorsal central and Volar central when the Volar central and Dorsal central are paired with the Ulna zone and Radial zone. For correct identification of simultaneous double-location of haptic stimulation, the duty cycles of the haptic stimulation at locations at the Ulna zone and Radial zone may be dynamically varied with the duty cycles for haptic stimulation at the Volar and Dorsal central to effective haptic perception..

5.6 Study Phase 3: Sensory Substitution Strategies (Haptic Feedback)

The choice of sensory substitution strategy for haptic feedback was explored in the phase 3 study. Two strategies were investigated: situational awareness and instruction. For situational awareness, sensor data about the remote environment are conveyed to operators via haptic feedback, with operators expected to make decisions on controlling the robot with the information provided. In this case, the success of the tele-operation depends on the successful interpretation of the haptic information provided, promoting the need for phase 1 and phase 2 studies. In employing the 'instruction' strategy, an operator is provided with instructions on how to carry out the tele-operation task. This may be particularly useful in applications where assistance is provided to operators and all they must do is to control the robot.

In this task, four participants were asked to change the orientation of a robot gripper based on the haptic stimulation from the wrist worn device. The device was worn on the non-dominant hand. The aim of the task was to understand a suitable strategy to convey haptic feedback to operators carrying out a gripper rotation task.

The haptic wristband contains two vibrating motors controlled by a Wi-Fi enabled control circuit. Two haptic motors were positioned at locations on the left and right of the wrist to signify the direction in which the gripper should be rotated. A range of 40% - 100% PWM duty cycles was used to power the motors. Vibration intensity increases as the duty cycle is increased. The location of the vibrating motor indicates the direction in which participants were to rotate the gripper. As the duty cycle increases (rising edge of the wave shown in figure 5.35, the gripper should be rotated away from its start position in the direction indicated by the location of vibrating motor. As the vibration intensity decreases, the gripper should be rotated in the opposite direction. If the rate at which the orientation is changed remains constant, the gripper should be back to its initial orientation when the vibration stops. The blue line on the positive section of figure 5.35 shows the duty cycle plot for the left haptic motor while the orange line shows that of the right haptic motor. Jaco[2] robot joystick was used to control the orientation of the robot gripper by simple clockwise and anticlockwise twist of the joystick. Figure 5.35 shows the plot of the preprogramed PWM duty cycle of the haptic feedback.

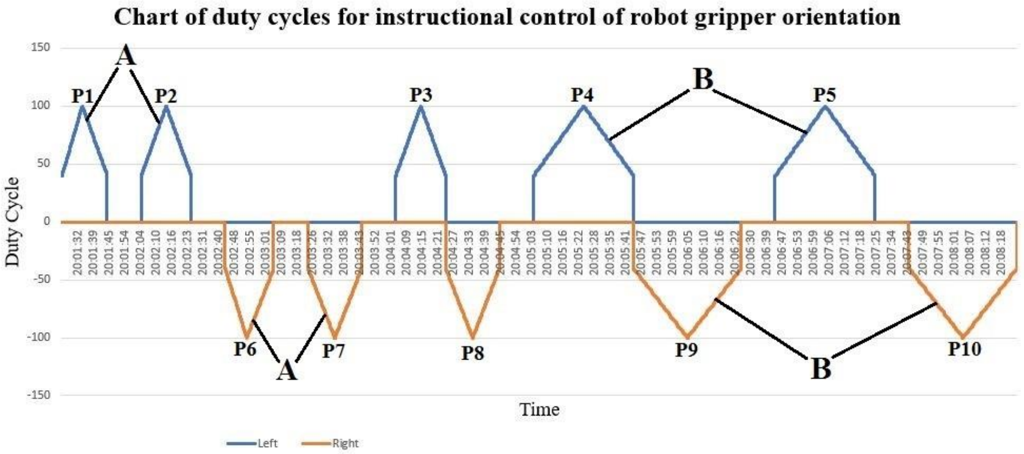

Figure 5.35: Duty cycle plot for instructional control of the robot gripper orientation

5.6.1 Results

For each participant, this phase was carried out in seven (7) minutes. The total rise and fall times for the parts labelled A (10 seconds) in Fig. 5.35 is half that of the part labelled B (20 seconds). The rest periods lasted for 10 seconds each. Each waveform of haptic stimulation contains five (5) peaks which may be used to make comparisons between the plots.

To understand how participants interpreted the perceived haptic stimulation, gripper orientation values as controlled by participants were plotted against time. Comparisons were made based on the peaks of the plots, as well as the rising and falling edges of the waves. Participants carried out the task with and without video views of the remote robot end.

5.6.1.1 Gripper Orientation Plots for Participant 1

1. **With Video Feedback of the Robot End**

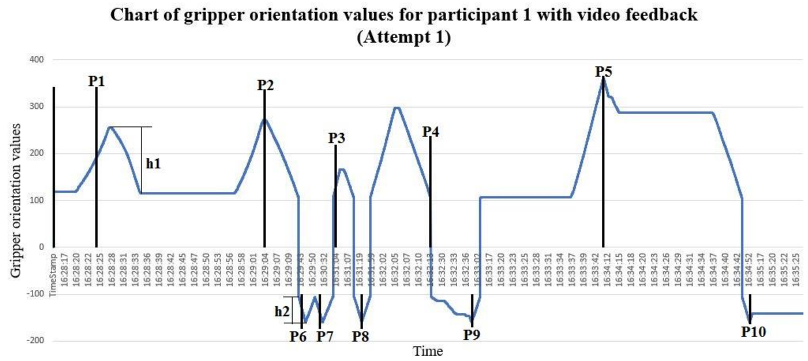

Figure 5.36: Chart of gripper orientation values for participant 1 with video feedback (Attempt 1)

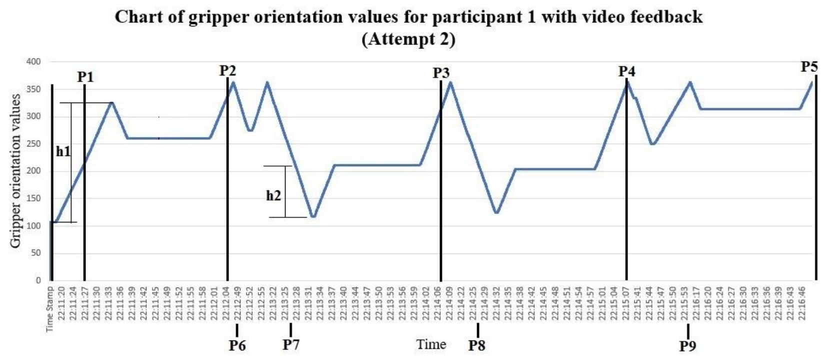

Figure 5.37: Chart of gripper orientation values for participant 1 with video feedback (Attempt 2)

2. **Without Video Feedback of the Robot End**

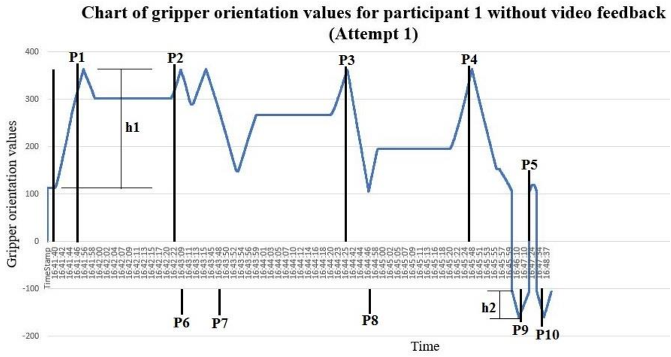

Figure 5.38: Chart of gripper orientation values for participant 1 without video feedback (Attempt 1)

5.6.1.2 Gripper Orientation Plots for Participant 2

1. **With Video Feedback of the Robot End**

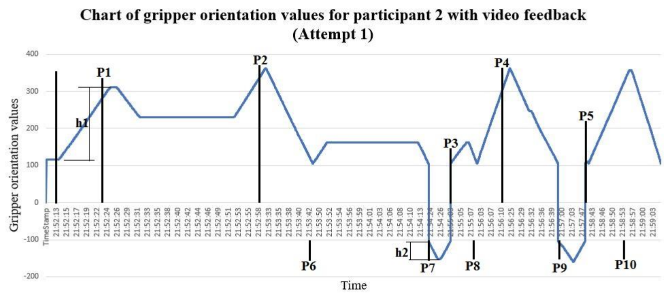

Figure 5.39: Chart of gripper orientation values for participant 2 with video feedback (Attempt 1)

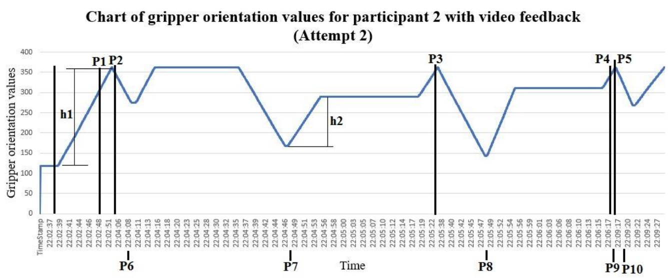

Figure 5.40: Chart of gripper orientation values for participant 2 with video feedback (Attempt 2)

2. **Without Video Feedback of the Robot End**

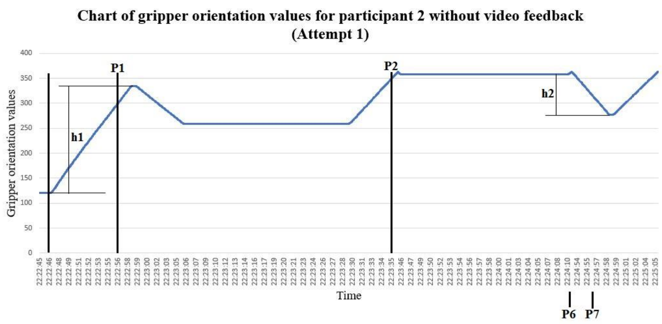

Figure 5.41: Chart of gripper orientation values for participant 2 without video feedback (Attempt 1)

5.6.1.3 Gripper Orientation Plots for Participant 3

1. **With Video Feedback of the Robot End**

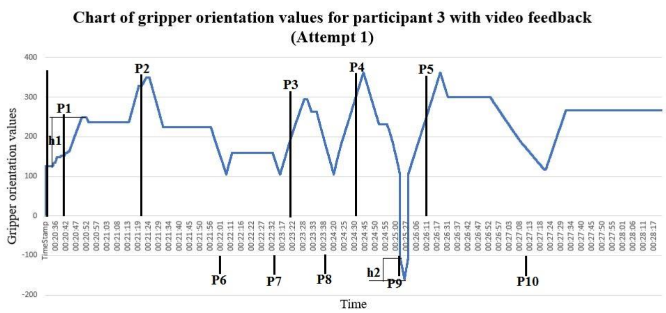

Figure 5.42: Chart of gripper orientation values for participant 3 with video feedback (Attempt 1)

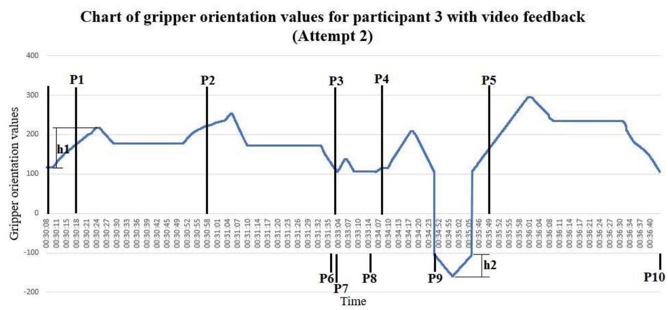

Figure 5.43: Chart of gripper orientation values for participant 3 with video feedback (Attempt 2)

2. **Without Video Feedback of the Robot End**

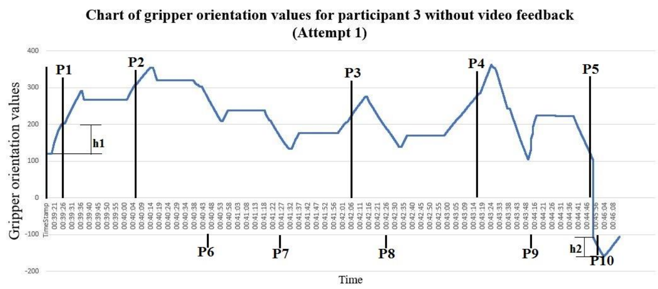

Figure 5.44: Chart of gripper orientation values for participant 3 without video feedback (Attempt 1)

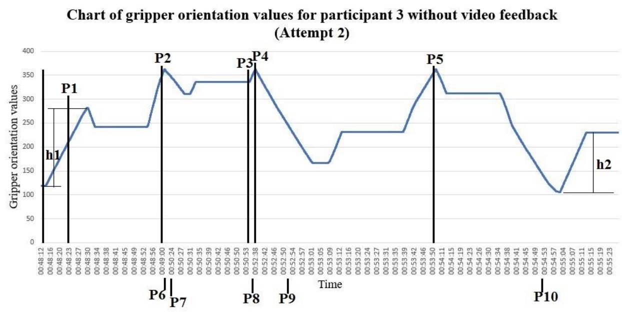

Figure 5.45: Chart of gripper orientation values for participant 3 without video feedback (Attempt 2)

5.6.1.4 Gripper Orientation Plots for Participant 4

1. **With Video Feedback of the Robot End**

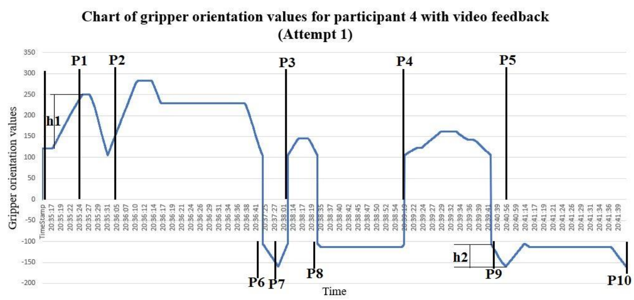

Figure 5.46: Chart of gripper orientation values for participant 4 with video feedback (Attempt 1)

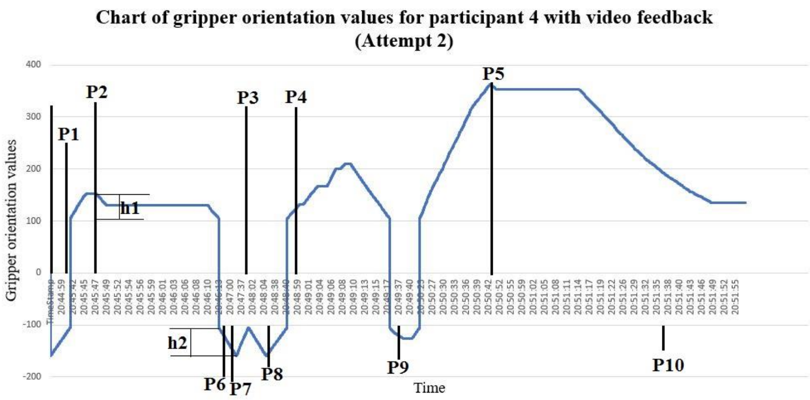

Figure 5.47: Chart of gripper orientation values for participant 4 with video feedback (Attempt 2)

5.7 Conclusion and Discussion

The first aim of the phase 1 study was to determine the minimum detectable haptic intensity (MDHI) across different locations on the wrist. MDHI was measured by recording the duty cycles (of PWM powering each haptic motor) for the least haptic intensities participants could pinpoint at different locations across the wrist. The study was carried out by all participants with and without the introduction of the same video distraction. The video distraction used was an interview on David Attenborough's career [59] on nature. Determining the MDHI was done by increasing the duty cycle of each haptic stimulation until participants could pinpoint the correct location of stimulation on the wrist. This study phase was repeated four times with varying duration of haptic stimulation (DHS): 250 ms, 500 ms, 750 ms, and 1000 ms.

Analysis was carried out on the recorded MDHI for each duration of haptic stimulation (DHS) using 2-way repeated measures ANOVA to investigate differences in MDHI between different locations across the wrist and to evaluate the effect of video distraction on MDHI (study phase 1, aim 2). For all duration of haptic stimulation (250 ms, 500 ms, 750 ms, and 1000 ms) considered, there was significant main effect of locations of stimulation on MDHI. Irrespective of the duration of haptic stimulation (DHS), the MDHI of the different locations of stimulation on the wrist are significantly different. The similarities in MDHI between different locations of haptic stimulation on the wrist varied depending on the duration of haptic stimulation (DHS). For all duration of haptic stimulation, there was similarity in MDHI between the Ulna zone and the Radial zone. However, as DHS increases MDHI similarities between the Dorsal central and the Volar central increases. The effect of distraction was significant for all the different values of duration of haptic stimulation considered. In general, results show that at lower values of duration of haptic stimulation (DHS), distractions reduced participants' abilities to detect lower haptic intensities. As DHS increases, the effect of distraction reduces. Also, for the durations of haptic stimulation considered, there was no effect of the interaction between locations of stimulation and distraction.

The effect of DHS on MDHI at each point on the wrist was also investigated. For each location of haptic stimulation, as the duration of haptic stimulation (DHS) increases, MDHI reduces. This trend can be noticed with and without video distractions. Paired t Test also revealed that there was significant difference between MDHI across DHS for each point of haptic stimulation as shown in Table 5.10. To investigate possible relationships between the MDHI at the different locations and the wrist size, bivariate correlations were carried out. Results show no correlations for most of the comparisons except at the top of the wrist with duration stimulation = 1000 ms. We can conclude that in the development of wrist-worn haptic devices, wrist size does not affect MDHI but dynamic changes in the duration and intensity of stimulation may improve haptic perception. Results from this phase of the study were therefore used in the next phase of the study where participants' haptic perception performance was evaluated.

The overall ILHSP was investigated for SSI and SDSI. This means that the mean performance scores of SSI and SDSI combinations were calculated. For SSI, there was no significant difference in ILHSP between scenarios 1-4 (phase 2 study, aim 1). However, overall ILHSP scores for scenario 5 was significantly different from scenarios with significantly different mean MDHI. This suggests that the use of results from the phase 1 study are useful for haptic device calibration. It also confirms that haptic stimulation become easier to perceive as the intensity of stimulation increases (phase 2 study, aim 2). ILHSP scores were generally low for SDSI. Even though overall ILHSP scores for SSI were high, it was important to examine ILHSP scores for individual location across the wrist.

Results showed that effect of locations of haptic stimulation on participants' abilities to identify locations of stimulation varies for various DHS. Likewise, the effect of video distraction on abilities to pinpoint locations of stimulation was different for different values of DHS. Across scenarios, with and without video distraction, scenario 5 resulted in the highest ILHSP scores for all locations examined across the wrist. For all scenarios, the Volar central had the highest ILHSP scores across the wrist(phase 2 study, aim 3). In order to eradicate the possibility of chance and false alarms, sensitivity of the the different locations across the wrist for each scenario was calculated. The Volar central was identified as the most sensitive with the Radial zone identified as the least sensitive location on the wrist (phase 2 study, aim 4). It was also important to examine the possibility of pinpointing two locations that are simultaneously stimulated. Overall, it was difficult for participants to identify two simultaneously stimulated locations. This may be attributed to the difference in haptic sensitivity of the different locations since the same intensity of haptic stimulation was used for all locations across the wrist. For all scenarios, in scenario 5, participants recorded highest ILHSP scores. In scenario 1 participants recorded the least ILHSP scores. In most cases when the Drsal central and Radial zone were simultaneously stimulated, participants reported that they felt the stimulation at the Dorsal central. This remained the same when the Dorsal central and Ulna zone were simultaneously stimulated. When the Volar central and Radial zone were simultaneously stimulated, participants mostly reported feeling the stimulation at the Volar central. Similar perception was reported when the Volar central and Ulna zone were simultaneously stimulated.

Plots of the gripper orientation values reveal how participants changed the gripper orientation based on the information perceived through the wrist-worn haptic device. Figures in section 5.6.1 show the difference in the amplitudes of the gripper orientation waveform. Each waveform represents the trajectory of the robot gripper. h1 represents the amplitude of the orientation waveform when the initial direction of rotation of the gripper is to the left while h2 represents the orientation waveform when initial direction of gripper rotation is to the right for each haptic stimulation. The positive and negative sections of the waveform would be symmetrical if the rate at which participants changed the gripper orientation was constant. The difference in the values of h1 and h2 implies a difference in trajectories and even though all the participants received similar haptic stimulation, the gripper trajectories were different in all cases. From figure 5.37, figure 5.40, figure 5.41, and figure 5.45 the wave plot is entirely positive which is not a representation of figure 5.35.

Points P1-P10 show the peak locations of the haptic stimulation. If the haptic peaks coincide with the peaks of the gripper trajectories, it implies that participants were able to change the gripper orientation in real time. For all participants (as well as for all attempts), the time between the peaks varied. The difference in waveform (time between the stimulation peak and the trajectory peak) is as a result of

1. participants' sensitivity to haptic stimulation,
2. the difference in the participants' reaction times and
3. the rate at which they change the gripper orientation (Often influenced by differing motor skills [31]).

Participants' perception of haptic stimulation can be improved by calibrating the haptic device for each participant. The problem with the rate at which participants can change the gripper orientation can be solved by keeping the speed of gripper rotation constant. Since the reaction times vary for different people, it is recommended that haptic feedback is used to convey instantaneous state of the robot and not instructions for real time applications.

Video feedback of the remote end provided participants with additional information of the instantaneous orientation of the gripper and may therefore lead to increase in the rate at which the orientation of the gripper is changed.

This chapter establishes that there exists difference in MDHI at different locations across the wrist. Results also show that the different locations across the wrist can be correctly pinpointed and performance varies based on different parameters. In chapter 6, we explored the participants' abilities to pinpoint locations of stimulation in a real-world tele-operated task. The aim was to explore the possibility of conveying more than one type of sensor data through the same wrist-worn haptic feedback device. The effect of task repetition on learning with regard to feedback modalities was also examined.

CHAPTER 6

Investigating the Impact of Conveying Multiple Sensor Data using a Single Wrist-Worn Haptic Feedback Device and the Effect of Task Repetition

6.1 Introduction

The basic concepts of sensory and feedback modalities were examined in the first chapter of this thesis. The concepts cover how the human body receives and interprets information. This helps to understand how different sensory modalities can be used in order to effectively convey information. This thesis also explored the concept of sensory substitution, making it possible to convey sensory information the human senses would otherwise have not been able to receive.

During the study on investigating optimal sensory feedback modalities, different combinations of video feedback, peripheral vision feedback, haptic feedback, and verbal collaboration were used to provide feedback on the orientation of the gripper during a simple pick-and-empty task. What is yet to be explored in this thesis is to convey of multiple sensor data via these different feedback modalities. The information received by the operator may be conveyed in two formats. The first format is to convey the information as instructions on what to do, while in the second format, operators are provided with information and allowed to make decisions on how to carry out a task. In the study carried out in chapter five, results showed that providing operators with instantaneous information about the remote environment and enabling them to make control decisions increases the accuracy with which tasks can be carried out.

Based on the way feedback modalities are designed, they may also be classified either as extreme discrete or continuous. Extreme discrete displays project the specific upper and lower bounds of the measured parameter. On the other hand, continuous displays provide variations of the feedback with the final decision left to the user. For example, the use of different colours to convey points of a measured parameter may be classified as extreme, while the use of different shades of the same colour to convey a measured parameter may be classified as continuous. Depending on the experimental design, different feedback modalities may be employed using either of the two information display classifications. It may however feel more natural to convey continuous environmental data using the continuous convey classification.

As the need to convey more sensor data to operators increases, it is important to explore the different ways through which information can be conveyed via the limited feedback modalities that are available. Results from the haptic feedback study in chapter five show that sensitivity to haptic stimulation varies at different locations on the wrist. Results also show that participants were able to identify these different locations of haptic stimulation. In this chapter, we explore the use of a wrist-worn haptic device to convey two different types of sensor data using the continuous display as participants carried out simple assistive task of controlling a robot arm to pick up a jar filled with rice grains and emptying the content into a bowl.

6.2 Hypotheses

The focus of this final phase of the study was to test the following hypotheses:

1. The use of additional feedback (gripper proximity and orientation) improves the accuracy with which participants carry out the task at each stage (stage 1 accuracy is gripper orientation and proximity, stage 2 accuracy is gripper proximity).
2. Participants' performance improves with task repetition. Performance is measured through task completion time, gripper proximity to the table, gripper orientation before grasp, and gripper trajectory.
3. Participants' performance further improves with task repetition and feedback.
4. Two different types of sensor information can be interpreted using the same wrist-worn haptic feedback device.

6.3 Design/Setup

The study setup used is located in the Assisted Living Studio of the Bristol Robotics Laboratory, Bristol. Figure 6.1 shows the study environment and hardware setup. The robot environment (fig. 6.1a) has a Kinova robot arm [88] hung from the ceiling railing. Four (4) video cameras were also installed in the robot environment to capture robot movements from four (4) different angles. Wi-Fi enabled orientation and proximity sensors were attached to the robot gripper to measure vertical alignment and proximity of the gripper to horizontal surfaces (cooking surface and table) respectively. The study setup used here is different from that used in the study investigating optimal feedback modalities.

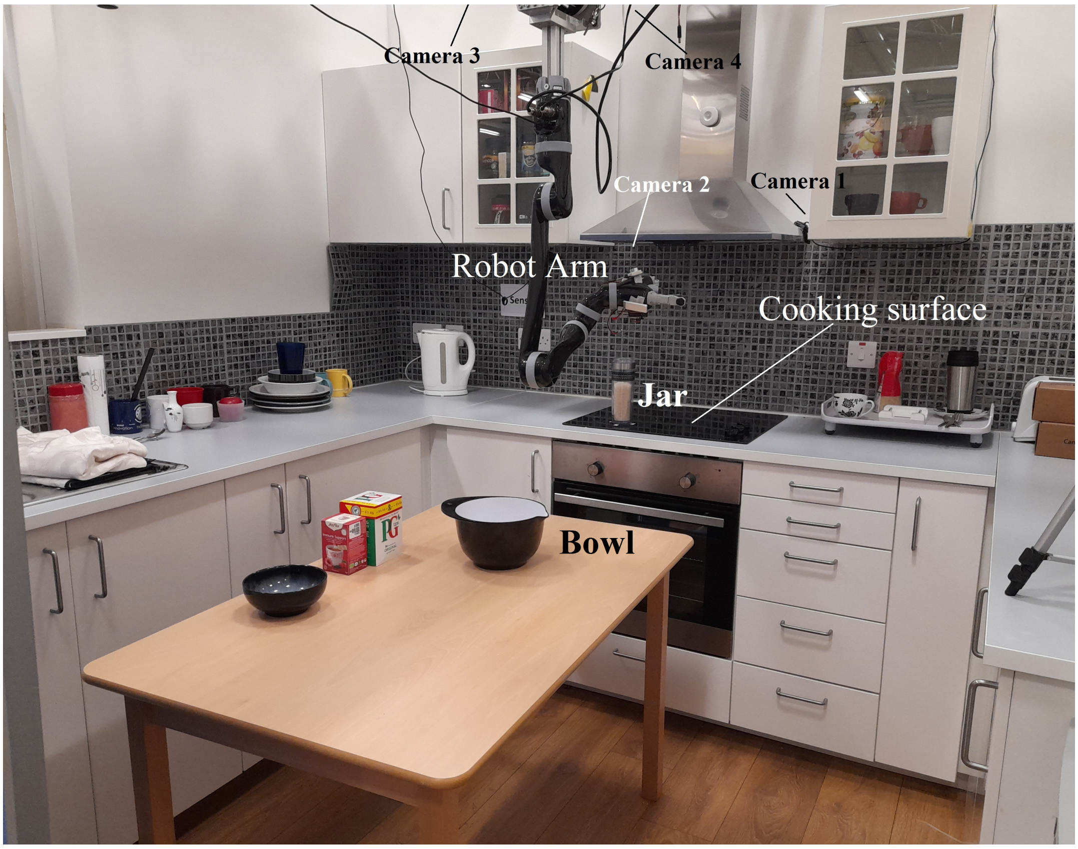

(a)

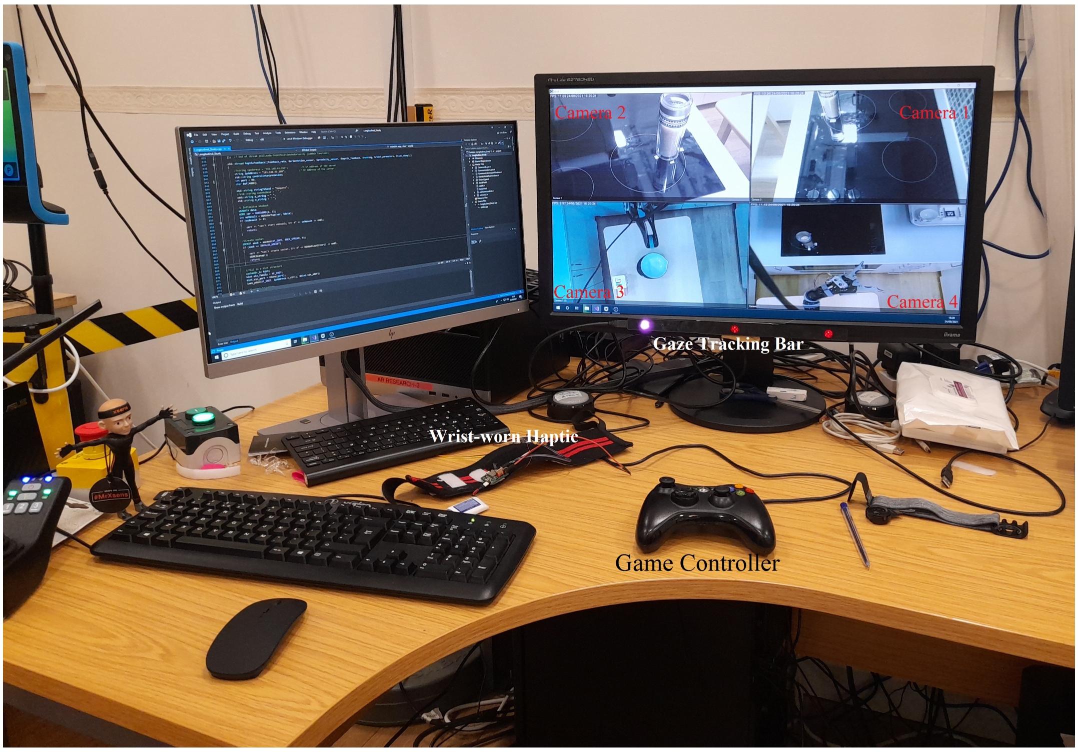

(b)

Figure 6.1: Study setup (a) robot environment, (b) operator workstation

The change in setup was carried out to increase the authenticity of the study for an assisted living scenario. Attaching the robot arm to a table, as was done in the previous setup, limits the work space in which the arm can be used. However, attaching the robot to the ceiling railing ensures that we could use all the degree of freedom of the robot to increase the work space of the robot.

Figure 6.1b shows the operator workstation. Real-time video from the four cameras installed in the robot environment are displayed on the screen to the right. An X-box game controller was adapted to control the robot. Proximity and orientation readings were conveyed to participants via the wrist-worn haptic device.

Data collection and processing was carried out at the tele-operation work station. For the study, C++ programming language was used to write the control program written to perform data collection and processing. The control program employed the use of threads to handle different tasks. Robot parameters were polled from the robot in a thread while communication between the proximity and orientation sensors were in separate threads.

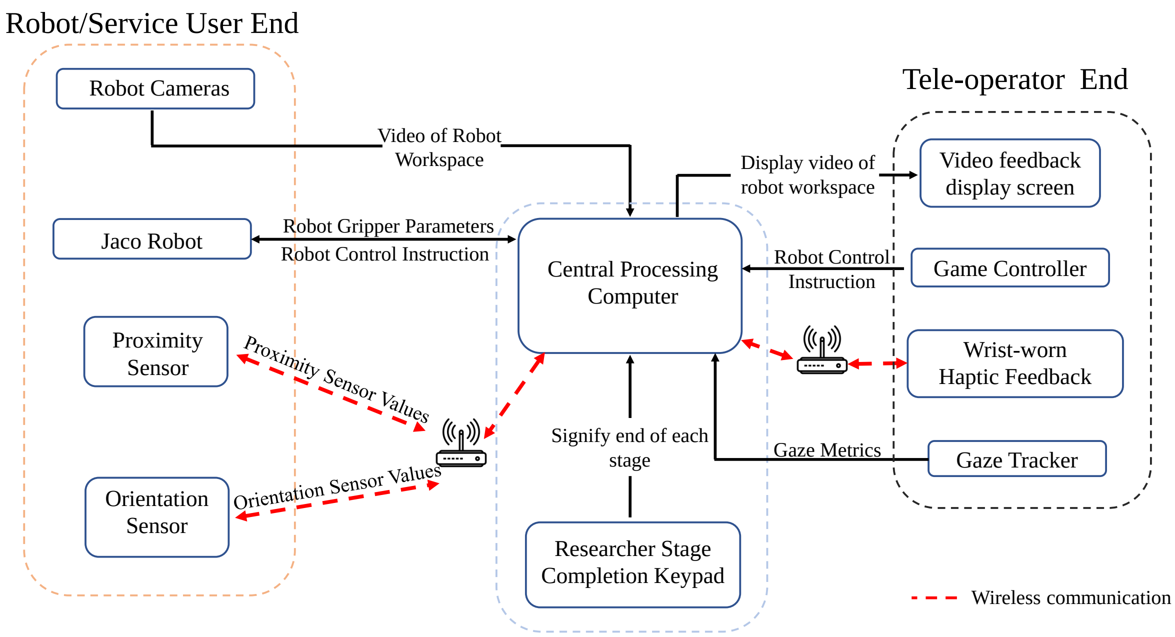

Figure 6.2: Block Diagram showing hardware and software interactions

Fig. 6.2 shows the block diagram of the hardware and software interactions for the study.

For this study, only video feedback and haptic feedback were used to convey information about the remote environment. The haptic device had three motors located at the Ulna zone, Volar central and Radial central of the wrist (fig. 6.3). Haptic motors at the Ulna zone and Radial zone of the wrist were used to convey the direction of gripper orientation (left or right) while the haptic motor at the Volar central of the wrist was used to convey proximity information.

Gripper orientation information was conveyed by increasing the amplitude of haptic stimulation as the alignment of the gripper deviates from its vertical reference position. The amplitude of haptic stimulation can be changed by increasing or reducing the duty cycle of the pulse width modulation. As the gripper orientation deviates from its vertical alignment, the amplitude of vibration of the motor corresponding to the direction of deviation increases. In order to convey proximity information, as the gripper gets closer to surfaces, the amplitude of the motor at the Volar central increases. The proximity motor only starts to vibrate if the gripper is within 20 cm of the horizontal surface. Video feeds from the four cameras installed on the robot environment was displayed in four quadrants on the video display screen at the operator workstation.

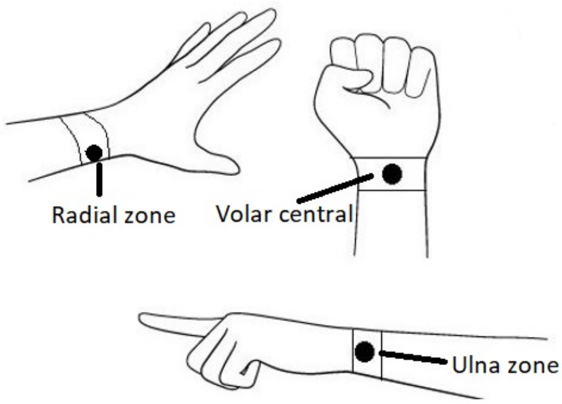

Figure 6.3: Motor positions across the wrist for the study

6.4 Study Procedure

Prior studies carried out were cross-sectional studies. This means that participants were involved in the study for only a few attempts. The effect of the use of feedback modalities were studied. However, the effect of increased number of trials on participants' abilities to interpret feedback data was not investigated. Additionally, in previous studies, whilst video feedback of the remote environment was provided to participants, only one additional sensor data (gripper orientation values) was conveyed to participants, albeit via different combinations of feedback modalities. In this study participants were required to carry out a simple pick-and-empty task while being provided with video feedback of the robot work environment as well as gripper proximity and orientation data. The proximity and orientation information was provided via a wrist-worn haptic feedback device. In the study, participants were required to control a robot arm to pick up a jar containing grains of rice and to empty the content into a bowl. The task was divided into four (4) stages.

1. Free-space translation and rotation of the gripper from its start position to a position close enough for grasp.

2. Grasping the jar and making free-space translation to a position where it's content can be emptied.

3. Free-space rotation and translation of the jar to empty its content.

4. Free-space translation and rotation of the emptied jar to its pickup position.

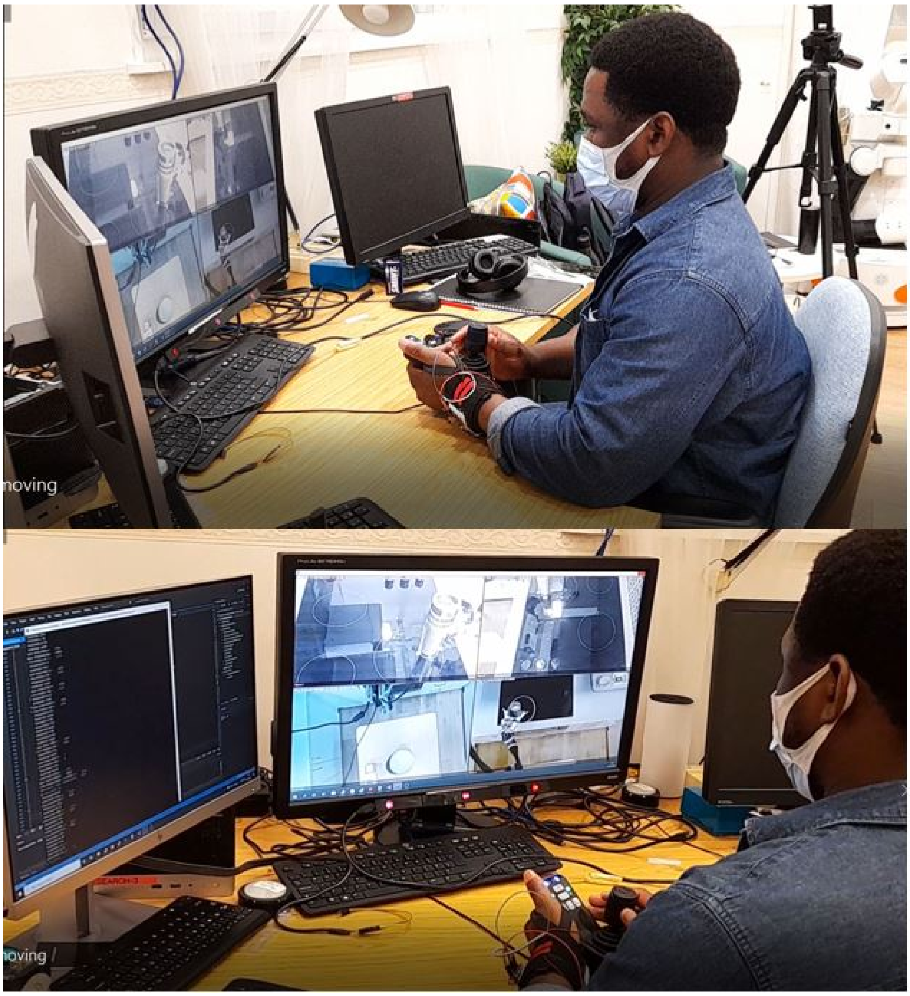

Figure 6.4: Operator interface showing a human operator

15 people (Male=11, Female=4) participated in the study and signed the consent form (Appendix A). Participants were randomly divided into two groups. Group 1 was the control group. Participants in group 1 were required to carry out the task using only video feedback of the robot work space. However, participants in group two were provided with supplementary information about the gripper orientation and proximity via the wrist-worn haptic device. All participants repeated the task five (5) times on four (4) different days, resulting to 20 attempts per participant over a four day period. For all participants, the longest study duration was on the first day with an average of forty minutes. The study completion time reduced thereafter.

(a)

(b)

Figure 6.5: Gripper parameters, (a) Stage 1 proximity and orientation (b) Stage 2 proximity

The study involved two independent variables (days and attempts) and four dependent variables (task completion time, gripper orientation, gripper proximity, gripper trajectory). The effect of other factors including supplementary feedback, gaming experience, and robot experience were also investigated. The task completion time is further classified into: total task completion time (TTCT), stage 1 task completion time (S1TCT), stage 2 task completion time (S2TCT), stage 3 task completion time (S3TCT), and stage 4 task completion time (S4TCT). Gripper proximity was also divided into two: Stage 1 gripper proximity and Stage 2 gripper proximity. Stage 1 gripper proximity (S1GP) is the vertical distance between the gripper and cooking surface while stage 2 gripper proximity (S2GP) is the vertical distance between the gripper and the table. Gripper trajectory is the distance the the gripper travelled in the x,y, and z planes (in meters) as the task is carried out. Participants were also required to complete a NASA Task Load Index (NASA TLX) questionnaire daily as they participated in the study. The NASA TLX questionnaire is designed to investigate participants' perceived mental demand, physical demand, temporal demand, performance, effort, and frustration in relation to the task which may be used to evaluate the overall workload experienced by each participant.

Table 6.1: Measured parameters

S/N	**Parameter**	**Interpretation**
1	Total task completion time (TTCT)	Total time taken to complete the task
2	Stage 1 task completion time (S1TCT)	Time taken to complete stage 1 of the task
3	Stage 2 task completion time (S2TCT)	Time taken to complete stage 2 of the task
4	Stage 3 task completion time (S3TCT)	Time taken to complete stage 3 of the task
5	Stage 1 Gripper Proximity	The vertical distance of the gripper to the kitchen cabinet (cm)
6	Stage 2 Gripper Proximity	The vertical distance of the gripper to the table (cm)
7	Gripper trajectory	The distance travelled by the gripper throughout the task (m)
8	NASA TLX questionnaire	The questionnaire was completed daily to provide insight into participants' perceived mental demand, physical demand, temporal demand, performance, effort, and frustration.

6.5 Result

In order to make accurate inferences, the sample size needed to provide statistical power of 0.95 was calculated (using the G*Power statistical software) to be 14 for two groups of participants and number of measurements of 20. Shapiro-Wilk's test for normality shows that the data was normally distributed. Two-way repeated measures ANOVA was therefore carried out on the data.

6.5.1 Task Completion Time

The task completion time is the time taken to complete the task. Total task completion time, stage 1 task completion time (S1TCT), stage 2 task completion time (S2TCT), stage 3 task completion time (S3TCT), and stage 4 task completion time (S4TCT) were analysed.

6.5.1.1 Total Task Completion Time

This is described as the total time taken to complete the task in seconds. Table 6.2 below shows the total task completion time for all days and the corresponding attempts for each day. The table shows changes in the total task completion time as participants repeated the task.

Table 6.2: Total task completion time for days and corresponding attempts

Day	Attempt	Mean total task completion time			
		Supplementary Feedback		No Supplementary Feedback	
		Mean	Standard Deviation	Mean	Standard Deviation
1	1	293.5777	147.5700	275.5990	90.3143
	2	244.0632	84.2494	224.3361	56.3420
	3	216.1181	62.3898	237.2811	106.5511
	4	203.8572	73.7023	203.3111	48.2126
	5	191.462	53.0626	193.7613	48.6862
2	1	229.4030	62.0167	195.7537	53.5552
	2	195.5537	61.0373	165.1947	30.0215
	3	184.1900	57.3275	158.0324	33.7817
	4	168.1787	44.0251	155.1363	30.9405
	5	191.8163	68.6131	150.0526	32.7115
3	1	176.1550	70.7182	148.6042	23.3087
	2	205.0244	75.5482	145.4366	23.1392
	3	161.7260	31.2390	152.6797	30.0631

Continued on next page

Table 6.2 – continued from previous page

Day	Attempt	Mean total task completion time			
		Supplementary Feedback		No Supplementary Feedback	
		Mean	Standard Deviation	Mean	Standard Deviation
	4	157.9627	26.9901	164.1423	45.0214
	5	144.83.56	20.7377	159.7079	29.2048
4	1	177.4634	53.8000	152.7357	23.7054
	2	157.0496	34.6881	142.4896	22.6733
	3	155.0664	29.7363	143.6029	30.2835
	4	160.0279	36.5570	146.3009	37.5333
	5	153.3280	14.9651	144.7020	36.3098

Table 6.3: Estimated marginal means for total task completion time

	Supplementary Feedback		Gaming Experience (GE)		Robot Experience (RE)	
	No Supplementary Feedback	Supplementary Feedback Used	No GE	Has GE	No RE	Has RE
Mean Total task completion time (seconds)	184.483	193.052	224.206	171.048	205.375	155.553

Mauchly's Test of Sphericity indicated that the assumption of sphericity has not been violated (assumption met) for days ($\chi^2(5) = 3.435$, $p = 0.636$), and attempts ($\chi^2(9) = 15.421$, $p = 0.089$).

There was significant main effect of the day the task was carried out on the overall task completion time, ($F(3,24) = 48.720$, $p < 0.001$, $\eta_p^2 = 0.859$). The effect of task attempt on the overall task completion time was also found to be significant ($F(4,32) = 17.398$, $p < 0.001$, $\eta_p^2 = 0.685$). There was significant interaction Days*Attempt ($F(12,96) = 4.347$, $p < 0.001$, $\eta_p^2 = 0.352$). The interactions Days*Supplementary Feedback, and Days*Gaming Experience was not significant. However, the interactions Days*Robot Experience, as well as Attempt*Robot experience were significant.

The test of between subject effect showed no significant effect of each factor (feedback, gaming experience, and robot experience) and their interactions.

Table 6.3 shows the estimated marginal means of the total task completion time. Pairwise comparison shows no significant difference in total task completion time for the use of supplementary feedback and without the use of supplementary feedback. Pairwise comparisons with and without gaming experience ($p = 0.013$) and with and without robot experience ($p = 0.003$) were significant.

Plots for the estimated marginal means are shown in figure 6.6.

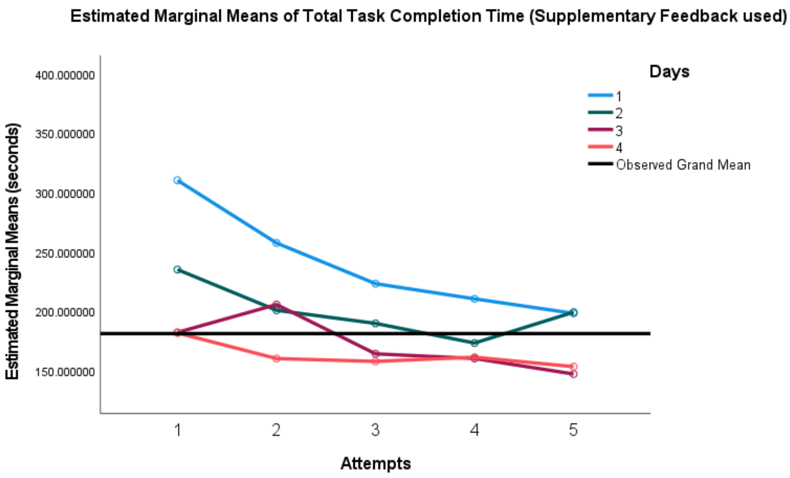

(a)

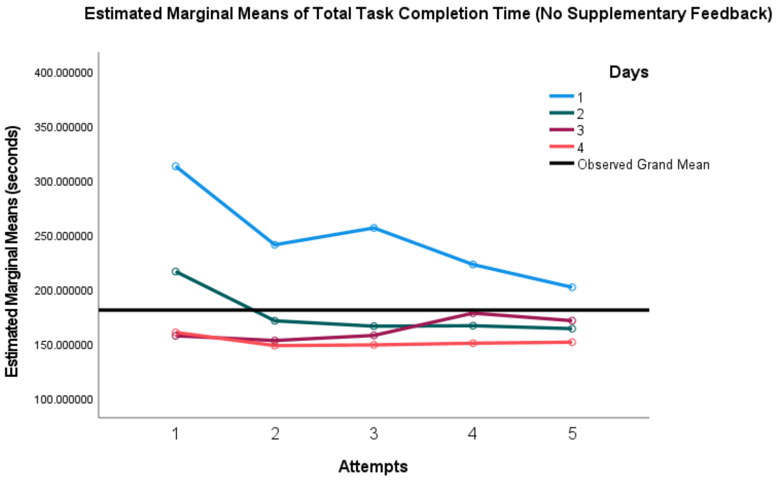

(b)

Figure 6.6: Plots of estimated marginal mean (a) supplementary feedback used, (b) no supplementary feedback Used

Pairwise comparisons for total task completion time between day 1 and days 2, 3, and 4 were significant ($p < 0.001$). Comparison between days 2 and 3 was not significant ($p = 0.124$), likewise between days 2 and 4 (p = 0.473) but was significant for days 3 and 4 (p = 0.017). Significant improvement in total task completion time after the first day was noticed every 2 days (8 attempts). For each day the task was carried out, there was significant improvement in total task completion time between attempts 1 and attempts 2,3,4, and 5. However there was no significant improvement after the second attempt. We further investigated for differences in total task completion time between the last attempt for each day by carrying out paired samples t test for the mentioned attempts.

Table 6.4: Mean task completion time for last daily attempts (attempt 5))

Last Daily Attempts	**Mean TTCT (s)**	**Standard error**
Day 1	192.612	48.938
Day 2	170.934	56.002
Day 3	155.029	26.818
Day 4	151.201	27.409

Paired samples t test shows that there was significant difference in total task completion times between day 1 and day 3 ($p < 0.001$), as well as between day 1 and day 4 ($p = 0.001$)

Table 6.5: Mean task completion time for last daily attempts (attempt 5) with and without supplementary feedback

Last Daily Attempts	With Supplementary Feedback		Without Supplementary Feedback	
	Mean TTCT (s)	Standard Deviation	Mean TTCT (s)	Standard Deviation
Day 1	191.462	53.063	193.761	48.686
Day 2	191.816	68.616	150.053	32.711
Day 3	144.839	20.738	159.708	29.205
Day 4	153.328	14.965	144.702	36.340

Table 6.6: Mean task completion time for last daily attempts (attempt 5) with and without gaming experience

Last Daily Attempts	Gaming Experience		Without gaming experience	
	Mean TTCT (s)	Standard Deviation	Mean TTCT (s)	Standard Deviation
Day 1	181.130	46.270	234.712	38.459
Day 2	149.408	36.589	249.863	42.412
Day 3	145.412	23.500	177.423	16.346
Day 4	146.632	30.136	157.751	8.400

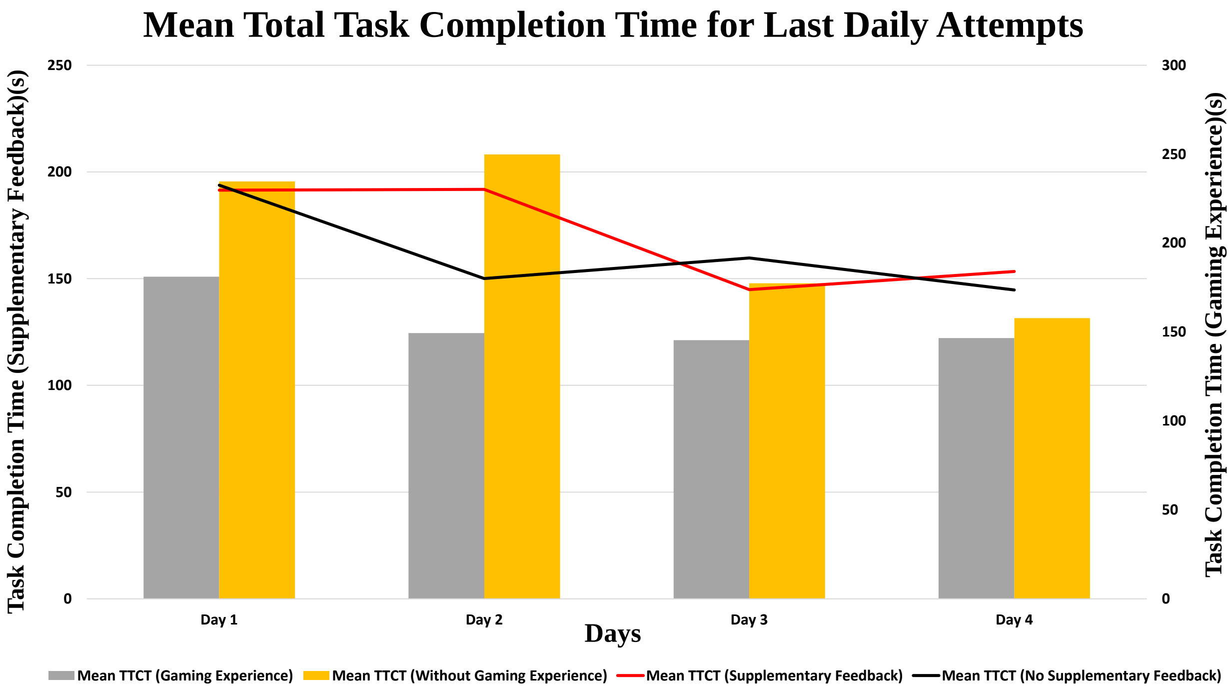

Figure 6.7: Task completion time for last daily attempts (attempt 5)

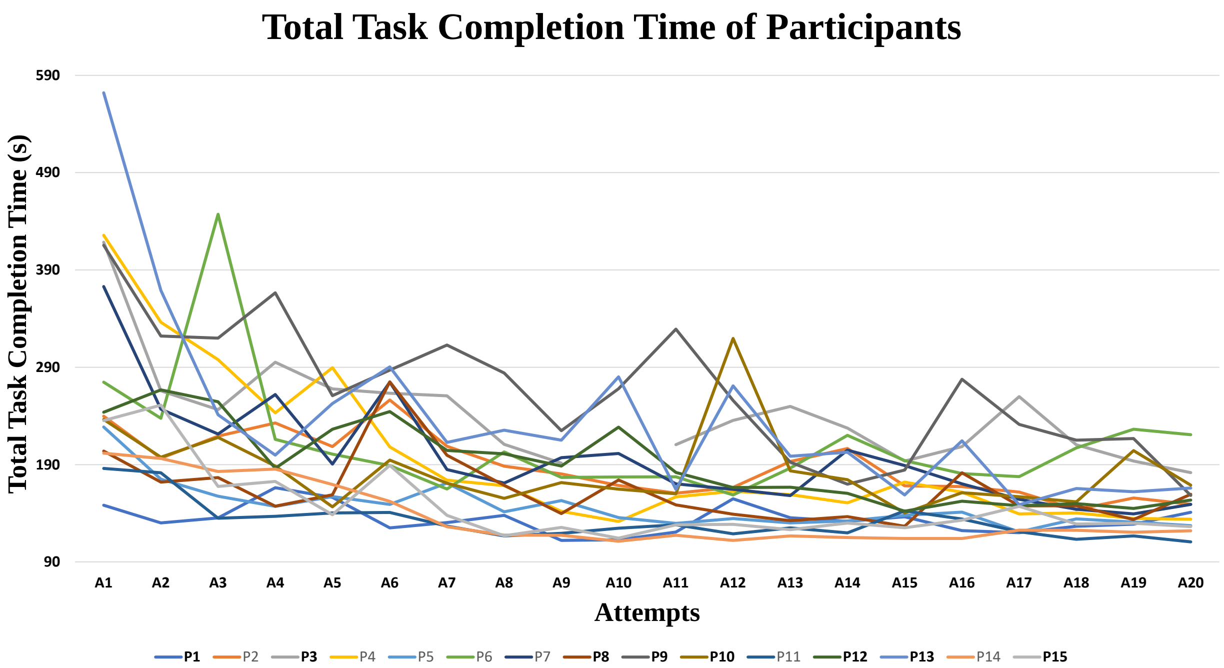

Figure 6.8: Task completion time for all participants

6.5.1.2 Stage 1 Task Completion Time

Stage 1 task completion time is the time it takes to move the robot from its home position to a position just before the fingers are closed for grasp. This involves translation and rotation of the gripper. The task completion time for stage 1 is provided in table 6.7.

Table 6.7: Stage 1 task completion time for days and corresponding attempts

Day	Attempt	Mean total task completion time			
		Supplementary Feedback		No Supplementary Feedback	
		Mean	Standard Deviation	Mean	Standard Deviation
1	1	123.1711	74.0014	90.9881	21.1955
	2	87.6275	41.5529	78.3511	16.3201
	3	75.7503	16.2776	72.5635	18.0018
	4	75.7600	18.4654	74.5706	21.8685
	5	71.4367	18.6974	69.0134	14.5856
2	1	85.5287	26.0098	70.9661	23.7329
	2	67.0231	17.1986	60.5923	13.4829
	3	65.1843	21.6816	55.4485	10.5224
	4	60.3658	15.6524	55.4884	11.7825
	5	61.2506	13.5488	56.0117	14.3237
3	1	61.1226	12.8383	57.9826	12.4915
	2	78.4337	48.6372	52.2951	9.0510
	3	61.0437	14.7483	57.5979	14.2811
	4	58.6657	11.4679	61.5169	21.2706
	5	53.8003	6.5041	59.6643	14.3487
4	1	56.1561	7.6285	53.5879	12.6534
	2	52.1319	3.6404	52.3443	9.8264
	3	54.0345	7.2507	56.5258	19.1902
	4	60.5122	20.2597	58.4952	20.2644
	5	60.3923	9.3167	56.9237	22.6119

Table 6.7 shows the task completion time for stage 1 of the task for participants with and without supplementary feedback.

A two-way repeated measures ANOVA was carried out on the data. Mauchly's Test of Sphericity indicated that the assumption of sphericity has not been violated (assumption met, $p > 0.05$) for days ($\chi^2(5) = 4.886$, $p = 0.434$). However, the assumption of sphericity was violated for attempts ($\chi^2(9) = 23.885$, $p = 0.006$) and since $\epsilon < 0.75$, we report the Greenhouse-Geisser corrected results.

There was significant main effect of the day the task was carried out on the task completion time for stage 1, ($F(3,24) = 31.405$, $p < 0.001$, $\eta_p^2 = 0.797$). The effect of task attempt on the task completion time for stage 1 was also found to be significant ($F(1.891, 15.126) = 7.225$, $p =$

0.007, $\eta_p^2 = 0.475$). The interaction days and attempt ($F(12,96) = 3.881$, $p < 0.001$, $\eta_p^2 = 0.327$) was significant. Interaction days and gaming experience, as well as days and robot experience were significant.

The test of between subject effect showed no significant effect of each factor (feedback, gaming experience, and robot experience) and their interactions.

Table 6.8 shows the estimated marginal means of the time taken to complete stage 1 of the task.

Table 6.8: Estimated marginal means for stage 1 task completion time

	Supplementary Feedback		Gaming Experience (GE)		Robot Experience (RE)	
	No Additional Feedback	Additional Feedback Used	No GE	Has GE	No RE	Has RE
Mean task completion time (seconds) for stage 1	68.223	69.465	82.002	62.265	74.102	58.327

Pairwise comparison of task completion time for stage 1 (S1TCT) between participants with feedback and without feedback was not significant ($p = 0.841$). Pairwise comparison of S1TCT for gaming experience was significant ($p = 0.023$). Likewise, pairwise comparison of S1TCT for robot experience was also significant ($p = 0.023$).

Table 6.9 shows the estimated daily marginal means for S1TCT.

Table 6.9: Daily estimated marginal means for S1TCT

Days	Mean S1TCT (seconds)
1	87.574
2	67.464
3	62.551
4	57.787

Pairwise comparison of daily S1TCT between day 1 and days 2,3, and 4 were significant ($p < 0.001$). However, comparisons between day 2, 3 and 4 were not significant. For each daily attempt, pairwise comparisons among all attempts were not significant.

Figure 6.9 shows the plots of estimated marginal means for S1TCT.

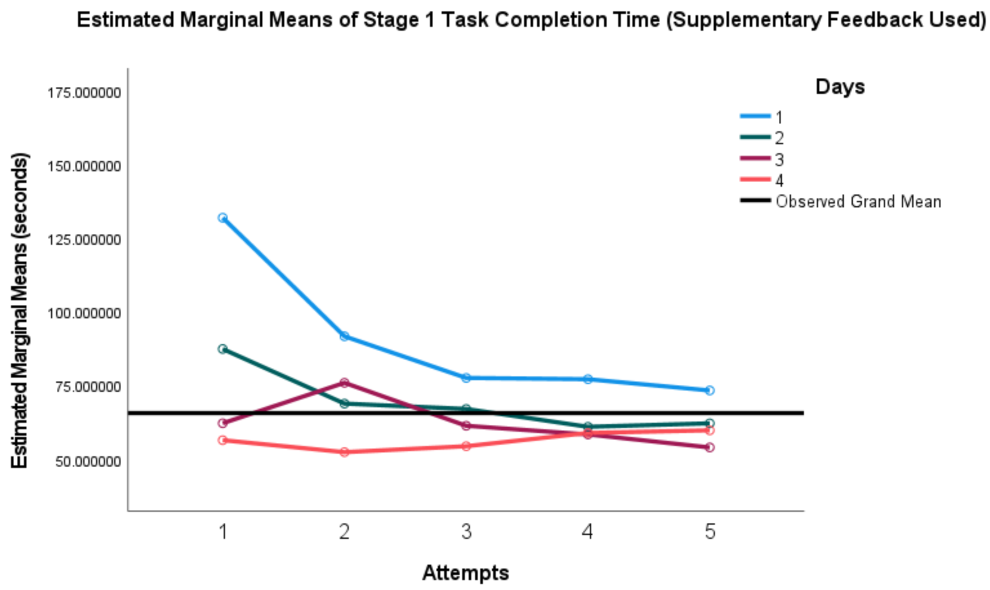

(a)

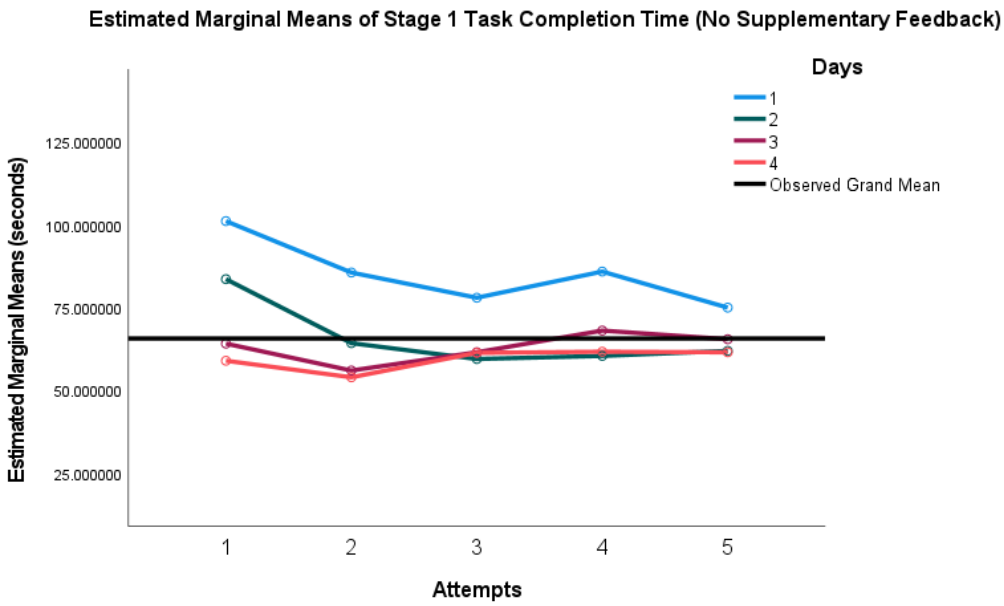

(b)

Figure 6.9: Plots of estimated marginal mean for stage 1 task completion time (a) Supplementary feedback used, (b) No supplementary feedback used

Further analysis was carried out on stage 1 task completion time between attempts 5 of all the days. Table 6.10 shows the mean S1TCT for attempts 5. Paired samples test of S1TCT between day 1 and day 2 was significant ($p = 0.003$). Likewise, paired samples test of SITCT between day

1 and day 3 was significant. There was also a significant difference in S1TCT between day 1 and and day 4. All other comparisons were not significant.

Table 6.10: Mean S1TCT for last daily attempts (attempt 5))

Last Daily Attempts	**Mean S1TCT (s)**	**Standard error**
Day 1	70.225	16.159
Day 2	58.631	13.667
Day 3	58.737	13.239
Day 4	58.650	16.104

Table 6.11: Mean S1TCT for last daily attempts (attempt 5) with and without supplementary feedback

Last Daily Attempts	With Supplementary Feedback		Without Supplementary Feedback	
	Mean S1TCT (s)	Standard Deviation	Mean S1TCT (s)	Standard Deviation
Day 1	71.437	18.698	69.013	14.586
Day 2	61.251	13.549	56.012	14.324
Day 3	53.800	6.504	59.664	14.349
Day 4	60.392	9.317	56.924	22.612

Table 6.12: Mean S1TCT for last daily attempts (attempt 5) with and without gaming experience

Last Daily Attempts	Gaming Experience		Without gaming experience	
	Mean S1TCT (s)	Standard Deviation	Mean S1CT (s)	Standard Deviation
Day 1	86.717	20.402	181.741	82.762
Day 2	54.525	12.138	73.687	6.696
Day 3	54.314	9.750	65.599	13.392
Day 4	57.069	18.706	64.484	1.020

Figure 6.10 shows the plot of S1TCT for participants. It shows the difference in S1TCT for participants with and without supplementary feedback. Figure 6.10 also shows the difference in S1TCT for participants with and without prior gaming experience. In figure 6.11, S1TCT plots for all participants are shown. 'A' represents attempts and 'P' represents participant. Participants with feedback appear in bold.

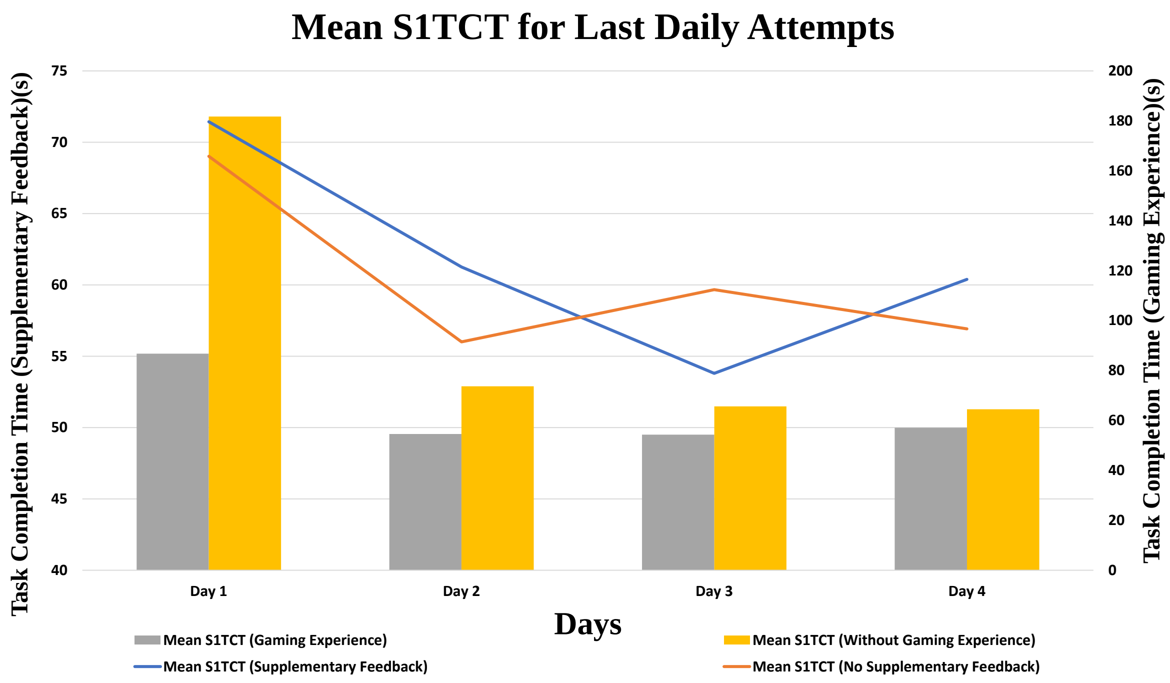

Figure 6.10: Stage 1 Task completion time for daily attempts 5

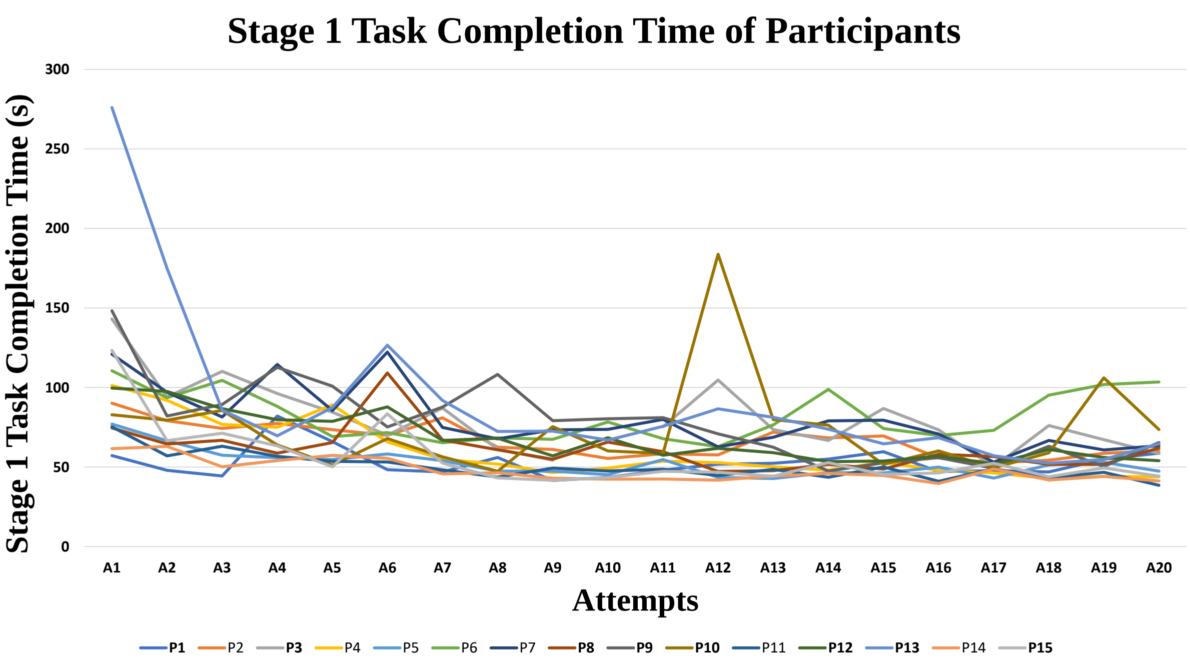

Figure 6.11: Stage 1 Task completion time for all participants

6.5.1.3 Stage 2 Task Completion Time

Stage 2 task completion time is the time it takes to close the gripper and move the jar away from the cooking cabinet towards the table, to a location just above the container in which the content of the jar is to be emptied. The task completion time for stage 2 is provided in table 6.13.

Table 6.13: Stage 2 task completion time for days and corresponding attempts

Day	Attempt	Mean total task completion time			
		Supplementary Feedback		No Supplementary Feedback	
		Mean	Standard Deviation	Mean	Standard Deviation
1	1	86.6423	59.4945	81.7265	32.0290
	2	69.6575	34.9667	57.3508	25.5268
	3	65.4190	25.4916	61.8585	26.6593
	4	64.8100	40.7675	52.4525	19.4100
	5	48.8425	15.9509	44.9935	15.3733
2	1	56.8553	20.8281	58.1544	23.7153
	2	55.8022	25.6619	38.3611	8.8378
	3	54.1624	28.0334	38.5271	10.1279
	4	49.0790	22.5257	35.4152	9.1943
	5	62.5020	40.4951	33.8861	9.3862
3	1	48.7970	25.5266	35.1562	6.1154
	2	63.7930	27.5042	34.8815	6.1054
	3	45.2789	10.6647	36.3224	9.4586
	4	45.7471	16.9233	42.7524	20.8552
	5	38.8274	16.1154	41.9122	10.0766
4	1	57.1582	32.0002	40.5238	9.7764
	2	40.6648	10.1028	35.0531	8.7590
	3	40.4207	12.8675	31.7626	5.4122
	4	43.6913	21.7206	32.6817	4.0365
	5	38.6104	5.5682	32.9692	5.5434

Table 6.13 shows the task completion time for stage 2 of the task for participants with and without supplementary feedback.

Mauchly's Test of Sphericity indicated that the assumption of sphericity has not been violated (assumption met, $p > 0.05$) for days ($\chi^2(5) = 9.650$, $p = 0.089$) and for attempts ($\chi^2(9) = 10.258$, $p = 0.345$).

There was significant main effect of the day the task was carried out on the task completion time for stage 2, ($F(3,24) = 22.254$, $p < 0.001$, $\eta_p^2 = 0.736$). The effect of task attempt on the task completion time for stage 2 was also found to be significant ($F(4,32) = 15.875$, $p < 0.001$, $\eta_p^2 = 0.665$). The interaction days and attempt ($F(12,96) = 4.205$, $p < 0.001$, $\eta_p^2 = 0.345$) was significant. Interactions Days*Robot experience ($p = 0.003$), Attempt*Gaming experience

($p = 0.022$), Days*Attempts*Supplementary Feedback ($p = 0.009$), Days*Attempts*Gaming experience ($p = 0.015$), Games*Attempts*Supplementary Feedback*Gaming Experience ($p = 0.010$) were all significant.

The test of between subject effect showed significant effect for supplementary feedback ($F(1,8) = 6.762$, $p = 0.032$), Gaming Experience ($F(1,8) = 9.859$, $p = 0.014$), and Supplementary Feedback*Gaming Experience ($F(1,8) = 7.007$, $p = 0.028$).

Table 6.14 shows the estimated marginal means of the time taken to complete state 2 of the task.

Table 6.14: Estimated marginal means for stage 2 task completion time

	Supplementary Feedback		Gaming Experience (GE)		Robot Experience (RE)	
	No Supplementary Feedback	Supplementary Feedback Used	No GE	Has GE	No RE	Has RE
Mean task completion time (seconds) for stage 2	68.223	69.465	82.002	62.265	74.102	58.327

Pairwise comparison of task completion time for stage 2 (S2TCT) between participants with supplementary feedback and without supplementary feedback was not significant (p=0.056). Pairwise comparison of S2TCT for gaming experience was significant ($p = 0.002$). Likewise, pairwise comparison of S2TCT for robot experience was also significant ($p = 0.003$).

Table 6.15 shows the estimated daily marginal means for S2TCT.

Table 6.15: Daily estimated marginal means for S2TCT

Days	Mean S2TCT (seconds)
1	67.816
2	50.559
3	45.233
4	40.822

Pairwise comparison of daily S2TCT between day 1 and days 2 ($p = 0.008$), 3 ($p = 0.003$), and 4 ($p = 0.001$) were significant. However, comparison between days 2 and 3 was also significant. For each daily attempt, pairwise comparisons between attempt 1 and attempts 3, 4, and 5 were significant.

Figure 6.12 shows the plots of estimated marginal means for S2TCT.

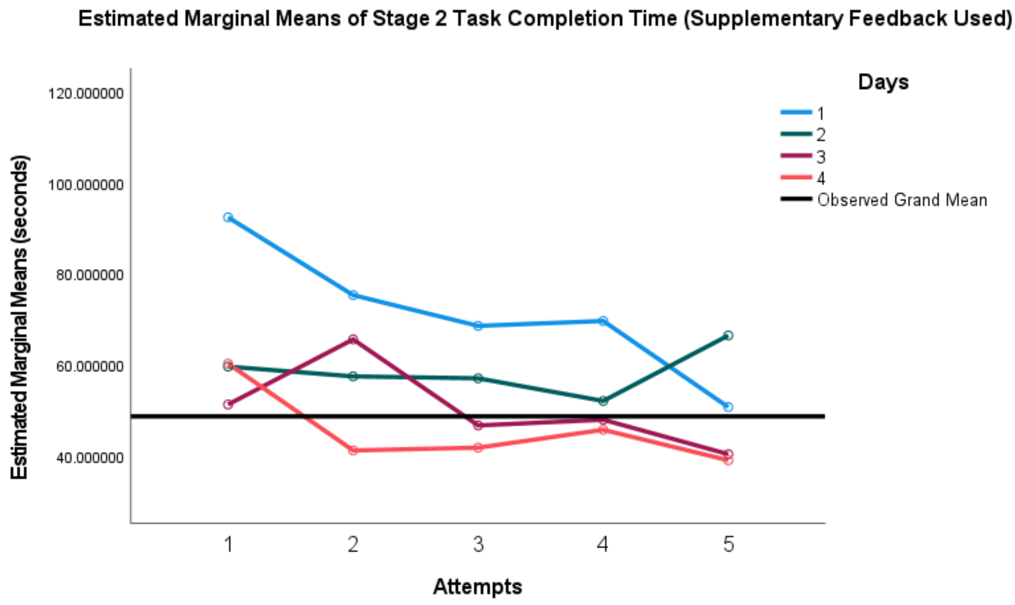

(a)

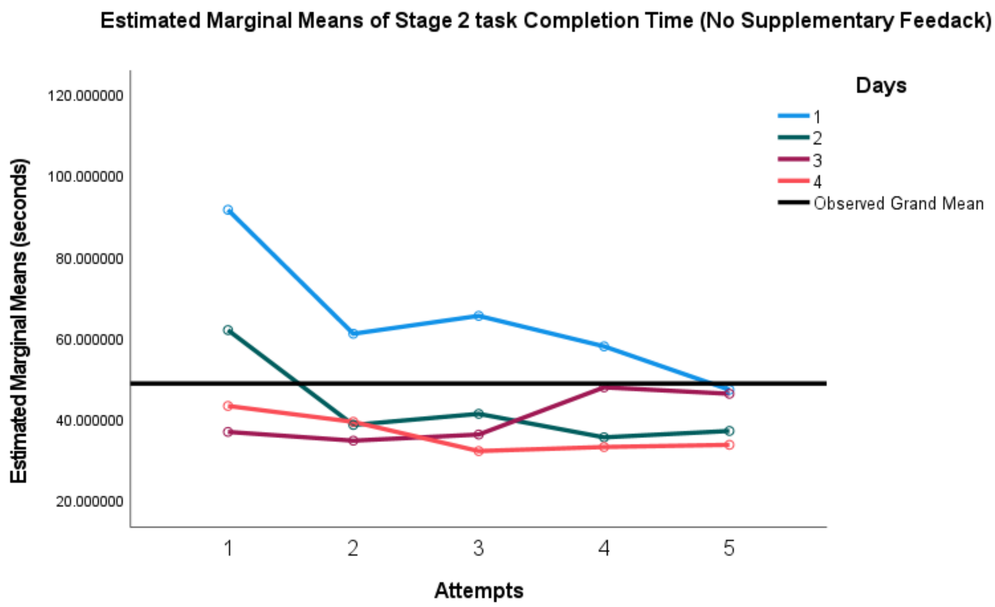

(b)

Figure 6.12: Plots of estimated marginal mean for stage 2 task completion time (a) supplementary feedback used, (b) no supplementary feedback used

Further analysis was carried out on stage 2 task completion time between attempts 5 of all the days. Table 6.16 shows the mean S2CT for attempts 5. Paired samples test shows a significant difference for S2TCT between day 1 and day 4.

Table 6.16: Mean S2TCT for last daily attempts (attempt 5))

Last Daily Attempts	**Mean S2TCT (s)**	**Standard error**
Day 1	46.918	15.182
Day 2	48.194	31.905
Day 3	40.723	12.612
Day 4	35.790	6.088

Table 6.17: Mean S2TCT for last daily attempts (attempt 5) with and without supplementary feedback

Last Daily Attempts	With Supplementary Feedback		Without Supplementary Feedback	
	Mean S2TCT (s)	Standard Deviation	Mean S2TCT (s)	Standard Deviation
Day 1	48.842	15.951	44.994	15.373
Day 2	62.502	40.495	33.886	9.386
Day 3	38.827	16.116	41.912	10.077
Day 4	38.610	5.568	32.969	5.543

Table 6.18: Mean S2TCT for last daily attempts (attempt 5) with and without gaming experience

Last Daily Attempts	Gaming Experience		Without gaming experience	
	Mean S2TCT (s)	Standard Deviation	Mean S2TCT (s)	Standard Deviation
Day 1	43.371	12.801	59.924	18.869
Day 2	35.348	10.555	95.297	42.711
Day 3	36.070	7.345	56.137	18.869
Day 4	34.603	5.879	40.141	5.653

Figure 6.13 shows the plot of S2TCT for participants (from table 6.17 and table 6.18). It shows the difference in S2TCT for participants with and without feedback. Fig. 6.13 also shows the difference in S2TCT for participants with and without prior gaming experience. In fig. 6.14 S2TCT plots for all participants are shown. 'A' represents attempts and 'P' represents participant. Participants with feedback appear in bold.

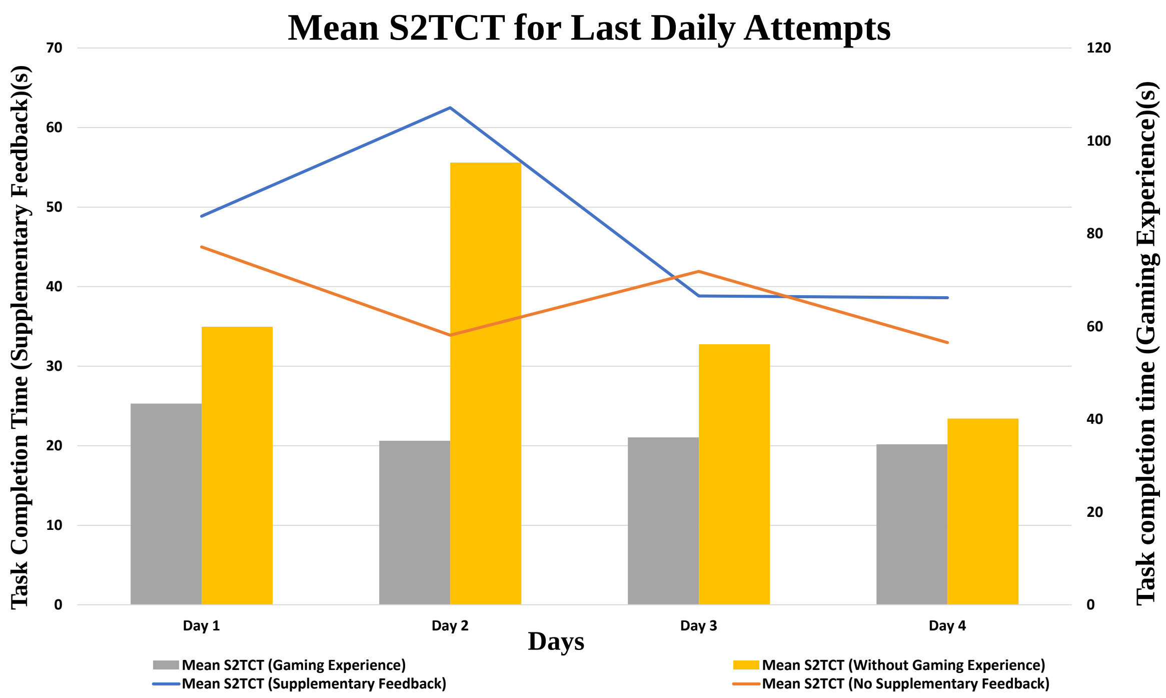

Figure 6.13: Stage 2 Task completion time for last daily attempts (Attempt 5)

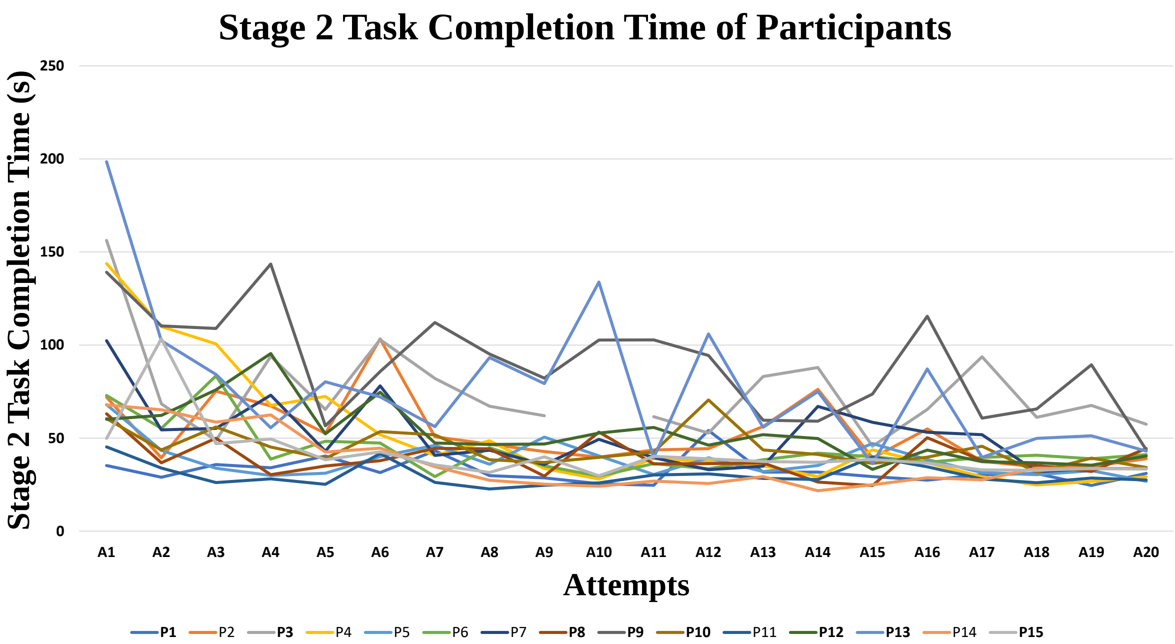

Figure 6.14: Stage 2 Task completion time for all participants

6.5.1.4 Stage 3 Task Completion Time

Stage 3 task completion time is the time it takes to empty the content of the jar into a bowl. This involves translation and rotation of the gripper. The task completion time for stage 3 is provided in table 6.19.

Table 6.19: Stage 3 task completion time for days and corresponding attempts

Day	Attempt	Mean total task completion time			
		Supplementary Feedback		No Supplementary Feedback	
		Mean	Standard Deviation	Mean	Standard Deviation
1	1	33.6914	10.8143	34.5920	10.9519
	2	30.9387	10.2386	27.7393	9.2662
	3	27.2528	6.3865	53.1553	66.4633
	4	23.7724	8.1626	28.8613	9.3433
	5	29.2504	8.106	27.7133	7.3898
2	1	32.4339	14.0703	23.3953	6.0778
	2	29.8102	16.000	23.7292	4.7142
	3	26.4194	9.0920	22.8983	5.4532
	4	23.4890	8.1426	21.1573	2.9296
	5	28.5939	16.0956	21.5529	3.4889
3	1	22.9842	7.2372	19.3659	4.1782
	2	22.4724	4.9933	22.7438	6.3628
	3	21.3429	4.7467	21.5990	4.7467
	4	20.0149	3.8699	24.0604	8.2063
	5	19.9475	2.6861	19.9624	7.7269
4	1	22.1775	3.2942	24.6504	10.3445
	2	23.5248	10.2315	20.7518	4.1145
	3	20.8490	3.1693	23.0754	7.0915
	4	20.9559	2.9559	23.9116	10.6370
	5	21.6289	3.3432	21.5753	6.1793

Table 6.19 shows the task completion time for stage 3 of the task for participants with and without supplementary feedback.

Mauchly's Test of Sphericity indicated that the assumption of sphericity was violated (for assumption to be met, p > 0.05) for days ($chi^2(5) = 14.464$, $p = 0.014$) and for attempts ($chi^2(9) = 46.388$, $p < 0.001$). Since $\epsilon < 0.75$, we report the Greenhouse-Geisser corrected results. There was significant main effect of the day the task was carried out on the task completion time for stage 3, ($F(1.513, 12.104) = 8.649$, $p = 0.007$, $\eta_p^2 = 0.519$). The effect of task attempt on the task completion time for stage 3 was however found not to be significant ($F(1.162, 32) = 0.825$, $p = 0.405$, $\eta_p^2 = 0.093$).

The test of between subject effect showed significant effect for Robot Experience ($F(1,8) =$

21.007, $p = 0.002$), Supplementary Feedback*Gaming Experience ($F(1,8) = 21.007$, $p = 0.013$), Supplementary Feedback*Robot Experience ($F(1,8) = 5.843$, $p = 0.042$).

Table 6.20 shows the estimated marginal means of the time taken to complete state 3 of the task.

Table 6.20: Estimated marginal means for stage 3 task completion time

	Supplementary Feedback		Gaming Experience (GE)		Robot Experience (RE)	
	No Supplementary Feedback	Supplementary Feedback Used	No GE	Has GE	No RE	Has RE
Mean task completion time (seconds) for stage 3	26.642	25.775	27.222	25.702	28.960	20.706

Pairwise comparison of task completion time for stage 3 (S3TCT) between participants with supplementary feedback and without supplementary feedback was not significant ($p = 0.680$). Pairwise comparison of S3TCT for gaming experience was also not significant ($p = 0.542$). Likewise, pairwise comparison of S3TCT for robot experience was significant ($p = 0.002$).

Table 6.21 shows the estimated daily marginal means for S3TCT.

Table 6.21: Daily estimated marginal means for S3TCT

Days	Mean S3TCT (seconds)
1	33.037
2	26.513
3	22.353
4	22.932

Pairwise comparison of daily S3TCT between day 1 and days 3 ($p = 0.027$), and 4 ($p = 0.011$) were significant.

Figure 6.15 shows the plots of estimated marginal means for S3TCT.

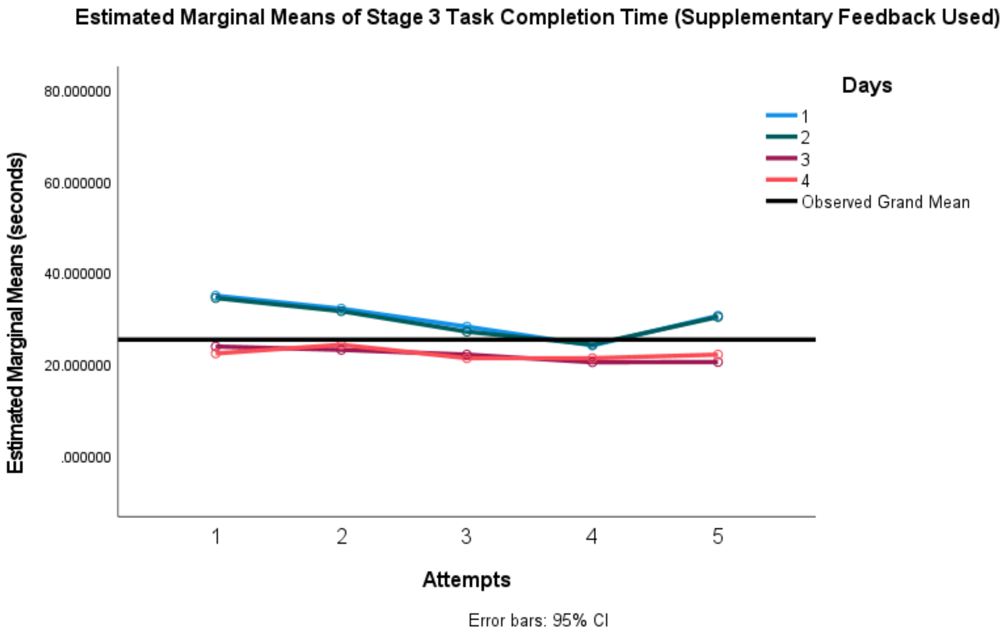

(a)

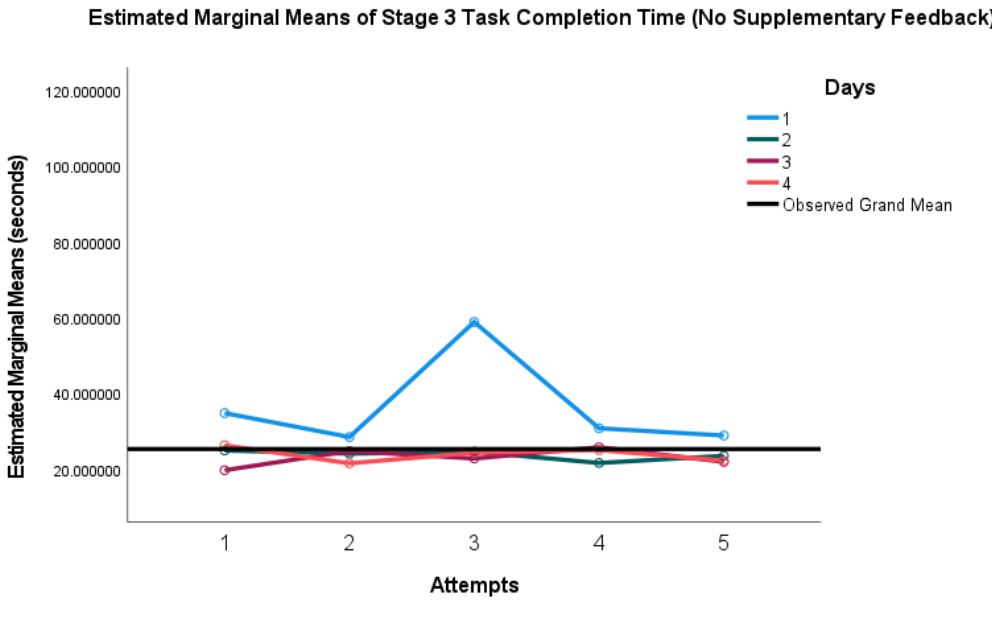

(b)

Figure 6.15: Plots of estimated marginal mean for stage 3 task completion time (a) supplementary feedback used, (b) No supplementary feedback used

In order to understand the learning process, we examined the changes in S3TCT for the final attempts of each day as participants carried out the task. Paired samples test shows a significant difference for S3TCT between day 1 and day 3 ($p < 0.001$), as well as for day 1 and day

4 ($p = 0.006$).

Table 6.22: Mean S3TCT for last daily attempts (attempt 5))

Last Daily Attempts	**Mean S3TCT (s)**	**Standard error**
Day 1	28.482	7.495
Day 2	25.073	11.770
Day 3	20.021	5.362
Day 4	21.791	4.657

Table 6.23: Mean S3TCT for last daily attempts (attempt 5) with and without supplementary feedback

Last Daily Attempts	With Supplementary Feedback		Without Supplementary Feedback	
	Mean S3TCT (s)	Standard Deviation	Mean S3TCT (s)	Standard Deviation
Day 1	29.250	8.106	27.713	7.390
Day 2	28.594	16.096	21.553	3.489
Day 3	19.947	2.686	19.962	7.727
Day 4	21.629	3.343	21.575	6.179

Table 6.24: Mean S3TCT for last daily attempts (attempt 5) with and without gaming experience

Last Daily Attempts	Gaming Experience		Without gaming experience	
	Mean S3TCT (s)	Standard Deviation	Mean S3TCT (s)	Standard Deviation
Day 1	26.698	7.007	35.024	6.157
Day 2	23.730	12.668	29.997	7.197
Day 3	19.187	6.031	22.770	1.927
Day 4	21.524	5.243	21.885	3.240

Figure 6.16 shows the plot of S3TCT for participants (from table 6.23 and table 6.24). It shows the difference in S3TCT for participants with and feedback. Figure 6.16 also shows the difference in S3TCT for participants with and without prior gaming experience. In figure 6.17 S3TCT plots for all participants are shown. 'A' represents attempts and 'P' represents participant. Participants with supplementary feedback appear in bold.

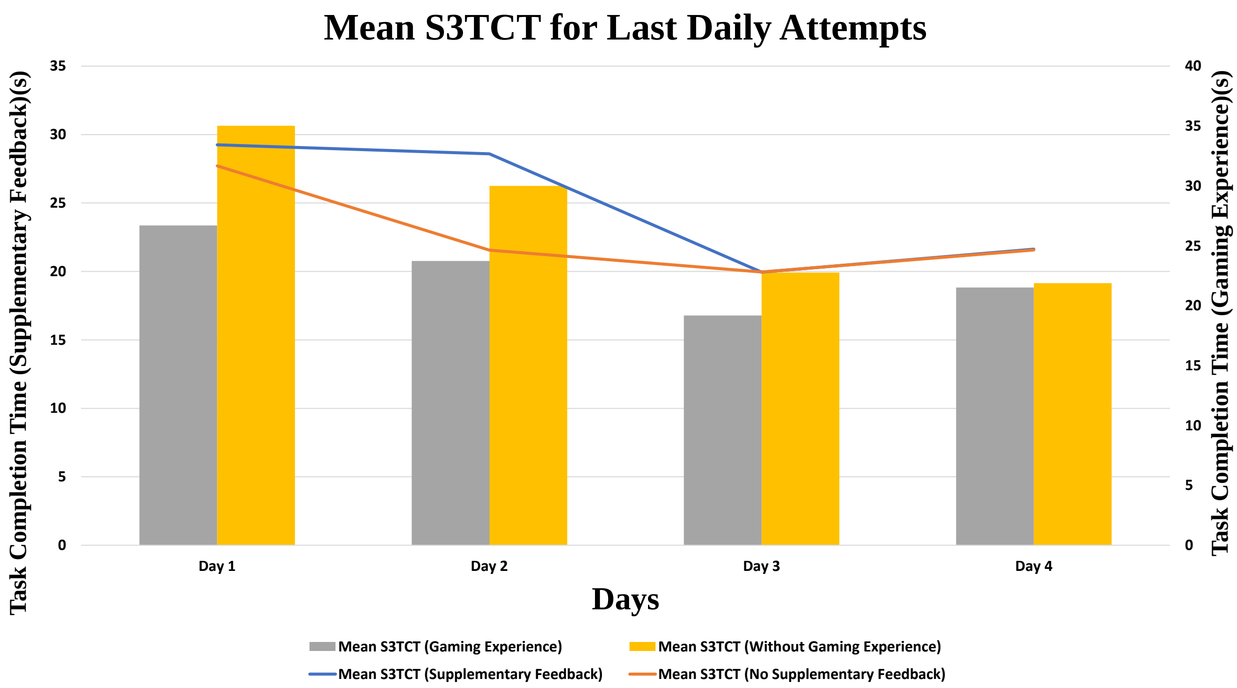

Figure 6.16: Stage 3 Task completion time for last daily attempts (Attempt 5)

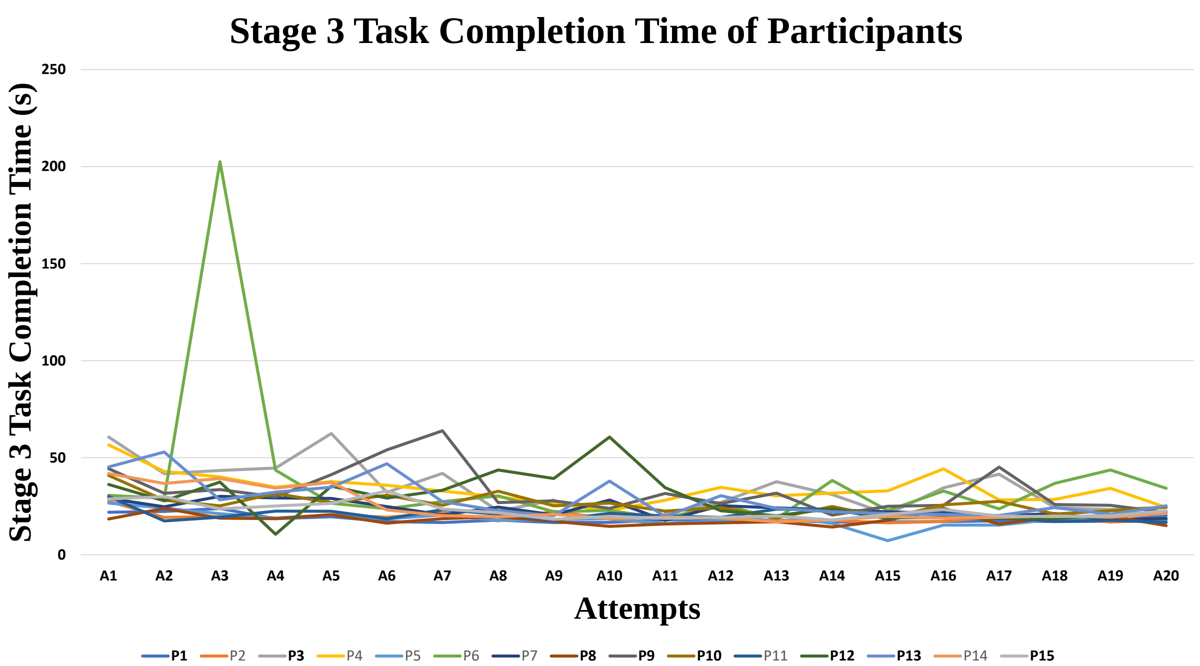

Figure 6.17: Stage 3 Task completion time for all participants

6.5.1.5 Stage 4 Task Completion Time

Stage 4 task completion time is the time it takes to return the jar back to its original pick-up location. The task completion time for stage 4 is provided in table 6.25.

Table 6.25: Stage 4 task completion time for days and corresponding attempts

Day	Attempt	Mean total task completion time			
		Supplementary Feedback		No Supplementary Feedback	
		Mean	Standard Deviation	Mean	Standard Deviation
1	1	50.0729	16.8273	68.2924	38.4258
	2	55.8396	23.9445	60.8950	20.2969
	3	47.6961	20.4711	49.7039	17.3005
	4	39.5153	23.6358	47.4267	14.9290
	5	41.9324	15.5253	52.0410	20.3260
2	1	54.5851	29.1771	43.2379	13.9976
	2	42.9181	16.6192	42.5122	11.1405
	3	38.2857	10.3259	41.1659	14.3198
	4	35.2449	7.8187	43.0753	14.9672
	5	39.4697	12.9430	38.6019	11.5430
3	1	43.2512	31.4955	36.0996	9.6443
	2	40.3257	13.0153	35.5162	8.5031
	3	34.0606	6.5265	37.1602	11.0086
	4	33.5350	7.8096	35.8125	7.0114
	5	32.2604	5.6339	38.1690	10.6444
4	1	41.9716	18.5629	33.9736	6.2402
	2	40.7281	16.5678	34.3403	9.4312
	3	39.7622	9.9241	32.2391	6.8962
	4	34.8685	8.0267	31.2124	8.7789
	5	32.6867	4.8071	33.2338	5.3701

Table 6.25 shows the task completion time for stage 4 of the task for participants with and without supplementary feedback.

Mauchly's Test of Sphericity indicated that the assumption of sphericity was violated for days ($chi^2(5) = 15.475$, $p = 0.009$) and for attempts ($\chi^2(9) = 19.851$, $p = 0.022$). Since $\epsilon < 0.75$, we report the Greenhouse-Geisser corrected results.

There was significant main effect of the day the task was carried out on the task completion time for stage 4, ($F(1.797, 14.379) = 13.815$, $p < 0.001, \eta_p^2 = 0.633$). The effect of task attempt on the task completion time for stage 4 was also found to be significant ($F(1.678, 13.426) = 7.628$, $p = 0.008, \eta_p^2 = 0.488$). Interaction Days*Attempt*Supplementary Feedback was significant ($p = 0.037$).

The test of between subject effect showed no significant effect of the factors (Feedback, Gaming

Experience, Robot Experience, and their interactions).

Table 6.26 shows the estimated marginal means of the time taken to complete state 4 of the task.

Table 6.26: Estimated marginal means for stage 4 task completion time

	Additional Feedback		Gaming Experience (GE)		Robot Experience (RE)	
	No Supplementary Feedback	Supplementary Feedback Used	No GE	Has GE	No RE	Has RE
Mean task completion time (seconds) for stage 4	43.760	41.450	47.912	39.951	45.188	37.438

Pairwise comparison of task completion time for stage 4 (S4TCT) between participants with supplementary feedback and without supplementary feedback was not significant (p=0.705). Pairwise comparison of S4TCT for gaming experience was also not significant ($p = 0.283$). Likewise, pairwise comparison of S4TCT for robot experience was not significant ($p = 0.198$).

Table 6.27 shows the estimated daily marginal means for S4TCT.

Table 6.27: Daily estimated marginal means for S4TCT

Days	Mean S3TCT (seconds)
1	54.538
2	43.268
3	37.134
4	35.480

Pairwise comparison of daily S4TCT between day 1 and days 3 ($p = 0.006$), and 4 ($p = 0.002$) were significant.

Figure 6.18 shows the plots of estimated marginal means for S4TCT.

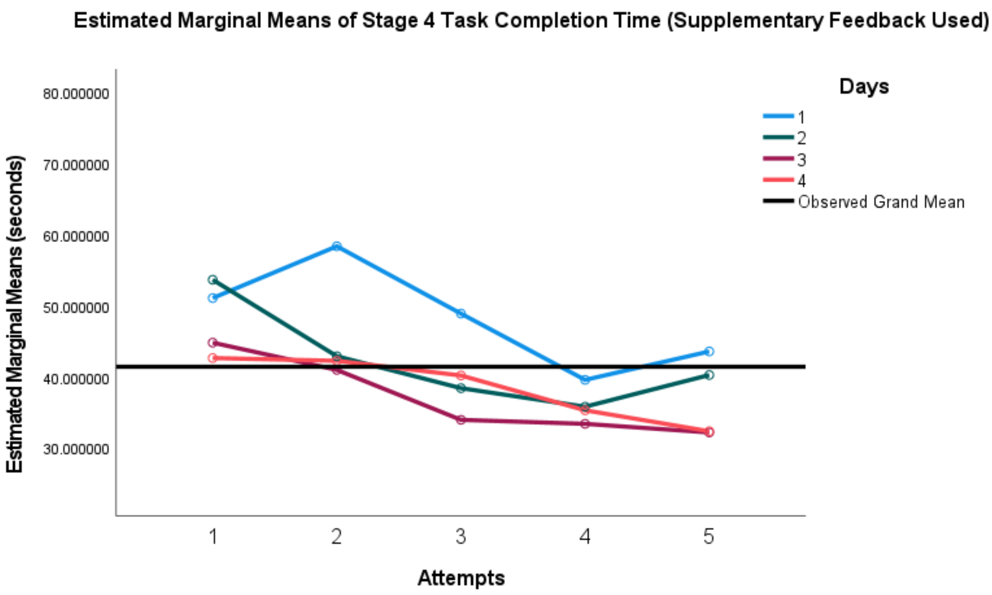

(a)

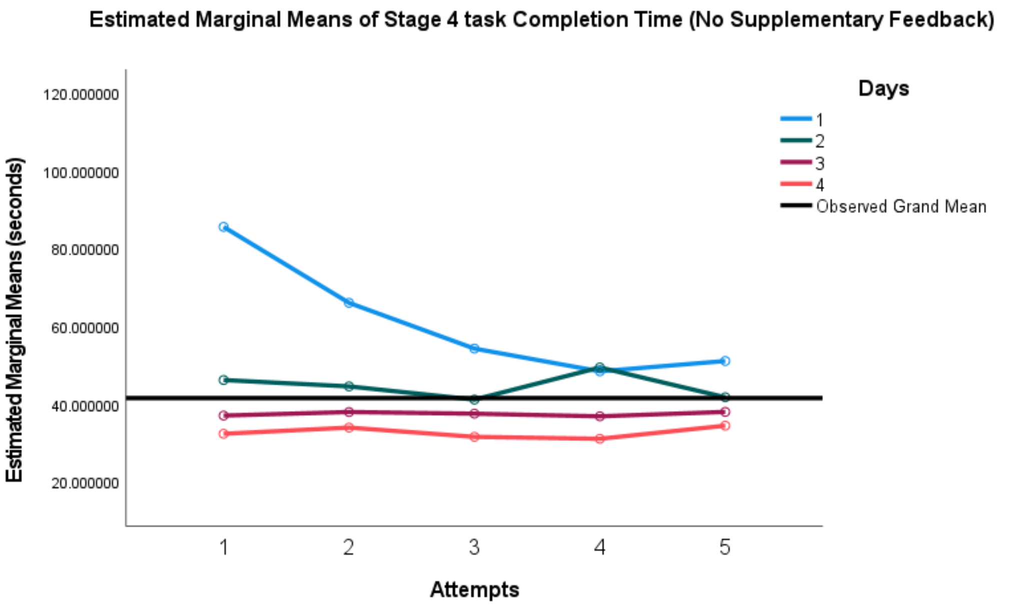

(b)

Figure 6.18: Plots of estimated marginal mean for stage 4 task completion time (a) supplementary feedback used, (b) No supplementary feedback Used

To fully understand changes in the values of S4TCT over the days examined, we further examined the changes in each daily last attempt. Paired samples test shows a significant difference for S4TCT between day 1 and day 3 ($p < 0.001$), as well as for day 1 and day 4 ($p = 0.006$). Table

6.28 shows the mean S4TCT values for final attempts of each day the study was carried out.

Table 6.28: Mean S4TCT for last daily attempts (attempt 5))

Last Daily Attempts	**Mean S4TCT (s)**	**Standard error**
Day 1	46.987	18.150
Day 2	39.035	11.790
Day 3	35.547	8.517
Day 4	33.525	5.199

Table 6.29: Mean S4TCT for last daily attempts (attempt 5) with and without supplementary feedback

Last Daily Attempts	With Supplementary Feedback		Without Supplementary Feedback	
	Mean S4TCT (s)	Standard Deviation	Mean S4TCT (s)	Standard Deviation
Day 1	41.932	15.525	52.041	20.326
Day 2	39.468	12.943	38.602	11.543
Day 3	32.260	5.633	38.169	10.644
Day 4	32.696	4.807	33.234	5.370

Table 6.30: Mean S4TCT for last daily attempts (attempt 5) with and without gaming experience

Last Daily Attempts	Gaming Experience		Without gaming experience	
	Mean S4TCT (s)	Standard Deviation	Mean S4TCT (s)	Standard Deviation
Day 1	46.578	19.619	48.485	14.578
Day 2	35.804	10.386	50.883	9.814
Day 3	35.841	9.710	32.917	3.843
Day 4	33.436	5.276	31.239	3.386

Figure 6.19 shows the plot of S4TCT for participants (from table 6.29 and table 6.30). It shows the difference in S4TCT for participants with and without feedback. Figure 6.19 also shows the difference in S4TCT for participants with and without prior gaming experience. In figure 6.20, S4TCT plots for all participants are shown. 'A' represents attempts and 'P' represents participant. Participants with feedback appear in bold.

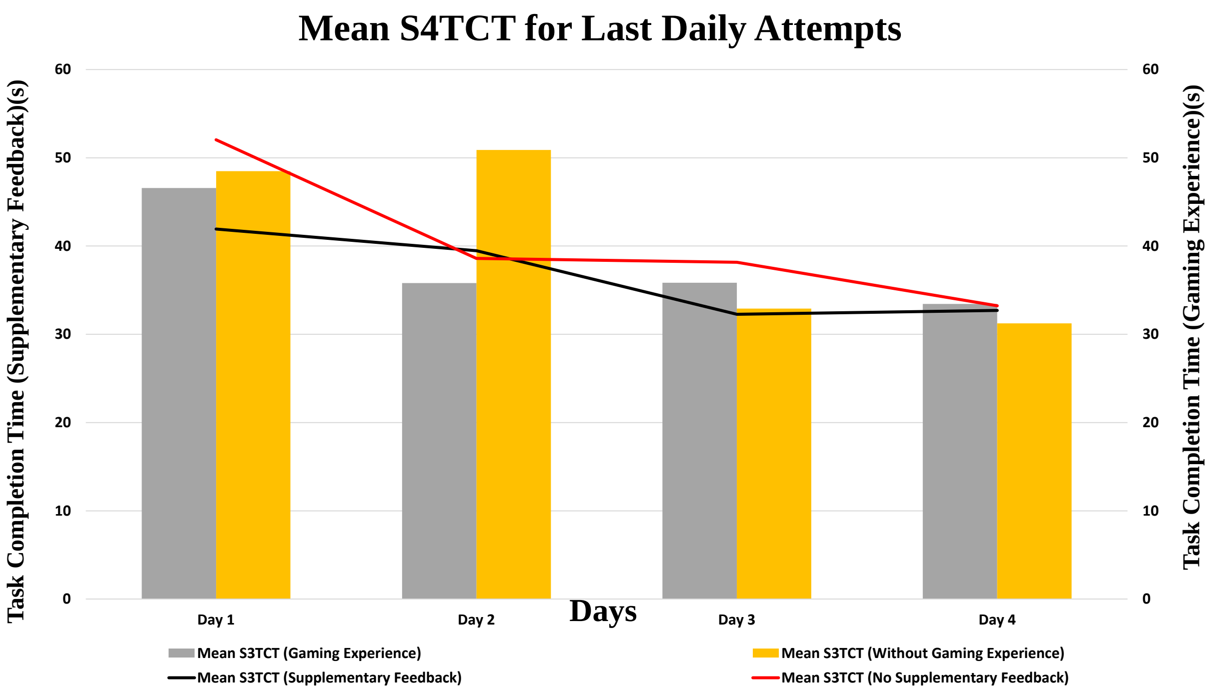

Figure 6.19: Stage 4 Task completion time for daily attempts 5

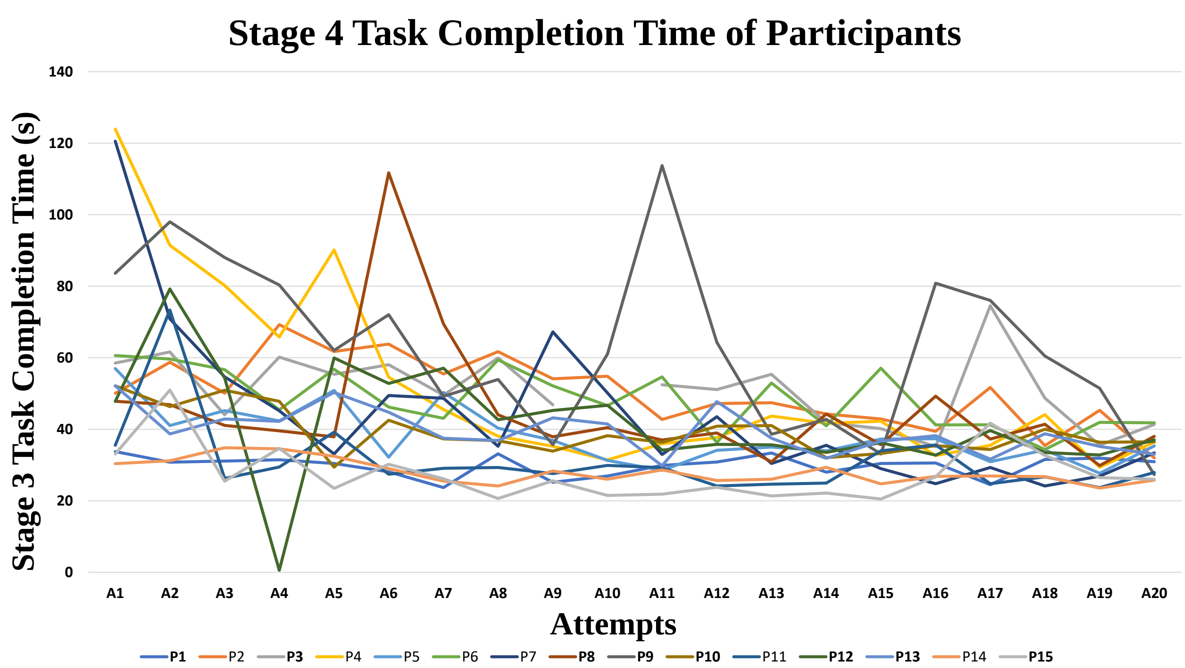

Figure 6.20: Stage 3 Task completion time for all participants

6.5.2 Gripper Orientation

In order to achieve good grasp, the orientation of the gripper needs to be vertically aligned with the jar to be grasped. The deviation of the gripper's vertically aligned position to the left or right is recorded on the scale of 1 to 50. Higher values mean that the gripper is farther away from the 'vertically aligned' position The focus here is the stage 1 gripper orientation, which is the orientation of the gripper just before grasp.

Table 6.31: Stage 1 gripper orientation deviation for days and corresponding attempts

Day	Attempt	Gripper Orientation Deviation			
		Supplementary Feedback		No Supplementary Feedback	
		Mean	Standard Deviation	Mean	Standard Deviation
1	1	4.3267	4.8672	3.4292	3.6950
	2	3.8140	1.9269	13.3821	10.3388
	3	4.4227	3.7965	5.3752	3.6157
	4	7.1213	10.8580	5.8978	5.9027
	5	6.1682	5.3849	4.0499	2.4227
2	1	3.5802	3.5784	10.9231	12.3885
	2	6.4954	4.8155	4.9404	3.8349
	3	8.9825	10.5774	11.8410	10.7076
	4	6.6407	7.1338	8.6330	9.6212
	5	6.9383	6.4481	14.9677	13.7167
3	1	6.3507	3.0297	6.4943	6.6244
	2	9.7236	8.3312	11.6139	17.2995
	3	2.8222	2.2879	3.6453	2.0774
	4	5.3369	5.5497	10.5127	13.1274
	5	9.5585	7.7834	7.6085	4.5030
4	1	6.2202	5.7024	4.8515	3.6323
	2	4.5262	3.3400	6.2162	4.9425
	3	10.5072	8.9972	6.2592	4.2073
	4	3.6113	2.6780	7.2048	7.9797
	5	7.2306	4.3396	5.7106	5.5344

Table 6.31 shows the gripper orientation deviations for participants with and without supplementary feedback. Higher values imply wrong orientation before grasp.

Mauchly's Test of Sphericity indicated that the assumption of sphericity was not violated for days ($\chi^2(5) = 3.044$, $p = 0.696$) and for attempts ($\chi^2(9) = 10.687$, $p = 0.313$).

Tests of within subject effects showed no significant effect of any of the independent variables (attempts and days) or their interactions. Likewise, test of between-subjects effects showed no significant effect of any of the factors (supplementary feedback, gaming experience, and robot experience).

Further analysis was carried out to compare the accuracy of gripper orientation for all final daily attempts. Table 6.32 shows the mean gripper deviation values. Paired samples t test reveals no significant difference between mean gripper deviation values for each of the attempts examined.

Table 6.32: Mean gripper orientation deviation of last daily attempts (attempt 5) for stage 1

Last Daily Attempts	**Mean Gripper deviation (s)**	**Standard error**
Day 1	5.109	4.159
Day 2	10.953	11.107
Day 3	8.465	5.984
Day 4	6.718	4.7637

Table 6.33: Stage 1 gripper deviation values for last daily attempts (attempt 5) with and without supplementary feedback

Last Daily Attempts	With Supplementary Feedback		Without Supplementary Feedback	
	Gripper deviation	Standard Deviation	Gripper deviation	Standard Deviation
Day 1	6.168	5.3848	4.050	2.423
Day 2	6.938	6.448	14.968	13.717
Day 3	9.559	7.783	7.608	4.503
Day 4	7.231	4.340	5.710	5.534

Table 6.34: Stage 1 gripper deviation values for last daily attempts (attempt 5) with and without gaming experience

Last Daily Attempts	Gaming Experience		Without gaming experience	
	Gripper Deviation	Standard Deviation	Gripper Deviation	Standard Deviation
Day 1	4.952	4.63	5.684	2.223
Day 2	11.532	12.219	8.826	6.838
Day 3	8.254	6.243	9.792	7.177
Day 4	6.797	5.450	5.274	1.080

Figure 6.21 shows the plot of gripper orientation deviations. There was no significant difference in gripper orientation deviation values between participants with feedback and participants without feedback. This is due to the possibility extracting gripper orientation visually from the camera view. This is peculiar to this study as a result of the camera view provided.

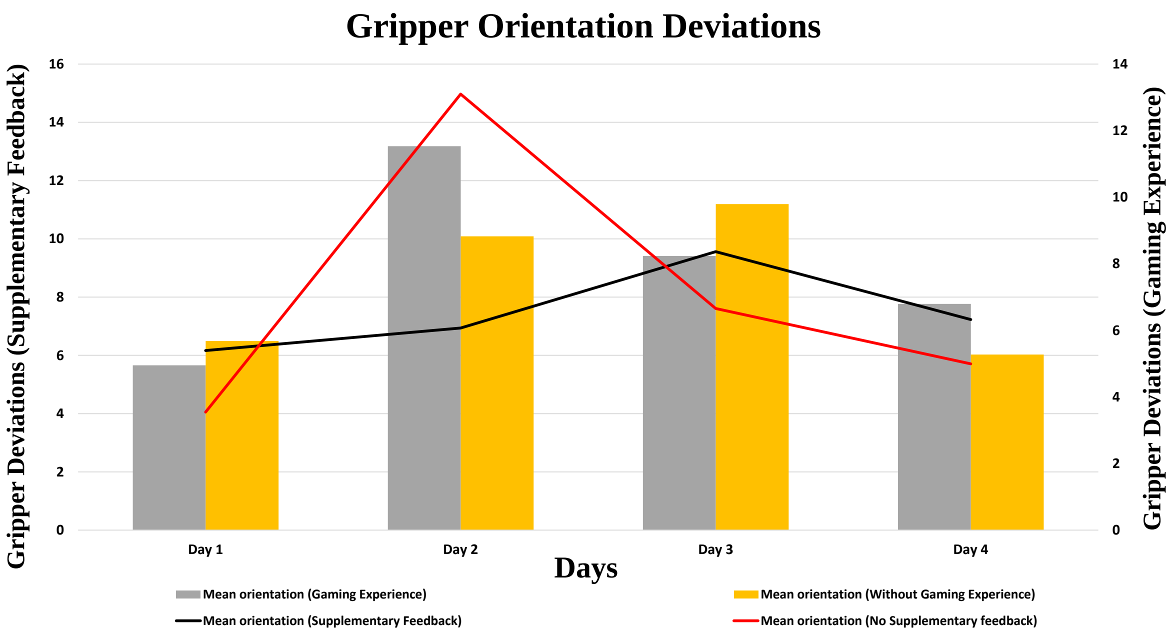

Figure 6.21: Stage 1 gripper orientation deviations for daily attempts 5

6.5.3 Gripper Proximity

To prevent participants from driving the robot into horizontal surfaces, a proximity sensor was attached to the robot gripper. As participants carried out the task, gripper proximity was measured at two stages of the task: stage 1 and stage 2. Stage 1 of the task involves positioning the gripper such that participants are about to grasp the jar. Gripper proximity in stage one was therefore measured against the cooking surface.

In stage 2 of the task, participants control the robot to a position close enough to the bowl. This also involves lowering the gripper close enough to the bowl, hence the need to measure the gripper proximity in stage 2.

6.5.3.1 Stage 1 Gripper Proximity

Table 6.35 shows the gripper proximities for participants with and without additional feedback. The gripper needs to be positioned such that it is close enough to the table for good grasp but not too close.

Mauchly's Test of Sphericity indicated that the assumption of sphericity was not violated (p> 0.05, sphericity assumed) for days ($\chi^2(5) = 3.512$, $p = 0.625$) and for attempts ($\chi^2(9) = 3.862$, $p = 0.924$).

Tests of within subject effects showed significant effect of the day the task was carried out, ($F(3,24) = 10.637$, $p < 0.001$, $\eta_p^2 = 0.571$). The effect of attempt on proximity was not significant, ($F(4,32) = 2.156$, $p = 0.097$, $\eta_p^2 = 0.212$). Interaction Days*Gaming Experience ($p = 0.012$), Attempts*Robot (p = 0.027) were significant. Test of between-subjects effects showed no significant effect of any of the factors.

Table 6.35: Stage 1 gripper proximity for days and corresponding attempts

Day	Attempt	Stage 1 Gripper Proximity (cm)			
		Supplementary Feedback		No Supplementary Feedback	
		Mean	Standard Deviation	Mean	Standard Deviation
1	1	3.7143	1.3801	4.4286	1.9024
	2	3.2857	1.3801	4.2857	1.1127
	3	3.4286	1.1339	5.5714	2.5072
	4	3.4286	1.3973	3.8571	2.4103
	5	3.4286	1.7183	3.7143	1.9761
2	1	3.4286	0.9759	4.2857	1.3801
	2	3.1429	1.3452	5.2857	3.2514
	3	3.8571	1.4639	5.0000	2.0000
	4	3.0000	1.1547	5.0000	1.9149
	5	3.8571	1.6762	4.8571	2.2678
3	1	4.0000	1.1547	4.5714	1.2724
	2	4.2857	1.1127	6.2857	2.1381
	3	4.2857	1.9761	5.1429	2.7946
	4	3.8571	1.5736	4.7143	2.6904
	5	3.0000	1.0000	4.5714	2.2254
4	1	3.7143	1.2536	3.7500	0.9574
	2	4.2857	0.9512	4.5714	1.9881
	3	3.7143	1.3801	6.1429	1.8645
	4	4.4286	1.5119	5.8571	1.6762
	5	4.1429	1.2150	5.1429	2.4103

Table 6.36 shows the estimated marginal means of gripper proximity for stage 1 of the task (S1Proximity).

Table 6.36: Daily estimated marginal means for stage 1 gripper proximity

Days	Mean S1 Proximity (cm)
1	3.958
2	4.408
3	4.708
4	4.994

Pairwise comparison of daily S1Orientation between day 1 and day 4 was significant (p = 0.002).

Figure 6.22 shows the plot of estimated marginal means of daily gripper proximity for stage 1 of the task.

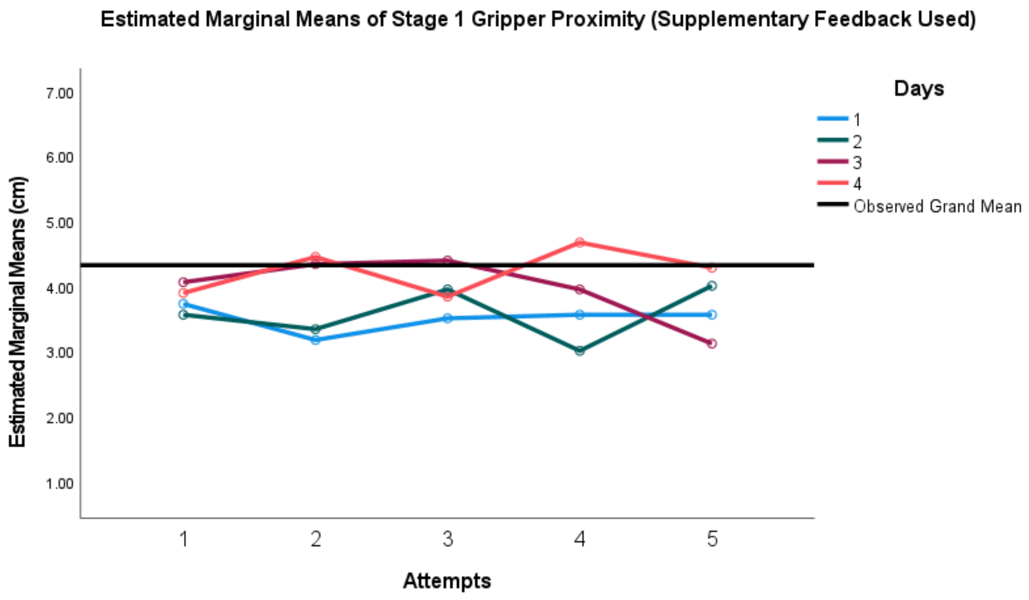

(a)

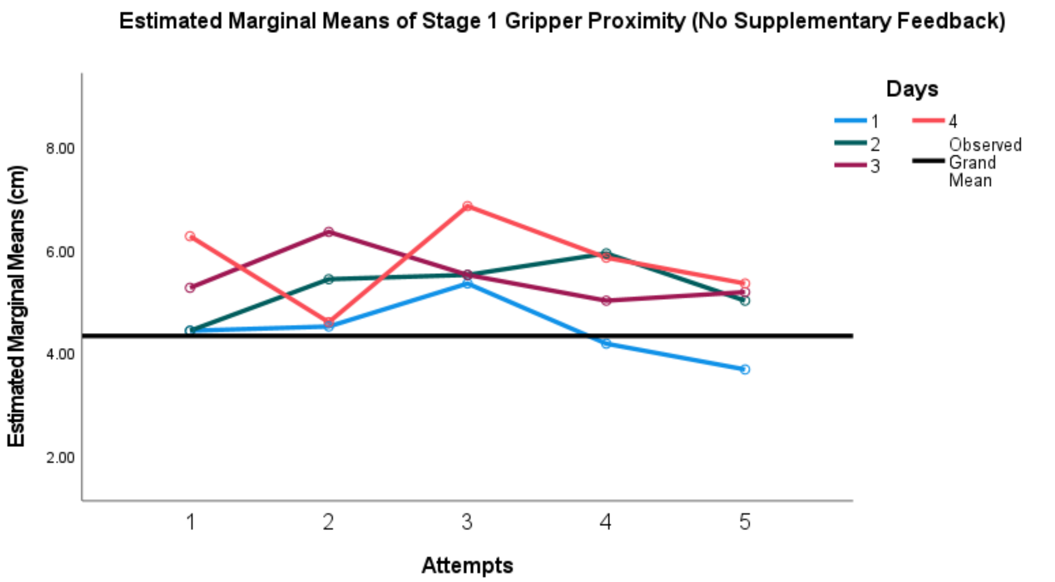

(b)

Figure 6.22: Plots of estimated marginal mean for stage 1 gripper proximity (a) supplementary feedback Used, (b) no supplementary feedback Used

Even though the effect of feedback was not significant due to the information gathered via the supplied camera views, the observed marginal mean in figure 6.22 shows that participants had relatively lower proximity values when supplementary feedback was used. The use of supplementary feedback allows the gripper to be moved close enough to the jar to be picked without driving the gripper into the cooking surface.

In order to understand the effect of learning (as a result of repeating the task), we examined the changes in gripper proximity values for each daily fifth attempt. Table 6.37 shows the mean gripper proximity values.

Table 6.37: Stage 1 gripper proximity values of last daily attempts (attempt 5) for stage 1

Last Daily Attempts	**Stage 1 Gripper proximity (cm)**	**Standard error**
Day 1	3.5714	1.7852
Day 2	4.3571	1.9848
Day 3	3.8667	1.8074
Day 4	4.7333	1.8697

Table 6.38: Stage 1 gripper proximity values for last daily attempts (attempt 5) with and without additional feedback

Last Daily Attempts	With Supplementary Feedback		Without Supplementary Feedback	
	S1 Gripper Proximity	Standard Deviation	S1 Gripper Proximity	Standard Deviation
Day 1	3.4286	1.7183	3.7143	1.9761
Day 2	3.8571	1.6762	4.8571	2.2678
Day 3	3.000	1.000	4.5714	2.2254
Day 4	4.1429	1.2150	5.1429	2.4103

Table 6.39: Stage 1 gripper proximity values for last daily attempts (attempt 5) with and without gaming experience

Last Daily Attempts	Gaming Experience		Without gaming experience	
	S1 Gripper Proximity	Standard Deviation	S1 Gripper Proximity	Standard Deviation
Day 1	3.6364	2.0136	3.3333	0.5774
Day 2	4.6364	2.1574	3.3333	0.5774
Day 3	3.7273	1.9540	4.0000	1.7321
Day 4	4.6364	2.1574	4.6667	0.5774

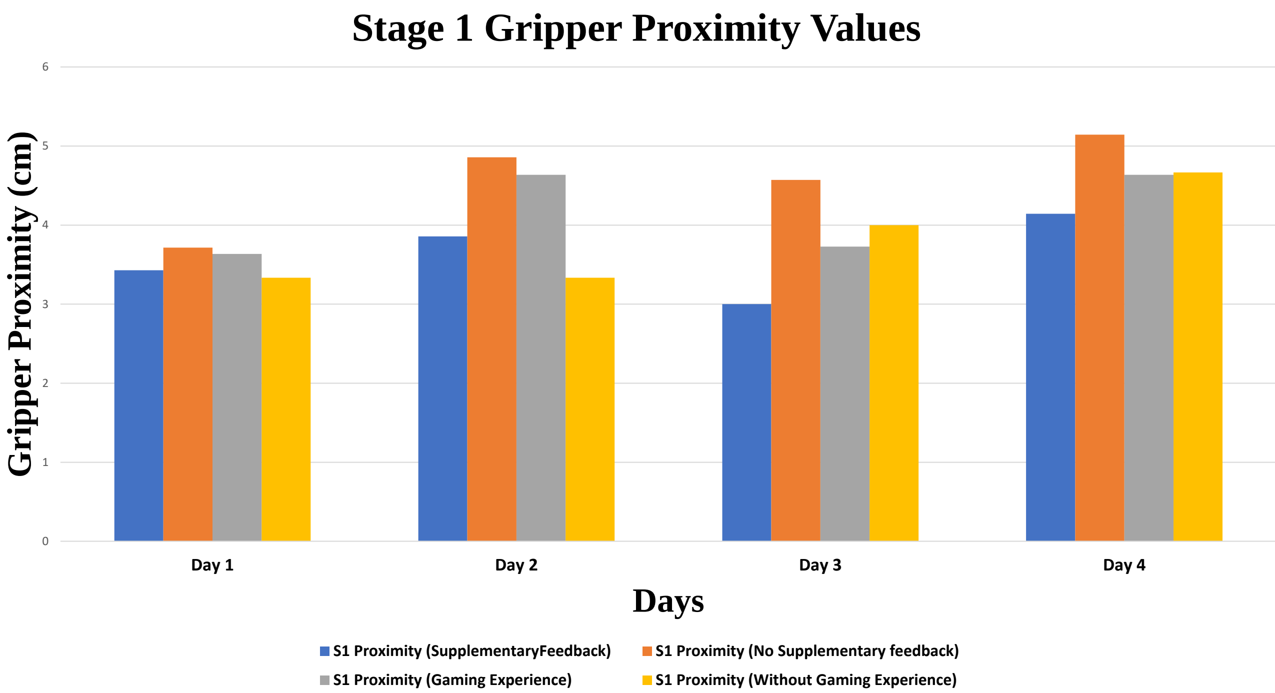

Figure 6.23: Stage 1 gripper proximity values for last daily attempts

6.5.3.2 Stage 2 Gripper Proximity

Moving the gripper close enough to the table before emptying the content may prevent spillage. Table 6.40 shows the mean distance of the gripper to surfaces before the content was emptied.

Table 6.40 shows the gripper proximity value for participants with and without supplementary feedback. The gripper needs to be positioned such that it is close enough to the table for good grasp but not too close.

Mauchly's Test of Sphericity indicated that the assumption of sphericity was not violated ($p > 0.05$, sphericity assumed) for days ($\chi^2(5) = 8.392$, $p = 0.140$) and for attempts ($\chi^2(9) = 13.524$, $p = 0.152$).

Tests of within subject effects showed no significant effect of the independent variables (days and attempts) on the gripper proximity. Test of between-subjects effects however showed significant effect of supplementary feedback on gripper proximity.

Table 6.40: Stage 2 gripper proximity for days and corresponding attempts

Day	Attempt	Stage 2 Gripper Proximity (cm)			
		Supplementary Feedback		No Supplementary Feedback	
		Mean	Standard Deviation	Mean	Standard Deviation
1	1	17.0000	8.2664	33.4286	8.8102
	2	22.0000	3.9581	30.7143	9.5344
	3	20.4286	6.3471	30.5714	15.7253
	4	27.0000	22.8400	29.0000	14.0831
	5	18.5714	5.2554	32.4286	9.3783
2	1	16.0000	6.0277	33.1429	6.2029
	2	15.5714	2.9358	31.0000	13.7235
	3	15.2857	2.7516	32.1429	7.0339
	4	16.8571	3.9340	33.0000	7.3485
	5	17.1429	3.8914	32.5714	4.0767
3	1	18.2857	4.9232	28.0000	11.3871
	2	16.1429	4.5251	28.1429	9.9738
	3	18.5414	5.9960	30.0000	13.5892
	4	19.0000	4.2817	28.0000	12.3828
	5	18.1429	5.8146	39.7143	26.6190
4	1	18.5714	4.5040	33.1429	2.7343
	2	19.1429	3.6253	30.2857	6.5247
	3	17.8571	2.6726	32.0000	5.0000
	4	17.0000	7.4162	32.1429	4.7759
	5	27.2857	23.0341	32.4286	6.8278

Table 6.41: Estimated marginal gripper proximity mean for stage 2

	Supplementary Feedback	
	No Supplementary Feedback	Supplementary Feedback Used
Mean gripper proximity (cm) for stage 2	32.525	18.878

Table 6.41 shows the estimated marginal means of gripper proximity for stage 2. Pairwise comparison of gripper orientation for participants with supplementary feedback and without supplementary feedback was significant ($p < 0.001$).

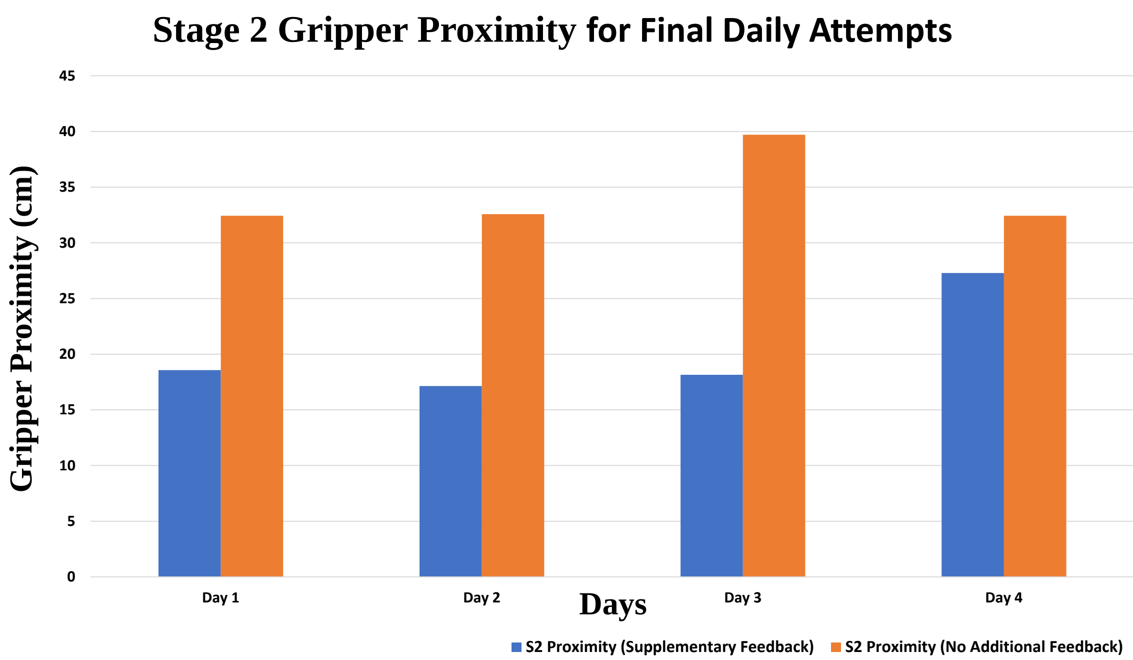

Figure 6.24: Stage 2 gripper proximity values for daily attempts 5

6.5.4 Gripper Path

The gripper path is a measure of the distance travelled by the gripper in the Cartesian coordinate as the task is carried out. The total gripper trajectory, stage 1 gripper trajectory, stage 2 gripper trajectory, stage 3 gripper trajectory, and stage 4 gripper trajectory were measured.

6.5.4.1 Total Gripper Trajectory

Table 6.42 shows the total gripper trajectories for participants with and without supplementary feedback.

Mauchly's Test of Sphericity indicated that the assumption of sphericity was not violated (p> 0.05, i.e sphericity assumed) for days ($chi^2(5) = 5.652$, $p = 0.345$) and for attempts ($chi^2(9) = 10.907$, $p = 0.667$).

Tests of within subject effects showed significant effect of Days ($F(3,27) = 18.697$, $p < 0.001$, $\eta_p^2 = 0.675$) and Attempt ($F(4,36) = 8.861$, $p < 0.001$, $\eta_p^2 = 0.496$). Interactions Days*Supplementary Feedback ($p = 0.027$), Attempts*Game ($p = 0.006$), and Days*Attempts*Game ($p = 0.009$) were also significant.

Test of between-subjects effects showed significant effect of supplementary feedback ($F(1,9) = 6.447$, $p = 0.032$) and gaming experience ($F(1,9) = 6.153$, $p = 0.035$) on the overall gripper trajectory.

Table 6.42: Total gripper trajectory for days and corresponding attempts

Day	Attempt	Total Gripper Trajectory (m)			
		Supplementary Feedback		No Supplementary Feedback	
		Mean	Standard Deviation	Mean	Standard Deviation
1	1	5.9607	1.4504	5.7354	1.5375
	2	5.6115	1.2747	5.2611	0.7873
	3	5.2374	0.7403	5.9538	2.5103
	4	5.6797	1.4458	5.0714	0.9784
	5	5.3774	0.9161	4.8693	0.4278
2	1	5.4337	0.6707	5.0527	0.5326
	2	5.0672	0.4786	4.4520	0.2868
	3	5.2337	0.9971	4.5323	0.2777
	4	5.0454	0.6824	4.4713	0.3774
	5	5.1428	2.6225	4.3692	0.4101
3	1	5.4514	1.9195	4.3062	0.1947
	2	5.6685	1.2938	4.6530	0.3574
	3	5.1047	0.4524	4.4012	0.2440
	4	4.9905	0.3620	4.5529	0.5538
	5	4.7943	0.4245	4.4062	0.3347
4	1	5.7835	1.5545	4.7072	0.4216
	2	5.2220	1.0206	4.4620	0.2898
	3	5.1587	1.0010	4.2940	0.4023
	4	5.2087	1.0861	4.3991	0.3856
	5	4.8619	0.4018	4.3618	0.2175

Table 6.43: Estimated marginal means for total gripper trajectory

	Supplementary Feedback		Gaming Experience (GE)		Robot Experience (RE)	
	No Supplementary Feedback	Supplementary Feedback Used	No GE	Has GE	No RE	Has RE
Mean total gripper trajectory	4.850	5.424	5.783	4.814	5.342	4.728

Table 6.43 shows the estimated marginal means of overall gripper trajectory. Pairwise comparison with feedback and without supplementary feedback was however not significant ($p = 0.055$). Pairwise comparison with gaming experience ($p = 0.012$), and experience with robots ($p = 0.030$) were significant.

Examining the daily estimated marginal means of gripper trajectory, as shown in table 6.43, pairwise comparison shows significant difference in gripper trajectory between day 1 and days 2 ($p = 0.007$), 3 ($p < 0.001$), and 4 ($p = 0.002$).

Pairwise comparisons show significant difference between attempt 1 and attempts 2 ($p = 0.027$), 4 ($p = 0.009$), and 5 ($p = 0.010$).

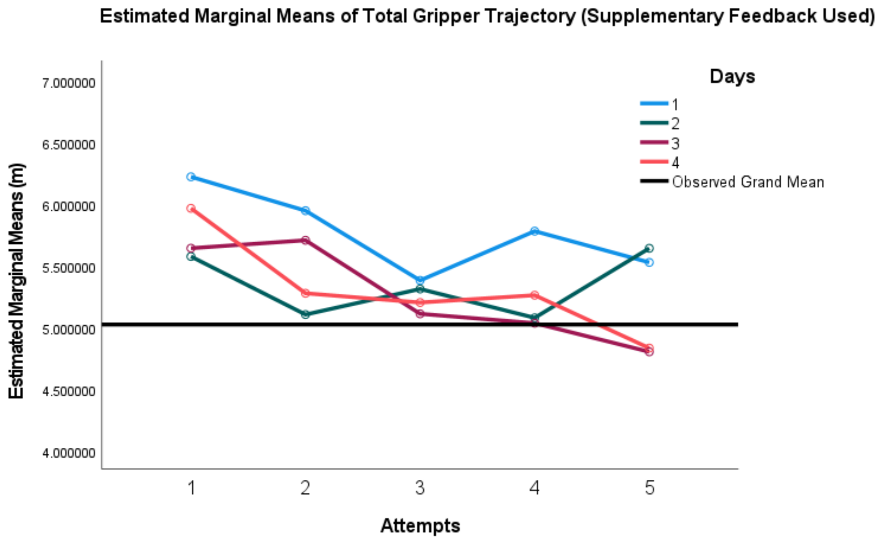

(a)

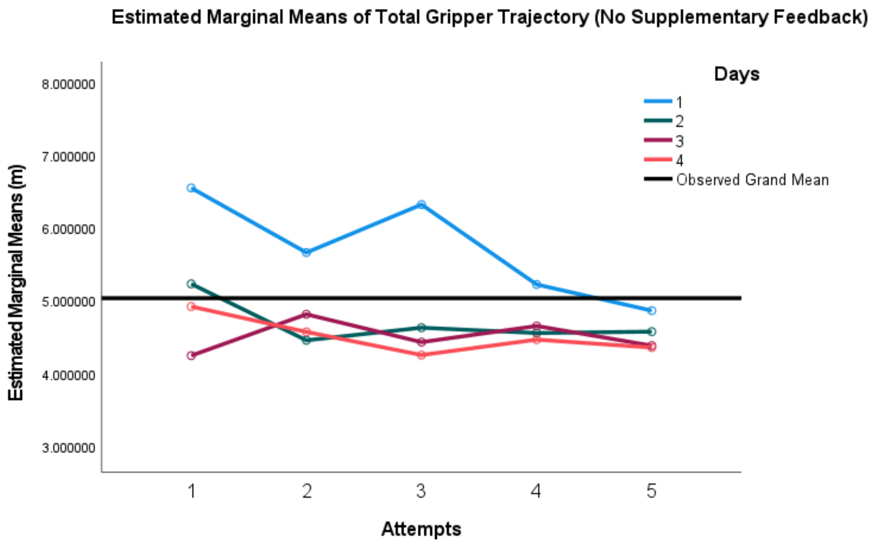

(b)

Figure 6.25: Plots of estimated marginal mean for total gripper trajectory (a) supplementary feedback used, (b) no Supplementary feedback used

Further analysis was carried out to examine changes in gripper trajectory at the end of all daily attempts. Paired samples test showed significant difference in total gripper trajectory on days 3 ($p = 0.005$) and 4 ($p = 0.006$).

Table 6.44: Mean gripper orientation deviation of last daily attempts (attempt 5)

Last Daily Attempts	**Overall Gripper Trajectory (m)**	**Standard error**
Day 1	5.140	0.7529
Day 2	4.782	1.9158
Day 3	4.613	0.4222
Day 4	4.629	0.4095

Table 6.45: Total gripper trajectory values for last daily attempts (attempt 5) with and without additional feedback

Last Daily Attempts	With Supplementary Feedback		Without Supplementary Feedback	
	Overall Gripper Trajectory (m)	Standard Deviation	Overall Gripper Trajectory (m)	Standard Deviation
Day 1	5.377	0.916	4.869	0.428
Day 2	5.143	2.622	4.369	0.410
Day 3	4.794	0.425	4.406	0.335
Day 4	4.862	0.401	4.362	0.218s

Table 6.46: Total gripper trajectory values for last daily attempts (attempt 5) with and without gaming experience

Last Daily Attempts	Gaming Experience		Without gaming experience	
	Overall Gripper Trajectory (m)	Standard Deviation	Overall Gripper Trajectory (m)	Standard Deviation
Day 1	4.946	0.434	5.916	1.341
Day 2	4.167	1.414	7.240	1.835
Day 3	4.589	0.396	4.709	0.608
Day 4	4.830	0.4535	4.955	0.281

Figure 6.26 shows the plots of overall gripper trajectory shown in table 6.45 and table 6.46. Participants without prior gaming experience had higher trajectories relative to participants

with prior gaming experience. Similarly, participants with supplementary feedback had recorded longer gripper trajectories.

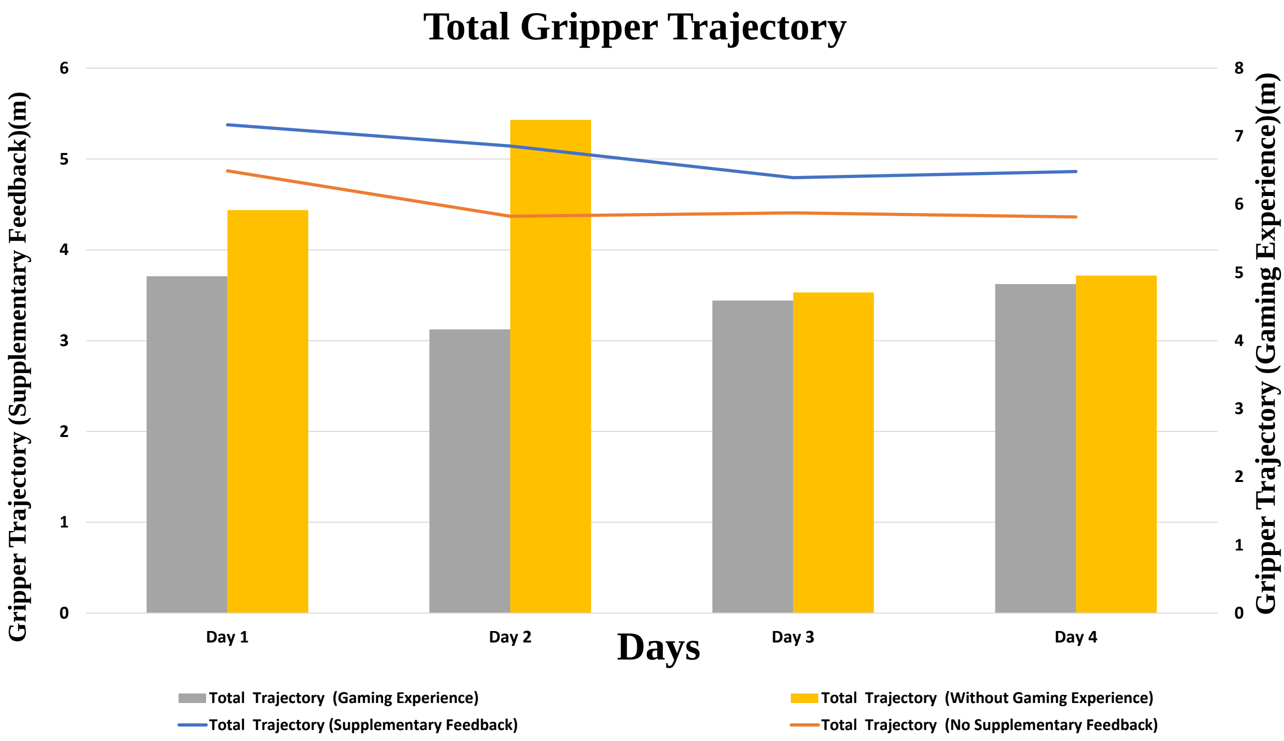

Figure 6.26: Overall gripper trajectory values for daily attempts 5

6.5.4.2 Stage 1 Gripper Trajectory

Table 6.47 shows the gripper trajectories for participants with and without supplementary feedback.

Table 6.47: Stage 1 gripper trajectory for days and corresponding attempts

Day	Attempt	Stage 1 Gripper Trajectory (m)			
		Supplementary Feedback		No Supplementary Feedback	
		Mean	Standard Deviation	Mean	Standard Deviation
	1	1.3058	0.4612	1.1964	0.3301
	2	1.2441	0.4225	1.2949	0.2641
1	3	1.0717	0.1469	1.1144	0.2404

Continued on next page

Table 6.47 – continued from previous page

Day	Attempt	Stage 1 Gripper Trajectory (m)			
		Supplementary Feedback		No Supplementary Feedback	
		Mean	Standard Deviation	Mean	Standard Deviation
	4	1.2865	0.2500	1.1819	0.3794
	5	1.1683	0.3290	1.1517	0.1690
2	1	1.2134	0.1573	1.1514	0.1460
	2	1.0871	0.1727	1.0400	0.1210
	3	1.0365	0.1195	0.9574	0.0825
	4	1.1689	0.4601	1.0003	0.0649
	5	1.0892	0.1453	0.9813	0.0776
3	1	1.1442	0.2294	1.0179	0.1002
	2	1.4282	0.9177	0.9809	0.0717
	3	1.0505	0.1823	0.9710	0.1032
	4	0.9871	0.0684	1.034	0.1281
	5	0.9775	0.0558	1.0168	0.1141
4	1	1.0823	0.1387	1.0725	0.1076
	2	0.9964	0.0858	1.0087	0.0681
	3	1.1271	0.2333	1.0419	0.1704
	4	1.1459	0.3938	1.0407	0.1401
	5	1.1154	0.2153	1.0211	0.1261

Mauchly's Test of Sphericity indicated that the assumption of sphericity was not violated (p> 0.05, i.e sphericity assumed) for days ($\chi^2(5) = 10.139$, $p = 0.074$) and but was violated for attempts ($\chi^2(9) = 21.589$, $p = 0.013$).

Tests of within subject effects showed significant effect of Days ($F(3,24) = 21.278$, $p < 0.001, \eta_p^2 = 0.727$) and Attempt ($F(4,32) = 2.836$, $p = 0.040, \eta_p^2 = 0.262$). Interactions Days*Feedback ($p = 0.034$), Days*Game ($p < 0.001$) were also significant.

Test of between-subjects effects showed no significant effect of all the factors on the stage 1 gripper trajectory.

Examining the daily estimated marginal means of gripper trajectory, pairwise comparison shows significant difference in gripper trajectory between day 1 and days 2 ($p < 0.001$), 3 ($p = 0.009$), and 4 ($p = 0.001$).

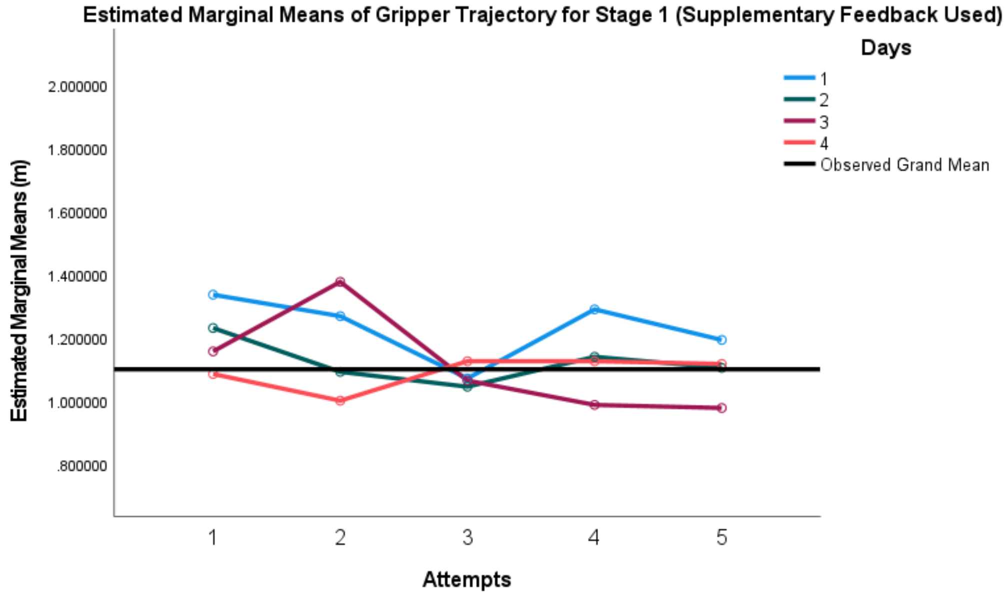

(a)

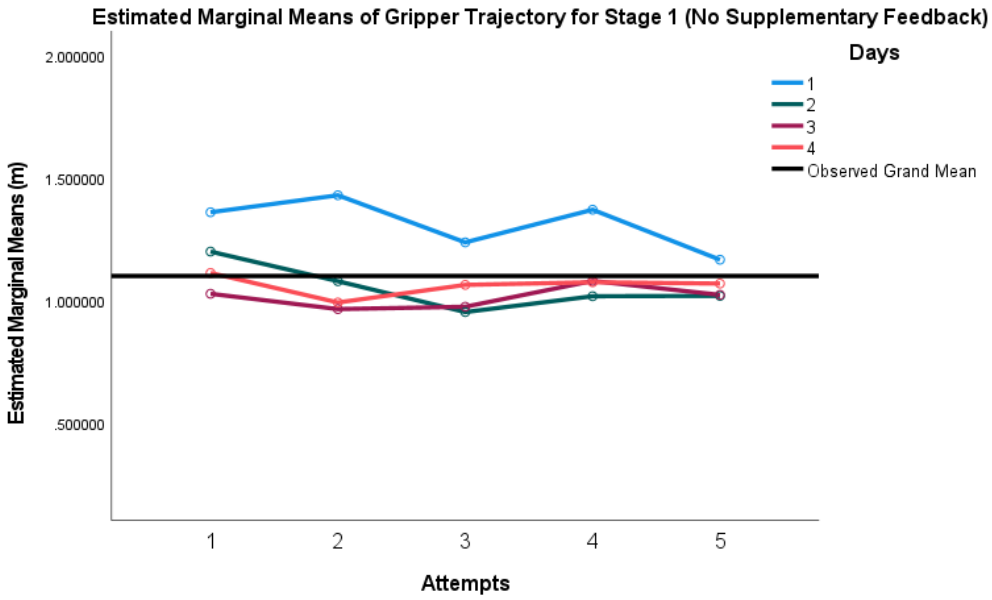

(b)

Figure 6.27: Plots of estimated marginal mean for stage 1 gripper trajectory (a) supplementary feedback used, (b) no supplementary feedback used

6.5.4.3 Stage 2 Gripper Trajectory

Table 6.48: Stage 2 gripper trajectory for days and corresponding attempts

Day	Attempt	Stage 2 Gripper Trajectory (m)			
		Supplementary Feedback		No Supplementary Feedback	
		Mean	Standard Deviation	Mean	Standard Deviation
1	1	2.6103	0.9523	2.4839	0.6833
	2	2.2644	0.6766	1.9243	0.3412
	3	2.0825	0.3032	2.2821	0.9601
	4	2.3118	0.6897	2.0961	0.6927
	5	1.9900	0.2538	1.7561	0.3548
2	1	2.0622	0.4465	2.0287	0.4269
	2	2.0146	0.2390	1.6850	0.1847
	3	2.1044	0.5802	1.7728	0.2465
	4	2.0234	0.4974	1.7420	0.3135
	5	2.5904	1.1221	1.6487	0.1632
3	1	2.1137	0.7528	1.6182	0.1001
	2	2.2660	0.3891	1.7578	0.1290
	3	1.9683	0.1305	1.6816	0.0858
	4	2.0813	0.3154	1.7834	0.3535
	5	1.9028	0.3013	1.6571	0.0837
4	1	2.4957	1.0244	1.8400	0.2140
	2	1.9680	0.4324	1.7049	0.2706
	3	2.0243	0.4866	1.5919	0.1919
	4	1.9990	0.6242	1.7024	0.1300
	5	1.7715	0.1284	1.6307	0.1822

Table 6.49: Estimated marginal means for stage 2 gripper trajectory

	Supplementary Feedback		Gaming Experience (GE)		Robot Experience (RE)	
	No Supplementary Feedback	Supplementary Feedback Used	No GE	Has GE	No RE	Has RE
Mean stage 2 gripper trajectory (m)	1.849	2.178	2.282	1.880	2.114	1.813

Table 6.48 shows the stage 2 gripper trajectories for participants with and without supplementary feedback.

Mauchly's Test of Sphericity indicated that the assumption of sphericity was violated (p< 0.05, i.e sphericity cannot be assumed) for days ($\chi^2(5) = 19.758$, $p = 0.002$) and but was not violated (p>0.05, sphericity assumed) for attempts ($\chi^2(9) = 11.208$, $p = 0.277$).

Tests of within subject effects showed significant effect of Days ($F(3, 9.719) = 5.600$, $p = 0.035$, $\eta_p^2 = 0.412$) and Attempt ($F(4, 32) = 16.348$, $p < 0.001, \eta_p^2 = 0.671$). Interactions Attempts*Game ($p < 0.001$), Days*Attempts ($p < 0.001$), Days*Attempts*Supplementary Feedback ($p = 0.005$), Days*Attempts*Game ($p = 0.002$) were also significant.

Test of between-subjects effects showed significant effect of feedback ($p = 0.024$) on the overall gripper trajectory.

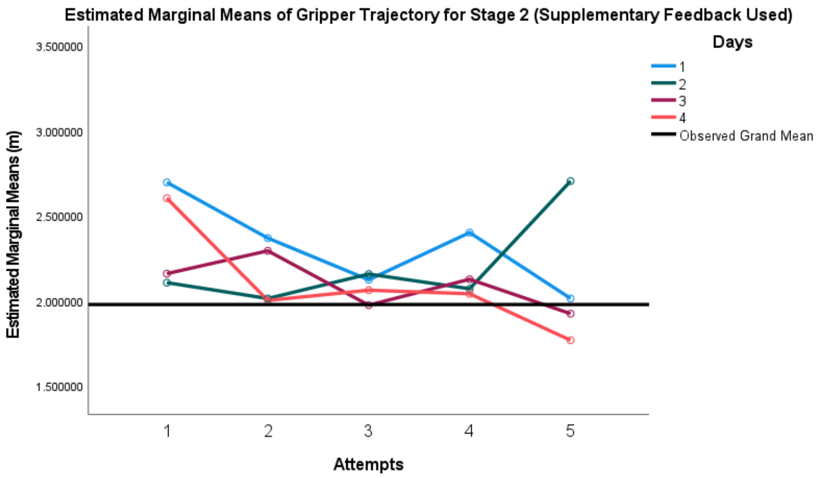

(a)

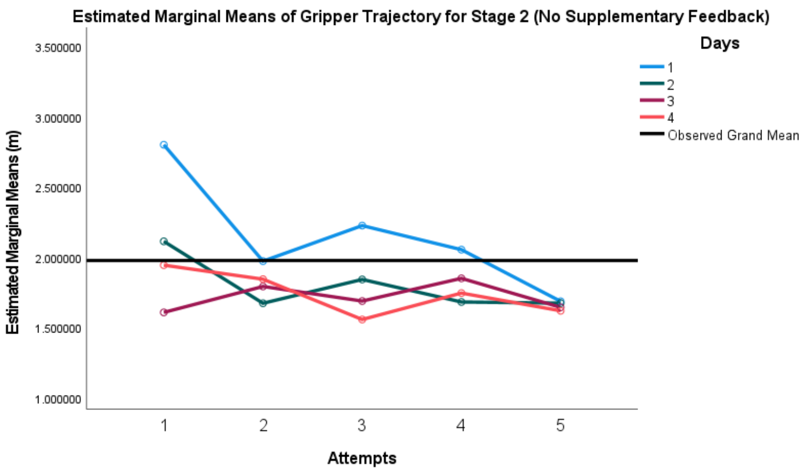

(b)

Figure 6.28: Plots of estimated marginal mean for stage 2 gripper trajectory (a) supplementary feedback used, (b) no supplementary feedback used

Table 6.49 shows the estimated marginal means of gripper trajectory for the independent variables. Pairwise comparison for supplementary feedback shows significant difference ($p = 0.032$). Likewise, there was significant pairwise difference for gaming experience ($p = 0.027$). Pairwise comparison for experience with robot was also significant ($p = 0.035$). Pairwise comparisons show significant difference between attempt 1 and attempts 2 ($p = 0.006$), 3 ($p = 0.008$), 4 ($p = 0.004$), and 5 ($p < 0.001$).

6.5.4.4 Stage 3 Gripper Trajectory

Table 6.50: Stage 3 gripper trajectory for days and corresponding attempts

Day	Attempt	Stage 3 Gripper Trajectory (m)			
		Supplementary Feedback		No Supplementary Feedback	
		Mean	Standard Deviation	Mean	Standard Deviation
1	1	0.1399	0.1269	0.0749	0.0760
	2	0.1463	0.1454	0.0885	0.1203
	3	0.1234	0.0961	0.7593	1.7970
	4	0.1891	0.1886	0.0541	0.0446
	5	0.2564	0.3017	0.1154	0.1454
2	1	0.1616	0.1623	0.1138	0.1333
	2	0.1721	0.1598	0.0411	0.0634
	3	0.1178	0.1749	0.0682	0.0884
	4	0.1691	0.2640	0.0470	0.0747
	5	0.1523	0.2355	0.0558	0.0610
3	1	0.1101	0.1082	0.0541	0.0927
	2	0.0862	0.0928	0.1461	0.1535
	3	0.1176	0.1108	0.1534	0.2846
	4	0.1043	0.1482	0.0493	0.0706
	5	0.0949	0.1446	0.0455	0.0686
4	1	0.1245	0.1559	0.1071	0.1126
	2	0.1295	0.1290	0.1579	0.1302
	3	0.1263	0.1066	0.0872	0.0937
	4	0.1487	0.1406	0.0609	0.0946
	5	0.1082	0.0875	0.0482	0.0739

Table 6.50 shows the stage 3 gripper trajectories for participants with and without supplementary feedback.

Mauchly's Test of Sphericity indicated that the assumption of sphericity was violated ($p < 0.05$, i.e sphericity cannot be assumed) for days ($\chi^2(5) = 25.551, p < 0.001$) and attempts ($\chi^2(9) = 26.536$, $p = 0.002$). Since $\epsilon < 0.75$, we report the Greenhouse-Geisser corrected results.

Tests of within subject effects showed no significant effect of all independent variables. Test of between-subjects effects was also not significant.

6.5.4.5 Stage 4 Gripper Trajectory

Table 6.51: Stage 4 gripper trajectory for days and corresponding attempts

Day	Attempt	Stage 4 Gripper Trajectory (m)			
		Supplementary Feedback		No Supplementary Feedback	
		Mean	Standard Deviation	Mean	Standard Deviation
1	1	1.9957	0.5085	1.9803	0.6838
	2	2.1087	0.5978	1.9544	0.4896
	3	2.0439	0.5006	1.7980	0.3325
	4	1.8759	0.9710	1.7393	0.2446
	5	1.9606	0.4242	1.8462	0.3039
2	1	2.0596	0.2925	1.7588	0.1866
	2	1.8521	0.2056	1.6862	0.1102
	3	1.9764	0.5318	1.7339	0.1872
	4	1.7337	0.2364	1.6820	0.2923
	5	2.0456	0.5909	1.6833	0.2725
3	1	2.1365	1.1000	1.6161	0.1253
	2	2.011	0.3648	1.7681	0.3122
	3	1.8652	0.1917	1.5952	0.3438
	4	1.8321	0.3484	1.6859	0.1580
	5	1.8829	0.2631	1.6868	0.2393
4	1	2.1687	0.6674	1.6876	0.1333
	2	2.0244	0.5831	1.5904	0.1485
	3	1.8656	0.4837	1.5730	0.1305
	4	1.9413	0.4020	1.5952	0.1660
	5	1.8221	0.1567	1.6618	0.1772

Table 6.51 shows the stage 4 gripper trajectories for participants with and without supplementary feedback.

Mauchly's Test of Sphericity indicated that the assumption of sphericity was not violated (p> 0.05, i.e sphericity assumed) for days ($\chi^2(5) = 25.551, p < 0.001$) but the assumption of sphericity was violated for attempts ($\chi^2(9) = 26.536$, $p = 0.002$). Since $\epsilon < 0.75$, we report the Greenhouse-Geisser corrected results.

Tests of within subject effects showed significant effect of Days on gripper trajectory for stage 4 ($F(3,24) = 10.539$, $p < 0.001, \eta_p^2 = 0.568$). However, test of within subject effect showed non-significant effect of attempt on gripper trajectory in stage 4 ($F(2.001, 16.006) = 3.519$, $p = 0.054$, $\eta_p^2 = 0.305$). Interactions Days*Feedback (p=0.004), Days*Game ($p = 0.005$), Days*Attempts*Feedback

($p = 0.038$), Days*Attempts*Game ($p = 0.007$), Days*Attempts*Feedback*Game ($p = 0.002$) were also significant. Test of between-subjects effects was not significant for all factors.

6.5.5 NASA Task Load Index

The NASA Task Load Index (NASA-TLX) is based on subjective workload assessment. It was originally developed for use in aviation but has been adopted for use in healthcare. The NASA-TLX scale is designed to measure subjective workload as a single variable by finding an average to six parameters: mental demand, physical demand, temporal demand, performance, effort, and frustration.

Participants filled the questionnaire (Appendix F) at the end of each day for which they participated in the study. The overall perceived workload is defined as the average of weighted ratings. Figure 6.29 shows the boxplot for the NASA-TLX mean daily overall perceived workload.

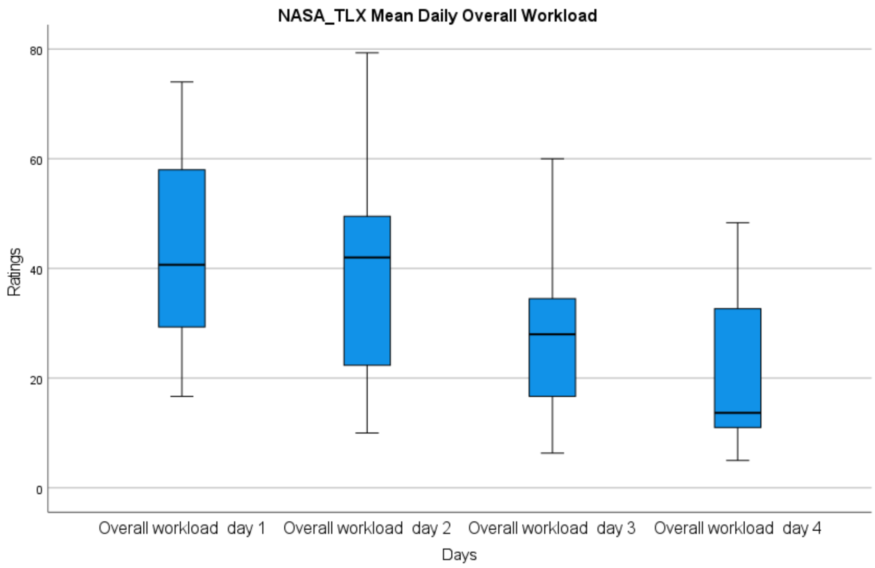

Figure 6.29: Boxplot for NASA-TLX Mean Daily Overall Workload

Table 6.52: Daily NASA-TLX Workload

Days	Mean	Std. Deviation
1	42.9560	18.2877
2	37.8000	21.3137
3	27.5327	15.1736
4	21.4220	16.0935

Table 6.52 shows the average daily NASA-TLX workload ratings. Figure 6.29 and table 6.52 show the reduction in daily perceived workload (PW) as participants repeated the task.

Paired samples t-test was conducted to compare correlation and examine the differences between perceived workload for each day. Table 6.53 and table 6.54 show the paired samples statistics and paired samples correlation for daily perceived workload respectively.

Table 6.53: Paired samples statistics for daily perceived workload (N=15)

		Mean	Std. Deviation
Pair 1	Perceived workload day 1	42.956	18.2877
	Perceived workload day 2	37.800	21.3137
Pair 2	Perceived workload day 1	42.956	18.2877
	Perceived workload day 3	27.533	15.1736
Pair 3	Perceived workload day 1	42.956	18.2877
	Perceived workload day 4	21.422	16.0935
Pair 4	Perceived workload day 2	37.800	21.3137
	Perceived workload day 3	27.533	15.1736
Pair 5	Perceived workload day 2	37.800	21.3137
	Perceived workload day 4	21.422	16.0935
Pair 6	Perceived workload day 3	27.533	15.1736
	Perceived workload day 4	21.422	16.0935

Table 6.54: Paired samples correlation for daily perceived workload (N=15)

		Correlation	Significance	
			One-sided p	Two-sided p
Pair 1	Perceived workload day 1 and Perceived workload day 2	0.874	< 0.001	< 0.001
Pair 2	Perceived workload day 1 and Perceived workload day 3	0.786	< 0.001	< 0.001
Pair 3	Perceived workload day 1 and Perceived workload day 4	0.687	0.003	0.006
Pair 4	Perceived workload day 2 and Perceived workload day 3	0.788	< 0.001	< 0.001

Continued on next page

Table 6.54 – continued from previous page

		Correlation	Significance	
			One-sided p	Two-sided p
Pair 5	Perceived workload day 2 and Perceived workload day 4	0.644	0.005	0.010
Pair 6	Perceived workload day 3 and Perceived workload day 4	0.906	< 0.001	< 0.001

Perceived workload for days 1 and 2 were strongly and positively correlated (r=0.874, p < 0.001). All other paired samples were also strongly and positively correlated (table 6.54).

Table 6.55: Paired samples test for daily perceived workload

		Mean	Std. Dev	t	df	Significance	
						One-sided p	Two-sided p
Pair 1	PW day 1 - PW day 2	5.156	10.371	1.925	14	.037	.075
Pair 2	PW day 1 - PW day 3	15.4233	11.328	5.273	14	<.001	<.001
Pair 3	PW day 1 - PW day 4	21.534	13.949	5.979	14	<.001	< .001
Pair 4	PW day 2 - PW day 3	10.267	13.221	3.008	14	0.005	0.009
Pair 5	PW day 2 - PW day 4	16.378	16.467	3.852	14	<.001	0.002
Pair 6	PW day 3 - PW day 4	6.111	6.855	3.452	14	0.002	0.004

As shown in table 6.55, there was a significant average difference between perceived workload for day 1 and perceived workload for day 2 (t_{14} = 1.925, p = 0.037). On average, perceived workload for day 1 was 5.156 points higher than perceived workload for day 2 (95% confidence interval[-0.5874, 10.8994]). There was also significant average difference between perceived workload for day 1 and perceived workload for day 3 (t_{14} = 5.273, p < 0.001). The perceived workload for day 1 was 15.423 points higher than perceived workload for day 3 (95% confidence interval[-9.150, 21.697]). The average difference between perceived workload for day 1 and perceived workload for day 4 was significant ($t_{14} = 5.979$, $p < 0.001$). The difference between average perceived workload for days 1 and 4 is 21.54 (95% confidence interval[13.809, 29.259]).

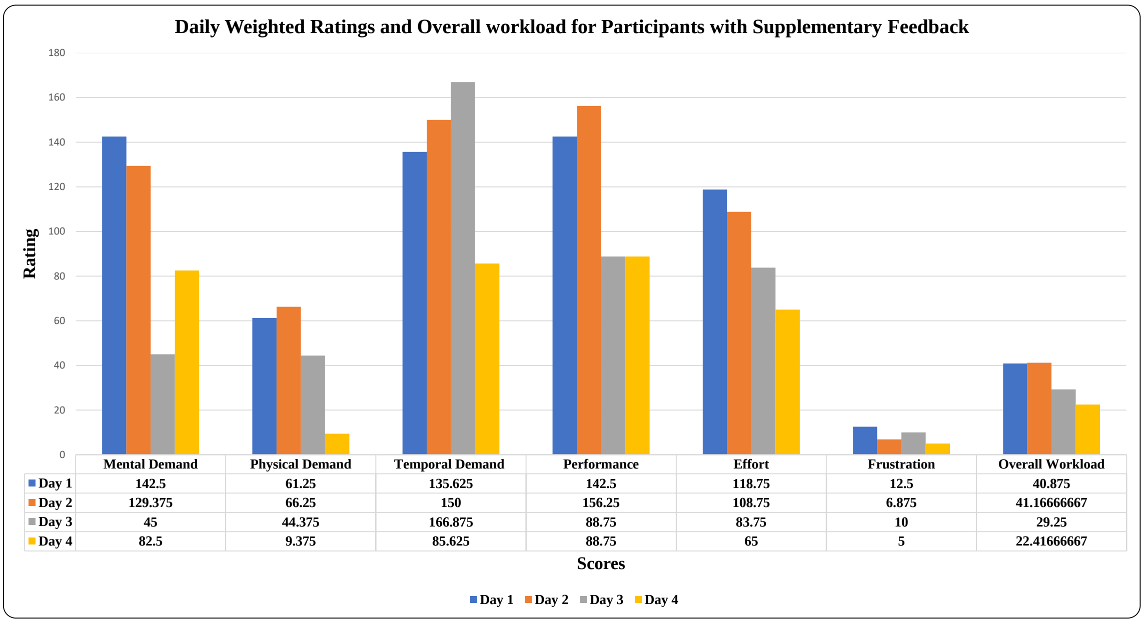

(a)

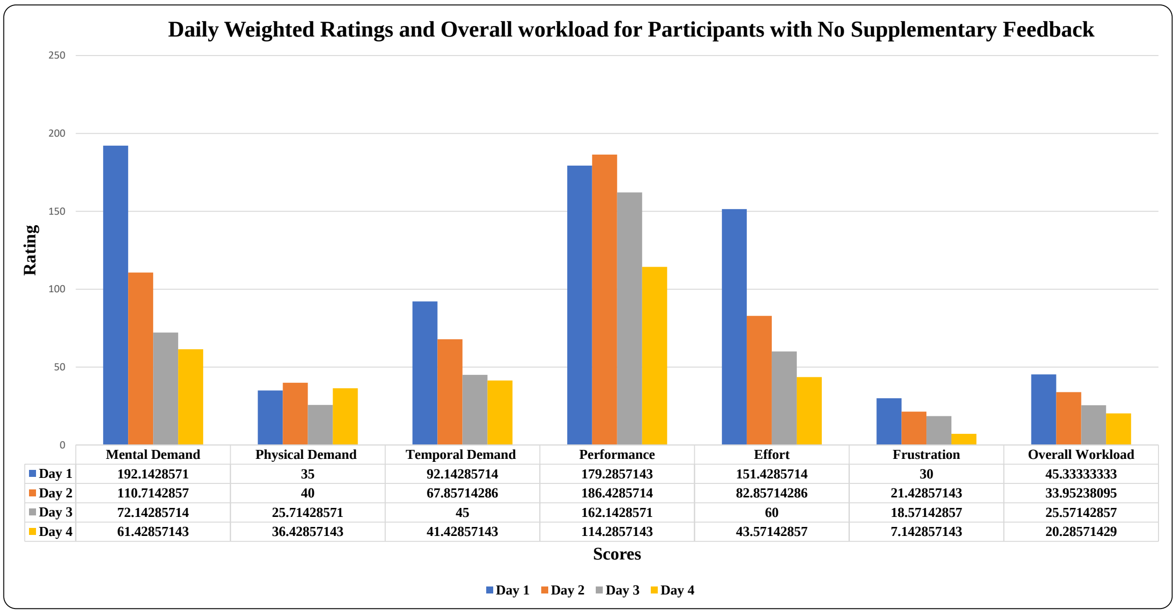

(b)

Figure 6.30: Histogram for daily rated scores (a) with supplementary feedback, (b) without supplementary feedback

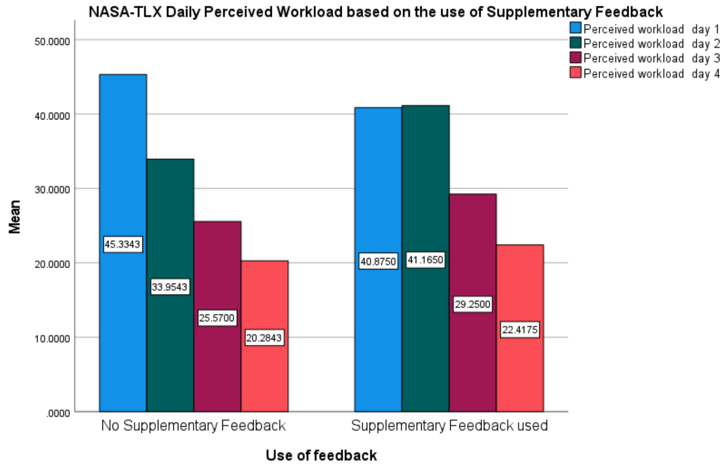

(a)

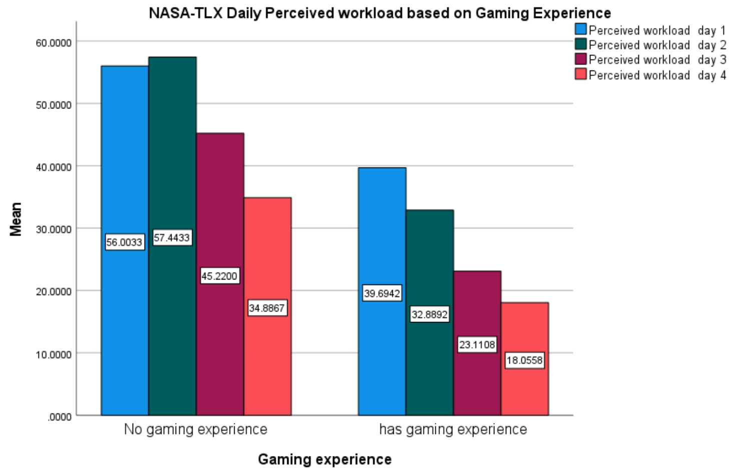

(b)

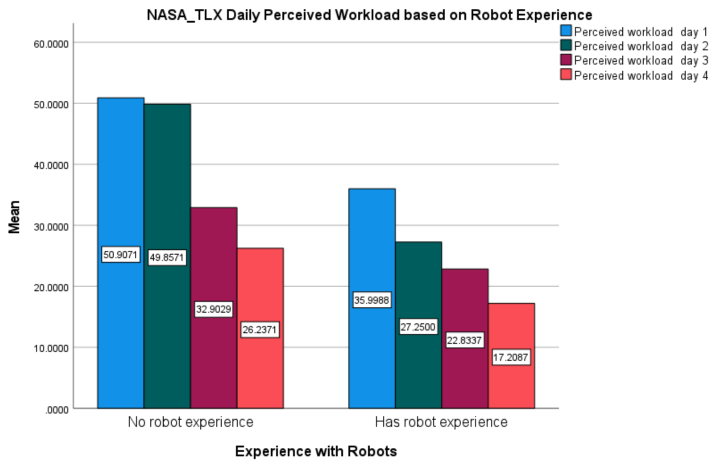

(c)

Figure 6.31: Daily perceived workload (a) with and without supplementary feedback, (b) with and without gaming experience, (c) with and without robot experience.

There was a significant average difference between perceived workload for day 2 and perceived workload for day 3 ($t_{14} = 3.008$, $p = 0.005$). On average, perceived workload for day 2 was 10.267 points higher than perceived workload for day 3 (95% confidence interval[2.946, 17.589]). There was also significant average difference between perceived workload for day 2 and perceived workload for day 4 ($t_{14} = 3.852$, $p < 0.001$). The perceived workload for day 2 was 16.378 points higher than perceived workload for day 4 (95% confidence interval[7.259, 25.497]).

The average difference between perceived workload for days 3 and 4 was significant ($t_{14} = 3.452$, $p = 0.002$). Perceived workload for day 3 was 6.111 points higher than the perceived workload for day 4 (95% confidence interval[2.314, 9.907]).

The daily changes in each of the questionnaire scores is shown in figure 6.30. Figure 6.30a shows the scores for participants with supplementary feedback while figure 6.30b shows the scores for participants without supplementary feedback.

For participants with and without supplementary feedback, daily subjective mental demand reduced with task repetition.

Whilst temporal demand reduced with daily repetition for participants without supplementary feedback, temporal demand increased with daily repetition for participants with supplementary feedback on gripper proximity and orientation. Overall, participants with supplementary feedback reported higher daily perceived workload than participants without supplementary feedback. Figure 6.31 shows the perceived workload based on the use of feedback, gaming experience, and robot experience.

Participants provided with feedback on gripper orientation and proximity reported higher daily perceived workload than participants who were not provided with supplementary feedback (fig. 6.31a).

Figure 6.31b shows that participants with no gaming experience reported higher daily workload than participants without prior gaming experience. For both groups, perceived workload reduced with daily repetition.

Likewise, participants with no prior experience with robots recorded higher daily workload than participants with prior experience with robots (fig. 6.31c). With daily repetitions however, perceived workload reduced.

6.6 Discussion

Understanding the effect of supplementary feedback modalities in tele-operation is very important as it may help to either reduce cognitive workload on operators or increase the ease with which tasks are carried out. In some cases, the use of supplementary feedback reduces task completion time and allows tasks to be carried out more safely. The study reported in this chapter focuses on investigating the possibility of conveying more than one type of sensor data through a single feedback modality and explores how task repetition can help operators to improve in their interpretation of haptic feedback stimulation. This is particularly important due to limited human senses. This chapter also demonstrates design iterations carried out on the haptic feedback device used in the study carried out in section 4.2. In the study reported in this chapter, a single wrist-worn haptic feedback device was used which is different from the section 4.2 study where two wrist-worn haptic feedback devices were used. In addition, the haptic feedback device used in section 4.2 was used to convey only one type of sensor data (gripper orientation) whereas in this chapter, the single wrist-worm haptic device was used to convey two different types of sensor data (gripper orientation and gripper proximity).

The provision of supplementary feedback modalities was not to make participants fully reliant on the supplementary feedback modalities, but to provide supplementary information that may be difficult to obtain from video feedback due to camera views, camera capabilities and camera design limitations. The impact of supplementary feedback was investigated to convey gripper proximity and gripper orientation data. This was carried out by investigating how two groups of participants performed when carrying out a simple tele-operation task. The first group was provided with supplementary feedback while the second group did not have supplementary feedback when carrying out the task.

One of the dependent variables investigated in the study is gripper proximity to the cooking surface and to the table. Proximity was measured in stage 1 and stage 2 of the task. How closely participants positioned the gripper to the cooking surface before grasp was measured in stage 1. Information about the gripper's proximity in stage 1 of the task was to ensure that participants do not drive the robot into the cooking surface but positioned to achieve good grasp. Even though there was no significant effect of supplementary feedback on gripper proximity for stage 1, participants that were provided with proximity information had lower proximity values that participants that were not provided with proximity information. From the design setup, positioning the gripper closer to the surface may allow for better grasp, hence making stage 3 task easier. One of the reasons attributed to non significant difference in gripper orientation between participants with feedback and participants without feedback is the field of view of camera 2 (Fig. 6.1). Camera 2 provides a close view of the jar before grasp, resulting to little or no need for supplementary feedback on the proximity of the gripper to the cooking surface. In order to successfully empty the content of the jar into the bowl, awareness of the the gripper's proximity to the table (in stage 2) before the content of the jar is emptied is important. High gripper proximity implies that the content will be emptied from a considerable height above the bowl, hence causing spillage. From camera 3 (fig. 6.1b), the camera was positioned vertically above the bowl, making it is difficult to visually gauge the gripper's proximity to the table. A crude approach by some of the participants was to move the jar close enough to the table or bowl for slight contact which gives an idea of the proximity. This may however be unsafe as the effect of such an approach may not be controllable. Participants who were provided with supplementary proximity feedback had significantly lower proximity to the table before emptying the content of the jar, hence they were able to avoid spilling the content of the jar.

Providing participants with supplementary feedback also made them aware of gripper's orientation and deviations from the 'aligned' position. Even through there was no significant effect of feedback on gripper orientation before grasp, participants that were provided with supplementary feedback reported that the gripper deviation prompts by the feedback device helped in correctly aligning the orientation of the gripper. This may be one of the reasons for lower frustration score in perceived workload by participants that were provided with supplementary feedback. The usefulness and effectiveness of the supplementary feedback therefore confirms the first hypothesis that the use of supplementary feedback improves the accuracy with which participants carry out the task.

Task completion time is defined in this study as the time taken to carry out the task, measured as total task completion time and task completion time for each stage of the task. The overall task completion time significantly reduced for each day and attempt the task was repeated. However, the reduction in the overall task completion time was not influenced by the use of feedback. Paired samples t-test showed significant reduction in total task completion time when the final daily attempts were compared. There was also significant effect of gaming experience and robot experience on total task completion time. Further analysis was therefore conducted to examine if the task completion time for each stage reduced with repetition and the use of feedback. For stage 1 of the task, completion time reduced as participants repeated the task but the reduction in the task completion time was not affected by the use of feedback or gaming and robot experience. When the last daily attempts were also compared, task completion time for stage 1 reduced with repetition. The reduction in stage 2 task completion time was found to be different between participants who used feedback and participants who did not. Participants provided with supplementary feedback had higher mean task completion time for stage 2 of the task. Gaming experience was also found to have significant effect on the task completion time for stage 2 as participants with gaming experience had lower completion time for stage 2. Feedback did not have significant effect on the completion time for stage 3. This is however expected due to the nature of stage 3 of the task. The completion time for stage 4 reduced as participants repeated the task, but feedback had not significant effect on the reduction. It was important to examine the completion time for each stage because the overall task completion time does not provide in-depth view of the changes in task completion time. This implies that the effect of feedback on the reduction of task completion time varies based on the stage of the task.

The effect of task repetition on gripper orientation was examined for participants with and without supplementary feedback. Gripper orientation was monitored for stage 1 of the task. Results show that neither feedback or task repetition had any significant effect on the accuracy with which participants vertically aligned the jar before grasp. This may be as a result of the information got from cameras 2 and 4. Participants were less reliant on supplementary feedback when sufficient information can be provided through video feedback, hence there is no significant effect of feedback. Gripper proximity did not significantly improve with task repetition but with the use of feedback. This again support the use of feedback by operators when carrying out such tasks.

The effects of task repetition and feedback was also examined on gripper trajectory, a measure of the distance travelled by the gripper. Overall gripper trajectory reduced as daily attempts were made. Participants that were provided with supplementary feedback had significantly longer overall trajectory relative to participants who were not provided with supplementary feedback. However, participants with gaming experience had shorter overall gripper trajectory than participants without prior gaming experience. Gripper trajectory for stage 1 showed that trajectory reduced significantly with daily attempts but the reduction was not effected by the use of feedback used or gaming and robot experience. Gripper trajectory reduced daily and with attempts as a result of feedback used. Participants that were provided with feedback had significantly longer trajectory. This may be explained due to that fact that stage 2 of the task involved more use for feedback. While gripper trajectory for stage 3 did not reduce with repetition, it did for stage 4. However, there was no significant effect of feedback, gaming experience or robot experience. The second hypothesis will neither be rejected not confirmed as the effect of task repetition was noticed in some of the parameters mentioned but not in all. Hypothesis 3 can however be confirmed as participants' performance was noticed to improve with the use of feedback and task repetition.

Analysis of the NASA-TLX load index questionnaire responses showed strong positive correlations between daily perceived workload. Paired samples t-tests also showed significant differences between daily perceived workload. In general, participants with supplementary feedback recorded higher daily perceived workload than participants that were not given supplementary feedback. Mental demand was perceived to reduce as participants repeated the task for all participants. However, temporal demand was perceived to increase by participants with supplementary feedback but perceived to reduce among participants without supplementary feedback. Participants that were not provided with supplementary feedback also recorded higher frustration as they carried out the task compared to participants that were provided with supplementary feedback.

Results from this study open up the possibilities of conveying more than one type of sensor data using a single wrist-worn haptic feedback device for real life applications, hence confirming the fourth hypothesis.

CHAPTER 7

Conclusions and Future Work

This chapter describes the work done to fulfil the aims and objectives of the PhD research. The aim of this PhD research was to identify optimal feedback modalities or combination of modalities for providing feedback to a tele-robotic operator and ensure minimal cognitive load for the operator. In this chapter, we also provide a summary of the main contributions of the PhD research and introduce guidelines for future research.

7.1 Conclusions

In order to provide an operator with as much information as possible about the remote environment it is important to consider how best to communicate this information and make it easy to interpret without increasing cognitive load. Investigations were carried out to identify sensor data to be conveyed to an operator for effective tele-operation. This was done within the context of a chosen experimental tele-operation task which was representative of an assisted living scenario. Within an assisted living context it is particularly important to consider the modalities of the feedback to ensure effective tele-operation as the operator would need to socially interact with the person being supported. Unlike other applications of tele-operation, such as in nuclear decommissioning and manufacturing, tele-operation of robots to provide support for older adults with assistive care needs and people with disabilities also requires emphasis on safe human-robot interaction since the tele-operated robot will come in close proximity to human users. This therefore requires consideration of a range of different sensors to capture information about the robot and the remote environment, which not only provide a high level of information but also can be interpreted through sensory modalities other than auditory and visual. The auditory and visual modalities within a tele-operated assistive robot task being key to reserve for social interaction with the person being supported.

The first research question was to determine what sensor data are required for effective tele-operation. The first study in chapter 4 showed that different gripper orientations resulted in different grasp forces and grasp outcomes. Some grasp orientations were sub-optimal resulting in the object not being grasped adequately. This suggested the need for capturing and communicating information about gripper orientation and grasp force in order to effectively carry out tele-operated pick and place tasks. Good and reliable off-the-shelf force sensors that could be used were expensive. As a result, customised force sensors had to be developed for this research as described in chapter 3. Force sensing resistors (FSRs) were initially employed to measure grasp force but bending limitations of the FSRs introduced inconsistencies into the readings from the FRSs. Barometric sensors where later used to develop Wi-Fi-enabled force sensors. The barometric force sensors were designed to be mounted at different locations on the fingers of the JACO robot gripper. However, there may be no need to measure grasp force if the objects to be grasped are rigid or if the maximum grasp force of the gripper does not exceed the maximum grasp force each object can withstand. In real-life applications where different objects with different properties are used, measuring grasp force may be important as confirmed in chapter 4. Literature review of studies on tele-operation shows that the most common sensor employed in robot tele-operation is the video camera which provides real-time visual information about the remote environment [143] [185]. In the studies carried out in chapter 4 and 6, web cameras were used to capture real-time video of the remote end. Visual feedback of the remote robot end was captured from different angles. Results from the second study in chapter 4 showed that visual feedback alone is not sufficient to provide information about the remote end due to limitations of the static cameras employed. In order to keep the number of cameras used to a minimum (to limit band width and keep the operator cognitive load low), we introduced proximity sensor into the setup in chapter 6 to provide additional information such as the robot gripper's proximity to surfaces. For the study in chapter 6, a 3-axis accelerometer board was developed with Wi-Fi capabilities to measure gripper orientation. For the previous study in chapter 4, gripper orientation was polled from the robot but the use of a different setup in chapter 6 prompted the design of the Wi-Fi enabled orientation sensor. Even though the sensors mentioned were identified in the context of assistive care provision, results gathered may be applicable in other application scenarios. For example, most tele-operation setup employ the use of visual feedback which also implies that the results relating to the choice of camera angles and supplementary feedback may also find use in other application scenarios also. The protocol followed to identify the sensors may be applied in other scenarios also.

The next research question was to identify software and hardware requirements for setting up efficient tele-operation systems. This question was answered throughout the PhD thesis. The hardware requirements involved the sensors and feedback devices described in chapter 3. Different iterations were carried out on the designs of the sensors and actuators as studies were carried out. Throughout the study, a Jaco robot arm was tele-operated to carry out the chosen task. Software was written in C++ and C programming languages to for the different sensors and feedback devices. A personal computer was designated as the central processing hub. Software was written to enable the PC communicate with the robot, sensors and feedback devices.

The next research question was to identify what feedback modality and combination of modalities are best suited for conveying sensor information to operators. The second study in chapter 4 was designed to identify optimal feedback modality or combination of modalities that can be used to convey sensor data to operators. Successful tele-operation was measured in this thesis in terms of task completion time, successful task completion, vertical gripper alignment before grasp, minimum gripper trajectory, ease of carrying out the task, safe gripper proximity, and perceived workload. The effect of verbal feedback was also investigated in chapter 4. In addition to visual display, additional feedback modalities were used to provide supplementary information about the remote robot. Supplementary information about the gripper orientation was displayed to participants using different combinations of peripheral vision, verbal feedback, and haptic feedback. Whilst the different scenarios yielded varying effects on task completion time, success of the task, accuracy with which the task was carried out, and the ease with which the task was carried out, decisions have to be made to prioritise which of the measured parameters is most important for specific tasks. Where multiple feedback modalities are used to display the same sensor data, participants sometimes ignored some modalities and focused on the feedback modality they feel more comfortable with. The introduction of feedback increased the ease with which the task was carried out but did not guarantee reduced task completion times even though task completion times were noticed to reduced with task repetition and gaming experience. Verbal feedback was reported to increase the ease with which participants carried out tele-operated tasks. A combinations of video feedback, peripheral vision feedback, and verbal collaboration was the optimal combination of feedback modalities based on the parameters measured. In addition to understanding the effect of different feedback modalities on the success of carrying out a task, gaze metrics was also demonstrated to be useful in understanding how participants interacted with the system. Feedback modalities may be used in two forms as confirmed in studies carried out. As confirmed in this thesis, there can be trade-off in the choice of different feedback modalities depending on the application. Whilst safety and task completion time may be the priority in an assistive care scenario, safety may be prioritised in the application of robot tele-operation in nuclear decommissioning. As much as safety is important in human robot interaction, we do not want to spend the whole day carrying out a single assistive care task. However, that may not be the case in nuclear decommissioning.

The next research question was what knowledge of haptic sensitivities can be used to improve haptic perception. With auditory and visual modalities reserved for social interaction with the person being supported, it was important to explore the use of other feedback modalities further. A Wi-Fi enabled wrist-worn haptic device was designed for use to provide feedback. In order to improve haptic perception, we carried out an investigation on the minimum detectable haptic intensity (MDHI) of different locations on the wrist in chapter 5. This was measured as percentages of duty cycle of pulse width modulation used to power the haptic motors embedded in the haptic feedback device. The results were used to calibrate the haptic device for an identification of location of haptic stimulation performance test for single-location identification (SSI) and simultaneous double-location identification (SDSI). For SSI, participants were asked to identify single locations of haptic stimulation. However, for SDSI participants were required to identify two locations that were simultaneously stimulated. Overall performance scores were higher for single location identification than it was for simultaneous double-location identification. For SSI performance and sensitivity scores were higher at the Volar central and Dorsal central respectively than at the Ulna zone and Radial zone. ILHSP was carried out for varying durations of haptic stimulation and video distraction. Single location stimulations were easier to identify and differentiate than simultaneous double-location stimulations. This suggests that it may be possible to convey different sensor data through different locations across the wrist. Likewise, it also suggests that haptic display may be improved by dynamically controlling haptic display parameters like durations of haptic stimulation and haptic intensity for different locations on the wrist. These results are also useful for different application scenarios that employ haptic feedback and haptic guidance.

The next research question was which sensory substitution strategies are best suited to convey sensor data. In chapter 5, two types of sensory substitution strategies were examined for the haptic feedback device. The first strategy was referred to in this thesis as instructional strategy. This involves the use of series of haptic stimulation to provide control instructions to operators. The second strategy provides situational awareness. With this strategy, sensor data are mapped to haptic stimulations in real time and the operator is allowed to make control decisions at will. Different locations on the wrists of participants were haptic stimulated to signal the direction of gripper orientation change. The plots of gripper orientation values showed that reaction time, haptic sensitivities and the speed with which the robot was controlled made it difficult for participants to change the gripper orientation in real time. This suggests that the situational awareness strategy is better when conveying information via haptic feedback.

The next research question was whether more than one type of sensor data can be conveyed through a single feedback modality as an operator carries out a task. In chapter 6, the display of multiple sensor data via a single wrist-worn haptic feedback device was investigated. This builds on results that demonstrated the possibility of differentiating haptic stimulation across different locations on the wrist. Information about gripper orientation and gripper proximity to surfaces were simultaneously conveyed to participants via a wrist-worn haptic feedback device using the situational awareness strategy. The effect of task repetition was examined to investigate changes in task completion time, accuracy of gripper orientation with repeated use of haptic feedback, the need for feedback for gripper proximity as a task was repeated, changes in gripper trajectory with task repetition, possible reduction on perceived workload due to task repetition and the use of feedback. Task repetition resulted in the reduction of overall task completion time. There was no significant difference in the reduction of overall task completion time between participants with supplementary feedback and participants without feedback. However, the effect of feedback on the reduction of task completion time was noticed in stages of the task that require supplementary sensor data. The significance of prior gaming experience on task completion time varied with the stages of the task and contributed to the overall changes in task completion time.

The next research question was what is the effect of task repetition on operator performance. The effect of the use of supplementary feedback was be noticeable when the information the feedback provided could be got from video feedback. In chapter 6, accuracy in terms of gripper proximity to the table improved with the use of feedback. task repetition did not improve gripper proximity accuracy in the study. This understanding can help in decision making when tele-operation systems are setup. The number of cameras employed to capture video information of the remote end may be reduced with the introduction of supplementary sensors. The use of feedback, prior gaming experience, prior robot experience, and task repetition have varying effects on the success of carrying out a tele-operated task. For the design of a tele-operation system, this thesis demonstrates different factors that may be considered and the parameters that can be measured when analysing the effects of these factors.

The use of supplementary feedback increased perceived workload which reduced with task repetition. Another advantage of the use of supplementary feedback was the reduction of frustration as the task was carried out. The use of supplementary feedback increased temporal demand on operators as they carried out tasks. It has been demonstrated in this thesis that multiple sensor data can be displayed to an operator carrying out real-life tasks and the understanding of the conveyed information increased with repetition.

7.2 Limitations and Recommendation for Future Works

The studies reported in this thesis have been able to answer the research questions to a certain extent, however given the constraints of the experiments, some limitations have been identified which may be addressed in future research.

The first limitation of this thesis is the difficulty of exploring all possible feedback modalities for the haptic feedback device. Of all the types of haptic feedback technologies (force, vibrotactile, electrotactile, ultrasound and thermal feedback), only vibrotactile feedback was explored for the design of the haptic feedback device in this thesis.

The next limitation of this thesis is the fidelity of chosen sensors. For example, the accuracy of proximity measurements may be higher if, say, a laser sensor was used to measure proximity of the gripper to the cooking surface and table instead of an ultrasound sensor.

The next limitation of this thesis is the possibility of the use of more combinations of feedback modalities. Possible feedback modalities and combinations of feedback modalities are not limited to the ones explored in this thesis. Other unexplored modalities may yield different results or may be easier to implement.

Another limitation of this thesis is the demographics of participants that volunteered for the study. The studies were carried out in an academic environment and participants were invited from that environment. A more diverse demographics will be a better representation of the society. Further research may be carried out with care givers and nurses as the operators in order to gather feedback from healthcare professionals that work in care giving environments. The feedback provided may be used to improve the design of tele-operation systems in this context.

The next limitation of this thesis is in the number of participants that took part in the studies. To increase statistical significance for future studies, the number of participants may be increased.

Another limitation of this thesis is the environment in which the study was carried out.The studies were carried out in a controlled environment and may not reflect other factors that may affect the results if the studies were to be replicated in real-world scenarios. Future studies may be carried out in real-world assisted living environments.

The next limitation of this thesis is that number of tasks carried out. However, the task was specifically considered because it comprised of key elements which will be part of a number of assistive tasks in an assisted living scenario.

For all the studies reported in this thesis, the same brand of robot was used. It may be important to compare different designs with different brands of robots. Ease of use scores by participants may also be different for different robot brands. Related to the choice of robot also is the range of motion each robot is capable of executing. This was however kept constant for all the studies carried out. It may also be important to carry out consultations with healthcare professionals on the requirements for designing such tele-operation systems in the early stages of the various software and hardware development and not relying only on literature. This may provide additional information needed to design feedback modalities.

For all the studies carried out, safety was introduced into the system by the principal researcher intervening. For real life applications, intelligent safety measures must be added to the system. Since the robots will operate in close proximity to humans, virtual force fields may be introduced to introduce a degree of safety.

Appendix A

APPENDIX A: CONSENT FORM

13/2/2018

Version 3

Consent Form

You have been invited to take part in this research study on "investigating optimal sensory feedback modalities for effective teleoperation of a robot to provide remote assistance for assisted living tasks" as described in the information sheet.

Please read the statements below and sign if you agree with them

- I have read and understood the information sheet about this study
- I have been given enough time to decide if I would like to participate and given the opportunity to ask questions about the study
- I have received satisfactory answers to all my questions
- I have received enough information about this study
- I understand that I am / the participant is free to withdraw from this study:
    - At any time (until such date as this will no longer be possible, which I have been told)
    - Without giving a reason for withdrawing
- Following discussion with the researcher about the activities involved in this study, I agree to one or more of the activities (as described in the information sheet)
- **Optional** - I am happy for the video recording to be digitally anonymised so that I cannot be recognised and used for dissemination as part of academic presentations at conferences and seminars.

  Please Tick if you agree with the anonymised use of your video as stated ☐
- I agree to take part in this study

Signed (participant)	Date:
Name in block letters:	
Researcher's Name:	
Researcher's Signature:	
This project is supervised by: Praminda Caleb-Solly	

Appendix B

APPENDIX B: DEMOGRAPHIC QUESTIONNAIRE

UWE Bristol University of the West of England

Bristol Robotics Laboratory

26/2/2018 Version 3

Demographic Questionnaire

Date: ………

Participant code: …………………………………………………………………………… (Researcher to insert code)

Gender:	Occupation:
Familiar with operating a robot? Yes/No If Yes – Please state what experience you have of operating a robot(s) Type of robot(s) operated: Number of weeks, months and years of experience of operating robots: _____Weeks _______Months ________Years	
Gaming experience? Yes/No If Yes – Please state what experience you have of playing computer games Types of computer games played most frequently: Including platform (Xbox, Kinect, VR, Windows, smart Phone, Playstation, Nintendo Wii) Number of weeks, months and years of experience of playing computer games: _____Weeks _______Months ________Years	
Age range (please circle) 18 – 25 26 – 35 36 -50 51-65 65+	

1. Are you presently on medications that may affect your level of concentration? Y/N
2. Do you have trouble distinguishing red, blue or green colours? Y/N
3. Have you been diagnosed of having tunnel vision? Or do you find it difficult identifying things in your peripheral vision? Y/N
4. Do you have any problems with your hearing (using a hearing aid or tinnitus)?
   - ☐ Using hearing aid
   - ☐ Tinnitus
5. Would you say you have a fear of or aversion to loud sounds? Y/N

Signed: Date:

Appendix C

Appendix C: Study Information Sheet

Version 3 26/2/2018

Information Sheet

PhD research study (Investigating optimal sensory feedback modalities for effective teleoperation of a robot to provide remote assistance for collaborative assisted living tasks)

Investigator: Joseph Oluwatobiloba Bolarinwa

Director of study: Praminda Caleb-Solly

1. Introduction

You have been invited to participate in the research study to explore the importance (timeliness, safety and accuracy) of feedback mechanisms in tele-operating a robotic arm (JACO2 robot) to carry out some collaborative assisted living tasks in the assisted living studio of the Bristol Robotics Laboratory. This study is important for my PhD research titled "Investigating optimal sensory feedback modalities for effective teleoperation of a robot to provide remote assistance for collaborative assisted living tasks".

Please read this form and ask any questions that you may have before participating in this study.

2. Purpose of Study

The purpose of this study is to examine the impact of sensory feedback using different modalities (peripheral vision) for the successful teleoperation of a robot arm in an assisted living environment. The ultimate aim of a tele-operated assistive robot would be to provide remote assistance to an older or younger adult with disabilities. Such a tele-operated system should be usable by anyone who is able to, and wants to help someone remotely while socially engaging with them. As such it is important to design a system that is intuitive and easy to use. We are trialling different ways of providing the tele-operator feedback – via sound, vision and touch, to find out which feedback modes help with remotely successfully carrying out teleoperation tasks. In this experiment, we will be using peripheral vision to provide information about the rotation of the gripper to the tele-operator.

3. What will I do if I decide to take part?

Upon agreeing to participate you will be tasked with tele-operating a JACO2 robot arm using the robot controller to pick up a jar filled with sunflower seeds and moved to a specified location. You will also be required to pour the content of the jar into another jar six (7) times with video feedbacks, peripheral vision feedback, haptic feedback, with and without collaboration with the principal investigator. The accuracy of execution and time taken to carry out the tasks will then be recorded.

For all the activities, we will be using the Tobii eye tracker to monitor where participants are looking at as they carry out various tasks. We shall also monitor some of vital body signals as tasks are carried out.

When the researcher contacts you to arrange your session he will also enquire if you need any support with understanding verbal or written instructions in English. If you do, you will be requested to bring along bring your interpreter that usually helps you with your work or study to support you during the experiment. During the experiments, the researcher will be present to guide you through the process and answer any questions you may have as you carry out the tasks. As you carry out the tasks, video recordings will be made of the process to study the different ways participants carry out the tasks. All video recordings will be anonymously analysed and stored.

Ultimately, this study will form part of my PhD study with results being published as part of a book, journal or conference proceedings.

4. Why you are invited

The reason you are being invited is because we need to conduct these experiments with people like yourself who in the future might use this approach to help a disabled friend or relative remotely. We want to ensure our system is easy and safe for everyone to use. As such previous experience with using a robot is not important though it will be considered in some of our analysis.

5. Is my participation compulsory?

Your participation is not compulsory – it is entirely optional. You will be required to sign a consent form and given a copy to keep if you choose to participate.

6. Right to Refuse or Withdraw

The decision to participate in this study is entirely up to you. You can stop participating in the study *at any time* without affecting your relationship with the investigators of this study. You don't have to answer questions you don't want to, and you can withdraw completely from the study at any point during the process. Additionally, you have the right to request that the investigator not use any of participation material and information up to 1 month after the study. In the case of such withdrawal please send a mail to:

The investigator: Joseph Bolarinwa joseph2.bolarinwa@live.uwe.ac.uk

7. Risks/Discomforts of Being in this Study

There are no foreseeable/expected risks posed by taking part in this study. However due to the nature of the study using sound and colour we have to make sure that people who have certain conditions are catered for in our experiments.

You will be asked to complete a questionnaire (attached with this information sheet) which will give the researcher the information needed to set up the experiment correctly for you.

If you are unsure of any of the questions or have any concerns please discuss these with the researcher prior to participating in the study.

Whatever group you are assigned, participating in the research will provide us with valuable data for our study.

8. Benefits of Being in the Study

There are no direct benefits in return for taking part in this study but your participation helps us understand better the impact of feedback mechanisms in carrying out tele-operation tasks.

9. Confidentiality and data protection

All personal data will be stored confidentially. The records of this study will be kept strictly confidential. Research records will be kept in a locked file, and all electronic information will be stored in secure storage devices. All data gathered will also be used anonymously.

10. Right to Ask Questions and Report Concerns

You have the right to ask questions about this research study and to have those questions answered by me before, during or after the research. If you like, a summary of the results of the study will be sent to you.

11. Who has checked to make sure the study is properly conducted and what do I do if I decide to participate or have concerns during the study?

This research has been approved by the University of the West of England's Research Ethics Committee.

If you wish to participate please contact:

Joseph Bolarinwa
PhD student, Bristol Robotics Laboratory
University of the West of England
Tel: 07480955398 or Email: joseph2.bolarinwa@live.ac.uk

If you have any concerns about this research after participating in the study please contact my supervisor:

Dr Praminda Caleb-Solly
Associate Professor, Bristol Robotics Laboratory
University of the West of England
Tel: 01173283178 or Email Praminda.caleb-solly@uwe.ac.uk

APPENDIX D

Appendix D: System Usability Scale Questionnaire

UWE Bristol University of the West of England

brl Bristol Robotics Laboratory

System Usability Scale (Robot Controller)

After completing the tasks, please tell us about your experience of controlling the JACO2 arm you have used – referred to below as 'the system'. Your response will help us understand what aspect of the system you found easy to use and what aspects you believe can be improved upon. Please read each statement and indicate how strongly you agree or disagree with the statement by circling one number on each scale. Please be aware that the 10 statements in the questionnaire alternate between being positively phrased and negatively phrased.

(Note: totally disagree = 1; totally agree = 5)

1. I think that I would be happy to use this system frequently.

1	2	3	4	5

2. I found the system unnecessarily complex.

1	2	3	4	5

3. I thought the system was easy to use.

1	2	3	4	5

4. I think that I would need the support of a technical person to be able to use this system.

1	2	3	4	5

5. I found the various functions in this system were well integrated.

1	2	3	4	5

6. I thought there was too much inconsistency in this system.

1	2	3	4	5

7. I would imagine that most people would learn to use this system very quickly.

1	2	3	4	5

8. I found the system very cumbersome to use.

1	2	3	4	5

9. I felt very confident using the system.

1	2	3	4	5

10. I needed to learn a lot of things before I could get going with this system.

1	2	3	4	5

Robot Controller

1. How functional* do you feel the Robot controller is?

   *Functionality can be viewed as a set of functions that the Robot controller is equipped with

   Please score how you feel on a scale of 0 (Robot controller is completely non-functional) to 5 (Robot controller is completely functional).________________

   Please tell us why you gave this score (Robot controller functionality):

2. How responsive do you feel the robot Robot controller is?

   Please score how you feel on a scale of 0 (robot Robot controller is completely non-responsive) to 5 (robot Robot controller is completely responsive). _________

   Please tell us why you gave this score (robot Robot controller responsiveness):

3. How much do you feel that your control of the robot was affected by the robot Robot controller responsiveness?

   Please score how you feel on a scale of 0 (not at all) to 5 (to a great extent). _________

   Please tell us why you gave this score:

Summary Table

Please grade on a scale of 1 -10

	Peripheral vision	Verbal collaboration	Haptic feedback	Ease of use (1 - 10)	How useful was the feedback from end users (1 - 10)
Condition 1 (No Feedback)	X	X	X		NA
Condition 2 (Verbal collaboration)	X	√	X		
Condition 3 (Peripheral Vision)	√	X	X		NA
Condition 4 (Peripheral vision and verbal collaboration)	√	√	X		
Condition 5 (Haptic feedback)	X	X	√		
Condition 6 (Haptic feedback and verbal collaboration)	X	√	√		
Condition 7 (Haptic feedback, Peripheral vision and verbal collaboration)	√	√	√		

What do you think could be improved in the collaboration with end users?

____

____

Appendix E

Appendix E: Study Protocol

Experiment Protocol

1. Upon arrival, provide participants with study information and consent form. Briefly explain what participants will have to do, how long the test will take (instructions below) and answer the questions participants have towards the experiment. Participant must sign the consent form before carrying out with the experiment.
2. Provide participants with Demographic questionnaire.
3. Connect 4 web cameras, the Jaco2 USB, the researcher's input button, and the USB mouse to the USB hubs that are connected to the PC. Because of the data load from the cameras, we split the 4 cameras to different hubs.
   Hub 1: 2 web cameras, Jaco2 USB, researcher's input button
   Hub 2: 2 web cameras, USB mouse
4. Start the IP camera viewer 4 to get the camera feeds from the 4 cameras on the robot end. Use win + G to start recording the web camera views.
5. Open the 'Stage_Completion' Arduino IDE, identify the port number and upload the c code to the Arduino.
6. Start the experiment's C++ code using visual studio. In the Code, type in the Arduino's port number and change the text files' names to the names of the participants. Remember to signify the order number of the experiment.
7. Put on the Cam coder to record the participants' behaviour/reactions during the experiment.
8. Help participants put on the Tobii pro eye tracker glasses. Attach the appropriate lenses where necessary. Turn it on and calibrate. Start recording the data.
9. Put Empatica wristband on participants' non-dominant hand. Turn it on and connect to the app on the mobile device. Explain how to put a marker on the wristband (by pressing a button until it blinks).
10. Allow participants practice using the controller to move the robot around for about 5 minutes. Practice moving the robot forward and backward, left and right, up and down, rotating the gripper as well as opening and closing the gripper.
11. Put the jars in their respective positions, 1 and 2, and pour the sunflower seeds into the jar in position 1.
12. Put the Jaco2 arm in its home position and rotate to angle 150.273
13. Start HRI task (counterbalancing order is provided below (include this order)). Ask participant to put the first marker and start the trial.

14. Once participants have completed the first stage, ask participant to put a second marker on the Empatica E4 wristband). The markers should be added at the completion of each stage.

    Stage 1: Moving the arm from the home position to grasp the jar in position 1.

    Stage 2: Move the grasped jar from position 1 to position 2 and empty the content into jar 2.

    Stage 3. Move the emptied jar back to position one.

15. After each task
    I. Stop the cam coder
    II. Save the recording on the eye tracker tablet
    III. Save the camera viewer 4 screen recording
    IV. Stop the Empatica measurements
    V. Change the file names in the C++ code
    VI. Empty the content of jar 2 back into jar 1
16. After HRI task has been completed, participants are given post study questionnaire.
17. After completion of the questionnaire, debrief participant.

Counter Balancing order

i. Carry out the task without peripheral vision and without collaboration with researcher. Visual feedback is provided though.
ii. Carry out the task without peripheral vision but in collaboration with researcher. Visual feedback is provided though.
iii. Carry out the task with peripheral vision and camera feedback, but without collaboration with researcher.
iv. Carry out the task with peripheral vision and camera feedback in collaboration with the researcher.

Participants	Order
1,5,9,13,17	i,ii,iii,iv
2,6,10,14,18	ii,iii,iv,i
3,7,11,15,19	iii,iv,i,ii
4,8,12,16,20	iv,i,ii,iii

Parameters measured	How measurement takes place	
Time	In code	
Stage completion/Time taken	Researcher input	
Stage Success	Researcher input	
Participants' video	External camera	
Participants' focus	Eye Tracker	
Participants' Vital signals	Empatica wrist band	
Robot end recording	Recording of monitor screen	

Participant instructions

Task Description

Thank you again for accepting to take part in this experiment. You will be required to move the robot from the home position to pick up a jar, move the jar to a new position and empty the content into another jar at that location. The task will be carried out in collaboration with the researcher who will engage in verbal conversations with you.

Robot Controller

Please feel free to play around with the robot controller to get used to how it works. Practice moving the robot forward and backwards, up and down, left and right. Also, practice opening and closing the gripper. You can do a mock movement from the home position to the pick-up position and final position.

Camera Feedback

To carry out the task, you will be provided with camera feeds from four cameras on a screen. The feeds provide you with visuals of what is happening on the robot end.

Peripheral Vision

Whilst you are expected to focus on the camera feeds, information about the gripper orientation will be provided on another screen as colour changes of the screen. It is expected that you receive this information through your peripheral vision. The information will help you vertically align the gripper with the jar to be picked up.

When the screen turns green, it implies that the gripper is aligned with the jar and can be grasped. When it turns light blue it means that the gripper is slightly aligned to the left and to correct the alignment, the controller knob should be turned slightly to the right. When the screen turns dark blue, it implies that the gripper is aligned further to the left and the gripper knob should be turned further to the right. If the screen turns light red, it means that the gripper is aligned slightly to the right and the gripper knob should be slightly turned to the left. When the screen turns deep red, it means that the gripper is turned further to the right and the gripper knob should be turned further to the left.

Eye Tracker

The Tobii eye tracker is used to monitor your gaze during the experiment.

Video Recording

We will also be taking a video recording your reactions during the experiment. This will be used for further analysis of performance. The data will be used only for further analysis and will be kept securely in a locked draw accessible only to study researcher and his supervisor.

Stress Checker

During the experiment, you will be asked to wear a device on your non dominant hand to help monitor your heart rate, skin temperature and skin electro-dermal activity (sweat).

APPENDIX F

Appendix F: NASA TLX Questionnaire

Pairwise Subscale Comparisons

Effort or **Performance**	**Temporal Demand** or **Frustration**
Temporal Demand or **Effort**	**Physical Demand** or **Frustration**
Performance or **Frustration**	**Physical Demand** or **Temporal Demand**
Physical Demand or **Performance**	**Temporal Demand** or **Mental Demand**
Frustration or **Effort**	**Performance** or **Mental Demand**
Performance or **Temporal Demand**	**Mental Demand** or **Effort**
Mental Demand or **Physical Demand**	**Effort** or **Physical Demand**
Frustration or **Mental Demand**	

Subject ID: ______________________________ **Task ID:** ___________________________________

RATING SHEET

MENTAL DEMAND

Low **High**

PHYSICAL DEMAND

Low **High**

TEMPORAL DEMAND

Low **High**

PERFORMANCE

Good **Poor**

EFFORT

Low **High**

FRUSTRATION

Low **High**

Bibliography

[1] 3D Systems, Haptic Devices, 2021.

[2] A. Acemoglu, J. Krieglstein, D. G. Caldwell, F. Mora, L. Guastini, M. Trimarchi, A. Vinciguerra, A. L. C. Carobbio, J. Hysenbelli, M. Delsanto, O. Barboni, S. Baggioni, G. Peretti, and L. S. Mattos, 5g robotic telesurgery: Remote transoral laser microsurgeries on a cadaver, IEEE Transactions on Medical Robotics and Bionics, 2 (2020), pp. 511–518.

[3] Adafruit, Vibrating Mini Motor Disc, 2019.

[4] Adolphus, Methods of empirical research, 2018.

[5] Age UK, New analysis shows number of older people with unmet care needs soars to record high | Age UK 2018.

[6] M. Ahn, H. J. Kwon, and J. Kang, Supporting Aging-in-Place Well: Findings From a Cluster Analysis of th Journal of Applied Gerontology, 39 (2020), pp. 3–15.

[7] M. Akçayir and G. Akçayir, Advantages and challenges associated with augmented reality for education: A Educational Research Review, 20 (2017), pp. 1–11.

[8] A. Al-Ibadi, S. Nefti-Meziani, and S. Davis, Active Soft End Effectors for Efficient Grasping and Safe Ha IEEE Access, 6 (2018), pp. 23591–23601.

[9] M. Alemi, A. Ghanbarzadeh, A. Meghdari, and L. J. Moghadam, Clinical Application of a Humanoid Robot in Pediatric Cancer Interventions, International Journal of Social Robotics, 8 (2016), pp. 743–759.

[10] F. Amirabdollahian, S. Livatino, B. Vahedi, R. Gudipati, P. Sheen, S. Gawrie-Mohan, and N. Vasdev, Prevalence of haptic feedback in robot-mediated surgery: a systematic review of literature, Journal of Robotic Surgery, 12 (2018), pp. 11–25.

[11] N. D. Anderson, Teaching signal detection theory with pseudoscience, Frontiers in Psychology, 6 (2015), p. 762.

[12] R. ANDERSON AND M. SPONG, Bilateral control of teleoperators with time delay, in Proceedings of the 1988 IEEE International Conference on Systems, Man, and Cybernetics, vol. 1, 1988, pp. 131–138.

[13] Y. ANSARI, M. MANTI, E. FALOTICO, Y. MOLLARD, M. CIANCHETTI, AND C. LASCHI, Towards the development of a soft manipulator as an assistive robot for personal care of elderly pe International Journal of Advanced Robotic Systems, 14 (2017), p. 1729881416687132.

[14] M. K. APOSTOLOS, H. ZAK, H. DAS, AND P. S. SCHENKER, Multisensory feedback in advanced teleoperations: benefits of auditory cues, in Sensor Fusion V, P. S. Schenker, ed., vol. 1828, International Society for Optics and Photonics, SPIE, 1992, pp. 98–105.

[15] S. F. ATASHZAR, I. G. POLUSHIN, AND R. V. PATEL, A small-gain approach for nonpassive bilateral telerobotic rehabilitation: Stability analysis and controller synthesis, IEEE Transactions on Robotics, 33 (2017), pp. 49–66.

[16] M. AUS DER WIESCHEN, K. FISCHER, K. KUKLIŃSKI, L. JENSEN, AND T. SAVARIMUTHU, Multimodal Feedback in Human-Robot Interaction: An HCI-Informed Comparison of Feedback Mo jan 2020, pp. 990–1017.

[17] V. BANTHIA, Y. MADDAHI, S. BALAKRISHNAN, AND N. SEPEHRI, Haptic-enabled teleoperation of base-excited hydraulic manipulators applied to live-line maintenance, in 2014 IEEE/RSJ International Conference on Intelligent Robots and Systems, 2014, pp. 1222–1229.

[18] J. BARDI, What is Virtual Reality, 2020.

[19] M. BEGUM, R. WANG, R. HUQ, AND A. MIHAILIDIS, Performance of daily activities by older adults with dementia: The role of an assistive robot, in 2013 IEEE 13th International Conference on Rehabilitation Robotics (ICORR), vol. 2013, IEEE, jun 2013, pp. 1–8.

[20] A. BEJCZY AND W. S. KIM, Predictive displays and shared compliance control for time-delayed telemanipulation, in EEE International Workshop on Intelligent Robots and Systems, Towards a New Frontier of Applications, 1990, pp. 407–412 vol.1.

[21] J. BIMBO, C. PACCHIEROTTI, M. AGGRAVI, N. TSAGARAKIS, AND D. PRATTICHIZZO, Teleoperation in cluttered environments using wearable haptic feedback, in 2017 IEEE/RSJ International Conference on Intelligent Robots and Systems (IROS), 2017, pp. 3401–3408.

[22] D. Black, S. Lilge, C. Fellmann, A. V. Reinschluessel, L. Kreuer, A. Nabavi, H. K. Hahn, R. Kikinis, and J. Burgner-Kahrs, Auditory Display for Telerobotic Transnasal Surgery Using a Continuum Robot, Journal of Medical Robotics Research, 04 (2019), p. 1950004.

[23] J. Bolarinwa, I. Eimontaite, S. Dogramadzi, T. Mitchell, and P. Caleb-Solly, The use of different feedback modalities and verbal collaboration in tele-robotic assistance, in 2019 IEEE International Symposium on Robotic and Sensors Environments (ROSE), 2019, pp. 1–8.

[24] J. Bolarinwa, A. Smith, A. Aijaz, A. Stanoev, and M. Giuliani, Demo: Untethered haptic teleoperation for nuclear decommissioning using a low-power wireless control technology, in IEEE INFOCOM 2022 - IEEE Conference on Computer Communications Workshops (INFOCOM WKSHPS), 2022, pp. 1–2.

[25] J. Bradbury, Taste perception: cracking the code, PLoS Biology, 2 (2004), p. E64.

[26] A. Bradford, The Five (and More) Senses, oct 2017.

[27] F. Brizzi, L. Peppoloni, A. Graziano, E. D. Stefano, C. A. Avizzano, and E. Ruffaldi, Effects of Augmented Reality on the Performance of Teleoperated Industrial Assembly Tasks in a IEEE Transactions on Human-Machine Systems, 48 (2018), pp. 197–206.

[28] P. Caleb-Solly, A brief introduction to ... Assistive robotics for independent living, Perspectives in Public Health, 136 (2016), pp. 70–72.

[29] G. Chance, A. Camilleri, B. Winstone, P. Caleb-Solly, and S. Dogramadzi, An assistive robot to support dressing - strategies for planning and error handling, in 2016 6th IEEE International Conference on Biomedical Robotics and Biomechatronics (BioRob), 2016, pp. 774–780.

[30] G. Chance, A. Jevtić, P. Caleb-Solly, G. Alenyà, C. Torras, and S. Dogramadzi, "Elbows Out"—Predictive Tracking of Partially Occluded Pose for Robot-Assisted Dressing, IEEE Robotics and Automation Letters, 3 (2018), pp. 3598–3605.

[31] J. Y. C. Chen, E. C. Haas, and M. J. Barnes, Human Performance Issues and User Interface Design for Teleoperated Robots, IEEE Transactions on Systems, Man, and Cybernetics, Part C (Applications and Reviews), 37 (2007), pp. 1231–1245.

[32] K. Chen and A. H.-S. Chan, Use or non-use of gerontechnology–a qualitative study, International journal of environmental research and public health, 10 (2013), pp. 4645–4666.

[33] Z. Chen, B. Liang, T. Zhang, and X. Wang, Bilateral Teleoperation in Cartesian Space with Time-Va International Journal of Advanced Robotic Systems, 9 (2012), p. 110.

[34] K.-H. Cheng and C.-C. Tsai, Affordances of Augmented Reality in Science Learning: Suggestions for Journal of Science Education and Technology, 22 (2013), pp. 449–462.

[35] M. Cortese, M. Cempini, P. R. de Almeida Ribeiro, S. R. Soekadar, M. C. Carrozza, and N. Vitiello, A mechatronic system for robot-mediated hand telerehabilitation, IEEE/ASME Transactions on Mechatronics, 20 (2015), pp. 1753–1764.

[36] D. Dobbelstein, P. Henzler, and E. Rukzio, Unconstrained Pedestrian Navigation based on Vibro- may 2016.

[37] C. Domingues, M. Essabbah, N. Cheaib, S. Otmane, and A. Dinis, Human-Robot-Interfaces based on Mixed Reality for Underwater Robot Teleoperation, IFAC Proceedings Volumes, 45 (2012), pp. 212–215.

[38] Double, Double 3, 2020.

[39] I. El Rassi and J.-M. El Rassi, A review of haptic feedback in tele-operated robotic surgery, Journal of Medical Engineering & Technology, 44 (2020), pp. 247–254.

[40] F. Elise van Beek, Making Sense of haptics: Fundamentals of perception and implications for device Springer, Switzerland, Cham, 2017.

[41] S. R. Ellis, On Redundancy in the Design of Spatial Instruments, Human Factors and Ergonomics Society Annual Meeting Proceedings, 49 (2005), pp. 1561–1563.

[42] M. R. Endsley, Toward a theory of situation awareness in dynamic systems, Human Factors, 37 (1995), pp. 32–64.

[43] Engineering Acoustics Inc., Haptics, 2021.

[44] A. Falk, U. Fischbacher, and E. Fehr, Driving Forces Behind Informal Sanctions, Econometrica, 73 (2005), pp. 2017–2030.

[45] W. R. Ferrell, Remote manipulation with transmission delay, IEEE Transactions on Human Factors in Electronics, HFE-6 (1965), pp. 24–32.

[46] W. R. Ferrell and T. B. Sheridan, Supervisory control of remote manipulation, IEEE Spectrum, 4 (1967), pp. 81–88.

[47] M. D. Fletcher, J. Zgheib, and S. W. Perry, Sensitivity to haptic sound-localisation cues, Scientific Reports, 11 (2021), p. 312.

[48] C. FONG, R. DOTSON, AND A. BEJCZY, Distributed microcomputer control system for advanced teleoperation, in Proceedings. 1986 IEEE International Conference on Robotics and Automation, vol. 3, 1986, pp. 987–995.

[49] M. FRITSCHER, F. SITTNER, D. ASCHENBRENNER, M. KRAUSS, AND K. SCHILLING, The Adaptive Management and Security System for Maintenance and Teleoperation of Industrial Robots IFAC-PapersOnLine, 49 (2016), pp. 6–11.

[50] J. FROST, Central Limit Theorem Explained, 2020.

[51] Y. GAFFARY AND A. LÉCUYER, The Use of Haptic and Tactile Information in the Car to Improve Driving Safe Frontiers in ICT, 5 (2018), p. 5.

[52] P. GALAMBOS, A. ROKA, G. SOROS, AND P. KORONDI, Visual feedback techniques for telemanipulation and system status sensualization, in 2010 IEEE 8th International Symposium on Applied Machine Intelligence and Informatics (SAMI), IEEE, jan 2010, pp. 145–151.

[53] N. GAVISH, T. GUTIÉRREZ, S. WEBEL, J. RODRÍGUEZ, M. PEVERI, U. BOCKHOLT, AND F. TECCHIA, Evaluating virtual reality and augmented reality training for industrial maintenance and as Interactive Learning Environments, 23 (2015), pp. 778–798.

[54] V. GIRBÉS-JUAN, V. SCHETTINO, Y. DEMIRIS, AND J. TORNERO, Haptic and visual feedback assistance for dual-arm robot teleoperation in surface conditioning tasks, IEEE Transactions on Haptics, 14 (2021), pp. 44–56.

[55] P. GLIESCHE, T. KRICK, M. PFINGSTHORN, S. DROLSHAGEN, C. KOWALSKI, AND A. HEIN, Kinesthetic Device vs. Keyboard/Mouse: A Comparison in Home Care Telemanipulation, Frontiers in Robotics and AI, 7 (2020), p. 172.

[56] C. GONZÁLEZ, J. E. SOLANES, A. MUÑOZ, L. GRACIA, V. GIRBÉS-JUAN, AND J. TORNERO, Advanced teleoperation and control system for industrial robots based on augmented virtuality and haptic feedback, Journal of Manufacturing Systems, 59 (2021), pp. 283–298.

[57] K. GORIS, J. SALDIEN, B. VANDERBORGHT, AND D. LEFEBER, Probo, an Intelligent Huggable Robot for HRI Studies with Children, feb 2010.

[58] P. GREEN, J. HILL, J. JENSEN, AND A. SHAH, Telepresence surgery, IEEE Engineering in Medicine and Biology Magazine, 14 (1995), pp. 324–329.

[59] B. GURUS, David Attenborough on His Decades-Long Career | Natural History Masterclass, 2018.

[60] A. HACINECIPOGLU, E. I. KONUKSEVEN, AND A. B. KOKU, Evaluation of haptic feedback cues on vehicle teleoperation performance in an obstacle avoidance s
IEEE, 2013, pp. 689–694.

[61] K. Z. HAIGH, L. M. KIFF, AND G. HO, The Independent LifeStyle Assistant: Lessons Learned, Assistive Technology, 18 (2006), pp. 87–106.

[62] C. HANSEN, D. BLACK, C. LANGE, F. RIEBER, W. LAMADÉ, M. DONATI, K. J. OLDHAFER, AND H. K. HAHN, Auditory support for resection guidance in navigated liver surgery, The International Journal of Medical Robotics and Computer Assisted Surgery, 9 (2013), pp. 36–43.

[63] W. HARRIS, Types of Haptic Feedback | HowStuffWorks, 2018.

[64] T. HASSAN, A. HAMEED, S. NISAR, N. KAMAL, AND O. HASAN, Al-zahrawi: A telesurgical robotic system for minimal invasive surgery, IEEE Systems Journal, 10 (2016), pp. 1035–1045.

[65] J. HEATH, PWM: Pulse Width Modulation: What is it and how does it work?, 2017.

[66] P. HEBERT, J. MA, J. BORDERS, A. AYDEMIR, M. BAJRACHARYA, N. HUDSON, K. SHANKAR, S. KARUMANCHI, B. DOUILLARD, AND J. BURDICK, Supervised Remote Robot with Guided Autonomy and Teleoperation (SURROGATE): A framework
in 2015 IEEE International Conference on Robotics and Automation (ICRA), 2015, pp. 5509–5516.

[67] H. HEDAYATI, M. WALKER, AND D. SZAFIR, Improving Collocated Robot Teleoperation with Augmente
in Proceedings of the 2018 ACM/IEEE International Conference on Human-Robot Interaction, HRI '18, New York, NY, USA, 2018, Association for Computing Machinery, pp. 78–86.

[68] S. HIRCHE, A. BAUER, AND M. BUSS, Transparency of haptic telepresence systems with constant time
in Proceedings of 2005 IEEE Conference on Control Applications, 2005. CCA 2005., 2005, pp. 328–333.

[69] G. HIRZINGER, J. HEINDL, AND K. LANDZETTEL, Predictive and knowledge-based telerobotic control concepts, in Proceedings, 1989 International Conference on Robotics and Automation, 1989, pp. 1768–1777 vol.3.

[70] P. F. HOKAYEM AND M. W. SPONG, Bilateral teleoperation: An historical survey, Automatica, 42 (2006), pp. 2035–2057.

[71] H.-C. HU AND Y.-C. LIU, Passivity-based control framework for task-space bilateral teleoperation with
ISA Transactions, 70 (2017), pp. 187–199.

[72] L. Hung, C. Liu, E. Woldum, A. Au-Yeung, A. Berndt, C. Wallsworth, N. Horne, M. Gregorio, J. Mann, and H. Chaudhury, The benefits of and barriers to using a social robot PARO in care settings: a scoping review, BMC Geriatrics, 19 (2019), p. 232.

[73] IEEE Spectrum, Baxter, 2020.

[74] Interlink Electronics, FSR 402 Short, 2019.

[75] K. Ishac and K. Suzuki, Gesture based robotic arm control for meal time care using a wearable sensory jac in 2016 IEEE International Symposium on Robotics and Intelligent Sensors (IRIS), dec 2016, pp. 122–127.

[76] M. J. Islam, J. Hong, and J. Sattar, Person-following by autonomous robots: A categorical overview, The International Journal of Robotics Research, 38 (2019), pp. 1581–1618.

[77] W. A. Isop, C. Gebhardt, T. Nägeli, F. Fraundorfer, O. Hilliges, and D. Schmalstieg, High-Level Teleoperation System for Aerial Exploration of Indoor Environments, Frontiers in Robotics and AI, 6 (2019), p. 95.

[78] M. C. Jimenez and J. A. Fishel, Evaluation of force, vibration and thermal tactile feedback in prosthetic lin in 2014 IEEE Haptics Symposium (HAPTICS), 2014, pp. 437–441.

[79] R. S. Johansson and J. R. Flanagan, Coding and use of tactile signals from the fingertips in object manip Nature Reviews Neuroscience, 10 (2009), pp. 345–359.

[80] N. W. John, S. R. Pop, T. W. Day, P. D. Ritsos, and C. J. Headleand, The Implementation and Validation of a Virtual Environment for Training Powered Wheelchair Manoeu IEEE Transactions on Visualization and Computer Graphics, 24 (2018), pp. 1867–1878.

[81] C. Ju and H. Son, Evaluation of Haptic Feedback in the Performance of a Teleoperated Unmanned Ground International Journal of Control, Automation and Systems, 17 (2019), pp. 168–180.

[82] T. Kato, T. Higashi, and K. Shimizu, Teleoperation of a Robot Arm System Using Pneumatic Artificial Rub in 2010 International Conference on Broadband, Wireless Computing, Communication and Applications, IEEE, nov 2010, pp. 714–718.

[83] B. Kehoe, A. Matsukawa, S. Candido, J. Kuffner, and K. Goldberg, Cloud-based robot grasping with the google object recognition engine, in 2013 IEEE International Conference on Robotics and Automation, 2013, pp. 4263–4270.

[84] N. Kehtarnavaz, N. C. Griswold, and J. K. Eem, Comparison of mono- and stereo-camera systems for autonomous vehicle tracking, in Applications of Artificial Intelligence IX, M. M. Trivedi, ed., vol. 1468, International Society for Optics and Photonics, SPIE, 1991, pp. 467–478.

[85] H.-Y. KIM, Statistical notes for clinical researchers: assessing normal distribution (2) using skewness
Restorative dentistry & endodontics, 38 (2013), pp. 52–54.

[86] K. KIM AND J. E. COLGATE, Haptic Feedback Enhances Grip Force Control of sEMG-Controlled Prosth
IEEE Transactions on Neural Systems and Rehabilitation Engineering, 20 (2012), pp. 798–805.

[87] U. KIM, D.-H. LEE, Y. B. KIM, D.-Y. SEOK, J. SO, AND H. R. CHOI, S-surge: Novel portable surgical robot with multiaxis force-sensing capability for minimally invasive surgery, IEEE/ASME Transactions on Mechatronics, 22 (2017), pp. 1717–1727.

[88] KINOVA, KINOVA JACO™ Prosthetic robotic arm user guide, tech. rep., 2018.

[89] J. K. KOEHN AND K. J. KUCHENBECKER, Surgeons and non-surgeons prefer haptic feedback of instrun
Surgical Endoscopy, 29 (2015), pp. 2970–2983.

[90] K. KRAFT AND W. D. SMART, Seeing is comforting: Effects of teleoperator visibility in robot-mediated health care, in 2016 11th ACM/IEEE International Conference on Human-Robot Interaction (HRI), 2016, pp. 11–18.

[91] R. KRAUT, M. MILLER, AND J. SIEGEL, Collaboration in performance of physical tasks, CSCW '96, ACM, 1996, pp. 57–66.

[92] J. KRITHIKADATTA, Normal distribution, Journal of conservative dentistry : JCD, 17 (2014), pp. 96–97.

[93] I. A. KULING, K. GIJSBERTSE, B. N. KROM, K. J. VAN TEEFFELEN, AND J. B. F. VAN ERP,
Haptic Feedback in a Teleoperated Box & Blocks Task BT - Haptics: Science, Technology, Applicati
Cham, 2020, Springer International Publishing, pp. 96–104.

[94] O.-H. KWON, S.-Y. KOO, Y.-G. KIM, AND D.-S. KWON, Telepresence robot system for english tutoring, in 2010 IEEE Workshop on Advanced Robotics and its Social Impacts, 2010, pp. 152–155.

[95] C. K. Y. LAM LOONG MAN, Y. KOONJUL, AND L. NAGOWAH, A low cost autonomous unmanned ground vehicle, Future Computing and Informatics Journal, 3 (2018), pp. 304–320.

[96] D. LAWRENCE, Stability and transparency in bilateral teleoperation, IEEE Transactions on Robotics and Automation, 9 (1993), pp. 624–637.

[97] H. R. LEE, H. TAN, AND S. SABANOVIC, That robot is not for me: Addressing stereotypes of aging in as
in 2016 25th IEEE International Symposium on Robot and Human Interactive Communication (RO-MAN), IEEE, aug 2016, pp. 312–317.

[98] J. S. LEE, Y. HAM, H. PARK, AND J. KIM, Challenges, tasks, and opportunities in teleoperation of excavator toward human-in-the-loop construction automation, Automation in Construction, 135 (2022), p. 104119.

[99] K.-H. LEE, V. PRUKS, AND J.-H. RYU, Development of shared autonomy and virtual guidance generation sys in 2017 14th International Conference on Ubiquitous Robots and Ambient Intelligence (URAI), IEEE, jun 2017, pp. 457–461.

[100] L. D. LEE, HEE RIN; RIEK, Reframing Assistive Robots to Promote Successful Aging, ACM Transactions on Human-Robot Interaction (THRI), 7 (2018).

[101] S. LI, R. RAMESHWAR, A. M. VOTTA, AND C. D. ONAL, Intuitive Control of a Robotic Arm and Hand System With Pneumatic Haptic Feedback, IEEE Robotics and Automation Letters, 4 (2019), pp. 4424–4430.

[102] Z. LI, P. MORAN, Q. DONG, R. J. SHAW, AND K. HAUSER, Development of a tele-nursing mobile manipulator for remote care-giving in quarantine areas, in 2017 IEEE International Conference on Robotics and Automation (ICRA), 2017, pp. 3581–3586.

[103] Z. LI AND C. SU, Neural-Adaptive Control of Single-Master–Multiple-Slaves Teleoperation for Coordinated M IEEE Transactions on Neural Networks and Learning Systems, 24 (2013), pp. 1400–1413.

[104] C. LIU, C. ISHI, AND H. ISHIGURO, Auditory scene reproduction for tele-operated robot systems, Advanced Robotics, 33 (2019), pp. 415–423.

[105] S. LIVATINO, D. C. GUASTELLA, G. MUSCATO, V. RINALDI, L. CANTELLI, C. D. MELITA, A. CANIGLIA, R. MAZZA, AND G. PADULA, Intuitive Robot Teleoperation Through Multi-Sensor Informed Mixed Reality Visual Aids, IEEE Access, 9 (2021), pp. 25795–25808.

[106] R. LOOIJE, M. A. NEERINCX, J. K. PETERS, AND O. A. B. HENKEMANS, Integrating Robot Support Functions into Varied Activities at Returning Hospital Visits, International Journal of Social Robotics, 8 (2016), pp. 483–497.

[107] J. LUO, W. HE, AND C. YANG, Combined perception, control, and learning for teleoperation: key technologies, Cognitive Computation and Systems, 2 (2020), pp. 33–43.

[108] H. LV, G. YANG, H. ZHOU, X. HUANG, H. YANG, AND Z. PANG, Teleoperation of Collaborative Robot for Remote Dementia Care in Home Environments, IEEE Journal of Translational Engineering in Health and Medicine, 8 (2020), pp. 1–10.

[109] S. MACHACA, G. UNG, AND J. D. BROWN, Towards an Understanding of the Utility of Dual-Modality H
IEEE Transactions on Medical Robotics and Bionics, 2 (2020), pp. 574–577.

[110] Y. MADDAHI, K. ZAREINIA, AND N. SEPEHRI, An augmented virtual fixture to improve task performance in robot-assisted live-line maintenance, Computers Electrical Engineering, 43 (2015), pp. 292–305.

[111] Y. MAE, T. INOUE, K. KAMIYAMA, M. KOJIMA, M. HORADE, AND T. ARAI, Direct teleoperation system of multi-limbed robot for moving on complicated environments, in 2017 IEEE International Conference on Robotics and Biomimetics (ROBIO), 2017, pp. 1171–1174.

[112] A. T. MAEREG, A. NAGAR, D. REID, AND E. L. SECCO, Wearable Vibrotactile Haptic Device for Stiffness Discrimination during Virtual Interactions, Frontiers in Robotics and AI, 4 (2017), p. 42.

[113] N. MARTURI, A. RASTEGARPANAH, C. TAKAHASHI, M. ADJIGBLE, R. STOLKIN, S. ZUREK, M. KOPICKI, M. TALHA, J. A. KUO, AND Y. BEKIROGLU, Towards advanced robotic manipulation for nuclear decommissioning: A pilot study on tele-operati
in 2016 International Conference on Robotics and Automation for Humanitarian Applications (RAHA), dec 2016, pp. 1–8.

[114] T. MASOOD AND J. EGGER, Augmented reality in support of Industry 4.0—Implementation challenges
Robotics and Computer-Integrated Manufacturing, 58 (2019), pp. 181–195.

[115] N. MAVRIDIS, G. PIERRIS, P. GALLINA, N. MOUSTAKAS, AND A. ASTARAS, Subjective difficulty and indicators of performance of joystick-based robot arm teleoperation with a
in 2015 International Conference on Advanced Robotics (ICAR), 2015, pp. 91–98.

[116] C. MEEKER, T. RASMUSSEN, AND M. CIOCARLIE, Intuitive Hand Teleoperation by Novice Operators U
in 2018 IEEE International Conference on Robotics and Automation (ICRA), IEEE, may 2018, pp. 1–7.

[117] L. MELI, C. PACCHIEROTTI, AND D. PRATTICHIZZO, Sensory subtraction in robot-assisted surgery: Fingertip skin deformation feedback to ensure safety and improve transparency in bimanual haptic interaction, IEEE Transactions on Biomedical Engineering, 61 (2014), pp. 1318–1327.

[118] ——, Experimental evaluation of magnified haptic feedback for robot-assisted needle insertion and pa
The International Journal of Medical Robotics and Computer Assisted Surgery, 13 (2017), p. e1809.

[119] C. K. MENSA AND K. M. YAP, Utilising tele-operation and mobile application in identifying materials of varie
in 2017 IEEE International Symposium on Haptic, Audio and Visual Environments and Games (HAVE), 2017, pp. 1–6.

[120] F. MICHAUD, P. BOISSY, D. LABONTE, H. CORRIVEAU, A. GRANT, M. LAURIA, R. CLOUTIER, M.-A. ROUX, D. IANNUZZI, AND M.-P. ROYER, Telepresence robot for home care assistance, in AAAI Spring Symposium: Multidisciplinary Collaboration for Socially Assistive Robotics, 2007.

[121] D. MIKHALCHUK, What is a haptic feedback (haptics)?, 2017.

[122] M. MINAMOTO, Y. SUZUKI, T. KANNO, AND K. KAWASHIMA, Effect of robot operation by a camera with the eye tracking control, in 2017 IEEE International Conference on Mechatronics and Automation (ICMA), aug 2017, pp. 1983–1988.

[123] MINDSPACE SOLUTIONS, Comparing and Inverting Egocentric and Exocentric Perspectives and Panoramas, 2007.

[124] MINITAB, Using the t-value to determine whether to reject the null hypothesis, 2019.

[125] F. MIYAZAKI, S. MATSUBAYASHI, T. YOSHIMI, AND S. ARIMOTO, A new control methodology toward advanced teleoperation of master-slave robot systems, in Proceedings. 1986 IEEE International Conference on Robotics and Automation, vol. 3, 1986, pp. 997–1002.

[126] L. MOORE, M. WILSON, E. WAINE, R. MASTERS, J. MCGRATH, AND S. VINE, Robotic technology results in faster and more robust surgical skill acquisition than traditional laparoscop
Journal of Robotic Surgery, 9 (2015), pp. 67–73.

[127] A. MORRIS, R. DONAMUKKALA, A. KAPURIA, A. STEINFELD, J. T. MATTHEWS, J. DUNBAR-JACOB, AND S. THRUN, A robotic walker that provides guidance, vol. 1, IEEE, 2003, pp. 2–30 vol.1.

[128] M. MOSTEFA, L. K. E. BOUDADI, A. LOUKIL, K. MOHAMED, AND D. AMINE, Design of mobile robot teleoperation system based on virtual reality, in 2015 3rd International Conference on Control, Engineering & Information Technology (CEIT), 2015, pp. 1–6.

[129] M. R. MOTAMEDI, J.-P. ROBERGE, AND V. DUCHAINE, The Use of Vibrotactile Feedback to Restore Texture Recognition Capabilities, and the Effect of Subject T
IEEE Transactions on Neural Systems and Rehabilitation Engineering, 25 (2017), pp. 1230–1239.

[130] N. MURAUER, Comparison of Scan-Mechanisms in Augmented Reality-Supported Order Picking Proce
nov 2018.

[131] A. NACERI, D. MAZZANTI, J. BIMBO, D. PRATTICHIZZO, D. G. CALDWELL, L. S. MATTOS, AND N. DESHPANDE, Towards a Virtual Reality Interface for Remote Robotic Teleoperation, in 2019 19th International Conference on Advanced Robotics (ICAR), 2019, pp. 284–289.

[132] P. NADRAG, L. TEMZI, H. ARIOUI, AND P. HOPPENOT, Remote control of an assistive robot using force feedback, in 2011 15th International Conference on Advanced Robotics (ICAR), IEEE, jun 2011, pp. 211–216.

[133] S. NEUMEIER, N. GAY, C. DANNHEIM, AND C. FACCHI, On the Way to Autonomous Vehicles Teleoperated Driving, in AmE 2018 - Automotive meets Electronics; 9th GMM-Symposium, 2018, pp. 1–6.

[134] K. A. NICHOLS AND A. M. OKAMURA, A framework for multilateral manipulation in surgical tasks, IEEE Transactions on Automation Science and Engineering, 13 (2016), pp. 68–77.

[135] M. NIEMELÄ, L. VAN AERSCHOT, A. TAMMELA, I. AALTONEN, AND H. LAMMI, Towards Ethical Guidelines of Using Telepresence Robots in Residential Care, International Journal of Social Robotics, (2019).

[136] NODEMCU, NodeMcu, 2021.

[137] K. OBAYASHI, N. KODATE, AND S. MASUYAMA, Socially Assistive Robots and Their Potential in Enhan
Journal of the American Medical Directors Association, 19 (2018), pp. 462–463.

[138] OHMNILABS, OHMNI® TELEPRESENCE ROBOT, 2020.

[139] D. S. PAMUNGKAS AND W. CAESARENDRA, Overview Electrotactile Feedback for Enhancing Human Co
Journal of Physics: Conference Series, 1007 (2018), p. 012001.

[140] G. I. PARISI, E. STRAHL, AND S. WERMTER, Robust fall detection with an assistive humanoid robot, in 2014 IEEE-RAS International Conference on Humanoid Robots, IEEE, nov 2014, pp. 1013–1013.

[141] A. PARSA AND A. FARHADI, New coding scheme for the state estimation and reference tracking of nonl
European Journal of Control, (2020).

[142] A. D. PEARLE, P. F. O'LOUGHLIN, AND D. O. KENDOFF, Robot-Assisted Unicompartmental Knee Arthroplasty, The Journal of Arthroplasty, 25 (2010), pp. 230–237.

[143] L. Pérez, Í. Rodríguez, N. Rodríguez, R. Usamentiaga, and D. F. García, Robot Guidance Using Machine Vision Techniques in Industrial Environments: A Comparative Review, Sensors (Basel, Switzerland), 16 (2016), p. 335.

[144] X. Perrin, R. Chavarriaga, C. Ray, R. Siegwart, and J. d. R. Millán, A comparative psychophysical and EEG study of different feedback modalities for HRI, in Proceedings of the 3rd international conference on Human robot interaction - HRI '08, New York, New York, USA, 2008, ACM Press, p. 41.

[145] J. Pineau, M. Montemerlo, M. Pollack, N. Roy, and S. Thrun, Towards robotic assistants in nursing homes: Challenges and results, Robotics and Autonomous Systems, 42 (2003), pp. 271–281.

[146] M. E. Pollack, L. Brown, D. Colbry, C. E. McCarthy, C. Orosz, B. Peintner, S. Ramakrishnan, and I. Tsamardinos, Autominder: an intelligent cognitive orthotic system for people with memory impairment, Robotics and Autonomous Systems, 44 (2003), pp. 273–282.

[147] G. Pollard and R. Ashton, Heart rate decrease: a comparison of feedback modalities and biofeedback with Biological Psychology, 14 (1982), pp. 245–257.

[148] Precision Microdrives, AB-029 : Vibration Motors - Voltage vs Frequency vs Amplitude, 2015.

[149] L. Pu, W. Moyle, C. Jones, and M. Todorovic, The Effectiveness of Social Robots for Older Adults: A Systematic Review and Meta-Analysis of Randomi The Gerontologist, 59 (2018), pp. e37–e51.

[150] D. Purves, A. George, F. David, K. Lawrence, L. Anthony-Samuel, M. James, and W. Mark, Vision: The Eye, Neuro science, Sinuauer Associates, Sunderland, 2001.

[151] Quanser, QUARC REAL-TIME CONTROL SOFTWARE, 2021.

[152] M. Radi, J. Artigas, C. Preusche, and H. Roth, Transparency Measurement of Telepresence Systems BT - Haptics: Perception, Devices and Scenarios, Berlin, Heidelberg, 2008, Springer Berlin Heidelberg, pp. 766–775.

[153] I. Rae, B. Mutlu, and L. Takayama, Bodies in motion: Mobility, presence, and task awareness in telepresence, in Proceedings of the SIGCHI Conference on Human Factors in Computing Systems, CHI '14, New York, NY, USA, 2014, Association for Computing Machinery, p. 2153–2162.

[154] J. Raisamo, R. Raisamo, and V. Surakka, Comparison of Saltation, Amplitude Modulation, and a Hybrid M IEEE Transactions on Haptics, 6 (2013), pp. 517–521.

[155] G. RAJU, G. VERGHESE, AND T. SHERIDAN, Design issues in 2-port network models of bilateral remote manipulation, in 1989 IEEE International Conference on Robotics and Automation, Los Alamitos, CA, USA, may 1989, IEEE Computer Society, pp. 1316,1317,1318,1319,1320,1321.

[156] J. REBELO AND A. SCHIELE, Performance analysis of time-delay bilateral teleoperation using impedan in 2015 International Conference on Advanced Robotics (ICAR), jul 2015, pp. 28–33.

[157] G. RECKTENWALD, Basic PWM Properties Pulse Width, 2011.

[158] N. L. ROBINSON, T. V. COTTIER, AND D. J. KAVANAGH, Psychosocial Health Interventions by Social Robots: Systematic Review of Randomized Controlled J Med Internet Res, 21 (2019), p. e13203.

[159] S. ROBINSON, M. JONES, P. ESLAMBOLCHILAR, R. MURRAY-SMITH, AND M. LINDBORG, "I Did It My Way": Moving Away from the Tyranny of Turn-by-Turn Pedestrian Navigation, oct 2010.

[160] ROBOTIQ, Applications, 2021.

[161] U. ROBOTS, UNIVERSAL ROBOT UR5e, 2021.

[162] D. RODRIGUEZ, C. PEREZ, M. JAGERSAND, AND P. FIGUEROA, A comparison of smartphone interfaces for teleoperation of robot arms, in 2017 XLIII Latin American Computer Conference (CLEI), 2017, pp. 1–8.

[163] J. RUBIN, What Is Haptics? Part 2: Vibrotactile (Vibration) Feedback | HaptX, 2017.

[164] H. SAEIDI, F. MCLANE, B. SADRFAIDPOUR, E. SAND, S. FU, J. RODRIGUEZ, J. R. WAGNER, AND Y. WANG, Trust-based mixed-initiative teleoperation of mobile robots, in 2016 American Control Conference (ACC), 2016, pp. 6177–6182.

[165] H. SANTACRUZ-REYES, L. G. GARCIA-VALDOVINOS, H. JIMENEZ-HERNANDEZ, T. SALGADO-JIMENEZ, AND L. A. GARCIA-ZARCO, Higher order sliding mode based impedance control for dual-user bilateral teleoperation under unk in 2015 IEEE/RSJ International Conference on Intelligent Robots and Systems (IROS), 2015, pp. 5209–5215.

[166] T. SATO AND S. HIRAI, Language-aided robotics teleoperation system for advanced teleoperation, in ICAR Proc. of Int. Conference on Advanced Robotics, 1985.

[167] P. SCHLEER, P. KAISER, S. DROBINSKY, AND K. RADERMACHER, Augmentation of haptic feedback for teleoperated robotic surgery, International Journal of Computer Assisted Radiology and Surgery, 15 (2020), pp. 515–529.

[168] C. SCHROETER, S. MUELLER, M. VOLKHARDT, E. EINHORN, C. HUIJNEN, H. VAN DEN HEUVEL, A. VAN BERLO, A. BLEY, AND H.-M. GROSS, Realization and user evaluation of a companion robot for people with mild cognitive impairments, in 2013 IEEE International Conference on Robotics and Automation, IEEE, may 2013, pp. 1153–1159.

[169] SEEED, Grove - Haptic Motor, 2021.

[170] K. SHIRRIFF, Arduino - SecretsOfArduinoPWM, 2009.

[171] P. SHULL, K. BARK, AND M. CUTKOSKY, Skin nonlinearities and their effect on user perception for rotational in 2010 IEEE Haptics Symposium, 2010, pp. 77–82.

[172] Y. SILVA, W. SIMÖES, M. TEÓFILO, E. NAVES, AND V. LUCENA, Training environment for electric powered wheelchairs using teleoperation through a head mounted disp in 2018 IEEE International Conference on Consumer Electronics (ICCE), 2018, pp. 1–2.

[173] J. SMISEK, M. M. VAN PAASSEN, AND A. SCHIELE, Haptic guidance in bilateral teleoperation: Effects of guidance inaccuracy, in 2015 IEEE World Haptics Conference (WHC), 2015, pp. 500–505.

[174] J. R. SMITH, E. GARCIA, R. WISTORT, AND G. KRISHNAMOORTHY, Electric field imaging pretouch for robotic graspers, in 2007 IEEE/RSJ International Conference on Intelligent Robots and Systems, IEEE, oct 2007, pp. 676–683.

[175] J. E. SOLANES, A. MUÑOZ, L. GRACIA, A. MARTÍ, V. GIRBÉS-JUAN, AND J. TORNERO, Teleoperation of industrial robot manipulators based on augmented reality, The International Journal of Advanced Manufacturing Technology, 111 (2020), pp. 1077–1097.

[176] Y. SONG, S. GUO, L. ZHANG, AND M. YU, Haptic feedback in robot-assisted endovascular catheterization, in 2017 IEEE International Conference on Mechatronics and Automation (ICMA), 2017, pp. 404–409.

[177] SOUND ENGINEERING ACADEMY, Human Voice Frequency Range - Sound Engineering Academy, 2010.

[178] W. STAAB, Auditory Icons, Earcons, and Speech, 2019.

[179] B. C. STAHL AND M. COECKELBERGH, Ethics of healthcare robotics: Towards responsible research and innov Robotics and Autonomous Systems, 86 (2016), pp. 152–161.

[180] L. STATISTICS, Testing for Normality using SPSS Statistics, 2018.

[181] M.-H. STOLTZ, V. GIANNIKAS, D. MCFARLANE, J. STRACHAN, J. UM, AND R. SRINIVASAN, Augmented Reality in Warehouse Operations: Opportunities and Barriers, IFAC-PapersOnLine, 50 (2017), pp. 12979–12984.

[182] H. SU, J. LI, K. KONG, AND J. LI, Development and experiment of the internet-based telesurgery with microhand robot, Advances in Mechanical Engineering, 10 (2018), p. 1687814018761921.

[183] G. R. SUTHERLAND, S. LAMA, L. S. GAN, S. WOLFSBERGER, AND K. ZAREINIA, Merging machines with microsurgery: clinical experience with neuroArm., Journal of neurosurgery, 118 (2013), pp. 521–529.

[184] G. R. SUTHERLAND, Y. MADDAHI, L. S. GAN, S. LAMA, AND K. ZAREINIA, Robotics in the neurosurgical treatment of glioma, Surgical neurology international, 6 (2015), pp. S1–S8.

[185] S. SUZUKI AND R. SUDA, A vision system with wide field of view and collision alarms for teleoperation ROBOMECH Journal, 1 (2014), p. 8.

[186] A. TAKHMAR, I. G. POLUSHIN, A. TALASAZ, AND R. V. PATEL, Cooperative teleoperation with projection-based force reflection for mis, IEEE Transactions on Control Systems Technology, 23 (2015), pp. 1411–1426.

[187] H. TAN, R. GRAY, J. J. YOUNG, AND R. TAYLOR, A haptic back display for attentional and directional cueing, (2003).

[188] M. TAVAKOLI, A. AZIMINEJAD, R. V. PATEL, AND M. MOALLEM, Tool/tissue interaction feedback modalities in robot-assisted lump localization, in 2006 International Conference of the IEEE Engineering in Medicine and Biology Society, vol. 1, IEEE, aug 2006, pp. 3854–3857.

[189] TOBIIPRO, Tobii Pro Glasses 2, 2021.

[190] O. TOKATLI, P. DAS, R. NATH, L. PANGIONE, A. ALTOBELLI, G. BURROUGHES, E. T. JONASSON, M. F. TURNER, AND R. SKILTON, Robot-assisted glovebox teleoperation for nuclear industry, Robotics, 10 (2021).

[191] H.-R. TSAI AND J. REKIMOTO, ElasticVR, in Extended Abstracts of the 2018 CHI Conference on Human Factors in Computing Systems - CHI '18, New York, New York, USA, 2018, ACM Press, pp. 1–4.

[192] F.-W. TUNG, Child Perception of Humanoid Robot Appearance and Behavior, International Journal of Human–Computer Interaction, 32 (2016), pp. 493–502.

[193] ULTRAHAPTICS, What is haptic feedback? - Ultrahaptics, 2018.

[194] ULTRALEAP, What is Haptic feedback, 2021.

[195] UNITED NATIONS, World Population Ageing, tech. rep., United Nations, New York, NY, USA, 2017.

[196] J. VAN OOSTERHOUT, J. G. W. WILDENBEEST, H. BOESSENKOOL, C. J. M. HEEMSKERK, M. R. DE BAAR, F. C. T. VAN DER HELM, AND D. A. ABBINK, Haptic Shared Control in Tele-Manipulation: Effects of Inaccuracies in Guidance on Task Execution., IEEE transactions on haptics, 8 (2015), pp. 164–175.

[197] S. VASUNILASHORN, B. A. STEINMAN, P. S. LIEBIG, AND J. PYNOOS, Aging in Place: Evolution of a Research Topic Whose Time Has Come, Journal of Aging Research, 2012 (2012), p. 120952.

[198] M.-A. VITRANI, C. POQUET, AND G. MOREL, Applying virtual fixtures to the distal end of a minimally invasive surgery instrument, IEEE Transactions on Robotics, 33 (2017), pp. 114–123.

[199] K. WADA, T. SHIBATA, T. SAITO, AND K. TANIE, Robot assisted activity for elderly people and nurses at a day service center, vol. 2, IEEE, 2002, pp. 141–1421 vol.2.

[200] M. WALKER, Z. CHEN, M. WHITLOCK, D. BLAIR, D. A. SZAFIR, C. HECKMAN, AND D. SZAFIR, A mixed reality supervision and telepresence interface for outdoor field robotics, in 2021 IEEE/RSJ International Conference on Intelligent Robots and Systems (IROS), 2021, pp. 2345–2352.

[201] B. WEBER AND C. EICHBERGER, The Benefits of Haptic Feedback in Telesurgery and Other Teleoperation Sy Cham, 2015, Springer International Publishing, pp. 394–405.

[202] S. WEINSTEIN, Intensive and extensive aspects of tactile sensitivity as a function of body part, sex, and later The skin senses. Proceedings of the First International Symposium March,, 1966 Talla (1968), pp. 195–222.

[203] J. G. W. WILDENBEEST, D. A. ABBINK, C. J. M. HEEMSKERK, F. C. T. VAN DER HELM, AND H. BOESSENKOOL, The Impact of Haptic Feedback Quality on the Performance of Teleoperated Assembly Tasks, IEEE Transactions on Haptics, 6 (2013), pp. 242–252.

[204] K. WINKLE, P. CALEB-SOLLY, A. TURTON, AND P. BREMNER, Social Robots for Engagement in Rehabilitative Therapies: Design Implications from a Study with Thera

in ACM/IEEE International Conference on Human-Robot Interaction, Chicago, 2018, ACM New York, pp. 289–297.

[205] G. YANG, H. LV, Z. ZHANG, L. YANG, J. DENG, S. YOU, J. DU, AND H. YANG, Keep Healthcare Workers Safe: Application of Teleoperated Robot in Isolation Ward for COVID-19 Chinese Journal of Mechanical Engineering, 33 (2020), p. 47.

[206] T.-H. YANG, D. PYO, S.-Y. KIM, Y.-J. CHO, Y. D. BAE, Y. M. LEE, J. S. LEE, E. H. LEE, AND D. KWON, A new subminiature impact actuator for mobile devices, in 2011 IEEE World Haptics Conference, 2011, pp. 95–100.

[207] G. YIN, M. J.-D. OTIS, P. E. FORTIN, AND J. R. COOPERSTOCK, Evaluating Multimodal Feedback for Assembly Tasks in a Virtual Environment, Proc. ACM Hum.-Comput. Interact., 3 (2019).

[208] A. A. YUSOF, T. KAWAMURA, AND H. YAMADA, Operational Evaluation of a Construction Robot Tele-op TRANSACTIONS OF THE JAPAN FLUID POWER SYSTEM SOCIETY, 43 (2011), pp. 8–15.

[209] T. ZHAN, K. YIN, J. XIONG, Z. HE, AND S.-T. WU, Augmented Reality and Virtual Reality Displays: Perspectives and Challenges, iScience, 23 (2020), p. 101397.

[210] X. ZHANG, D. LIN, H. PFORSICH, AND V. W. LIN, Physician workforce in the United States of America: forecasting nationwide shortages, Human resources for health, 18 (2020), p. 8.

[211] Q. ZHAO, D. TU, S. XU, H. SHAO, AND Q. MENG, Natural human-robot interaction for elderly and disabled healthcare application, in 2014 IEEE International Conference on Bioinformatics and Biomedicine (BIBM), IEEE, nov 2014, pp. 39–44.

[212] J. ZHU, Y. CHEN, M. XU, E. DONG, H. ZHANG, AND X. TANG, Graphical Force and Haptic Feedback Teleoperation System for Live Power Lines Maintaining Rob in 2019 IEEE International Conference on Mechatronics and Automation (ICMA), 2019, pp. 2565–2570.

[213] Z. A. ZOOK, J. J. FLECK, T. W. TJANDRA, AND M. K. O'MALLEY, Effect of Interference on Multi-Sensory Haptic Perception of Stretch and Squeeze, in 2019 IEEE World Haptics Conference (WHC), 2019, pp. 371–376.